NTNU – Trondheim
Norwegian University of
Science and Technology

History Matching a Full Field Reservoir Simulation Model

The Jette Field

Kjetil Lorentzen

Petroleum Geoscience and Engineering
Submission date: June 2014
Supervisor: Jon Kleppe, IPT
Co-supervisor: Eirik Espe, Weatherford Petroleum Consultants AS

Norwegian University of Science and Technology
Department of Petroleum Engineering and Applied Geophysics

ACKNOWLEDGEMENTS

This Master's thesis has been carried out during the Spring of 2014 at the Norwegian University of Science and Technology, Department of Petroleum Engineering and Applied Geophysics, in collaboration with Weatherford Petroleum Consultants AS.

First and foremost I would like to express my sincere gratitude towards my supervisors Eirik Espe, Senior Reservoir Engineer at Weatherford Petroleum Consultants AS, and Jon Kleppe, Professor at the Department of Petroleum Engineering and Applied Geophysics, for their guidance, discussions and valuable insights throughout the completion of this Master's thesis. I would also like to thank all employees at Weatherford Petroleum Consultants AS for their support and help during my work with this thesis.

Finally, a great thanks goes to Det norske oljeselskap ASA for allowing me to work with their dynamic reservoir model of the Jette field.

Kjetil Lorentzen

Trondheim, June 2014

ABSTRACT

Reservoir models are used for understanding and prediction of reservoir performance. The Jette dynamic reservoir model were not capable of representing reservoir performance at Jette and experienced problems with prediction of reservoir performance. Oil production at Jette were overestimated and it was of interest to history match the Jette dynamic reservoir model in order to increase understanding and obtain a more realistic representation of the reservoir.

In this thesis, the upscaled Jette dynamic reservoir model from project work by Lorentzen (2013) has been manually history matched. Perturbations to the model have been performed in a trial and error fashion, in accordance with the most recent geologic understanding and knowledge of the Jette reservoir. Attention has been focused on validation of model input as well as only making realistic changes to the model in order to obtain a reasonable representation of the Jette reservoir.

Most perturbations during history matching of the Jette dynamic reservoir model were performed using Petrel, a complementary software to the ECLIPSE 100 reservoir simulator used to run the Jette model. During validation of input, reservoir characterization were improved by replacing the old fluid model with two new fluid models and establishing a compartmentalized reservoir by inclusion of sealing faults. As a result of this, new lift curves were created in order to run the model constrained by tubinghead pressure during prediction of reservoir performance. Updates to well completions were also needed. The main history matching parameters have been permeability, aquifer size and connectivity in addition to vertical flow barriers representing black shales and calcite stringers. Permeability has been perturbed according to interpreted well tests in order to promote linear flow.

The Jette dynamic reservoir model is considered to be successfully history matched. Well D-1H is capable of accurately replicating historical performance data when running constrained from both allocated oil rate and tubinghead pressure. Well E-1H also experience a reasonable match. However, with a slight mismatch in water production and bottomhole pressure from 15th of November 2013, possibly caused by an overestimate of oil in the model.

Prediction of reservoir performance at Jette, using the history matched model, were performed for the period between 1st of March 2014 and 1st of January 2020. Prediction runs were constrained by tubinghead pressure and no seam effect was observed when crossing over from history mode. However, oil production in well E-1H is slightly overestimated. A

total of four prediction scenarios were selected to investigate the effect of gas lift rate at Jette, they found oil production to increase with increasing gas lift rate.

History matching of the Jette dynamic reservoir model has established a better understanding of the mechanisms controlling reservoir behavior at Jette. Hence, the process of history matching has clearly added value to the Jette dynamic reservoir model as it can now be used with greater accuracy and less uncertainty when conducting simulation studies in the future.

SAMMENDRAG

Reservoarmodeller blir brukt til å forstå og forutsi oppførselen til et reservoar. Den dynamiske reservoarmodellen til Jette var ikke i stand til å representere oppførselen til reservoaret og opplevde problemer med å predikere korrekt produksjon. Oljeproduksjonen på Jette ble overestimert, noe som førte til en interesse for å historietilpasse den dynamiske reservoarmodellen for å kunne øke forståelsen og samtidig oppnå en mer realistisk representasjon av reservoaret.

I denne oppgaven har den dynamiske reservoarmodellen til Jette som ble oppskalert i prosjektoppgaven av Lorentzen (2013) blitt historietilpasset manuelt. Endringer i modellen har blitt utført i en prøv og feil prosess, i samsvar med den seneste geologiske forståelse og kunnskap om reservoaret på Jette. Fokus har vært på å validere data som var tilstede i den eksisterende reservoarmodellen samtidig som endringer skulle være så realistiske som mulig. På denne måten ble det forsøkt å oppnå en realistisk representasjon av reservoaret på Jette.

De fleste endringer under historietilpasningen av den dynamiske reservoarmodellen har blitt utført i Petrel, et komplementært program til reservoarsimulatoren ECLIPSE 100 som har vært brukt til å kjøre Jette-modellen. Under validering av data ble karakteriseringen av reservoaret forbedret ved å erstatte den gamle fluid-modellen med to nye fluid-modeller og opprettelse av et kompartmentalisert reservoar ved å legge til forseglende forkastninger. Som et resultat av dette ble det opprettet nye løftekurver for bruk til prediksjon av produksjon når brønnene er styrt på brønnhodetrykk. Det ble også foretatt oppdateringer av brønnkompletteringer. Permeabilitet, akviferstørrelse samt vertikale strømningsbarrierer er parameterne som hovedsaklig er blitt endret under historietilpasningen. Vertikale strømningsbarrierer er representert ved skifrige lag og stringere av kalsitt. Permeabiliteten har blitt endret for å oppnå lineær strømning i reservoaret, som påvist av brønntester.

Historietilpasningen av den dynamiske reservoarmodellen til Jette er ansett for å være vellykket. Brønn D-1H er i stand til å følge historiske produksjonsdata tett både når brønnen er styrt på brønnhodetrykk og når brønnen er styrt av allokert oljerate. Brønn E-1H opplever også en god tilpasning til historiske data, men opplever et økende avvik i produksjon av vann samt bunnhullstrykk fra 15. November 2013. Avviket er trolig forårsaket av for masse olje i reservoarmodellen.

Det har blitt utført prediksjon av reservoaroppførsel ved bruk av den historietilpassede reservoarmodellen i perioden 1. Mars 2014 til 1. Januar 2020. Prediksjonene ble styrt på

brønnhodetrykk og det ble ikke observert noen sømeffekt i overgangen fra historisk modus til prediksjonsmodus. Det ble derimot observert at oljeproduksjonen i brønn E-1H er blitt noe overestimert. Totalt fire scenarioer for prediksjon ble forberedet for å kunne vurdere effekten til valg av gassløftrate på Jette. Prediksjonene konkluderte med at økt gassløftrate resulterer i økt oljeproduksjon.

Historietilpasning av den dynamiske reservoarmodellen på Jette har ført til en dypere forståelse av mekanismene som styrer oppførselen i reservoaret på Jette. På grunnlag av de oppnådde resultat er det tydelig at historietilpasningen har tilført verdi i den dynamiske reservoarmodellen siden den nå kan bli brukt med større presisjon og mindre usikkerhet under framtidige simuleringsstudier.

TABLE OF CONTENT

LIST OF FIGURES

LIST OF TABLES

1 INTRODUCTION

Det norske oljeselskap operates the Jette field which is one of the smallest oil fields on the norwegian continental shelf. Jette was discovered in 2009 and production started in May 2013. Production from Jette is the first oil produced by Det norske oljeselskap as operator and represents an important cash flow for the company. Jette produces from two standalone subsea wells tied back to Jotun. Due to its small size Jette would never have been developed had it not been for the possibility to tie back with already existing infrastructure at Jotun (Lorentzen, 2013).

During development of Jette it was created a reservoir model in order to predict reservoir performance. Reservoir models are extensively used in the development and management of oilfields throughout the world in order to optimize production and assess economics. Production from Jette has unfortunately not met with expectations from predictions made with the current reservoir model. Jette has experienced a rapid decline in oil production, indicating that the reservoir model is not a realistic representation of the reservoir and not capable of predicting future reservoir performance. Prediction of future reservoir performance is an important feature of a reservoir model, if not the most important. Hence, the reservoir model should be updated in order to correctly represent reservoir behavior and be able to predict future reservoir performance. This process is known as history matching and is what will be performed in this Master's thesis.

The common workflow in a simulation study is to build a dynamic reservoir model, validate it towards available data and make production forecasts. Production forecasts are used to evaluate alternative development scenarios and establish a cash flow prediction (Fanchi, 2006). Reservoir management decisions are based on cash flow predictions. Hence, it is important to have reliable cash flow predictions in order to make good decisions for the future of the oil company. If production forecasts are found not to represent the actual reservoir behavior it is common to perform history matching of the reservoir model. History matching is the process of updating the reservoir model to incorporate all available field information such that the model is capable of replicating past reservoir performance. It is assumed that a reservoir model capable of simulating past reservoir performance will reduce uncertainty, improve reservoir understanding and enhance the accuracy of predicted future reservoir performance (Gilman and Ozgen, 2013).

Unfortunately, it has not been possible for reservoir engineers at Det norske oljeselskap to obtain a history matched reservoir model of Jette. There is much uncertainty related to the current Jette dynamic reservoir model and its input making history matching difficult. This includes allocated production rates, lack of core data and geological understanding, fluid sampling in addition to numerical problems such as dispersion and convergence issues. It is of great interest to reduce uncertainty to the above mentioned by obtaining a history matched model.

The Jette dynamic reservoir model will be history matched during this Master's thesis. Manual history matching will be performed on the upscaled Jette dynamic reservoir model created during project work by Lorentzen (2013). The Jette dynamic reservoir model will be updated to accurately represent recorded production data by calibrating certain parameters. Selection of what parameters to update in the model will be based on thorough studies of all available data from Jette, provided by Det norske oljeselskap. In addition to updating the model, current input to the Jette dynamic reservoir model should be validated in order to ensure that the model is a realistic representation of the reservoir. The history matched model will be used to make simple predictions of future reservoir performance at Jette. New predictions of reservoir performance after history matching of the Jette dynamic reservoir model is believed to give a more realistic representation of the future reservoir performance and will be of great interest to Det norske oljeselskap when making reservoir management decisions in the future.

There are several applications of a history matched Jette dynamic reservoir model which encourage the matching process. This includes, in addition to prediction of reservoir performance, sensitivity studies, the possibility to evaluate alternative development plans for increased oil production or evaluation of any other reservoir management decision. Having a history matched Jette dynamic reservoir model will allow Det norske oljeselskap to make sound reservoir management decisions and hopefully increase oil production from Jette.

2 HISTORY MATCHING

Accurate reservoir models are of great help when making decisions related to reservoir management. They can reduce risk of investment in field development and predict reservoir performance under various operating condtions. It is imparative that if a reservoir model is to accurately represent the reservoir it will need to be conceptually similar to the real life reservoir. To test and validate that the simulation model is similar to the reservoir a process known as history matching is performed (Mattax and Dalton, 1990). During history matching past performance of the reservoir is simulated and the model is updated in order to match actual historical performance. The final history matched model is assumed to accurately represent the reservoir and be able to predict reservoir performance (Gilman and Ozgen, 2013).

2.1 INTRODUCTION TO HISTORY MATCHING

The purpose and primary objective of history matching reservoir models is to reduce uncertainty, improve reservoir understanding, validate the reservoir simulation model and enhance the accuracy to predictions of reservoir performance. It is assumed that if the reservoir model is capable of replicating past reservoir performance it can be used to reasonably predict future performance (Gilman and Ozgen, 2013). History matching is the process by which the model input, such as the geological description or fluid properties, are changed to obtain a match towards recorded data. Recorded data can be phase rates and cumulative production, pressures, tracers, temperatures, salinity etc. (Gilman and Ozgen, 2013). Matching as much of the historical data as possible will effectively reduce uncertainty and improve confidence in the current reservoir characterization (Ertekin, Abou-Kassem and King, 2001). However, uncertainty can never be reduced below the uncertainty inherent in the historical data itself.

History matching is often a time consuming, expensive and frustrating process since reservoir performance can be complex, with numerous interactions that as a whole can be difficult to understand (Mattax and Dalton, 1990). Especially choosing what parameters to alter in order to improve match can be a daunting task. Common practice is to choose and alter those parameters which are considered the most uncertain (Gilman and Ozgen, 2013;

Ertekin, Abou-Kassem and King, 2001). During history matching it is important that changes made to the reservoir model are consistent with reservoir description. This is because of the non-unique nature of the history matching problem. History matching is an inverse problem of which we know the output and seek to identify what input it results from (Gilman and Ozgen, 2013). Due to the shear amount of variables affecting reservoir performance there will be numerous combinations which will yield output similar to historical data. This means that history matched models can be falsely obtained if the reservoir is not understood properly or unrealistic changes are performed on reservoir parameters. Wrong reservoir characterization can yield a good history match, however it will not be able to predict the reservoir performance. Unfortunately, there is no way of controlling that the reservoir characterization obtained during history matching is correct. Other than to ultimately verify if the model was able (or fail) to correctly predict the reservoir performance (Gilman and Ozgen, 2013). A summary of why history matching is such a difficult task is listed in Table 2.1.1.

Table 2.1.1 – Issues making history matching difficult (Gilman and Ozgen, 2013)

- If considered strictly as an inverse problem, history matching is an ill-conditioned mathematical problem that is non-unique and thus has a large (infinite?) set of solutions.
- The physics of most models is nonlinear – in many cases strongly nonlinear – meaning it is not easy or even possible to clearly isolate changes in the output data to changes in the input data.
- The key input parameters that affect the output in such a way to improve the history match is not always apparent.
- Extensive sensitivity studies are generally required to gain a good understanding of the reservoir model.
- Some input parameters are stochastic in nature, particularly data describing the geological scenario.
- Production data are inherently biased – particular old data – and often associated with large errors.

A properly history matched reservoir model will contribute to better understanding of the current status of the reservoir, fluid distribution and fluid movement, including verification of the current depletion mechanism. It is also possible to obtain information about operating problems such as casing leaks or improper fluid allocation between wells (Mattax and Dalton, 1990).

A typical history matching process consists of the steps listed in Table 2.1.2 (Ertekin, Abou-Kassem and King, 2001). In essence the history matching process consists of starting with an initial model, performing a simulation run constrained by chosen historical data and then comparing it against the matching criterias. If the model is not matched changes will be made to the most uncertain parameters governing the problem to be resolved. The model is

rerun and compared with historical data and the process is repeated until a satisfactory match is obtained (Mattax and Dalton, 1990; Gilman and Ozgen, 2013). No standard matching criterias exist, but the match can be judged by whether the reservoir model is good enough to permit the objectives of the study to be met (Mattax and Dalton, 1990).

Table 2.1.2 – Stepwise description of a history matching process (Ertekin, Abou-Kassem and King, 2001)

1.	Define objectives for the history matching process.
2.	Determine what method to use for history matching. This should be dictated by the objectives of the history match, resources available for the history match, the deadlines for the history match and the data available.
3.	Determine the historical production data to be matched and the criteria to be used to describe a successful match. These should be dictated by the availability and quality of the production data and by the objectives of the simulation study.
4.	Determine what reservoir parameters that can be adjusted during the history match and the confidence range for these. The parameters to be chosen should be those least accurately known with the most significant impact on reservoir performance.
5.	Run the simulation model with the best available input data.
6.	Compare the results of the history match run with the historical production data chosen in step 3.
7.	Make changes to parameters selected in step 4 within the range of confidence in order to improve history match.
8.	Repeat steps 5 through 7 until the criteria established for a succesful match in step 3 are met.

2.2 ESTABLISHING REALISM IN THE INITIAL RESERVOIR MODEL

Before initialization of a major history matching process it is important to assess how well the reservoir model represents the actual reservoir. The initial reservoir model will need to incorporate the best available static and dynamic data about the reservoir if a realistic history match is to be obtained. This is due to the non-unique nature of the history matching problem, as described in Chapter 2.1. Accuracy of the results from predictions are shown to be highly dependent on the starting geological model and simplifying assumptions employed during reservoir characterization. Reservoir models can never provide a unique answer, hence they can only show which models are not plausible. Because of this more focus needs to be directed at better reservoir characterization and ensuring that simulation models ends up giving realistic answers consistent with the geology of the reservoir (Gilman and Ozgen, 2013).

Reservoir simulation usually begins with reservoir characterization. Reservoir characterization can be considered the process of bringing together diverse sources of data

and expert opinions to develop a most realistic model of the reservoir to be used for evaluation (Gilman and Ozgen, 2013). These data will form the foundation for reservoir understanding and the prediction of future performance. It is important that when building the initial model a multidisciplinary approach be used in order to transfer competency between geologists and engineers to establish a common foundation for understanding of the reservoir and underlying assumptions. Today most characterization processes of reservoirs are associated with building a static geological model from available data. This ensures that the model is constrained and consistent with a set of static information which, in theory, will reduce uncertainty associated with the model (Gilman and Ozgen, 2013). The task of establishing a realistic initial model relies heavily upon experience, judgement and intuition in order to account for the many different measurement scales, illustrated in Figure 2.2.1, in data while also addressing the uncertainty from sparse data sets. Table 2.2.1 lists the data sources that will need to be integrated in order to establish a realistic model.

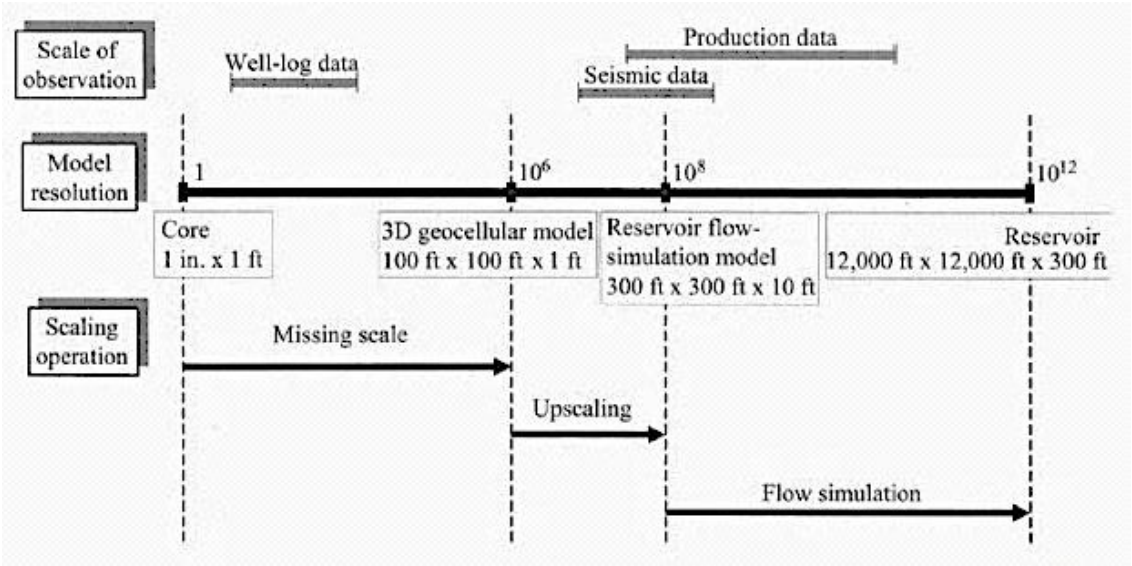

Figure 2.2.1: Comparison of various measurement scales and the scales typically used in modeling. The reference unit is defined such that a core corresponds to an order of 1, and the other units are compared with this (Caers, 2005).

Table 2.2.1 – Data sources needed to be integrated in the initial model (Gilman and Ozgen, 2013)

- ***Geological interpretation***: From outcrops, cross sections, analogy and expert opinion the depositional environment and architectural elements can be understood.
- ***Well logs:*** Estimates of properties such as porosity, saturation and permeability along the well can be established. Well logs also enables stratigraphic top picks to be selected.
- ***Cores:*** Measurements on cores will establish basic flow characterization for permeability and relative permeability in addition to facies description, storage (porosity) and other data derived from special core analysis (SCAL).
- ***Geochemistry:*** Analysis of PVT may provide data for compartmentalization and compostional grading estimates. PVT is also used to establish a fluid characterization.
- ***Seismic:*** Data forming the basis for structural analysis and property distribution based on seismic attributes. 4D seismic can also improve understanding of how the reservoir is depleted.
- ***Drilling records:*** Surveys from drilling operations dictate where the wells are to be located within the model and what zones to be completed.
- ***Production profiles:*** Data about reservoir geometry and flow regimes can be derived from production profiles. Pressure transient analysis can also indicate estimates of permeability.
- ***Repeat formation test (RFT):*** Measurement of saturation and pressure along the wellbore at different times can help discover flow barriers and locate what parts of the reservoir are being produced.

It is obvious that the process of integrating all available data to form a realistic initial model to perform history matching on is a time consuming and difficult process. Figure 2.2.2 illustrates the general workflow for characterizing a reservoir and preparing a simulation model. Most data incorporates a wide span on uncertainty, and will need to be verified before being incorporated in the model. In addition to uncertainty related to properties of the reservoir, there is also uncertainty in measured data such as fluid rates and pressures. Even laboratory measurements and fluid samples from the reservoir may have a high degree of uncertainty. For systems with a commingled production stream additional uncertainty is introduced from back-allocation of fluids between wells. All uncertainty will have to be assessed if the initial model for history matching is to be as realistic as possible.

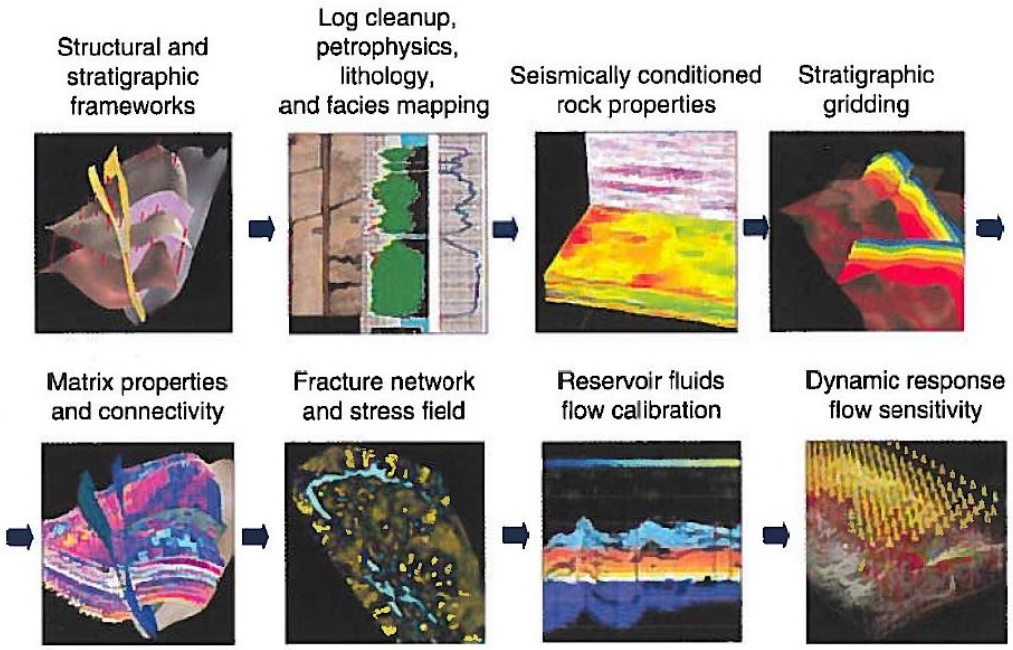

Figure 2.2.2: General workflow during characterization and building of a simulation model (Gilman and Ozgen, 2013).

Once a satisfactorily characterized model is established this will form the starting point for the history matching process. At this stage the model will be simulated and perturbations will be performed on various parameters to improve match towards recorded data. It is stated that if the reservoir characterization is close to the real description of the reservoir this will speed up the cumbersome process of history matching, and the reservoir model will converge towards a match more rapid than if the model includes a poor reservoir description (Gilman and Ozgen, 2013). This highlights the importance of forming a solid understanding of the reservoir and using this information already in the early stages of history matching.

2.3 HISTORICAL RESERVOIR PERFORMANCE DATA

In order to perform and achieve a history match of a reservoir model some sort of historical performance data must exist (Ertekin, Abou-Kassem and King, 2001). These data can be production rates of different phases, pressures or any other historic data describing reservoir performance. By constraining the wells in a simulation model with a chosen type of performance data one is able to compare the calculated model response with any of the other types of data available. For instance, one may specify the model to be simulated with wells constrained by oil rate. The model will calculate the corresponding rates of gas and water according to mobility and pressure, these in turn can be compared with measured rates. The

history match will be validated based on how good it matches the historical reservoir performance. There is usually some sort of deviation between the behavior of the simulation model and the actual reservoir. This establishes the need to predetermine a criteria used to describe a successful match.

The following three sub chapters will elaborate on important aspects related to the selection of historical reservoir performance data used to constrain the model, what reservoir performance data to match and what constitutes a successful match.

2.3.1 CONSTRAINING THE RESERVOIR MODEL

A dynamic reservoir simulation model reflect the discretized version of the partial differential equations which describe multiphase flow within the reservoir. Similar to solving partial differential equations we need a set of boundary conditions, in addition to the initial conditions during initialization, to obtain a solution. These boundary conditions can be either a Neumann-type or a Dirichlet-type. A Neumann-type boundary condition specifies the rate of a given phase produced from within the reservoir while the Dirichlet-type specifies the pressure, either bottomhole pressure (BHP) or tubing head pressure (THP), which the well operates at (Gilman and Ozgen, 2013). The most commonly used boundary condition (well constraint) is to specify the production rate of individual wells. The choice of production data to specify depends on the hydrocarbons present in the reservoir. If the reservoir produces oil it is of course common to specify the oil rate, and similarily gas rate in a gas reservoir. If an oil reservoir produces at high gas-oil ratios (GOR) or high water cuts (WC) it might be better to constrain production by either gas or water rate (Ertekin, Abou-Kassem and King, 2001). The reason for choosing rate constraints are due to these data being more readily available. It is only lately that pressure sensors are installed downhole to record pressure performance data continuously. Another reason to specify oil rate is to accurately account for production of the most valuable fluid (Gilman and Ozgen, 2013).

Performance data should be scrutinized before being used to constrain wells in the simulation model. Uncertainties in performance data need to be assessed and minimized to represent the historical performance of the reservoir as realistically as possible. A source of uncertainty could be back-allocation of phase rates in commingled production streams. Allocation of production inevitably introduces uncertainty in the data but is neccessary in order to obtain rates which can be used to constrain wells or to match model production

against. Other sources that might cause uncertainty are metering of rates at test separator or multiphase flow meters (MPFM). If changes are performed to the well stream these must be accounted for before using the metered rates. This could be to account for gas routed for gas lift systems, gas used as fuel or gas flared off (Gilman and Ozgen, 2013; Ertekin, Abou-Kassem and King, 2001). It is worth noting that the resulting history match will never be more certain than the uncertainty inherent in the reservoir performance data used to obtain a match.

If performance data are found representative it will need to be tabulated and prepared in order to be entered into the reservoir model. The time specification of historical data may vary depending on the availability and amount of data (Gilman and Ozgen, 2013). If large amounts of data exists it might be necessary to specify historic well performance (either rate or pressure constraint) on a monthly basis. In comparison, a relatively young field might specify historical well performance on a daily basis. The reason for this is that the simulator must print a report at all times when historical performance data are entered, this will lead to time consuming simulations if large amounts of data are specified. The engineer performing history matching will need to use sound judgement to obtain an efficiently running model with representative performance data. Reducing the need for timesteps when specifying historical performance data less frequently introduces the need for averaging of the historical data. This implies that data might not be correctly represented if large variations exists in the data sets, when averaging over months for instance. This problem can be seen from Figure 2.3.1.1, where historical oil rate is measured on a daily basis and then averaged in order to be entered in a model on a monthly basis. It is obvious that the two rates presented in Figure 2.3.1.1 would represent two very different responses in terms of BHP.

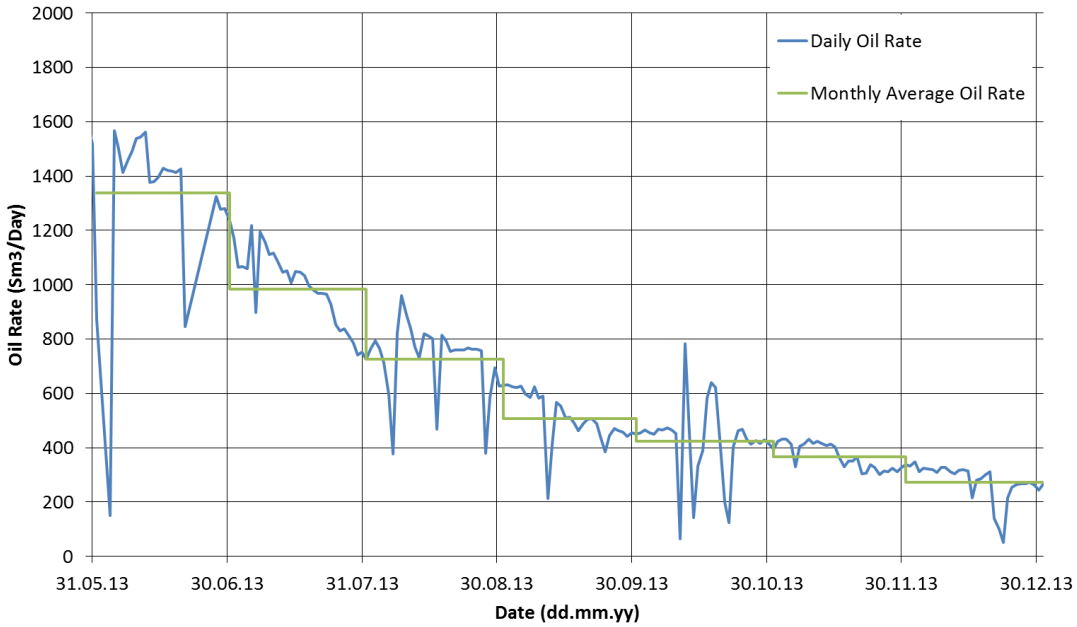

Figure 2.3.1.1: Historical oil rate represented on both daily and monthly basis. The monthly basis is an average of the daily oil rate and prepared in order to reduce amount of data input in a simulation run. Averaging of historical input data will change the response given from the simulation model.

2.3.2 RESERVOIR PERFORMANCE DATA TO BE MATCHED

Having decided on which performance data will constrain wells, the reservoir simulation model will have to be run and compared with other historical performance data. Selection of what production or injection data to match during history matching depends on availability and quality of data (Ertekin, Abou-Kassem and King, 2001). The quality of a history match is proportional to the amount and accuracy of the available data (Gilman and Ozgen, 2013). Also, matching multiple parameters describing reservoir performance will increase confidence to predictions performed later with the history matched model (Ertekin, Abou-Kassem and King, 2001). This is due to the non-unique nature of the history matching problem, since a match towards multiple parameters will make the resulting history matched model more unique and reduce uncertainty in the prediction of reservoir performance (Baker et al., 2006). However, if data has not been measured accurately it might not be necessary to run an excessive history matching process to match these data exactly. What parameters to match and what tolerances to match these data against should be governed by uncertainty in the data (Ertekin, Abou-Kassem and King, 2001).

Table 2.3.2.1 lists the most commonly available performance data that can be matched during history matching of reservoir models. As with data used to constrain the model, data specified to be matched should also be scrutinized. When matching past reservoir

performance data it is important that changes made to the model honors both the static geomodel and reservoir physics, mentioned in more detail in Chapter 2.1 (Gilman and Ozgen, 2013). The various points listed in Table 2.3.2.1 will be described briefly below.

Table 2.3.2.1 – Possible types of performance data to match (Gilman and Ozgen, 2013)

- Rates, Ratios and Volumes
- Static Pressures
- Pressure and Saturation Profiles
- Flowing Pressures
- Production and/or Injection Profiles
- Salinity
- Compositions
- Interference Tests
- 4D Seismic

Rates, Ratios and Volumes:

When constraining wells with a given phase rate, the simulator will honor the specified phase rate. The goal of the history matching then becomes to accurately represent production of the remaining (unspecified) phases. It is common to view the historical and calculated rates, together with water cuts, gas-oil ratio (GOR), and cumulative production of all phases all on the same plot (Gilman and Ozgen, 2013). Any mismatch between the reservoir model and the historical data will easily be spotted on such a plot. Besides using phase ratios such as GOR and water cut, a commonly used observation is the breakthrough time of a given phase. This is because it will help characterize vertical and lateral flow barriers (Gilman and Ozgen, 2013). If either water or gas production is not present, it will be hard to match the reservoir model correctly because less data is available for comparison with model calculations (Mattax and Dalton, 1990).

Phase ratios, water cut and GOR, can in addition to the above mentioned be used to assess relative mobility of the phases, as well as verification of the displacement efficiency (Gilman and Ozgen, 2013). Displacement efficiency is also effectively monitored and assessed from the breakthrough time. This is because breakthrough time is dependent on geology, zonation, interwell transmissibility and mobility ratio (Ertekin, Abou-Kassem and King, 2001). GOR behavior is experienced to be strongly related to PVT characteristics (Gilman and Ozgen, 2013). A sudden increase in GOR will indicate that reservoir pressure close to the well has fallen below the bubblepoint pressure such that the oil will boil and gas will come out of solution.

Static Pressures:

Static pressures used for history matching are obtained from observation wells or pressure-transient analysis (PTA). Analysis of pressure buildup data will provide several interpretations useful for history matching, such as average reservoir pressure (within drainage area), permeability-thickness, skin, flow regime and reservoir geometry. The reservoir model should be modified in order to reflect the results obtained from PTA (Gilman and Ozgen, 2013). Pressures from observation wells will help establish estimates of interwell permeability-thickness (Mattax and Dalton, 1990). If compared with permeability-thickness obtained from PTA a greater confidence to this data can be achieved.

It is possible to use static pressures obtained from buildup tests during the history matching process, however this requires special considerations. A solution is to shut in the simulated well for the same amount of time as the buildup test and match shut in pressures. This calls for selection of small timesteps in the simulator, as the duration of most buildup tests are short. If a valid comparison between observed shut-in pressures and calculated pressures is to be obtained it is important that pressure is evaluated at the same location (datum) (Gilman and Ozgen, 2013). Also, measured pressure will usually not correspond directly to pressure calculated in grid blocks containing the wells. This is due to the horizontal dimension of the block being much larger than the wellbore radius, meaning that the grid block pressure, which is an average pressure in the volume represented by the grid block, corresponds to a pressure some distance away from the well. If a realistic comparison is to be performed between history and model, either calculated or historic pressure must be adjusted (Mattax and Dalton, 1990). Peaceman developed an equation (Equation 2.3.2.1) which expresses the shut-in time Δt_s at which the buildup pressure and grid block pressure should be compared. Shut-in time is expressed in hours and r_o is Peacemans wellblock-equivalent pressure radius (ft) (Gilman and Ozgen, 2013). The difference between grid block pressure and measured shut-in pressure is more pronounced for low permeability reservoirs.

$$\Delta t_s = 1688 \frac{\phi \mu c_t r_o^2}{k} \qquad \text{Equation 2.3.2.1}$$

Pressure and Saturation Profiles:

An important piece of information is the pressure vs. depth profiles obtained from repeat formation testing (RFT) or modular-dynamic testing (MDT). From a pressure vs. depth profile before start of production it is possible to determine the water-oil contact (WOC) and gas-oil contact (GOC) in the reservoir (Gilman and Ozgen, 2013). The contacts are found from gradients as illustrated in Figure 2.3.2.2. In mature reservoirs vertical flow barriers and bypassed zones will be identified as discontinuities in the pressure gradient. An example of vertical flow barriers are illustrated in Figure 2.3.2.2 where a pressure vs. depth profile is given for a reservoir section initially and after some time of production.

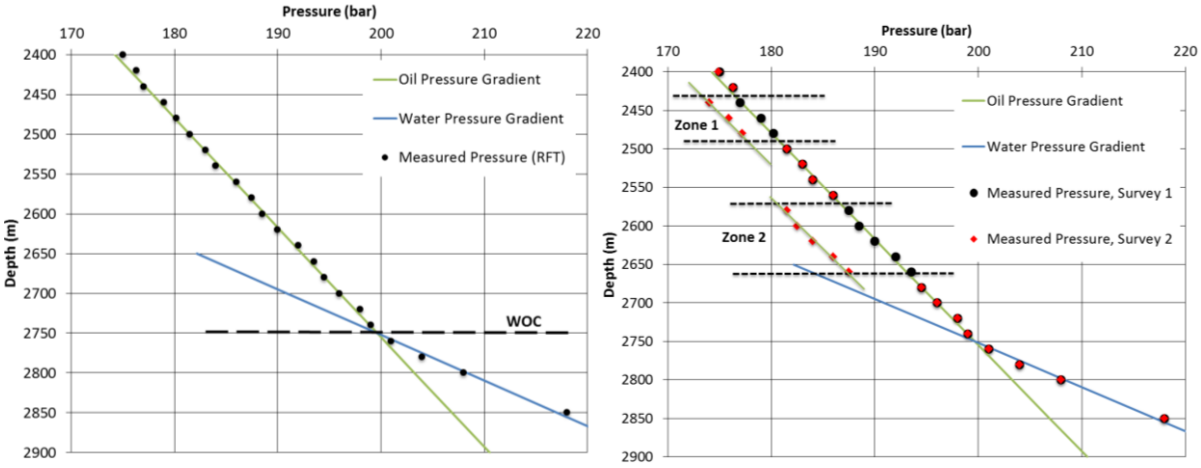

Figure 2.3.2.2: Plot of pressure vs. depth obtained from a RFT-run before production start (left) and some time after start of production (right). Gradients of oil and water indicate the initial fluid contact. Pressure surveys after start of production (right) indicate vertical flow barriers due to differential depletion in zone 1 and zone 2.

Saturation profiles along wells can be obtained from petrophysical interpretation of logs. The logged saturation profiles should be compared against the saturation profiles of wells in the simulation model to validate the distribution of fluids within the reservoir model. Due to differences in scale the comparison between model and log, in most cases, is only qualitative. However, if saturation profiles are obtained at different times throughout the life of the field these can help identify fluid movement in the reservoir (Gilman and Ozgen, 2013; Mattax and Dalton, 1990).

Flowing Pressures:

Measured BHP or THP can be matched in order to increase confidence of the calculated phase rates. This is because producing a given volume of each phase at the observed pressure

is less uncertain than producing the same volume not restricted from historical BHP or THP. In order to use THP the model needs to incorporate tables specifying vertical flow performance (VFP). These tables account for pressure loss between reservoir and wellhead, through the tubing, and is a strong function of fluid properties, flow rates, phase ratios and artificial lift projects applied to wells (Gilman and Ozgen, 2013).

Production and/or Injection Profiles:

Production logging tools (PLT) gives information about relative productivity or injectivity of zones in stratified reservoirs or reservoirs consisting of multiple flow units. Matching relative productivity ensures that fluids are produced from the correct zones in the reservoir. Production profiles will also help identify tight zones in the reservoir which will not contribute to production (Gilman and Ozgen, 2013).

Salinity:

In reservoirs produced with pressure support from water injection salinity can be used to differentiate between production of injected water and formation water if a difference in salinity exist between the two. This is similar to the use of tracers in injection projects. Tracers are effectively used to track fluid movement and breakthrough time. The difference in salinity between injected water and formation water is a natural tracer and it can easily be represented by the use of the tracer option available in most commercial reservoir simulators (Gilman and Ozgen, 2013).

Compositions:

In compositional reservoir models it is possible to track component mole fractions, similar as tracers and salinity described above. Reservoirs with compositional gradients will most often have separator gas chromatography information available for comparison with model compositions. Non-hydrocarbons such as CO_2 or H_2S is normally used during history matching of compositions (Gilman and Ozgen, 2013).

Interference Tests:

Interference test is similar to the use of static pressure from observation wells as described above. Single or multi rate tests allows us to make an interpretation of the connectivity between wells in the reservoir. If interference tests are to be reproduced in the reservoir model it requires small timesteps and consideration of grid size in order to minimize numerical dispersion and grid orientation effects (Gilman and Ozgen, 2013).

4D Seismic:

Time-lapse seismic, or 4D seismic, can yield useful information about fluid movement and how the reservoir is drained. However, it is not usually available since 4D seismic aquisition is expensive. Seismic response is dependent on rock and fluid density. If the change in rock density can be assumed neglible between seismic surveys, a repeat seismic should be able to highlight changes in fluid densities within the reservoir (Gilman and Ozgen, 2013). Figure 2.3.2.3 illustrates the response obtained from time-lapse seismic. If the resolution of the aquisitioned seismic is good it might be possible to compare the movement of fluids with that of the reservoir model during history matching to improve the realism and understanding of the matched model. It will be easier to apply 4D seismic in history matching of gas fields compared to oil fields since the seismic response will be improved due to a larger difference in density between fluids.

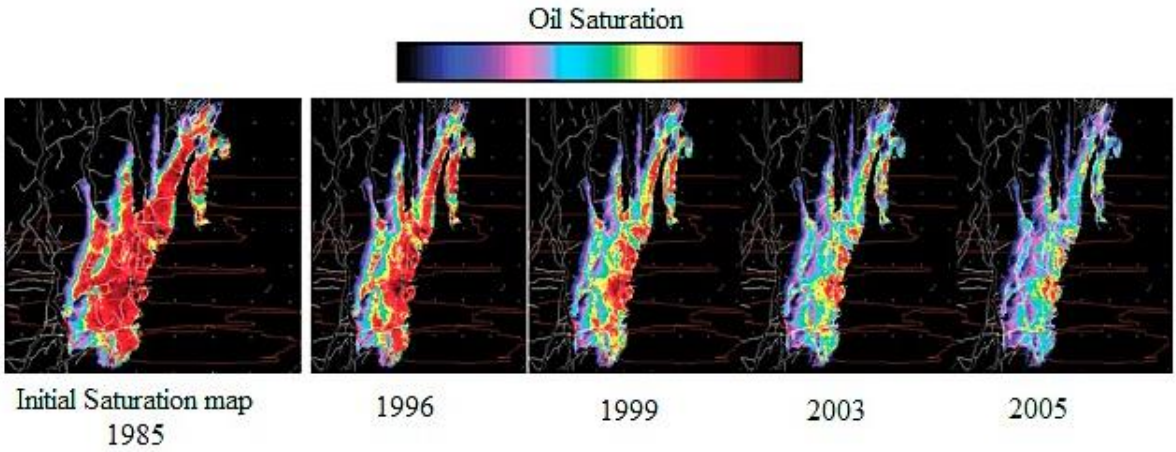

Figure 2.3.2.3: Time-lapse seismic (4d seismic) used to map fluid movement in the Gullfaks reservoir. There is a difference in seismic response between seismic surveys due to the change in fluid distribution from depletion of the reservoir (Sandø, Munkvold and Elde, 2009).

2.3.3 MATCHING CRITERIA

No standard matching criterias exist which will describe what is considered to be an accurately matched reservoir model (Baker et al., 2006). Because matching a reservoir model perfectly to historical performance data is next to impossible one needs to establish some sort of criteria which will constitute a successful match. This is difficult as all reservoirs are unique and criterias will be based on several parameters. A general method to judge the quality of the match is to assess wheter the reservoir model is good enough to permit the objectives of the study to be met (Mattax and Dalton, 1990). Baker et al. (2006) suggests that criterias should be based on the required accuracy of production forecasts simulated with the matched model. For instance, if a forecast accurate to within ± 20% of the project economics is required, the criterias needed to match on various performance data should be considered according to the required precision (Baker et al., 2006).

History matching usually tries to match as much performance data as possible to reduce uncertainty (described in Chapter 2.3.2). Most performance data will need different matching criterias based on the inherent uncertainty and how much they affect the model performance. For instance, matching cumulative oil production to a tighter tolerance than BHP is the general standard as oil production is much more important for project economics. Matching criterias may also change with time because the risk tolerance of most fields tightens as it is matured (Baker et al., 2006).

It is generally accepted that for a history match to be considered successful it must follow the trend of the reservoir performance being matched. This implies that drive mechanism and reservoir physics are correctly represented, at least to some degree, in the model. For the production forecasts based on the history match to be valid it is important to assess how the starting point of the forecast was reached. Figure 2.3.3.1 illustrates a history matched model where the cumulative gas production matches within a tolerance, but this is a mere coincidence as the model does not represent the gas rate through the history. It is obvious that even though the cumulative gas production is somewhat similar, this model does not represent the correct reservoir behavior, hence can not be considered a successful match (Baker et al., 2006).

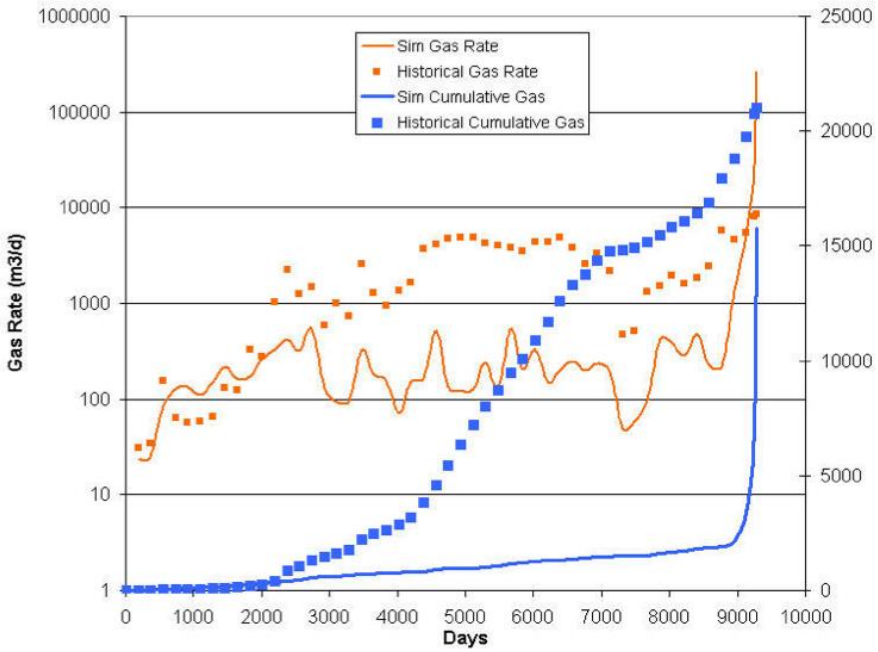

Figure 2.3.3.1: Comparison of simulated and historical gas rate and cumulative production. Simulation model obtains similar cumulative gas produced but does not reflect reservoir behavior, hence a model can meet matching criterias without necessarily representing a successful match (Baker et al., 2006).

Model performance can be assessed on a field level or individual well level when compared with the performance data required to match. It is expected that field performance match closer to recorded performance data than individual wells (Mattax and Dalton, 1990). Baker et al. (2006) has proposed a set of matching criterias to be used when determining if the history match is successful. The criterias are listed in Table 2.3.3.1 and assumes that the trend is followed in addition to meeting with the criterias. It is important to realize that a set of matching criterias should be established prior to history matching, and that these are individual for each reservoir. Tabulated matching criterias should only work as guidelines for establishing apropriate criterias.

Table 2.3.3.1 – Matching criterias used to describe a successful history match (Baker et al., 2006)

Parameter	Match Criteria
Cumulative production (Oil, gas and water)	± 10%
Production rate (Oil, gas and water)	± 10%
Bottomhole flowing pressure	± 20%
Field average pressure	± 10%

When a history matched model is considered successful and meets with the matching criterias it can be used to predict reservoir performance with the same accuracy and uncertainty reflected by the matching criterias. Due to the non-unique nature of the history matching problem, described in Chapter 2.1, severeal equiprobable history matched models can be

obtained. It is important to be aware of the fact that predictions from equiprobable history matched models will be different even though they all represent historical performance within the tolerance of the matching criterias. The effect is illustrated in Figure 2.3.3.2 where two models are close the first 15 years before experiencing a gradual increase of deviations arising from model differences.

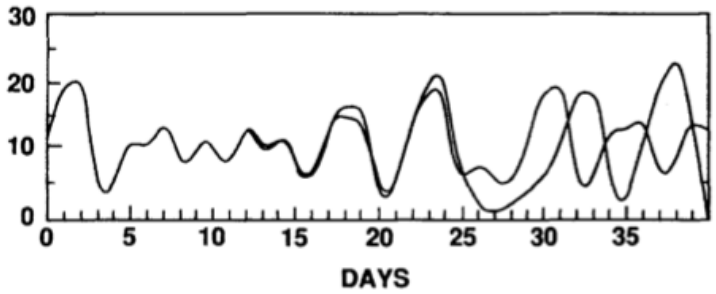

Figure 2.3.3.2: Two equiprobable history matched models exhibit similar behavior during the first 15 years when they are constrained by performance data. Predictions from 15 years and onwards diverge as a consequence of differences in reservoir description (Saleri, Toronyi and Snyder, 1992).

2.4 HISTORY MATCHING PARAMETERS

If a history match is to be obtained, one or more reservoir parameters will need to be selected and changed during the history matching process. Because of the non-unique nature of the history matching problem almost any reservoir parameter can be adjusted to achieve a history match (Ertekin, Abou-Kassem and King, 2001). Selection of history matching parameters is a difficult task considering that selected parameters and any adjustments performed on these will need to be consistent with the reservoir description. Because of this it is desirable to keep changes to the reservoir parameters with the most influence on the answer, hence attemt to find the simplest change which will result in a match (Carlson, 2006).

Selection of history matching parameters are usually performed according to uncertainty. Listing of reservoir model input data from most reliable to least reliable will form an hierarchy of uncertainty which will help guide what parameters to adjust during history matching. Uncertainty depends on multiple factors, such as quality of the aquired data, how it was sampled and interpretation of data to mention a few. Changes should be kept to those parameters with the highest degree of uncertainty, as listed in the hierarchy of uncertainty (Fanchi, 2006; Carlson, 2006). Adjustments performed on the most uncertain parameters are believed to result in the most geologically consistent history matches. Mattax and Dalton (1990) has listed (Table 2.4.1) reservoir and aquifer properties appropiate for alteration during

history matching in order of decreasing uncertainty. This means that properties at the top should normally be altered first. Aquifer data is considered the most uncertain, arising from a lack of data because oil companies seldom drill into the water zone.

Table 2.4.1 – History matching parameters in order of decreasing uncertainty (Mattax and Dalton, 1990)

1. Aquifer transmissibility, kh
2. Aquifer storage, φhc_t
3. Reservoir permeability thickness, kh
   - Includes vertical flow barriers and high conductivity streaks
   - Permeability anisotropy, k_v/k_h
4. Relative permeability and capillary pressure functions
5. Porosity and thickness
6. Structural definition
7. Rock compressibility
8. Oil and gas properties (PVT)
9. Fluid contacts, WOC and GOC
10. Water properties

Points 1 through 3 in Table 2.4.1 are the most used history matching parameters. This is because the remaining points are usually fairly known to geoscientists and reservoir engineers from well logs, SCAL, fluid sampling, pressure profiles and seismic surveys. Many more than those history matching parameters listed in Table 2.4.1 exist. In general, history matching parameters can be divided in two; those that affect volumetrics and those that affect fluid flow. An overview of what history matching parameters affect volumetrics and fluid flow are listed in Table 2.4.2. Uncertainty in volumetric parameters such as pore volume, aquifer properties, compressiblity, compartmentalization and fluid distribution can effectively be addressed and reduced from material balance calculations and decline curve analysis (Fanchi, 2006; Gilman and Ozgen, 2013).

Table 2.4.2 – History matching parameters affecting volumetric or fluid flow (Gilman and Ozgen, 2013)

Volumetric Parameters	Fluid Flow Parameters
Compartmentalization	Flow barriers (vertical and lateral)
Fluid contacts	High-permeability streaks
Drainage capillary pressure curve and endpoints	Conductive faults
Pore volume	Permeability distribution
Aquifer properties	Fracture properties
Leakage (fluid loss)	Porosity distribution
Fluid influx	Matrix-fracture exchange
Pore volume compressibility	Saturation function endpoints
Fluid composition distribution	Imbibition capillary pressure curves
PVT properties	Relative permeability curves

Fluid flow parameters such as the presence, extent and distribution of flow barriers and high-permeability streaks will almost always need to be adjusted during history matching. This is because geostatistics are having problems distributing and populating correct values for these properties as they are usually in each end of the permability scale, several standard deviations away from the mean, hence less probable to be correctly distributed (Gilman and Ozgen, 2013). Previous analysis will probably indicate locations where effort should be focused on addressing this issue.

It might be useful to perform a simulation run of the initial reservoir model to assess what history matching parameters needs to be adjusted in order to resolve the mismatch between model performance and historical performance. Since modifications made to history matching parameters needs to be consistent with the geological and reservoir description it is important that a span on uncertainty is determined for all parameters prone to change. Once a set of history matching parameters with a given range for adjustments are selected the actual history matching process will begin.

2.5 MANUAL HISTORY MATCHING

Manual history matching is the process of history matching a reservoir model based exclusively on manual perturbations to preselected history matching parameters. There exist no standardized method of how to conduct a manual history match and the approach will usually vary from engineer to engineer (Gilman and Ozgen, 2013). Manual history matching requires that the reservoir model is run the entire historical period to establish a comparison of the model to the known performance of the field. Once differences has been established the reservoir engineer can adjust simulation data in order to improve match (Ertekin, Abou-Kassem and King, 2001). The adjustments made will be applied in a trial and error fashion and relies heavily upon intuition and experience. For every adjustment the simulation model will have to be rerun and the resulting model performance assessed. Experience is valuable since it increases the understanding of reservoir mechanics and allows one to identify possible changes that might improve the match (Mattax and Dalton, 1990; Gilman and Ozgen, 2013).

It is imparative that manual history matching requires a good understanding of the field which is to be matched. Thorough studies of the field needs to be undertaken before initiating a history matching process because the time used to obtain a match may be severly prolonged if the personnel performing the matching does not fully understand the processes

taking place within the reservoir (Ertekin, Abou-Kassem and King, 2001). As described in Chapter 2.4 it is important to determine the history matching parameters with their respective range of uncertainty in order to perform perturbations which are consistent with geological, petrophysical and geophysical interpretations (Gilman and Ozgen, 2013). An important step in the early phase of history matching is to establish a criteria which the acceptability of the model will be judged by (point 3 in Table 2.1.2). This is to avoid the conundrum of when to stop the history match because a better match to the exact solution will almost always exist.

A general approach is to split the manual history matching process in two, a gross matching phase and a detailed matching phase. The purpose of the gross phase is to match average pressure levels and ensuring that the correct fluid volumes are withdrawn from the model. During the detailed phase focus is to match individual well performance according to preselected historical performance data and matching criterias (Ertekin, Abou-Kassem and King, 2001). The two stages, gross and detailed, will be described in more detail below.

2.5.1 GROSS MATCHING PHASE

The gross matching phase, or pressure matching phase, is concerned with matching the average reservoir pressure, regional pressure gradients and well pressures through time. The most commonly adjusted reservoir parameters affecting the pressure match are listed in Table 2.4.2 under volumetric parameters and includes aquifer size and connectivity, pore volume and system compressibility. If problems are experienced during matching of the average reservoir pressure it is possible that the initial volumes of fluids in place were wrong. Simple material balance calculations can be performed to reduce uncertainty and improve match to these parameters (Ertekin, Abou-Kassem and King, 2001). In case problems of matching pressure persist it is a chance that the starting model is not properly characterized (Chapter 2.2), requiring revision together with geologists and geophysicists. It is important that while history matching the model, one should not be afraid to go back to the static geomodel and change reservoir description as new knowledge is obtained from history matching (Gilman and Ozgen, 2013).

The main purpose of matching pressure is to ensure that the volumetrics of the reservoir are correct, also mentioned in Chapter 2.5. For the purpose of matching pressure behavior of individual wells it may be better to constrain wells by voidage, rather than a specific phase rate. This way the correct amount of fluids will be removed, not necessarily the

correct phase volumes, and an average pressure match can more easily be obtained. It is important that changes made to volumes of fluid in place is consistent with estimates from sensitivity studies prior to the history matching process (Ertekin, Abou-Kassem and King, 2001). Especially stock tank oil initially in place (STOIIP) cannot be varied much since it is a parameter reported to governments, hence careful studies are needed to change this.

A quick look at differences in pressure distribution between model and field will help discover the presence of sealing faults, unconformities, pinchouts and poor reservoir communication. If major pressure gradients exist in the field it is suggested that pressure transient analysis can help estimate changes that will improve match. Permeability is the main parameter changed to establish more correct pressure gradients within the reservoir (Mattax and Dalton, 1990). Equation 2.5.1.1 gives the pressure response from a well at given time and radius. As seen from this equation permeability is the parameter most likely to be changed in order to adjust the pressure differential. An example of how permeability can be adjusted to correct pressure gradients in a reservoir model is illustrated in Figure 2.5.1.1. The actual pressure gradient (solid line) indicates less pressure drop between wells than that calculated from the model (dotted line). Hence, a multiplication of between well permeability similar to the ratio of pressure drop between the actual and calculated gradient will improve match. However, these changes may of course disturb the response from previous perturbations, thus some iterations may be required to improve match with the knowledge from gradient analysis (Ertekin, Abou-Kassem and King, 2001).

$$\Delta P = P_i - P(r,t) = -70.6 \cdot \frac{q\mu B}{kh}\left(Ei\left(-\frac{948\varphi\mu c_t r^2}{kt}\right)\right) \qquad \text{Equation 2.5.1.1}$$

Pressure distribution and discontinuities in the reservoir are in some cases possible to obtain from RFT surveys as described in Chapter 2.3.2 and illustrated in Figure 2.3.2.2. Focus should be to match early time well pressures to prevent errors from growing. However, if matching of well pressure progressively deteriorates it may indicate errors away from the well. Distance to the source of mismatch can be calculated using the concept radius of investigation. Equation 2.5.1.2 used to calculate the radius of investigation, the distance pressure waves have propagated in the reservoir during time of continuous production *t*, is derived from pressure transient theory (Ertekin, Abou-Kassem and King, 2001).

$$r_{inv} = \sqrt{\frac{kt}{948\varphi\mu c_t}} \qquad \text{Equation 2.5.1.2}$$

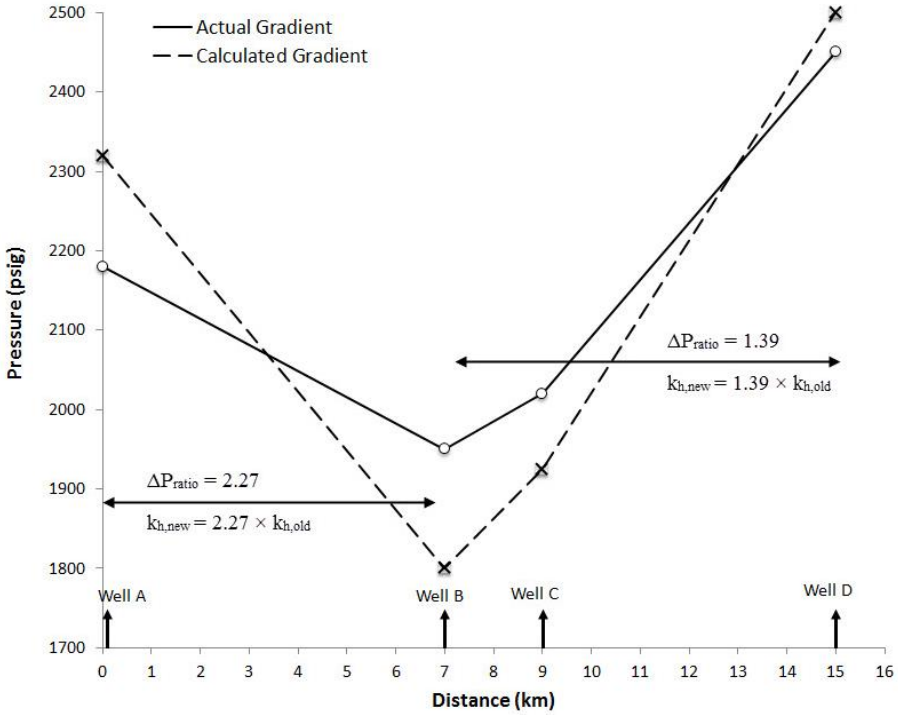

Figure 2.5.1.1: Difference between actual and calculated pressure gradients in a reservoir indicating that between well permeability is too low. Between well permeability is multiplied by a factor equal to the ratio of the actual and calculated pressure gradient (Mattax and Dalton, 1990).

2.5.2 DETAILED MATCHING PHASE

The detailed matching phase, or saturation matching phase, considers the matching of fluid movement. This includes matching production of oil, gas and water in addition to time of breakthrough and any other measurements available during the lifetime of the reservoir. The matching is performed on a well to well basis. It is difficult to obtain a match unless the reservoir model is reasonably complete and almost entirely consistent with the reservoir description, as described in Chapter 2.2 (Mattax and Dalton, 1990). However, it is still possible that certain wells cannot be matched, which may indicate casing-leak problems, tubing or other mechanical problems (Gilman and Ozgen, 2013).

It is obvious that the detailed matching phase may be frustrating to the practitioning engineer since changes applied to improve the match of fluid movement may affect the previously established pressure match (Ertekin, Abou-Kassem and King, 2001). To improve the efficiency of matching it is important to understand the major flow mechanisms in the

reservoir and identify the properties that are likely to influence the movement of oil, gas and water (Mattax and Dalton, 1990). Figure 2.5.2.1 illustrates an example of how water-oil ratio (WOR) was matched in a reservoir with coning. Initial simulations indicated that breakthrough times was too late compared with actual data. Permeability was increased such that coning was obtained with a good match in breakthrough time and WOR. In most reservoir models layers are relatively thick and high permeable layers may have been averaged with neighboring low permeability layers such that displacement efficiency is overestimated and breakthrough times estimated too late. Adding high permeable streaks can help match models that experience early breakthrough of water or gas.

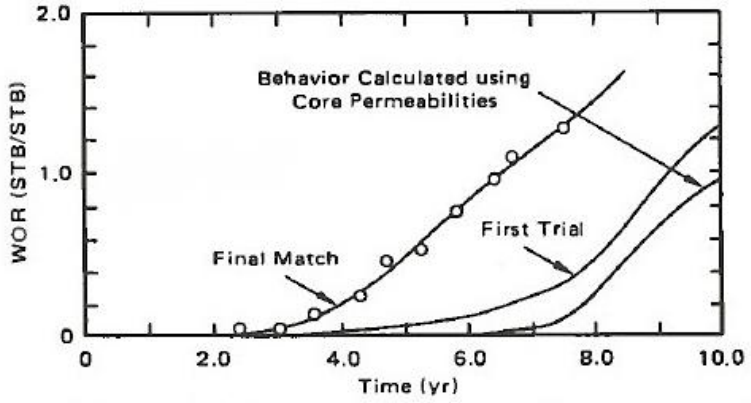

Figure 2.5.2.1: Reservoir model experiencing a poor initial match in WOR and time of breakthrough. When coning behavior was identified and added to the reservoir model the time of breakthrough was improved and a good WOR match obtained (Mattax and Dalton, 1990).

Parameters most often perturbed to obtain a saturation match are listed in Table 2.4.2 in the column *Fluid Flow Parameters*. It is not possible to generalize what parameters to change in order to obtain a match of fluid movement since every reservoir is unique. However, as was stated in Chapter 2.4 the best approach is to perturb parameters according to the hierarchy of uncertainty. Tools such as Buckley-Leverett, Stiles and Dykstra-Parsons analysis can help guide the history matching in the right direction as these analyses might indicate the required change in certain properties (Ertekin, Abou-Kassem and King, 2001). At the end of the detailed matching phase it is important to ensure that both pressure and saturation is matched according to the matching criterias set prior to the start of the history match.

Because perturbation of reservoir properties should be performed in the most geologically sound manner it is advised to avoid making localized near-well changes not consistent with the reservoir characterization. Ertekin, Abou-Kassem and King (2001) suggested an approach to minimize the use of localized near-well changes listed in Table

2.5.2.1. Following this systematic approach will ensure that changes preferentially are made globally before shifting to more localized changes. The selection where to apply changes, and what changes to apply, to improve match may not be a straightforward process and usually requires several iterations before an acceptable history match is established.

Table 2.5.2.1 – Order of how to apply changes to the reservoir model in the most geologically sound manner (Ertekin, Abou-Kassem and King, 2001)

Vertical adjustments	Areal adjustments
1. Global (all simulation layers)	1. Global (all grid cells)
2. Reservoirs (in fields made up of vertically stacked reservoirs)	2. Reservoir/Aquifer
3. Flow units within a reservoir	3. Fault blocks within a reservoir
4. Facies (in laminated reservoirs or flow units)	4. Facies (areal facies envelope)
5. Simulation layers	5. Regional
	6. Individual well

2.6 ASSISTED HISTORY MATCHING

Manual history matching is a tedious and time-consuming process as described in Chapter 2.5. Due to this much effort has been focused on automating the history matching process through the use of software assisted history matching techniques. Assisted history matching (AHM) techniques rely on non-linear optimizing techniques in order to achieve a best fit between observed and calculated data (Mattax and Dalton, 1990). During the use of AHM techniques perturbations are automatically performed by the software to predetermined history matching parameters within a given range of uncertainty. The AHM software then seeks to minimize an objective function (defined by the user), corresponding to finding the model with the least discrepancy between observed and calculated data (Mattax and Dalton, 1990; Rwechungura, Dadashpour and Kleppe, 2011).

AHM techniques follow the process illustrated in Figure 2.6.1. The starting point is selection of an initial reservoir model thought to be the most accurate representation of the reservoir (described in Chapter 2.2). After simulation of this model the response is used to calculate an objective function. The objective function (*OF*) defines the discrepancy between observed and calculated data and is commonly expressed with a least-square or weighted least-square formulation as given in Equation 2.6.1 and Equation 2.6.2 respectively. o_i and c_i express observed and calculated model response for given historical performance data at various points in time respectively, while W_i is a weighting factor used to put more or less importance on different data points (Mattax and Dalton, 1990; Rwechungura, Dadashpour and

Kleppe, 2011). Weights are also needed to scale data properly such that pressure differences are not more important than say water cut differences simply because of the magnitude of the numbers (Gilman and Ozgen, 2013). Observed data used in calculation of the objective function depends on historical performance data available with the most used types described in Chapter 2.3.

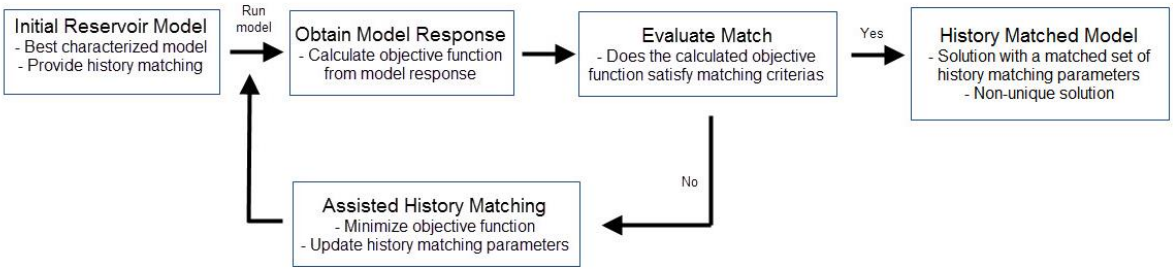

Figure 2.6.1: Workflow followed by AHM software.

$$OF = \sqrt{\sum (o_i - c_i)^2} \qquad \text{Equation 2.6.1}$$

$$OF = \sqrt{\sum (W_i \cdot (o_i - c_i)^2)} \qquad \text{Equation 2.6.2}$$

Once the objective function is calculated it is compared with matching criterias to assess if it is considered matched, if not the simulation model will need to be updated and rerun. Updates are made to predetermined history matching parameters with the goal of minimizing the objective function, hence to reduce discrepancy between observed and calculated data. If this process is to be successful the history matching parameters chosen prior to initiating AHM needs to be key inut parameters governing response of the model, described in more detail in Chapter 2.4. The selection of input parameters in AHM relies heavily on sensitivty analysis and experience, hence AHM will rely to some degree upon manual simulations. History matching parameters need to be specified with a minimum and maximum value to form a range for which the AHM software is allowed to vary the property within (Gilman and Ozgen, 2013). It is imparative that a large range of accepted values for history matching parameters and selection of multiple parameters will require large amount of simulations to minimize the objective function. Consequently effort should be focused on having a smoothly running model with short run times to speed up the AHM process. In most cases AHM is only used with a small set of history matching parameters as large amounts of variables makes it computationally difficult to converge to a clear solution. Due to this AHM is most often used

early in the history matching process, corresponding to the gross matching phase described in Chapter 2.5.1, since only a few global parameters are sensitized to isolate certain parameters (Gilman and Ozgen, 2013). AHM is also applicable in the late phase of history matching when the value range of parameters is narrowed and only slight tuning is needed. A major advantage of AHM is its ability to find several equiprobable solutions.

History matching parameters are updated differently depending on the applied AHM technique. This is because the AHM techniques utilize various minimization algorithms for improving the objective function. An overview of the most commonly used methods for AHM are listed in Table 2.6.1, further description of the methods will not be given as this thesis deals with manual history matching. The process of updating history matching parameters to minimize the objective function continues until the objective function is lowered to within the matching criteria, assuming that changes made to the model are realistic.

Table 2.6.1 – Methods for AHM
• Gradient Decent Methods • Experimental Design • Response-Surface Modeling • Parametric Methods • Ensemble Kalman Filters (EnKF) • Artificial-Intelligence Methods • Hybrid Methods

AHM is usually less time-consuming than manual history matching. However, the history matching process will never be completely automated due to the fact that it s not a process that can easily be put into a linear process free of subjective judgements from the engineer performing the history match. For instance, in manual history matching the quality of a match is dependent on visual inspection and comparison of calculated model response with historical performance. Considering Figure 2.6.2, it is obvious that manual history matching would consider Model 1 superior to Model 2 since the trend is good but time of breakthrough is too early. AHM software would consider Model 2 the best since this respresents a lower value in the objective function. It is obvious that engineering judgement would assist AHM software in this case and that the engineer is able to apply both experience and intuition to improve the history match. AHM supplies a strict mathematical solution to the history matching problem based on the definition of the objective function. It is obvious that some engineering judgement is needed, which cannot be replaced by optimization algorithms in various AHM software, however AHM is of great help when narrowing down

uncertainty of history matching parameters and holds the potential of reducing workload significantly (Gilman and Ozgen, 2013).

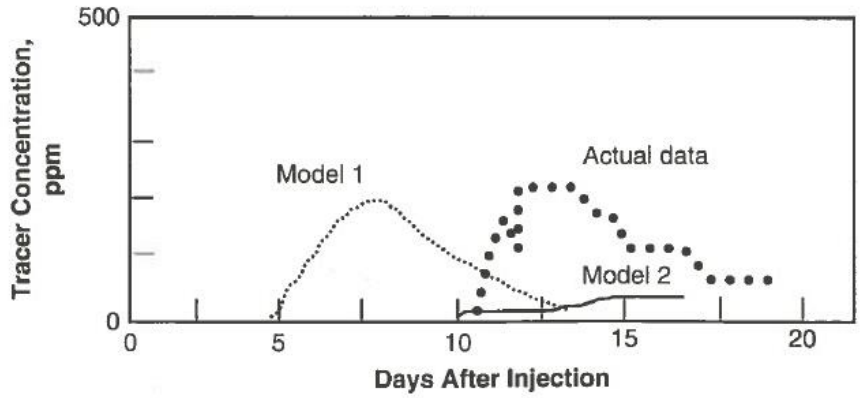

Figure 2.6.2: Two reservoir models with a large difference in response. It is obvious that Model 1 is the best match if trend is considered because if Model 1 is shifted forward in time it will match the actual data better than Model 2. However, Model 2 will have a lower value of the objective function than Model 1 and will be the best model according to AHM software unless Model 1 is shifted in time (Gilman and Ozgen, 2013).

2.7 USE OF GEOSTATISTICS DURING HISTORY MATCHING

Geostatistics are used to build high resolution geocellular models and its role during model building is seen from Figure 2.7.1. Caers (2005; p. 7) gives the following general definition of geostatistics: ”In its broadest sense, geostatistics can be defined as the branch of statistical sciences that studies spatial/temporal phenomena and capitalizes on *spatial relationships* to *model* possible values of variable(s) at unobserved, unsampled locations.” Figure 2.7.1 illustrates the population of facies and petrophysical properties according to spatial relationships derived from geological studies and measured well data. Geostatistics are restricted from geologic continuity and measured data when populating properties and will always constrain values to within a given range. Hence generated properties from geostatistics will remain realistic according to interpretations of the subsurface.

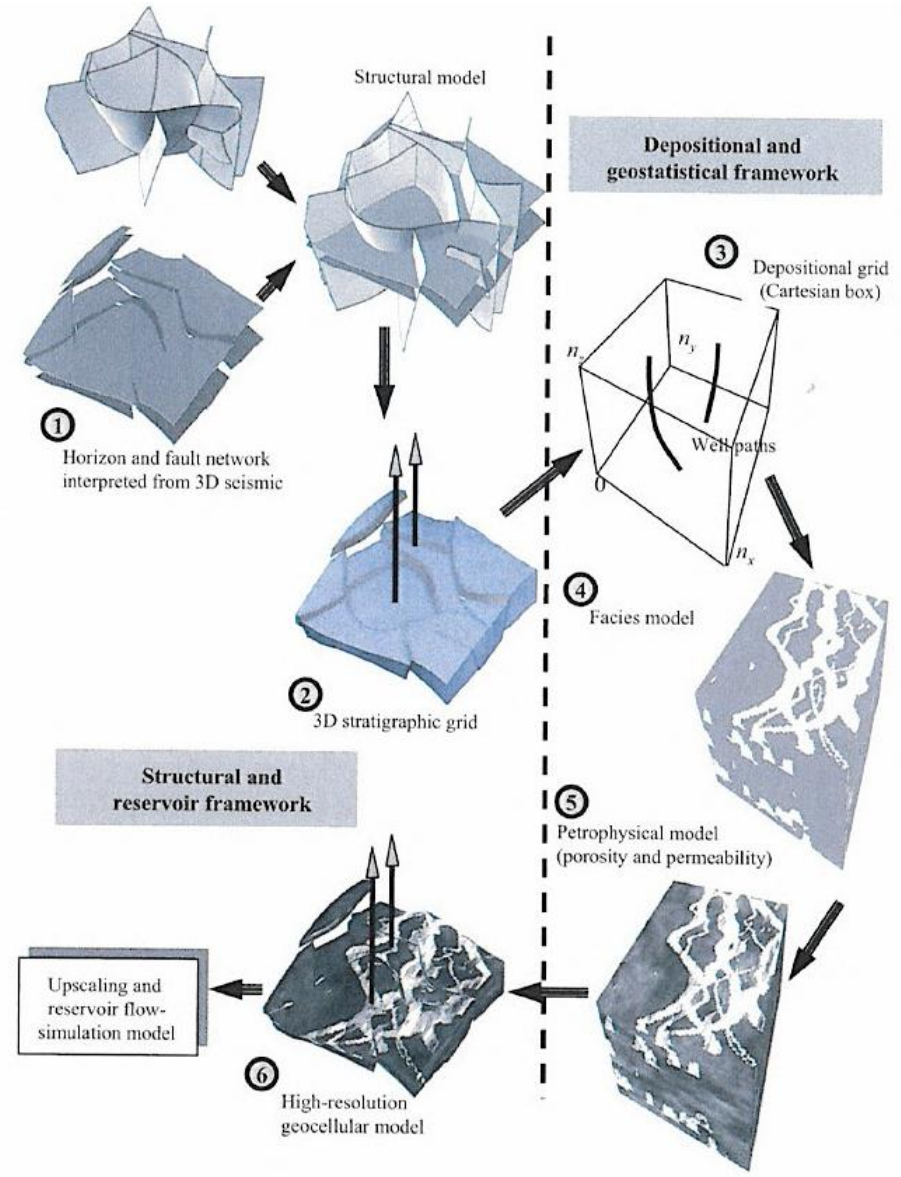

Figure 2.7.1: Stepwise workflow for building geocellular models with the role of geostatistics highlighted to the right (Caers, 2005).

As has been mentioned several times throughout this chapter, the goal of history matching is not just simply to obtain a match of dynamic data, but rather to produce models capable of predicting future reservoir performance to within some accepted tolerance. To do this it is necessary to reflect the subsurface heterogeneities as realistically as possible and to avoid making changes to the reservoir model that doesn't correspond with the geological continuity (Caers, 2005). During manual history matching changes can simply be made to the model which are not in accordance with the current reservoir characterization. By applying geostatistics in the history matching process it is possible to provide a geological constraint, allowing us to avoid unrealistic changes to the model. The geological constraints imposed by introducing geostatistics in the history matching process provides restrictions on perturbations

made to obtain a match. Restrictions could be either a permeability variogram or an object-based model with a seismic derived facies probability cube to mention but a few (Caers, 2005).

There is much to be said about geostatistics and how it is applicable in reservoir simulation, however focus here will be on the role and implementation of geostatistics during history matching. Two methods of how geostatistically constrained history matching is performed will be described briefly below. An illustration of the workflow in these two methods are given in Figure 2.7.2.

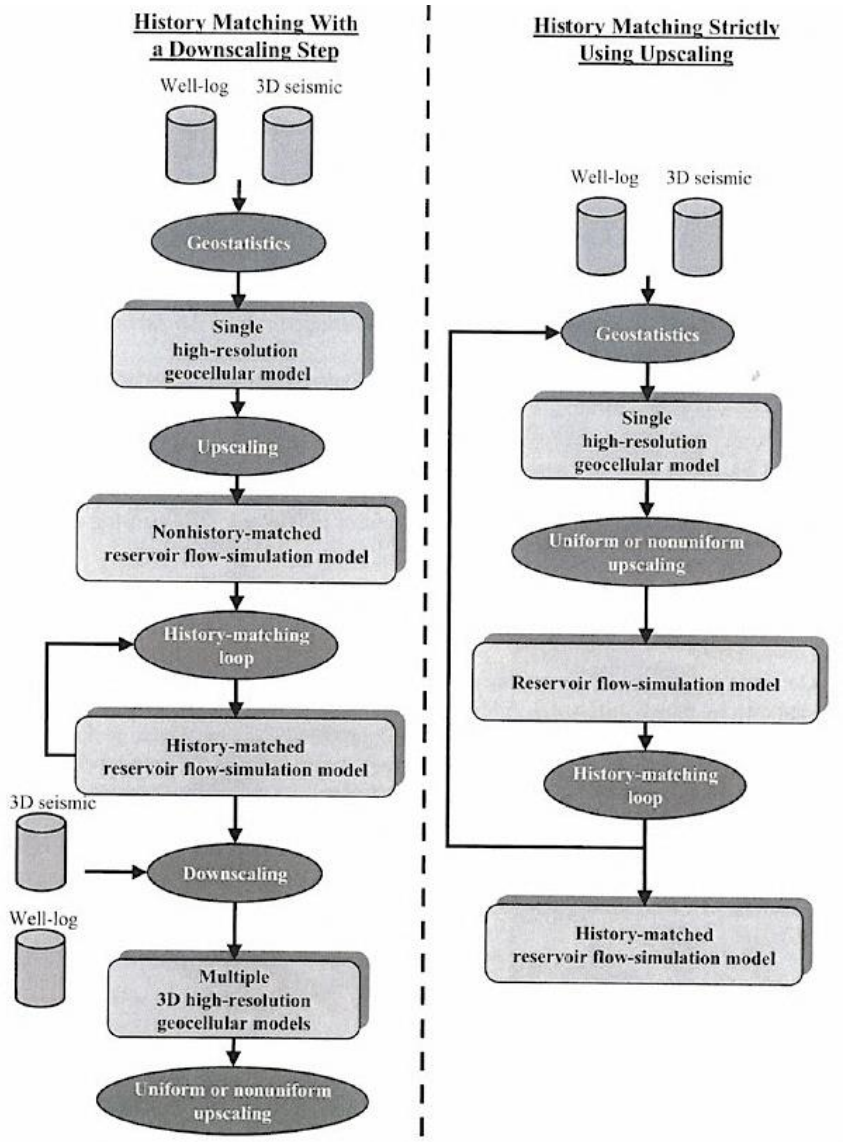

Figure 2.7.2: Workflow for geostatistically constrained history matching using two methods, history matching with a downscaling step (left) and history matching strictly using upscaling (right) (Caers, 2005).

2.7.1 HISTORY MATCHING USING A DOWNSCALING STEP

If dynamic data such as pressure and production is to be incorporated within the geocellular model flow simulations will need to be performed. Flow simulations are CPU-intensive and most often not feasible on high resolution geocellular models leading to the need for upscaling. Upscaling is performed to the geocellular model once it is deemed ready to incorporate dynamic data. The upscaled model is termed the initial model, or basecase model, and does not match historical performance data. Hence, the need for history matching. An iterative history matching loop is followed (Figure 2.7.2) where the model is simulated, compared with historical performance data and properties perturbed in order to minimize discrepancy. This process is similar to the manual history matching process described in Chapter 2.5. The iterative history matching loop results in a single matched model which then is downscaled into multiple (equiprobable) geocellular models. The reasoning for downscaling the history matched model is to reintegrate any fine-scale observations and establish geological continuity that might have been lost during history matching since the history matching was performed without explicit consideration of the seismic and well-log data used to construct the initial high resolution geocellular model (Caers, 2005). After downscaling has established geological continuity to the model it is upscaled to allow prediction of reservoir performance. The upscaled model created from one of multiple downscaled models doesn't neccessarily still match historical performance data, in this case another iteration of upscaling must be performed or another of the downscaled models should be upscaled.

Downscaling reservoir models consists of generating a high resolution model from coarse data. This process is shown in Figure 2.7.1.1 and highlights that several equiprobable high resolution models emanate from downscaling. Hence, downscaling is not unique and because several high resolution geocellular models are created an additional uncertainty to what model to use is created (Caers, 2005). During downscaling the high resolution geocellular model is constrained from both data points and a geological continuity model, illustrated in Figure 2.7.1.1. In this figure porosity is supplied as point data while two different geological continuity models (training image based and variogram based) are used to obtain several downscaled models. All are seen to match the supplied point data of porosity. The geological continuity model is represented by geostatistics. Further details of downscaling algorithms will not be covered here, for this the reader is advised to look up in the literature.

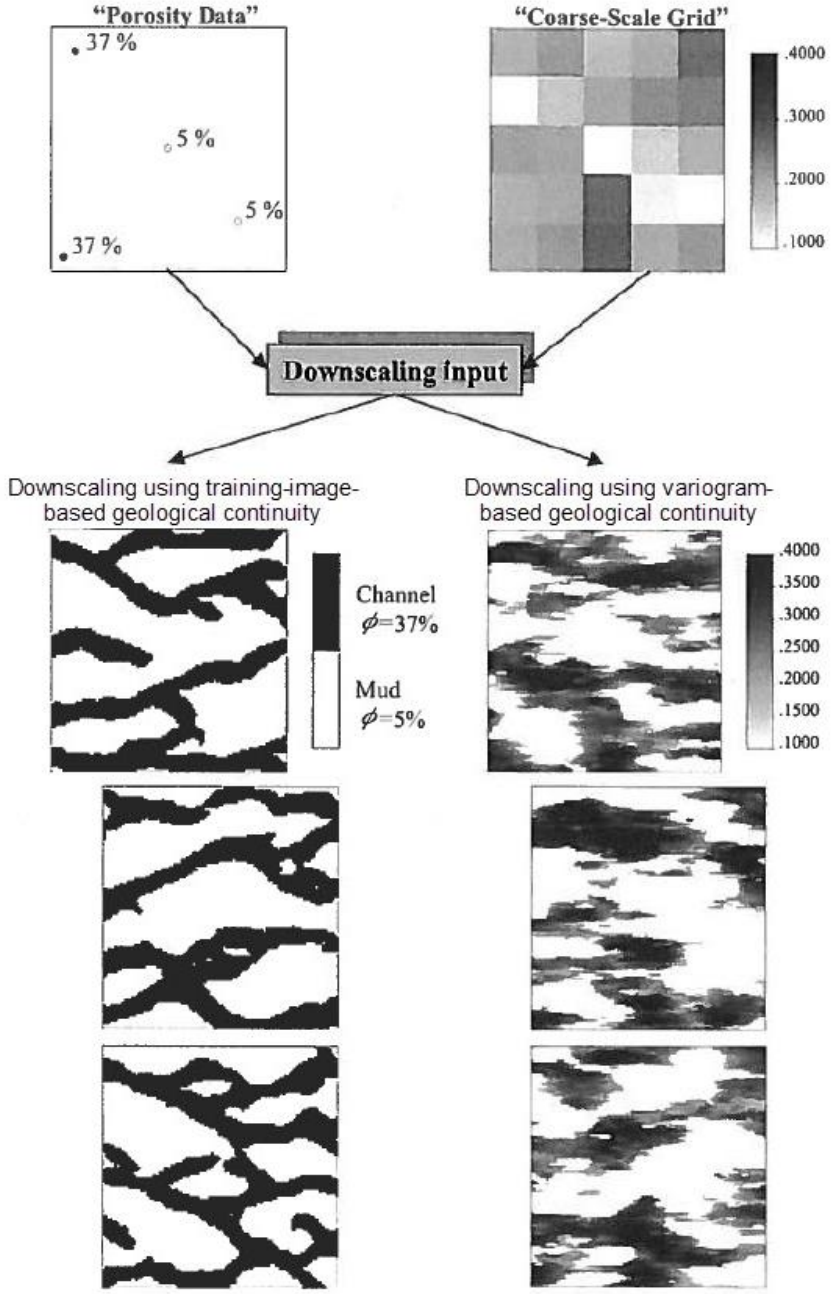

Figure 2.7.1.1: Downscaling a coarse 5x5 grid of porosity with different geological continuity models, training-image-based (left) and variogram-based (right). Several equiprobable downscaled models are obtained and they all match the supplied porosity data points (Caers, 2005).

History matching using a downscaling step involves two obvious pitfalls. Firstly, the inability of the upscaled model to model fine-scale geological flow conduits or barriers. Depending on the effect they have on reservoir flow this might result in an unsuccessful history match as the main flow mechanisms will not be captured in the model. Secondly, the downscaled model does not neccessarily match history anymore since fine-scale heterogeneity is reinstated. This prolongs the matching as another upscaling iteration will need to be performed (Caers, 2005).

2.7.2 HISTORY MATCHING STRICTLY USING UPSCALING

The history matching strictly using upscaling circumvents the limitations of downscaling mentioned in Chapter 2.7.1. Figure 2.7.2 illustrates the workflow when history matching strictly using upscaling. It is similar to the downscaling method in that a most realistic high resolution geocellular model is created and upscaled in order to allow flow simulations. The history matching procedure is slightly different since perturbations are performed directly on the high resolution geocellular model, rather than on the upscaled model. The perturbed geocellular model is then upscaled to perform flow simulations from which results are compared with historical performance (Caers, 2005). The history matching process is iterated until the model is satisfactorily matched.

Because perturbations are performed directly on the high resolution geocellular model which incorporates geological, well and seismic data, the history matching will have explicit control over geological consistency and data conditioning. However, geological consistent perturbations are needed to maintain geological consistency. If properties are perturbed without regard to the underlying geological continuity there is a possibility that the realism of the initial reservoir characterization and model is lost. Two methods of ensuring geological consistency when perturbing properties is probability perturbation and gradual deformation (Caers, 2005). The probability perturbation approach will be used as an example on how perturbations can be made geologically consistent. With the probability perturbation, changes are made to the probability distribution used to generate grid block properties, rather than changing grid block properties directly. Property maps created from sequential simulation methods are created according to a given probability distribution. The probability perturbation approach avoids making changes to the component controlling geological continuity and the amount of perturbation is controlled by a perturbation parameter *r*. This parameter, *r*, can be varied between 0 and 1, where 0 results in no change and 1 equals a completely new realization (Caers, 2005). Figure 2.7.2.1 illustrates how permeability is changed using various values for *r*. Notice that geological continuity is kept for all values of *r*, even for the value 1 which equals a completely new equiprobable realization of the geocellular model.

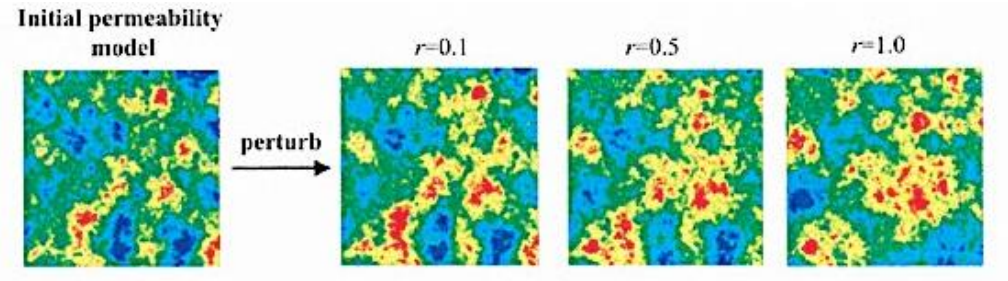

Figure 2.7.2.1: Perturbation of a permeability model using the probability perturbation method with various values of the perturbation parameter r governing the amount of perturbations performed to the model. When r equals 1 a new equiprobable realization is created (Caers, 2005).

Imparative for this method to be of any use is that upscaling errors, such as grid orientation effects or numerical dispersion, are small. This is because the upscaled model should have similar flow response as the high resolution geocellular model which has been perturbed. It doesn't make much sense to perturb the high resolution geocellular model to accurately reflect the geological continuity which is governing reservoir flow performance if this is missed in the upscaled model (Caers, 2005).

2.8 HISTORY MATCHING IN ECLIPSE 100

History matching of the Jette field will be performed using the commercially available reservoir simulator ECLIPSE 100 from Schlumberger. ECLIPSE 100 is considered the industry standard, however several other commercially available reservoir simulators exist. A description of ECLIPSE 100 and its capabilities is given in Appendix A. This section will give a brief description on how to perform history matching using ECLIPSE 100.

ECLIPSE 100 is constructed to operate wells in either historical or predictive mode. During historical mode wells are constrained by a set of historical data provided and entered in the simulator by the user. When the model runs constrained by given historical performance, remaining phases, pressures and production ratios are calculated by the simulator according to mobility ratios as described in Chapter 2.3. Historical data is entered using keywords WCONHIST and WCONINJH for production and injection wells respectively. Table 2.8.1 lists the various types of historical performance data that can be specified to constrain production and injection wells. Even though wells are constrained by only one type of historical performance data ECLIPSE 100 allows the user to enter all available historical performance data (restricted to types listen in Table 2.8.1). In this way historical production data will be written to the summary file and available for direct

comparison with the calculated reservoir performance of the reservoir simulator when plotted in a post-processing software (ECLIPSE Reference Manual, 2012). Calculation of THP requires specification of a VFP-table together with an artificial lift quantity specifying gas lift or any other type of artificial lift if present. The WCONHIST/WCONINJH keyword specifying historical data must be entered in the simulation data-file at every timestep data exist.

Table 2.8.1 – Historical performance data compatible with ECLIPSE 100 (ECLIPSE Reference Manual, 2012)

Production Wells	Injection Wells
Oil production rate	Oil injection rate
Water production rate	Water injection rate
Gas production rate	Gas injection rate
Liquid production rate	BHP
Reservoir voidage production rate	THP
BHP	
THP	
Artificial lift quantity	

The option of specifying reservoir voidage production rate is especially helpful during the gross matching phase (Chapter 2.5.1) since it ensures that the correct amount of fluid is withdrawn from the model. This way average reservoir pressure trends can be matched and help establish more correct volumes of fluid in place if deviations exist (ECLIPSE Reference Manual, 2012).

Changes needed to improve match can easily be made to the simulation model in ECLIPSE 100 during history matching. It can be applied either directly in the data-file using ECLIPSE 100 syntax or the model can be imported and updated using Petrel. Petrel is a shared earth software from Schlumberger, compatible with ECLIPSE 100, used to integrate the different disciplines involved in building, interpreting and updating reservoir models. It is recomended to update the simulation model using Petrel as this software offers more advanced options of making changes to the grid as compared with manual edits in the data-file. Petrel also lets the user visualize new property maps enabling better overview and quality control of inconsistencies in grid properties. However, changes using permeability or fault multipliers directly to the data-file in ECLIPSE 100 can be applied quickly to help speed up the matching process before applying the final changes in the updated simulation model in Petrel. This process will be followed during the matching of Jette and is described in detail in Chapter 7.

2.9 RESERVOIR PERFORMANCE FORECASTING

When a reservoir model is sufficiently history matched it is believed to model the reservoir more realistically and be able to predict future reservoir performance with greater accuracy than a reservoir model which has not been matched. Hence, the objective of history matching is to provide a model capable of predicting future reservoir performance under various operational scenarios to reduce uncertainty and answer questions related to optimal reservoir management (Gilman and Ozgen, 2013). The following discussion will give a short introduction to reservoir performance forecasting.

Reservoir performance forecasting is conducted on either green-field or brown-field reservoir models. Green-field models are described as young reservoirs with a limited amount of information and historical performance data. These models exist in early field life and is not matched or calibrated with historical performance data. Brown-field models are the opposite to green-field models and incorporate more information, often obtained after the field has been developed. Calibration and additional information is usually added during history matching. Hence, brown-field models are usually less uncertain than green-field models and are preferred when performing more detailed reservoir performance optimization and forecasting studies (Gilman and Ozgen, 2013).

Reservoir performance forecasting requires specification of a basecase. The basecase is established in order to compare reservoir performance under various operational scenarios. It is common to specify the basecase as a ”do-nothing” case where the future reservoir performance is simulated with the current reservoir management strategy. In other words, allowing the reservoir to produce at the current operating conditions (Ertekin, Abou-Kassem and King, 2001; Mattax and Dalton, 1990). When a basecase has been selected it is possible to specify and run various scenarios which is compared with the production from the basecase. Types of scenarios include drilling and placement of new wells, workover scheduling, facility upgrade planning, secondary and tertiary recovery planning and injection rate optimization (Gilman and Ozgen, 2013). Comparing various operational scenarios with the basecase will yield the incremental increase in oil or gas production resulting from the applied change in the subject scenario. It is recommended to change only one variable for each production scenario in order to isolate the effects from the change in the model (Ertekin, Abou-Kassem and King, 2001). If an incremental increase in production is large enough it may help justify application of the investigated operational scenario. Even though production forecasts will help evaluate the economics of expensive operations in order to enhance

production it is important to take model uncertainties and assumptions into account when making decisions about future reservoir management strategies.

There are a few things to consider when setting up simulations for performance forecasting. If performance forecasting is performed with a history matched model it requires new well specifications and well constraints. During history mode the model was constrained from specified historical performance, most often production rate (as described in Chapter 2.3.1). During predictive mode it is common to specify wells to operate at a given THP because pressure is most often kept constant at the separator inlet, hence it will be almost constant at the tubinghead as well. In order to make performance forecasts specifying THP to guide wells it is important that VFP-tables representing tubing performance is supplied to the simulator. Even though wells may be specified to operate at a given THP several well constraints can be specified, such as a maximum flow rate or minimum BHP. If any of these limits are reached the simulator will change well specifications so that they are constrained by the worst offended limit. When changing from history mode to prediction mode in a simulator there is a possibilty that an abrupt change in production performance will arise (Figure 2.9.1). This is most likely due to BHP and THP not being tuned during history matching (Gilman and Ozgen, 2013). The transition from history mode to prediction mode should be smooth and if a discontinuity as shown in Figure 2.9.1 exists this may be alleviated by tuning of well indices (well geometric factor). This process is known as calibration of wells and assumes that the only unknown is the near-well pressure drop (Gilman and Ozgen, 2013; Ertekin, Abou-Kassem and King, 2001). Figure 2.9.1 illustrates how well indices can be adjusted by reducing inflow performance in order to obtain a smooth transition from history mode to prediction mode. If changes are made to well indices it is important that the history match is checked in order to control that a change in well indices doesn’t affect the previously obtained history match.

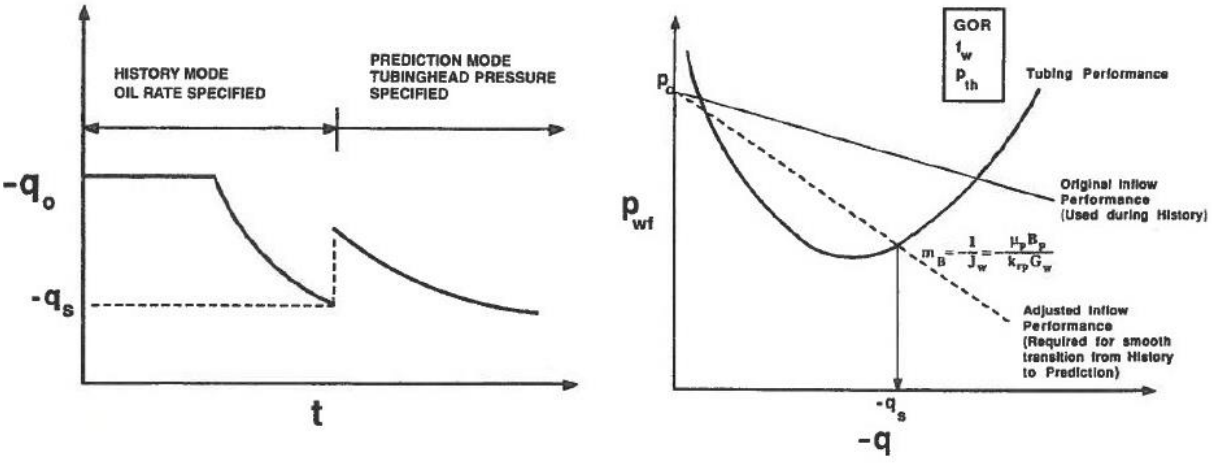

Figure 2.9.1: Transition from history mode to prediction mode with an abrupt change in oil production (left). Calibration of wells for a smooth transition can be performed by editing the inflow performance of the well (right). The dotted line in the right figure illustrates the required reduction in inflow performance of the well to transition smoothly from history mode to prediction mode (Ertekin, Abou-Kassem and King, 2001).

When conducting reservoir performance forecasts it is important that all available information is incorporated in order to create a prediction which is as realistic as possible. In addition to ensuring that the reservoir model is realistic factors such as unforseen political events, regularity of the field and human bias needs to be assessed. This is because most predictions are optimistic, they predict too high oil (or gas) production (Rajvanshi, Meyling and Haaf, 2012). Since most field developments are based on predicted production from reservoir models this may pose a threat to the economics of marginal fields if forecasted production is not met. Differences between forecasted production and actual production can be caused by a variety of reasons, listed in Table 2.9.1. Figure 2.9.2 illustrates the reasons for mismatch between predicted and actual performance listed in Table 2.9.1.

Table 2.9.1 – Possible reasons for differences between actual reservoir performance and predicted reservoir performance (Rajvanshi, Meyling and Haaf, 2012)
• Delay in production start-up. • Less rapid ramp-up because of inaccurate estimates about time of drilling. • Lower peak rates due to reservoir quality assumed too high. • Failed to incorporate important reservoir heterogeneities causing early breakthrough . • Inaccurate estimates and consideration of well regularity. • Steeper decline in production due to idealized assumptions about reservoir connectivity, pressure support and flood conformance. • Earlier cut-off due to problems with production together with economical considerations.

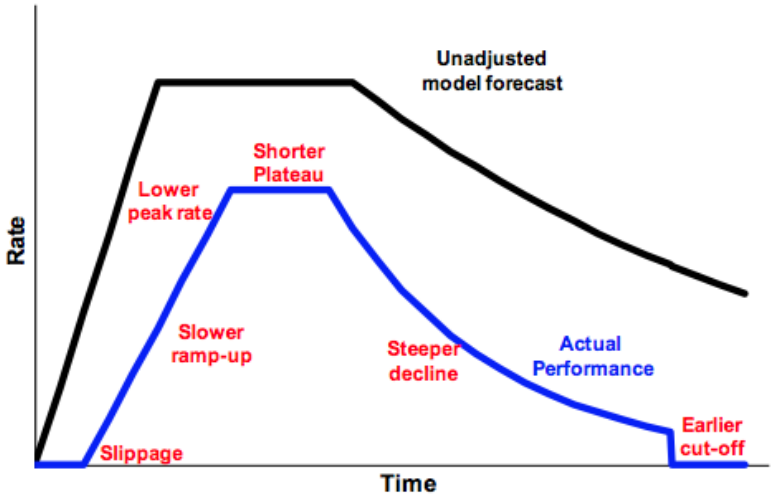

Figure 2.9.2: Possible reasons for differences between actual reservoir performance (blue line) and predicted reservoir performance (black line) (Rajvanshi, Meyling and Haaf, 2012).

3 THE JETTE FIELD

History matching of reservoir simulation models relies heavily upon understanding of the field and reservoir to be matched. This chapter will give a comprehensive introduction to the Jette Field. Parts of this chapter are based upon project work undertaken by the author during the fall of 2013 (Lorentzen, 2013) at the Norwegian University of Science and Technology (NTNU).

3.1 INTRODUCTION

The Jette field, former Jetta, is located in the north sea within production licences PL 027D, PL 169C and PL 504. The licences are part of blocks 25/7 and 25/8 which are part of a mature area on the norwegian continental shelf (NCS). The Jette Field is a small oil accumulation approximately six kilometers south of the Jotun field operated by ExxonMobil and was discovered by two exploration wells, 25/8-17 and 25/8-17A in october/november 2009 (Det norske oljeselskap ASA, 2011a; Lorentzen, 2013). The location of Jette can be seen from Figure 3.1.1.

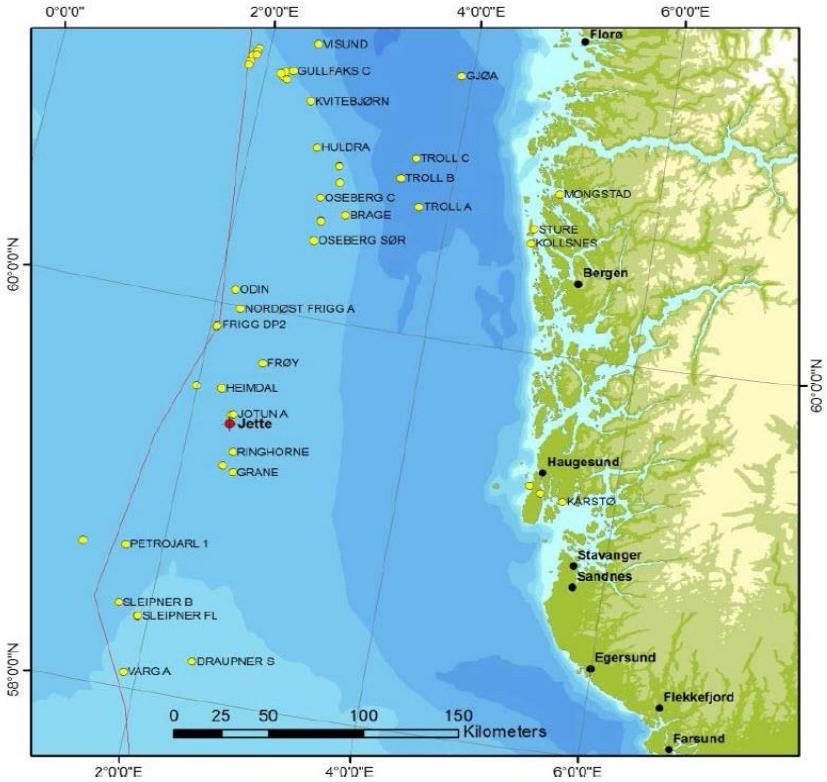

Figure 3.1.1: Location of the Jette field (Det norske oljeselskap ASA, 2013b).

The original licensees were Det norske oljeselskap ASA, Dana Petroleum AS, Bridge Energy Norge AS and Petoro AS. Bridge Energy Norge AS and Dana Petroleum AS backed out when Det norske oljeselskap ASA recommended to proceed with Plan for Development and Operations (PDO) in April 2011. Jette was devoloped by Det norske oljeselskap ASA and Petoro, respectively having 70% and 30% licence share, and is currently being produced from two horizontal standalone wells tied back to Jotun (Det norske oljeselskap ASA, 2011a; Lorentzen, 2013).

3.2 DEVELOPMENT OF JETTE

Oil was first discovered in 2009 from well 25/8-17. It showed a 27 meter oil column in the Heimdal formation at a vertical depth of 2100 meters. The amount of estimated reserves in place fell short of the licensees expectations. However, due to its proximity to Jotun it was decided to develop Jette (Det norske oljeselskap ASA, 2011a). The Jette field was developed with two satelite wells tied back to Jotun which is located six kilometres north of Jette. A schematic of the tie-back with Jotun can be seen in Figure 3.2.1 (Lorentzen, 2013).

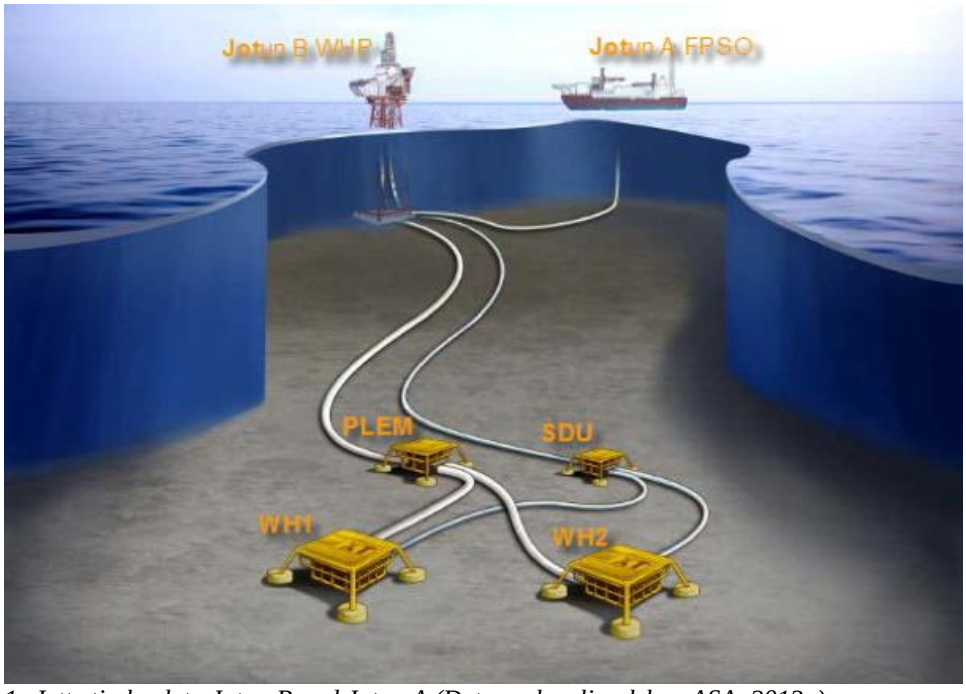

Figure 3.2.1: Jette tie-back to Jotun B and Jotun A (Det norske oljeselskap ASA, 2013a).

Development was performed as a fast-track project due to the requirement for tie-back with Jotun in order for Jette to be commercially viable. Jotun has produced oil since 1999 and is

currently in a late tail production. Due to this it was important that Jette would be developed and tied back to Jotun as fast as possible if reserves at Jette are to be produced before Jotun is plugged and abandoned. Jotun had a scheduled stop in production during the summer 2012 and connection from Jette was successfully established during this stop. The oil from Jette was found to be similar in composition to the produced oil from Jotun which made requirements for storage and processing easier. The Jette production stream is mixed with production from Jotun at the Jotun B platform before being transfered to the Jotun A FPSO where the oil is processed and stored. The gas will be processed and exported via the Statpipe System. Production from Jette started in May 2013 (Det norske oljeselskap ASA, 2011a and 2013a; Lorentzen, 2013).

3.3 GEOLOGY

Jette produces from the distal parts of the Paleocene Heimdal Formation. This is part of the same formation as the Tau West structure produced at Jotun (Det norske oljeselskap ASA, 2011a). Jette is structurally downfaulted from the Utsira High and is a combination of a structural trap to the west and a stratigraphical trap to the south and east pinching out towards the main NE-SW fault (Det norske oljeselskap ASA, 2013a, Lorentzen, 2013). The trap configuration together with indication of possible faults can be seen from Figure 3.3.1. It is believed that a fault located to the north isolates Jette from the close by Tau reservoir at Jotun. Even though Figure 3.3.1 indicate several potential faults, there is a high degree of uncertainty related to the existence of these faults (Lorentzen, 2013).

The Heimdal Formation is part of the Rogaland group. Apart from the Heimdal Formation, Rogaland consists of Balder, Sele, Lista and Ty Formations. The lithologies include claystone, tuffaceous claystone, sandstone, siltstone and occasional limestone stringers (Det norske oljeselskap ASA, 2010). The lithostratigraphy performed at Jette is based on cuttings and divisions are based on major lithological changes, LWD and offset well correlations. Heimdal which is the main reservoir zone is characterized to contain sandstone, claystone layers, minor siltstone interbeds and some limestone stringers. The sandstone grain size is predominantly fine to medium with some locally calcareous cement. A shale in the Lista Formation, which predominantly consists of claystone and siltstone, forms the sealing cap rock (Det norske oljeselskap ASA, 2010).

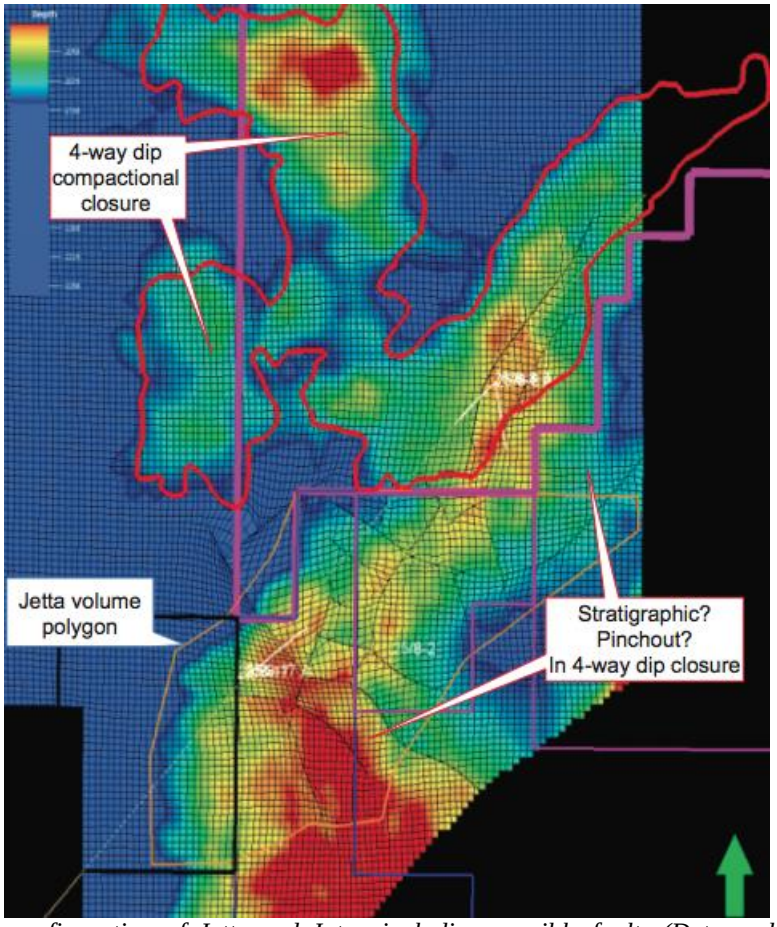

Figure 3.3.1: Trap configuration of Jette and Jotun including possible faults (Det norske oljeselskap ASA, 2011b).

Five facies types have been identified at Jette. These are Low Density Turbidite (LDT) sands, High Density Turbidite (HDT) sands, black shale, E-sequence (a type of mud) and calcite. No core samples have been taken at Jette but results from the extensive core coverage at Jotun, which is in the same Heimdal Formation, has been used to characterize facies (Det norske oljeselskap ASA, 2011b). The Heimdal formation was deposited as a sand-rich submarine-fan system and the reservoir is characterized as heterogeneous, with high permeability sandy turbidites interfingered by shale (Det norske oljeselskap ASA, 2011a; Lorentzen, 2013). Uncertainty surround the permeability of the Jette reservoir, as initial estimates from characterization indicated permeabilities ranging from hundreds of milliDarcy to several Darcys. This first interpretation has been questioned since well tests and production data have indicated permeabilities to be in the range from ten to hundred milliDarcy, well below the initial estimate (Lysne, Nakken, Totland et al., 2013; Lorentzen, 2013). Also, initial estimates of permeability is based on logs not properly calibrated because there exists no cores for which logs can be calibrated against. This makes log interpretations highly uncertain.

Correlations from cores taken at Jotun together with seismic data have shown that the sand deposits in the Heimdal Formation are affected by mounds in the below Ty Formation (Figure 3.3.2). This led to a compensational stacking sequence of sands interbedded by thin anoxic black shales. The black shale layers act as vertical flow barriers within the reservoir. However, sand injections in the upper Heimdal Formation are thought to improve vertical communication between layers (Det norske oljeselskap ASA, 2011a; Lorentzen, 2013).

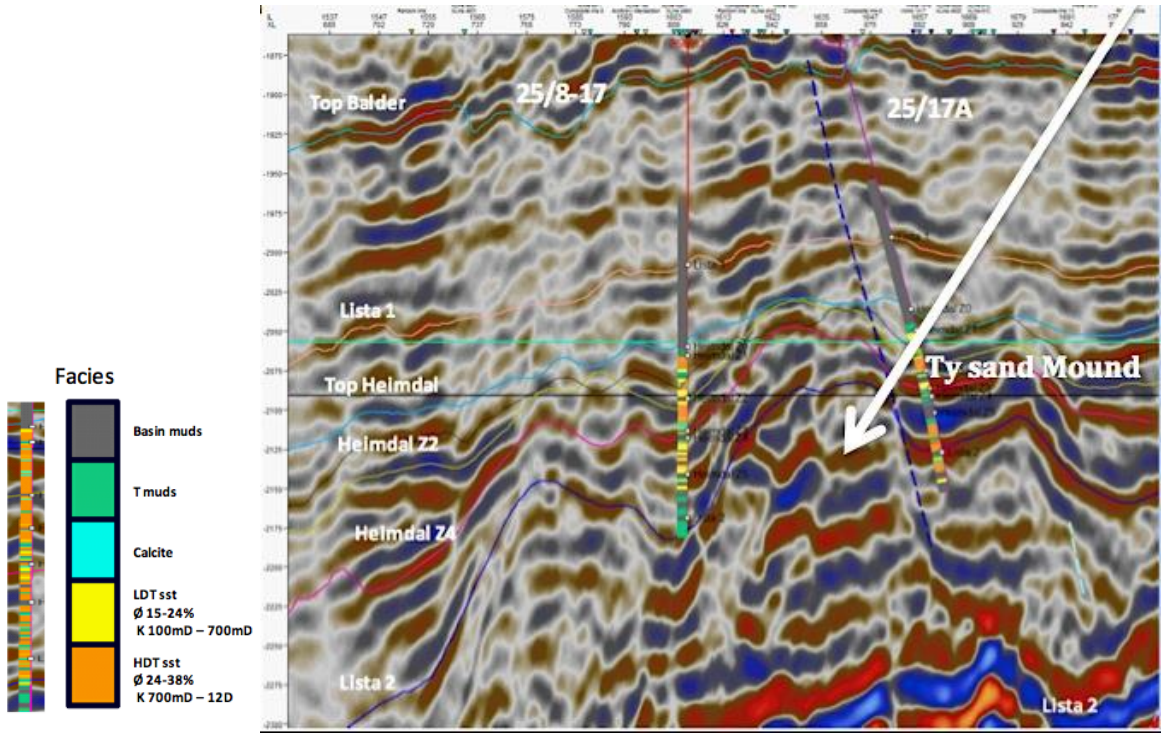

Figure 3.3.2: Seismic section illustrating a Ty mound between well 25/8-17 and 25/8-17A. Included are interpreted facies along wellbore together with facies description (Det norske oljeselskap ASA, 2011b).

3.4 RESERVOIR DESCRIPTION

Jette is a highly heterogeneous oil reservoir. The main reservoir facies has been identified as HDT sands which are sand rich amalgamating sandstones with good connectivity and high porosity (Det norske oljeselskap ASA, 2011b; Lorentzen, 2013). Well tests interpreted by Weatherford Petroleum Consultants AS in October 2013 resulted in an average horizontal reservoir permeability of 13 mD from well 25/8-D-1 AH T3 and 27.5 mD from well 25/8-E-1 H. Vertical permeability in well 25/8-E-1 H has been measured to be 20 mD, which leads to a k_v/k_h-ratio of 0.73 indicating that reservoir sands are relatively isotropic (Lysne, Nakken, Totland et al., 2013). The reservoir sands are thin and in general not more than 10 meters thick, interbedded with anoxic black shales and occasional calcite stringers. The calcite and

black shales are believed to restrict vertical communication in the reservoir (Det norske oljeselskap ASA, 2011a; Lorentzen, 2013). Log interpretation from the vertical well 25/8-D-1 H clearly indicate these sealing layers (Figure 3.4.1). Similar log responses of lithology can be seen in all vertical wells.

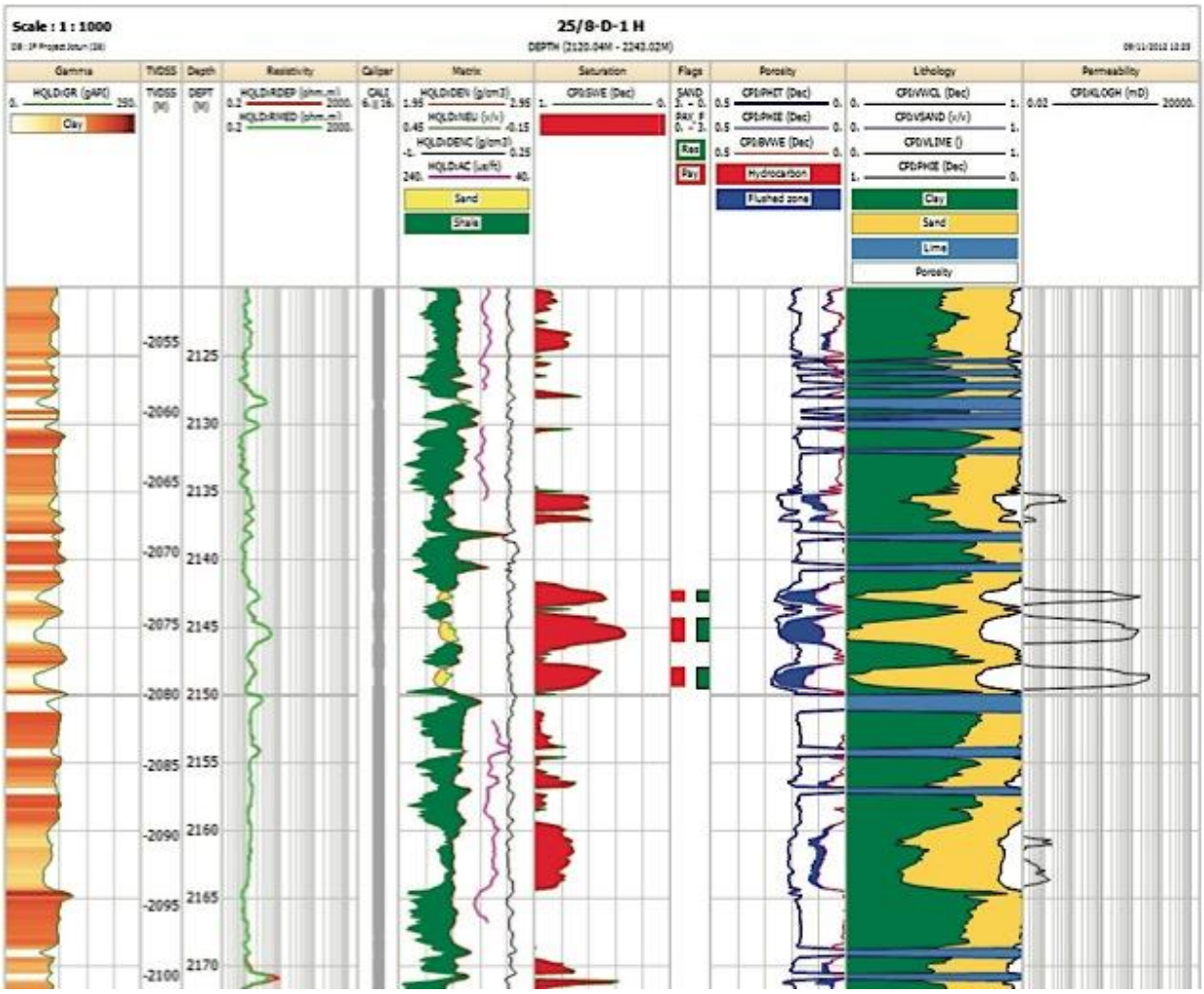

Figure 3.4.1: Log from the vertical pilot well 25/8-D-1 H indicating sealing layers due to black shales and calcite stringers (Det norske oljeselskap ASA, 2013d).

Jette is assumed to have good pressure support from a strong nearby aquifer (Figure 3.4.2), similar to the one at Jotun, resulting in a flank waterdrive. Several possible faults have been identified in the reservoir, seen in Figure 3.3.1 and Figure 3.4.2, but the presence of faults and degree of communication across faults is highly uncertain. When the dynamic reservoir model was built it was decided not to include any faults in the model (Det norske oljeselskap ASA, 2011a; Lorentzen, 2013). However, interpretation of buildup tests indicates that some sort of compartmentalization can be seen in well 25/8-D-1 AH T3 because it was not able to reach initial reservoir pressure as was done in well 25/8-E-1 H due to pressure maintenance from

the aquifer. Further analysis of pressure behavior in well 25/8-D-1 AH T3 indicates depletion and that aquifer support is limited or not present in the compartment being produced (Lysne, Nakken, Totland et al., 2013). Well tests has also indicated that both wells at Jette are producing under linear flow regimes.

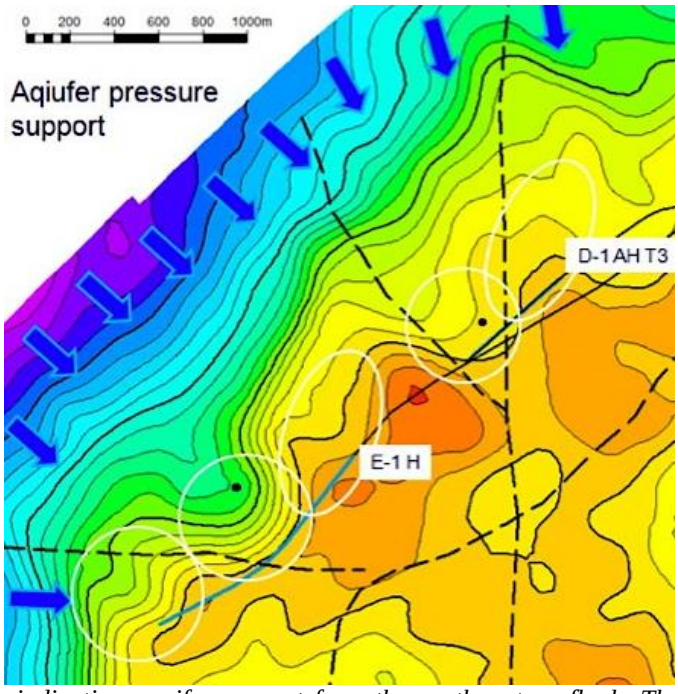

Figure 3.4.2: Schematic indicating aquifer support from the northwestern flank. The dashed lines represent possible faults (Det norske oljeselskap ASA, 2013a).

In the exploration of the field, well 25/8-17 encountered undersaturated oil while sidetrack 25/8-17A encountered oil with a possible overlying gas cap. However, no gas cap has been encountered with either of the two production wells, 25/8-D-1 AH T3 or 25/8-E-1 H. The water oil contact (WOC) was logged to a depth of 2091 mTVD MSL with an initial reservoir pressure of 197 bara. However, MDT tests indicate a WOC as high as 2086 mTVD MSL (Lorentzen, 2013). In Chapter 3.3 it was mentioned that a possible sealing fault exist between Jette and Tau. A fault may exist, but it is not sealing since pressure plots at Jette indicate communication with the nearby Tau wells 25/8-8 S/A/B, due to a 3 bar depletion from initial reservoir pressure without any production at Jette (Det norske oljeselskap ASA, 2013a; Lorentzen, 2013). Even though a hydraulic connectivity exists between Tau and Jette it is not believed that production from Tau will affect stock tank oil initially in place (STOIIP) at Jette because of the strong aquifer.

Three fluid samples have been collected at Jette. The first sample was taken from well 25/8-17 which first discovered oil at Jette, the second sample was taken from the pilot well

25/8-D-1 H and the third sample is a recombined sample from 25/8-E-1 H production collected at the test separator at Jotun A. There is introduced a high degree of uncertainty to which sample represents the reservoir fluid most correctly since all fluid samples yield different bubblepoint pressures and solution gas-oil ratios (R_{so}) (Lorentzen, 2013). PVT analysis performed on fluid samples from well 25/8-D-1 H indicated a bubblepoint pressure of 172.3 bara and solution gas-oil ratio of 125 Sm^3/Sm^3 (Ravnås and Skog, 2012). This is much higher than what had been measured on the first sample from well 25/8-17. The first sample yielded a bubblepoint pressure of 114.7 bara and solution gas-oil ratio of 87 Sm^3/Sm^3 (Sandvik and Ravnås, 2010). The third and final sample recombined from the separator indicated a bubblepoint pressure of 146.5 bara (Nielsen, Winsnes and Bjørsvik, 2013). The large variation in fluid properties observed from fluid samples at Jette supports the existence of faults and compartmentalization indicated by well tests. It is likely that several fluid systems exist within the Jette reservoir. Further discussion and information about the fluid system at Jette is given in Chapter 5.1.

Tau is a good analogue of the Jette reservoir since it is an extension of the Jette north area and produces from the same Heimdal Formation. Due to this, and the lack of cores from Jette, it was decided to use relative permeability curves from core samples taken at Tau to be used with the Jette model (Det norske oljeselskap ASA, 2011c; Lorentzen 2013). In addition porous plate (water and oil) measurements from well 25/8-5 S have been used to establish a leverett function from which capillary pressure has been derived (Det norske oljeselskap ASA, 2011b).

Measurements from logs in production wells 25/8-D-1 AH T3 and 25/8-E-1 H indicate a net to gross of 25.3% and 21.2% in the completed section respectively. The net criteria used during log interpretation is porosity greater than 15% and clay volume less than 40% (Det norske oljeselskap ASA, 2010). Net effective porosity was measured to be 24.3% and 25.0% for well 25/8-D-1 AH T3 and 25/8-E-1 H respectively (Lorentzen, 2013). As a comparison, nearby horizontal wellbores 25/8-B-5 and 25/8-B-17 at the Jotun field show a net to gross of 53% and 39% respectively. The net effective porosity is 29.1% and 28% respectively (Det norske oljeselskap ASA, 2013e). This infers that sands in the Heimdal Formation at Jette is of less quality and more heterogeneous compared to sands in the Jotun field.

The latest resource estimate indicates STOIIP of 11.2 MSm^3 and technical recoverable reserves of 1.039 MSm^3. This equals a recovery factor of 9.27%. According to a 2012 prognosis recoverable reserves were 1.11 MSm^3, but due to technical problems with drilling and completion in addition to thinner and less permeable sands, recoverable reserves were

reduced. With the current tie-in agreement Jette is assumed to produce until 31.12.2017 (Det norske oljeselskap ASA, 2013a; Lorentzen, 2013).

3.5 WELLS

Jette was originally planned developed with two standalone horizontal wells, Jette South and Jette North, tied back to Jotun B. Both wells were planned completed with 8½″ open hole section with a 5½″ production tubing with standalone mesh screens, inflow control devices (ICD) and swell packers. To alleviate risk it was decided that a pilot well from Jette South would penetrate the more uncertain northern parts of the reservoir to prove reservoir sands (Det norske oljeselskap ASA, 2011a; Lorentzen, 2013). Drilling operations commenced on the 13th of May 2012 with the drilling of pilot well 25/8-D-1 H. The 6th generation semi-submersible drilling rig Transocean Barents went of hire on the 26th of November 2012 after completing both wells, 25/8-D-1 AH T3 and 25/8-E-1 H (Det norske oljeselskap ASA, 2013b and 2013c; Lorentzen 2013).

The pilot well, 25/8-D-1 H, was finished on schedule. It proved thinner and less permeable sands than expected. Three sands with a gross thickness of about 5 meters was encountered, leading to a new correlation against nearby wells at Tau (Det norske oljeselskap ASA, 2013a; Lorentzen, 2013). A log section with interpreted lithology from well 25/8-D-1 H can be seen in Figure 3.4.1.

Drilling of the Jette South well proved challenging. A loss of wellbore resulted in sidetracking. Also the second track experienced wellbore instability issues and screens were not able to be run in hole to reach target depth (TD). The third and final track was finished with a reduction in length of the planned reservoir section. Although the reservoir section was reduced to 1200m only half of the 8½″ open hole section was completed with mesh screens, ICDs and swellpackers (Det norske oljeselskap ASA, 2013a and 2013b; Lorentzen, 2013). Due to drilling with WARP mud it is believed that overpressure in the wellbore may have caused fine particles from the mud to migrate into the formation causing deterioration of reservoir quality. There is also a possibility that insufficient clean-up has caused plugging of the sand screens in well 25/8-D-1 AH T3 (Lysne, Nakken, Totland et al., 2013).

As a result of the shorter reservoir section in the Jette South well, and the pilot well indicating thinner sands to the north, it was decided to target both wells to the South. Jette South was believed to prove more optimistic oil reserves than the un-drilled Jette North area.

This was based on a better definition of the South area due to the already drilled exploration wells 25/8-17, 25/8-17 A and the abandoned sidetracks of well 25/8-D-1 AH T3. However, a third well may be decided to be drilled at Jette North later in the life of the field (Det norske oljeselskap ASA, 2013a; Lorentzen, 2013).

The second well, 25/8-E-1 H, was drilled just south of the toe of 25/8-D-1 AH T3 (Figure 3.5.1). Due to the problems experienced in well 25/8-D-1 AH T3 when running in screens it was decided that 25/8-E-1 H would be completed without swell packers. This resulted in the entire $9^{½}''$ open hole reservoir section of 1220 m to be completed with standalone mesh screens and ICDs. Both production wells are considerably shorter than stated in the PDO owing to instability during drilling and completion (Det norske oljeselskap ASA, 2013a and 2013c; Lorentzen, 2013). Completion schematics of both wells, 25/8-D-1 AH T3 and 25/8-E-1 H, are listed in Appendix B.

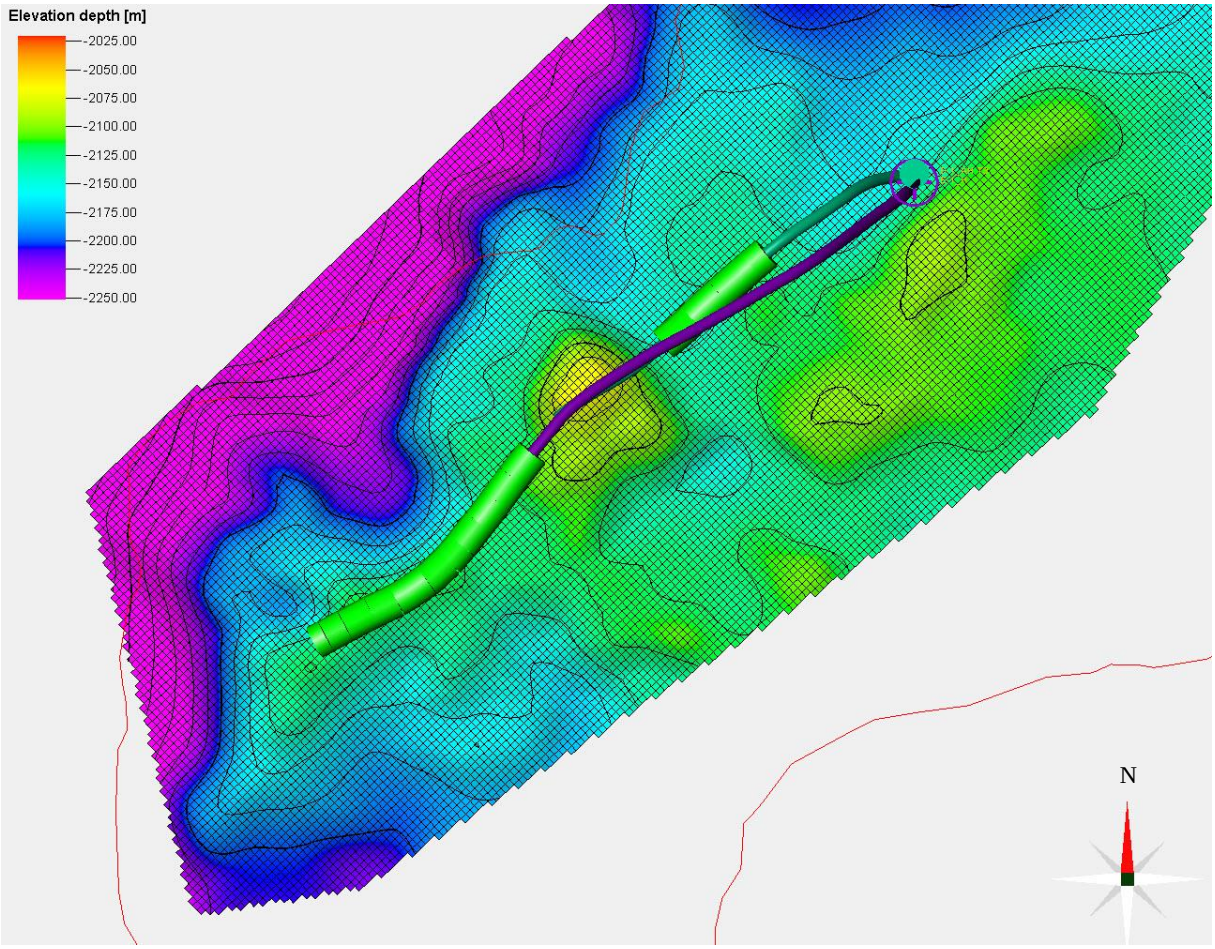

Figure 3.5.1: Location and trajectory of well 25/8-D-1 AH T3 (green) and 25/8-E-1 H (purple) in the geomodel. The light green encompassing both well trajectories reresent where the wells are completed.

It is not planned for any well interventions due to the short lifetime of the field. However, both wells are constructed in order to be able to perform interventions by drill stem, cabel,

coiled tubing or pump jobs from both rig or ship if needed (Det norske oljeselskap ASA, 2011a; Lorentzen, 2013).

3.6 PRODUCTION

Jette is developed with a subsea installation tied back to Jotun B (Figure 3.2.1). There are two standalone wells with connections for an umbillical and an 8″ flowline. The umbillical incorporates lines for hydraulic, chemicals, signal cabels and electric cabels. Individual well streams are connected to the pipeline end manifold (PLEM) where flow is commingled and tied back to Jotun B through an 8″ ID flowline (Det norske oljeselskap 2011a; Lorentzen, 2013). A schematic of the subsea installation at Jette is illustrated in Figure 3.6.1. The flowline connecting the PLEM to Jotun B is 5877m long following the seabed at a depth of 127m (Det norske oljeselskap ASA, 2013a; Lorentzen, 2013). The riser at Jotun B is 12″ ID and is further connected with an 8″ piping topside before being routed through a 10″ production line from Jotun B to Jotun A (Lysne, Nakken, Totland et al., 2013). The PLEM has the possibility for a third connection if it is decided to drill an additional well at Jette.

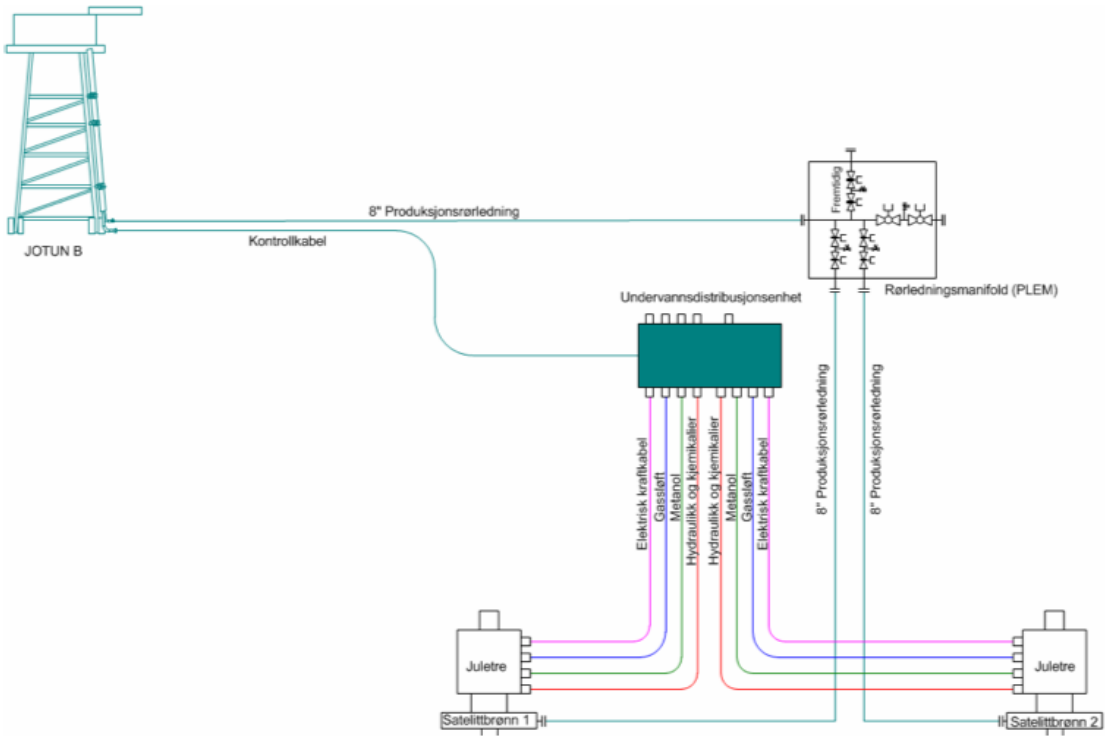

Figure 3.6.1: Schematic of the subsea installation at Jette (Det norske oljeselskap ASA, 2011a).

Production from Jette is processed and stored at Jotun A. Jotun A is a floating, production, storage and offloading unit (FPSO) with a storage capacity of 540,000 bbl oil. A test separator at Jotun A will be used to verify the measurements performed at Jotun B with the multi phase flow meter (MPFM) (Det norske oljeselskap ASA, 2011a; Lorentzen, 2013). The MPFM measures the flow rate of all phases in the flowline topside Jotun B. Other continuous measurements of special interest includes bottom hole pressure (BHP) and tubing head pressure (THP) from both wells. Table 3.6.1 specifies the design capacity of production from Jette which can be processed at Jotun A. These numbers represent the maximum production from the commingled flow from both wells, 25/8-D-1 AH T3 and 25/8-E-1 H. The minimum arrival pressure at Jotun B is calculated to be 20 bara (Det norske oljeselskap ASA, 2011a; Lorentzen, 2013).

Table 3.6.1 – Production capacity from Jette (Det norske oljeselskap ASA, 2011a)

Oil production	3,500 Sm^3/day
Gas production (including lift gas)	0.5 million Sm^3/day
Gas lift	0.2 million Sm^3/day
Water production	5,000 Sm^3/day
Total liquid production	5,000 Sm^3/day

Because of the aquifer support it was decided to develop and produce Jette without any water injection or other pressure maintenance projects. The oil is produced with gas lift and the supply of gas is an integrated part of the umbilical which is controlled from Jotun A (Lorentzen, 2013). Gas lift gas used at Jette is taken from production at Jotun. There are some uncertainty related to injected volumes of lift gas due to sensors reaching their measurement limit.

ExxonMobil operates the production of Jette on behalf of Det norske oljeselskap ASA. Jette was put on production 20th of May 2013. Monthly production rates can be seen in Figure 3.6.2. Production from Jette has not met with expectations from simulation forecasts and has experienced a steep decline in production and too early water breakthrough in well 25/8-E-1 H (Lorentzen, 2013). Monitoring of production has also indicated severe slugging due to unfortunate design of the riser system. It is believed that replacing the 12″ riser with an 8″ riser will prevent slugging and optimize production. A study on production optimization has addressed the issue of wells not producing to their full potential. The root causes of poor production are most likely due to well 25/8-D-1 AH T3 having plugged sand screens, formation damage, poor clean-up and unfortunate reservoir conditions. Well 25/8-E-1 H is believed to have its productivity reduced only from a poor clean-up. For comparison, well

25/8-D-1 AH T3 and 25/8-E-1 H have interpreted productivity indices of 1 Sm^3/d/bar and 11.2 Sm^3/d/bar respectively (Lysne, Nakken, Totland et al., 2013).

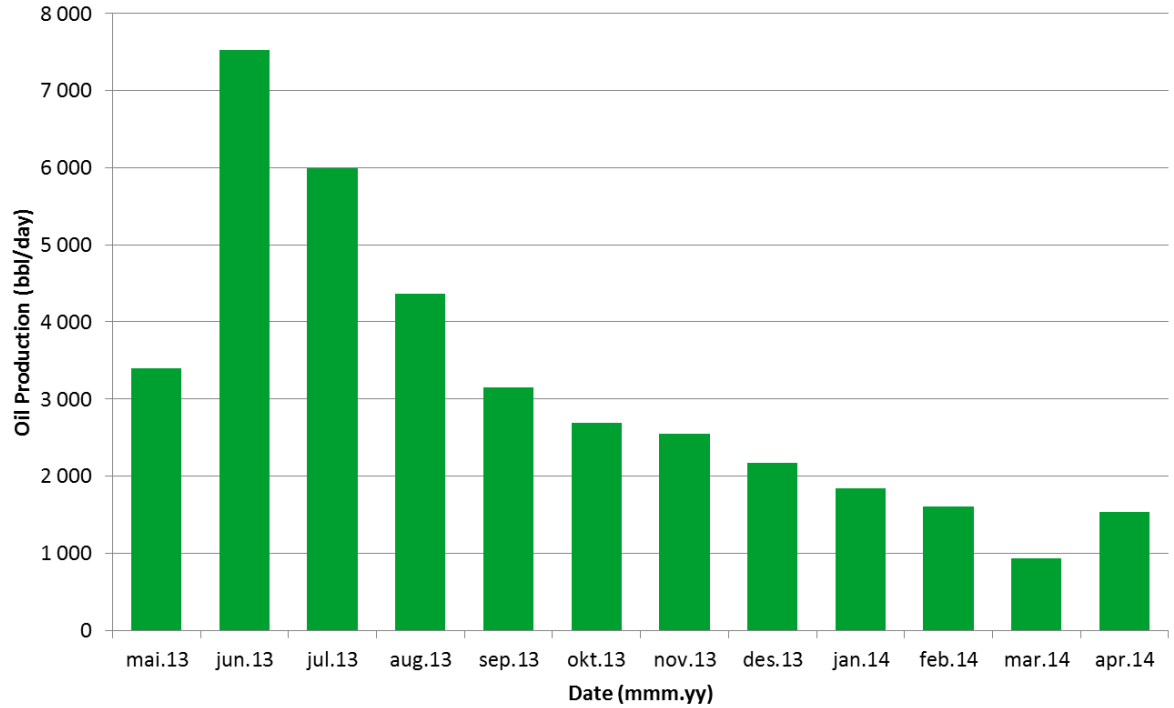

Figure 3.6.2: Monthly production rate at Jette between May 2013 and April 2014 (Det norske oljeselskap ASA, 2014).

4 JETTE DYNAMIC RESERVOIR MODEL

This chapter will describe the dynamic reservoir model which will be used in the process of obtaining a history match between model and actual field performance at Jette. The dynamic reservoir model is based upon the model provided by Det norske oljeselskap ASA (herof denoted Det norske). The provided model has previously been upscaled by the author to improve convergence issues and reduce run times. For further information of how the upscaling was performed the reader is adviced to look up the project report written by Lorentzen (2013). The dynamic reservoir model presented throughout this chapter will be used as a the initial model during the history matching process and form the basis for perturbations made to improve match. Before proceeding with history matching it is of interest to form a solid understanding of the model which will be used during the history matching process, namely the Jette dynamic reservoir model.

The Jette dynamic reservoir model is based on the geological model created by Det norske and runs in ECLIPSE 100 which is a commercial reservoir simulation software from Schlumberger, described in Appendix A. Jette is modeled in three dimensions with a black oil formulation containing three phases. It is initially undersaturated but evolves gas as reservoir pressure is lowered below the bubblepoint. Simulation starts on the 20th of May 2013 and runs until 1st of January 2020 (Lorentzen, 2013).

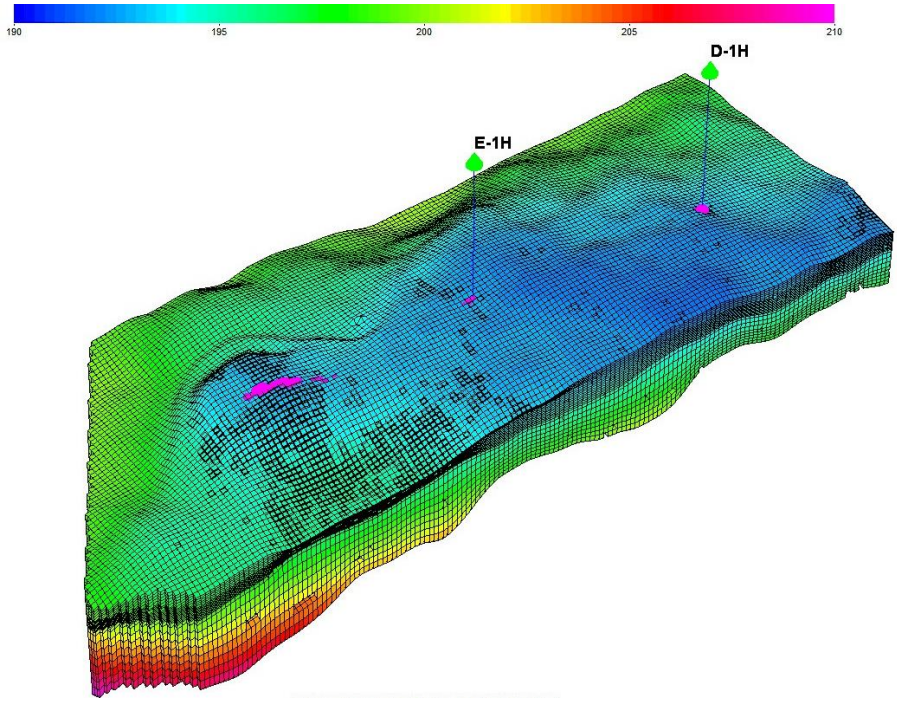

Figure 4.1: Jette dynamic reservoir model illustrated with pressure.

Upscaling of the Jette model resulted in grid dimensions of 166x69x25. This leads to a moderately sized reservoir model with 286,350 grid blocks of which 247,834 are active. The reduction of active grid blocks is due to a restriction in pore volume, leading to grid blocks with a pore volume less than 10 Sm^3 being set inactive. The Jette dynamic reservoir model including the two production wells 25/8-E-1 H and 25/8-D-1 AH T3, respectively E-1H and D-1H in the model, are illustrated in Figure 4.1. Lateral dimensions of grid blocks are 25m in both the X and Y-direction. Vertical dimensions vary considerably and will be described further in the following section.

4.1 MODEL GEOLOGY

The Jette dynamic reservoir model is based on the geological model and was directly cut from the original grid of the geological model. This can be seen from Figure 4.1.1 where the top horizon of the dynamic reservoir model is overlaid the grid of the static geological model. The northern parts of the geological model stretches into the nearby Jotun field and is not of interest during simulation due to the assumption of a no flow boundary between the two fields and minor pressure differentials caused by the presence of a strong aquifer as described in Chapter 3.4. The aquifer is included in the Jette dynamic reservoir model as a numerical aquifer connected along the entire north face of the model, capable of supplying close to complete pressure maintenance (Lorentzen, 2013).

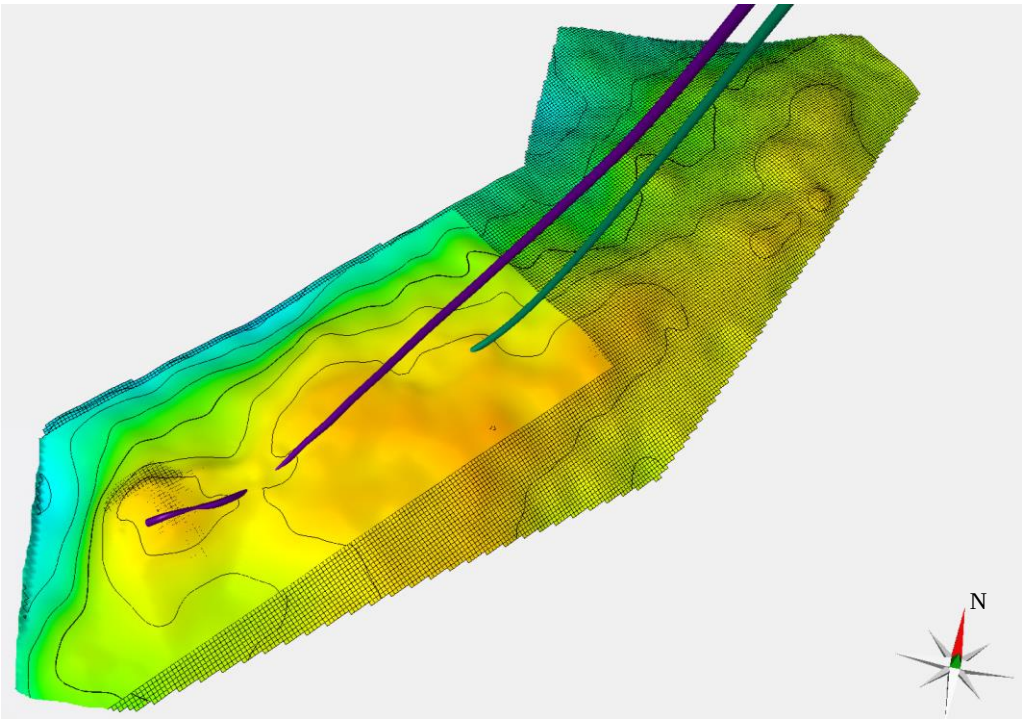

Figure 4.1.1: Horizon from the Jette dynamic reservoir model overlaid the geological model grid.

The layering of the Jette dynamic reservoir model is created according to a predefined reservoir zonation from the geological model. To reduce the number of cells in the model the zone of the cap rock and underlying sands (saturated with water) have been left out. This can be done as neither of these zones will affect reservoir performance. Figure 4.1.2 illustrates the reservoir zonation before removal of the two zones mentioned above, while Table 4.1.1 gives the number of grid layers and average dimensions of these in the Jette dynamic reservoir model (Lorentzen, 2013). During upscaling the grid was coarsened with a factor 3 in the three top zones while keeping the original dimensions of the bottom zone. This resulted in a reduction from 65 layers to the current number of 25. Numerical dispersion and grid orientation effects introduced from upscaling was found to be neglible (Lorentzen, 2013).

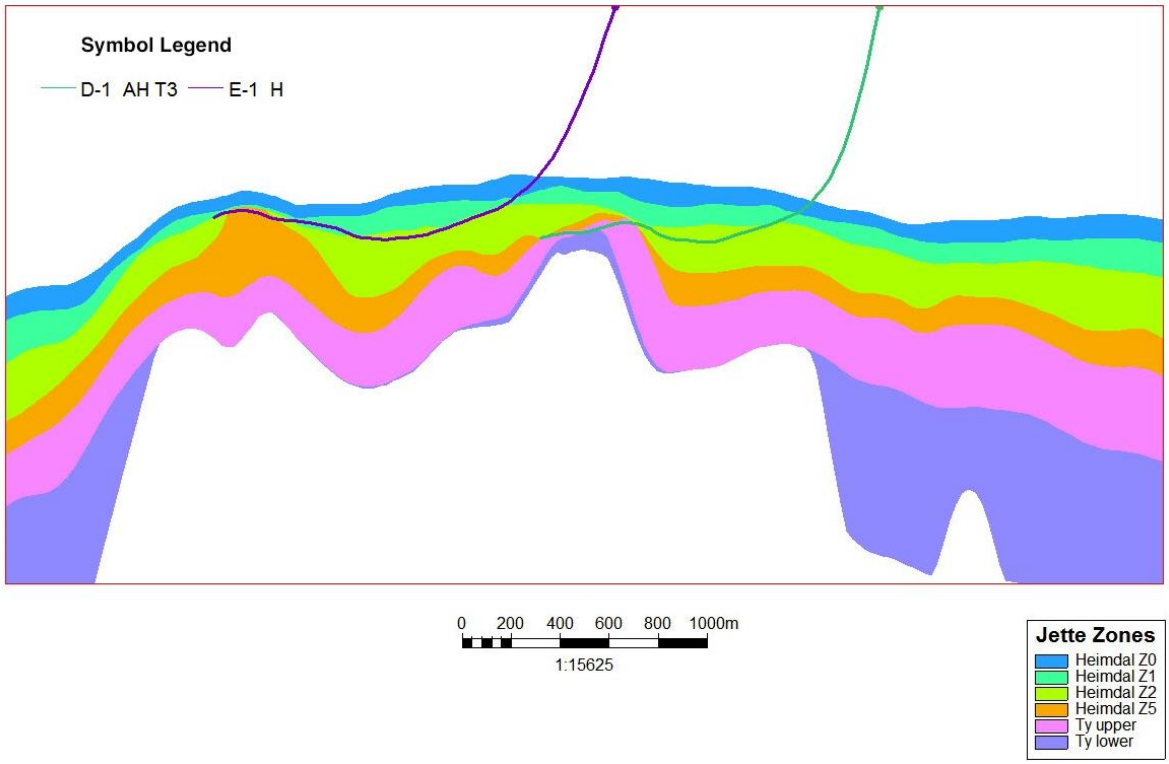

Figure 4.1.2: Cross section illustrating reservoir zonation including wells in the model.

Table 4.1.1 – Layering of the Jette dynamic reservoir model.

Zone	*Cell k-index range*	*Number of Cells in vertical direction*	*Average dimensions in vertical direction*
Heimdal Z1	1 – 5	5	3.74 m
Heimdal Z2	6 – 17	12	3.20 m
Heimdal Z5	18 – 20	3	7.42 m
Ty upper	21 – 25	5	7.45 m

Reservoir zonation is mainly due to the presence of distributed facies within the geological model. The facies types characterized at Jette was described in Chapter 3.3. Heimdal Z1 is the uppermost sand consisting predominantly of LDT sands while the Heimdal Z2 is the main reservoir zone containing mostly HDT sands and some LDT sands. Heimdal Z5 contains large amounts of black shale while Ty upper is a mixture of sands (Lorentzen, 2013). All zones contain small amounts of calcite. Facies were stochastically distributed within the different zones based upon the upscaled well properties. This ensures that interpreted facies in wells are honored in the dynamic model (Det norske oljeselskap ASA, 2011b).

Static reservoir parameters such as porosity and permeability are modeled based on facies and log interpretation. Porosity was calculated along the wells using the density log and correcting for shale and hydrocarbons. It was then upscaled to the grid and distributed according to facies type. HDT sands would yield high porosities while shale and calcite would yield very low porosities. The permeability was added to the grid from a porosity/permeability transform defined from core data collected at Jotun. Three transformations were defined based on facies type, one for HDT sand, one for LDT sand and one representing black shale, calcite and E-sequence. The transformations are given by Equation 4.1.1, Equation 4.1.2 and Equation 4.1.3 respectively (Det norske oljeselskap ASA, 2011b). The value range for each property by facies can be seen in Figure 3.3.2.

$$k_{HDT} = 10^{(8.37*\varphi_e+0.97)} \quad \text{Equation 4.1.1}$$

$$k_{LDT} = 10^{(15.42*\varphi_e-1.75)} \quad \text{Equation 4.1.2}$$

$$k_{Shale,Calcite,E-seq} = 10^{(21.02*\varphi_e-2.81)} \quad \text{Equation 4.1.3}$$

Values of permeability and porosity vary considerably throughout the model due to the stochastic distribution. The model was however implicitly homogenized when it was upscaled due to averaging of properties between neighboring cells. The Jette dynamic reservoir model assumes permeability in the X and Y-direction to be equal throughout the entire model. Histograms of the porosity and permeability distribution in the Jette dynamic reservoir model are illustrated in Figure 4.1.3.

The extent of faulting is a major uncertainty in the Jette model and it was not possible to prove the existence of faults. As a consequence no faults are present in the Jette dynamic reservoir model (Det norske oljeselskap ASA, 2011b).

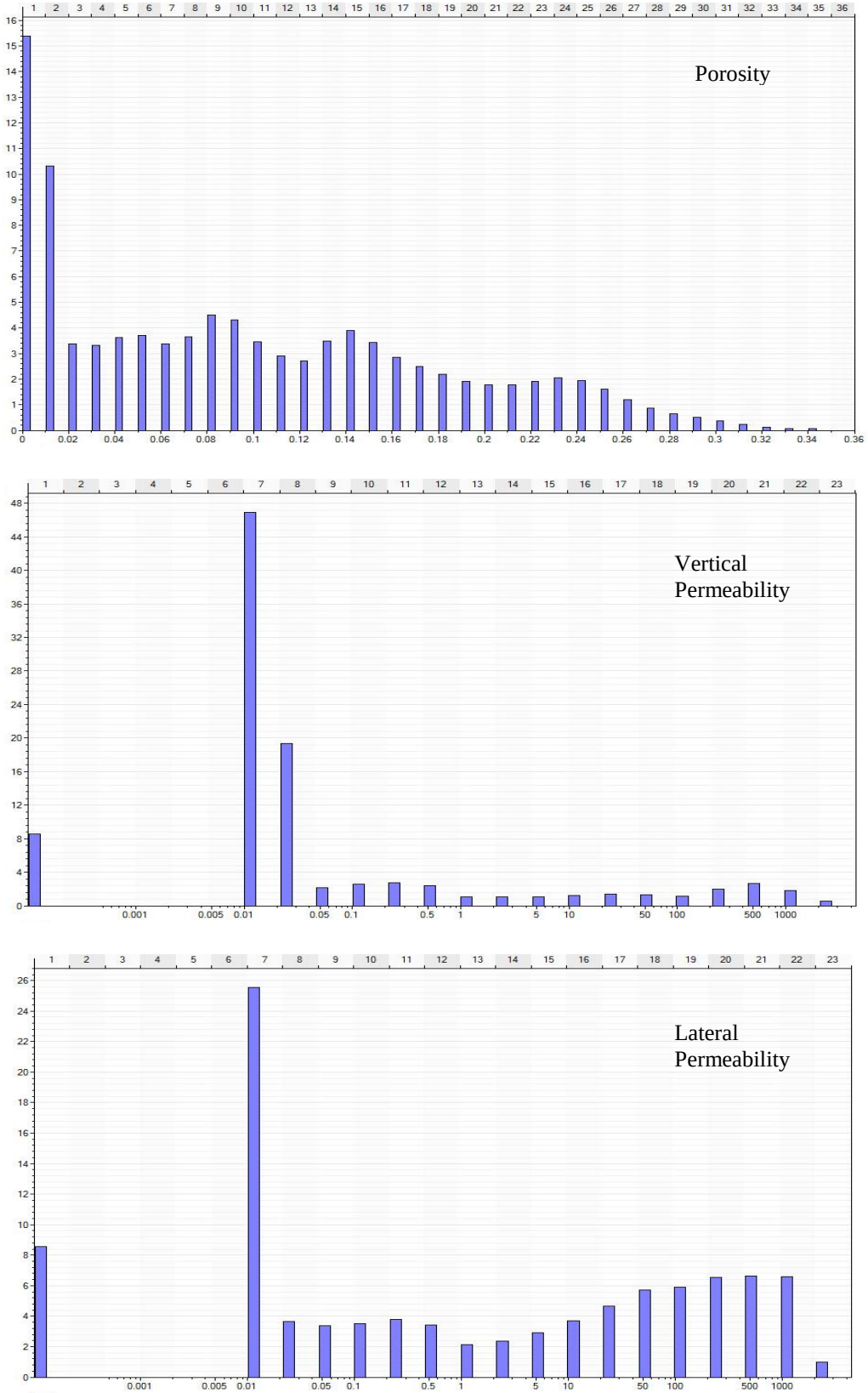

Figure 4.1.3: Histograms of porosity (top), vertical permeability (middle) and lateral permeability (bottom) in the Jette dynamic reservoir model, respectively in fraction, milliDarcy and milliDarcy.

4.2 DYNAMIC PROPERTIES

The most important model properties governing the dynamic behavior of the Jette dynamic reservoir model will be described in this section.

4.2.1 MODEL INITIALIZATION

The Jette dynamic reservoir model has been initialized from a WOC located at 2,091 mTVD MSL with a datum pressure of 195.9 bar. Initialization has been based on special core analysis (SCAL) from Jotun, using porous plate measurements on core plugs from well 25/8-5 S. The cores used represents the upper Heimdal Formation. A water saturation model was created by use of the Leverett J-function (Equation 4.2.1.1) (Det norske oljeselskap ASA, 2011b). P_c is the capillary pressure, σ the interfacial tension, φ the porosity and θ the contact angle.

$$J_{SI-units} = \frac{3.1419 * P_c}{\sigma * \cos(\theta)} \sqrt{\frac{Permeability}{\varphi}} \qquad \text{Equation 4.2.1.1}$$

To improve the correlation factor a normalization of water saturation, *SWN*, was performed and calculated using Equation 4.2.1.2 and Equation 4.2.1.3. H_{fwl} is the height above the free water level (Det norske oljeselskap ASA, 2011b).

$$J_{SI-units} = 0.003258 * H_{fwl} * \sqrt{\frac{Permeability}{\varphi}} \qquad \text{Equation 4.2.1.2}$$

$$SWN = 0.1601 * J^{-0.712} \qquad \text{Equation 4.2.1.3}$$

A correlation between irreducible water saturation, S_{wirr}, and porosity was established (Equation 4.2.1.4). It is based on a best fit curve from all measured S_{wirr} data at Tau (Det norske oljeselskap ASA, 2011b). S_{wirr} is calculated for all cells in the model. Then saturation table scaling is applied to scale the connate water saturation (*SWL*) to match the irreducible water saturation calculated from Equation 4.2.1.4. More information about the saturation scaling option in ECLIPSE 100 can be found in Appendix C.

$$S_{wirr} = 0.0001 * \varphi^{-4.968}$$ Equation 4.2.1.4

The final water saturation, *SWJ*, is calculated for all cells using Equation 4.2.1.5. Note that the maximum water saturation is set to 1 in order to honor the physics. Due to missing SCAL data for porosities lower than 21%, irreducible water saturation for porosities lower than 17% will be erroneously high. Due to this a maximum limit of 0.6 has been given to *SWL* which scales the irreducible water saturation (Det norske oljeselskap ASA, 2011b).

$$SWJ = SWN * (1 - S_{wirr}) + S_{wirr}$$ Equation 4.2.1.5

The resulting oil in place from initialization is 6,226,452 Sm^3. Volumetric calculations and uncertainty studies performed by Det norske has indicated an uncertainty span of oil in place approximately ±20% (Det norske oljeselskap ASA, 2013a).

The above described initialization process was followed on the model which was created by Det norske. This model was later upscaled by Lorentzen (2013) to form the current Jette dynamic reservoir model. Due to this *SWL* was upscaled, however it was shown that it was upscaled adequately accurate to represent the original *SWL* of the coarse grid (Lorentzen, 2013).

4.2.2 FLUID MODEL

The fluid model specified in the Jette dynamic reservoir model is based on the fluid sampled from well 25/8-D-1 H. A black oil fluid description is used, which represents the reservoir hydrocarbons as two phases (oil and gas) and their behavior as functions of pressure. The bubblepoint pressure of the oil is 170.9 bara and results in an undersaturated oil throughout the entire reservoir. Only one fluid region is used in the model. The solution gas-oil ratio used is specified to decrease downwards in the reservoir as indicated in Table 4.2.2.1 (Lorentzen, 2013). The solution gas-oil gradient was calculated from PVTSim with a specified temperature gradient of 3.5°C/100m.

It was previously mentioned (Chapter 3.4) that there is much uncertainty related to the fluid samples. This leads us to question the fluid model used in the Jette dynamic reservoir model. Further investigation and work with description of new fluid models will be presented later in this thesis.

Table 4.2.2.1 – Solution gas-oil ratio variation with depth	
R_{so} (Sm^3/Sm^3)	Depth (m TVD)
141.1	2,000.0
124.9	2,050.0
117.8	2,075.0
112.8	2,094.0

4.2.3 Relative Permeability and Capillary Pressure

The Jette dynamic reservoir model is modeled using relative permeability from Tau. It is assumed that Jette and Tau produce from similar sandstones in the Heimdal Formation. Figure 4.2.3.1 and Figure 4.2.3.2 illustrates water-oil imbibition relative permeability and gas-oil drainage relative permeability respectively.

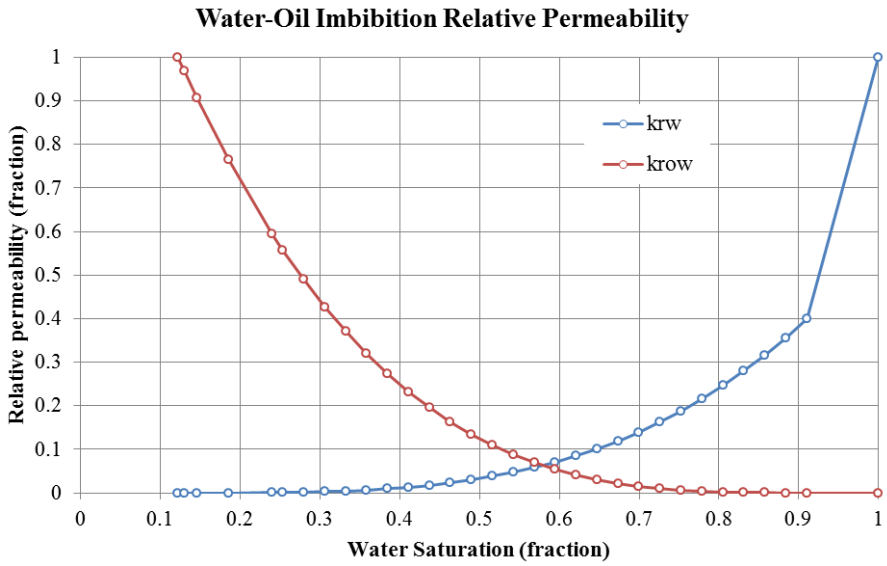

Figure 4.2.3.1: Water-oil imbibition relative permeability.

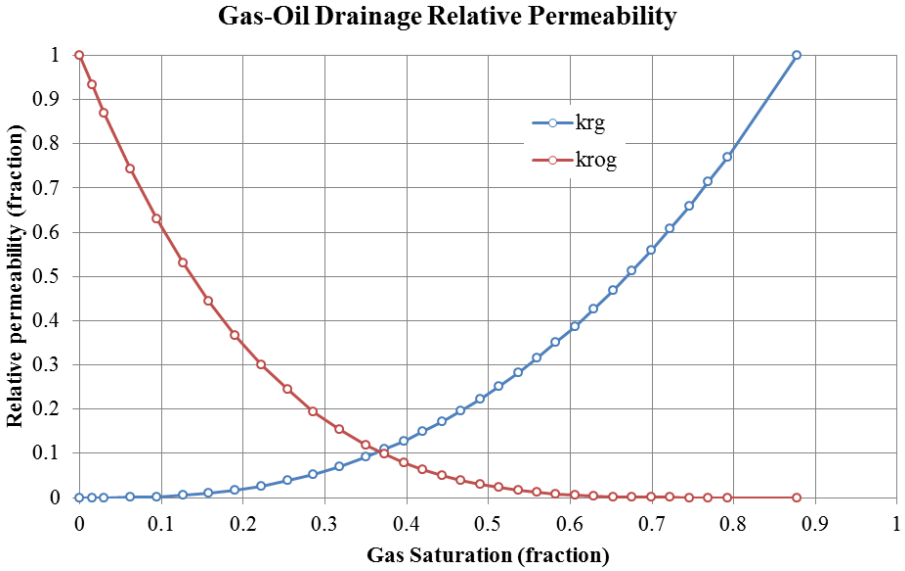

Figure 4.2.3.2: Gas-oil drainage relative permeability.

Capillary pressure used in the Jette dynamic reservoir model is derived from the Leverett J-function described in Chapter 4.2.1. The resulting capillary pressure calculated with the correlation using the Leverett J-function is illustrated in Figure 4.2.3.3. The Jette dynamic reservoir model uses scaling of maximum capillary pressure, *PCW*, in order to avoid excessive capillary pressures in the model. Gas-oil capillary pressure has been set to zero (Lorentzen, 2013).

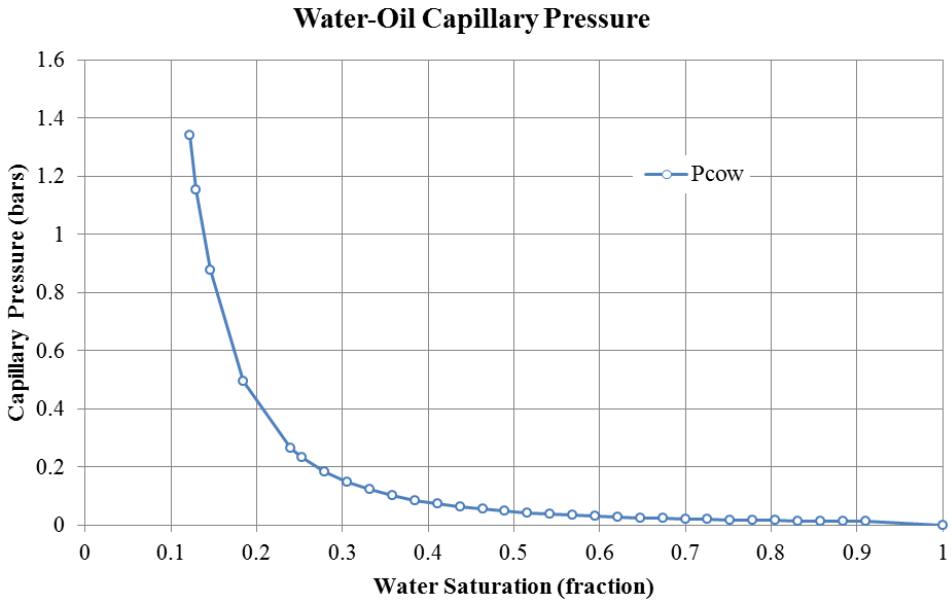

Figure 4.2.3.3: Water-oil capillary pressure from Leverett J-function.

4.2.4 PRODUCTION AND WELLS

Well 25/8-D-1 AH T3 and 25/8-E-1H are both included in the Jette dynamic reservoir model. For simplicity they are named D-1H and E-1H in the model respectively. The location of both wells can be seen in Figure 3.5.1 and Figure 4.1. The wells are run in history mode, controlled by liquid rate, from 20th of May until 13th of August from which they are set to operate in predictive mode. Restrictions imposed on wells during predictive mode are listed in Table 4.2.4.1. The model runs until 1st of January 2020 (Lorentzen, 2013).

Table 4.2.4.1 – Restrictions imposed on wells during predictive period

Well	*Oil rate*	*Gas rate*	*Liquid rate*	*BHP*	*Gas lift*
D-1H	300 Sm^3/day	270,000 Sm^3/day	3,500 Sm^3/day	50 bara	50,000 Sm^3/day
E-1H	800 Sm^3/day	270,000 Sm^3/day	3,500 Sm^3/day	50 bara	50,000 Sm^3/day

Tables specifying vertical lift performance (VFP) are specified and used to calculate the lift capacity in the wells and to represent the use of lift gas. THP can also be calculated in order to compare with measured values from pressure gauges at the wellhead. VFP-tables account for flow in the tubing between the reservoir and the wellhead, but does not consider the flowline between wellhead and Jotun B.

Well connections are extracted from Petrel, based upon trajectory and completions entered from deviation surveys. Skin is set to zero in both wells, there is however included a multiplier in productivity index (PI) to all connections of 0.03 and 0.07 for well D-1H and E-1H respectively. Well efficiencies are included to be 89.8% the first year of operations and 92.8% after this period (Lorentzen, 2013).

4.3 ASSUMPTIONS AND UNCERTAINTIES

During simulation and interpretation of results it is important to be aware of the inherent uncertainty and assumptions in the Jette dynamic reservoir model. It is difficult to quantify all of the assumptions and uncertainties in a reservoir model but the most pronounced in the Jette dynamic reservoir model will be listed below. Further discussion of uncertainty and assumptions will be addressed later in the thesis where found appropriate.

- Maximum permeability is given to be 4,500 milliDarcy.
- Lateral permeability is equal (k_x=k_y). Vertical permeability may be too low since it was upscaled using a harmonic averaging algorithm (Lorentzen, 2013).
- Pressure maintenance from a large (200 GSm^3) aquifer with good connectivity.
- Boundaries in the model are no flux boundaries (except for where the aquifer is connected). It is also assumed a sealing fault between Jette and Tau.
- There is not modeled any skin in either of the wells even though there are indications of formation damage due to use of WARP mud during drilling (Lysne, Nakken, Totland et al., 2013).
- Relative permeability used in the model is based on core samples from Tau.
- Water-oil capillary pressure is calculated from the Leverett J-function which may be inaccurate. There is also not specified any gas-oil capillary pressure which is a simplification.

- The fluid model used is uncertain due to three samples indicating completely different values of bubblepoint pressure.
- Instant gas re-solution is assumed (DRSDT=∞).
- Initialization is based upon the Leverett J-function derived from SCAL at Jotun which may not be representative of Jette. An assumption of 0.6 as the maximum value of the saturation table scaling factor *SWL* is made.
- There is uncertainty related to the stochastic modeling and population of properties since values are based on logs which has not been calibrated with cores from Jette (no cores available). Additional uncertainty is added to properties from the upscaling performed by Lorentzen (2013).
- A major uncertainty in the Jette model is the extent of faulting, sandstone injection and slumping which are features affecting vertical permeability (Det norske oljeselskap ASA, 2011b). Currently no faults are modeled.
- The degree of compartmentalization is uncertain.
- The completion length of well D-1H is uncertain due to operational challenges during drilling with chances of pack of and fluid loss material, such as $CaCO_3$, causing plugged sand screens (Lysne, Nakken, Totland et al., 2013).

5 VALIDATION OF INPUT DATA

If a realistic history match is to be obtained it is important that both static and dynamic input to the model are scrutinized in order to remove false data which is not representative of the reservoir. Validation of input data is performed before embarking on the actual history matching. As described in Chapter 2.2 a model which resembles the actual reservoir as closely as possible after characterization will faster converge towards a match and predict reservoir performance with greater confidence. This chapter will describe the validation process which has been performed in order to ensure that the reservoir model is characterized as accurate as possible before initiating the history match.

5.1 RESERVOIR FLUID DESCRIPTION

A correct fluid description needs to be established if the reservoir performance is to be modeled accurately. Understanding the PVT behavior of the reservoir fluid is vital in order to describe fluid dynamics in the reservoir (Dandekar, 2006). An erroneous fluid description can lead to false estimates of fluids in place due to errors in formation volume factors and problems calculating the amount of evolved gas in undersaturated reservoirs due to errors in bubble point pressure.

In Chapter 3.4 it was described that several fluid samples have been collected at Jette with varying values for bubble point pressure and GOR leading to uncertainty of which sample represents the reservoir most accurately. It was also mentioned in Chapter 4.2.2 that the current Jette dynamic reservoir model contains only one fluid model based on a fluid sample from well 25/8-D-1 H. According to the acquired fluid samples with such a wide span in fluid properties it is not sufficient to model the reservoir with only one fluid model. A summary of the acquired fluid samples with values of bubble point pressure and GOR are illustrated in Figure 5.1.1, clearly indicating a trend with increasing bubble point pressure and GOR from well 25/8-17 in the south to well 25/8-D-1 H in the north. This supports the theory that several fluid systems exist within the Jette reservoir due to compartmentalization and possible compositional gradients. The trend of more gas when going north is confirmed at Jotun where a gas cap exist.

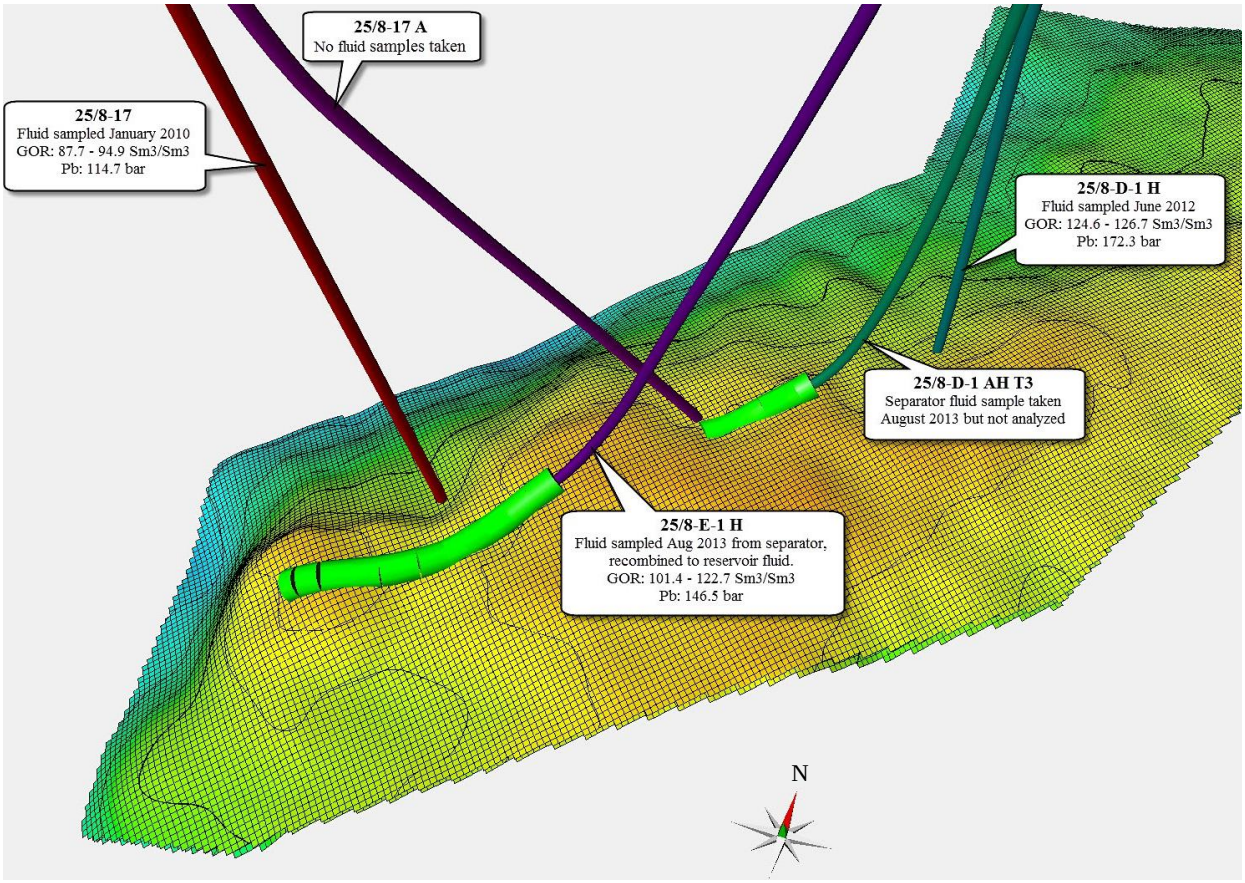

Figure 5.1.1: Overview of fluid sampling performed at Jette.

From Figure 5.1.1 it is possible that three fluid systems (compartments) exist at Jette. However, several compartments and fluid systems may exist if fluid samples had been recovered from well 25/8-17A and 25/8-D-1 AH T3. Due to the findings presented in Figure 5.1.1 it is concluded that the current fluid description in the Jette dynamic reservoir model is inadequate to represent the fluid system at Jette. It is believed that creation of two fluid models will give a valid representation of the fluid system at Jette. The two fluid models will be based on samples obtained from wells 25/8-E-1 H and 25/8-D-1 H. Hence, the Jette reservoir model will be updated to consist of two fluid models, one to the south representing the area where well 25/8-E-1 H produces from and one to the north where well 25/8-D-1 AH T3 produces from. When the recombined sample from well 25/8-E-1 H was obtained, a similar fluid sample was taken from 25/8-D-1 AH T3 but it was unfortunately not analyzed (Nielsen, Winsnes and Bjørsvik, 2013). Due to this the fluid sample from 25/8-D-1 H is the basis for the northern fluid model. There is believed to be a sealing fault between the two producing wells at Jette causing compartmentalization and the variations seen in fluid description. The addition of such a sealing fault to the Jette dynamic reservoir model will be described in Chapter 7.3.1.

5.1.1 CREATING NEW FLUID MODELS

The creation of new fluid models was conducted with use of PVTsim which is a software capable of simulating PVT and phase behavior of petroleum reservoir fluids. The main purpose of PVT software, such as PVTsim and others, is to simulate PVT experiments such as constant composition expansion (CCE), constant volume depletion (CVD), differential liberation (DL) and separator tests using a selected equation of state (EOS). The simulated experiments are compared with actual measurements from experiments on fluid samples performed by a laboratory and is tuned such that the EOS model in the software is able to represent the measured fluid behavior. The tuned EOS model, that matches with experiments from laboratory measurements, is then used to generate input tables for reservoir simulators (Dandekar, 2006). Most PVT software packages offers the possibility to export tables with either a compositional fluid description or the more commonly used black oil formulation.

Two fluid models are created and they will be referred to as fluid model 1 and fluid model 2 for simplicity. Fluid model 1 represents the southern part of the Jette reservoir and is based on a recombination of fluid samples (TS-9401 and TS-5075) from well 25/8-E-1 H collected at the test separator. The laboratory report of Nielsen, Winsnes and Bjørsvik (2013) was used and describes the fluid analysis performed on the fluid sample. Fluid model 2 represents the northern part of the Jette reservoir and is based on a bottomhole sample (PT-2550) taken in well 25/8-D-1 H. The fluid analysis report of Ravnås and Skog (2012) was used when creating the fluid model.

Both fluid samples were analyzed by Weatherford Laboratories. The experiments utilized during analysis includes constant mass expansion (CME), DL, single stage separator test, three-stage separator test and oil viscosity measurement. These experiments are conducted in order to establish the PVT behavior of the fluid which the EOS model in PVTsim will be tuned against. A reservoir temperature of 82.9°C was used in experiments for both samples. A brief description of how the different experiments are conducted together with a summary of results are given below.

Separator tests:

Figure 5.1.1.1 illustrates how a separator test is performed. The reservoir sample is initially at saturated conditions such that the volume of oil at the bubble point pressure can be measured. The sample is then brought to the first stage separator at a new pressure and temperature. The

gas which has come out of solution from the oil is removed and measured together with the volume of remaining oil in the separator (Whitson and Brulé, 2000). If this was a single stage separator test the sample would have been brought directly to standard conditions of 1 atm and 15 °C. Multistage separator tests include several separator stages, normally two or three, with different pressure and temperature conditions before ending up at standard conditions. The choice of pressure and temperature at each separator stage influences the final test results and sensitivity can be performed to obtain the optimum choice of separator conditions. The purpose of a separator test is to provide a basis for converting differential liberation data from a residual oil to a stock tank oil basis (Whitson and Brulé, 2000).

The fluid samples from Jette was analyzed in both a single stage separator test and a three-stage separator test. A summary of results are given in Table 5.1.1.1 and Table 5.1.1.2 respectively.

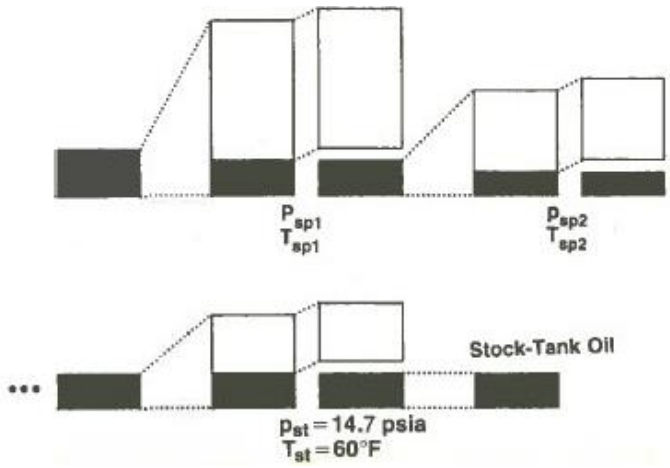

Figure 5.1.1.1: Multistage separator test showing how the saturated oil sample is brought through different separator stages at various pressure and temperature conditions before ending up at standard conditions (Whitson and Brulé, 2000).

Table 5.1.1.1 – Single stage separator results (Ravnås and Skog, 2012; Nielsen, Winsnes and Bjørsvik, 2013)

Sample	GOR (Sm^3/Sm^3)	Density of stock tank oil (kg/Sm^3)	Molecular weight of stock tank oil	Gas gravity
Recombination	112.8	838.9	197.9	0.969
PT-2550	126.4	844.3	204.3	0.912

Table 5.1.1.2 – Three stage separator results (Ravnås and Skog, 2012; Nielsen, Winsnes and Bjørsvik, 2013)

Sample	GOR (Sm^3/Sm^3)	B_o at P_{bp} (m^3/Sm^3)	Density of stock tank oil (kg/Sm^3)	Molecular weight of stock tank oil	Calculated density at P_{bp} (kg/m^3)
Recombination	101.4	1.341	830.7	187.6	701.1
PT-2550	121.7	1.414	840.9	199.0	686.4

Constant mass expansion:

CME, also called CCE, is an experiment used to determine bubblepoint pressure, density of undersaturated oil, isothermal compressibility of oil and two phase volumetric behavior of the oil at pressures below the bubblepoint. A test cell is filled with a known mass of reservoir fluid and kept at constant temperature throughout the test. The sample is initially at pressure above the bubblepoint to ensure single phase behavior. Pressure is lowered and volumetric behavior of the fluid is recorded. At the bubblepoint the measured volume will increase more rapidly due to the evolution of gas, thus create a discontinuity in the volumetric behavior. This discontinuity makes it easy to find the bubblepoint pressure from a pressure vs. volume plot (Whitson and Brulé, 2000). Figure 5.1.1.2 illustrates the concept of the CME together with the resulting pressure vs. volume plot indicating the bubblepoint pressure at the discontinuity.

A summary of the CME test performed on the Jette fluid samples are given in Table 5.1.1.3.

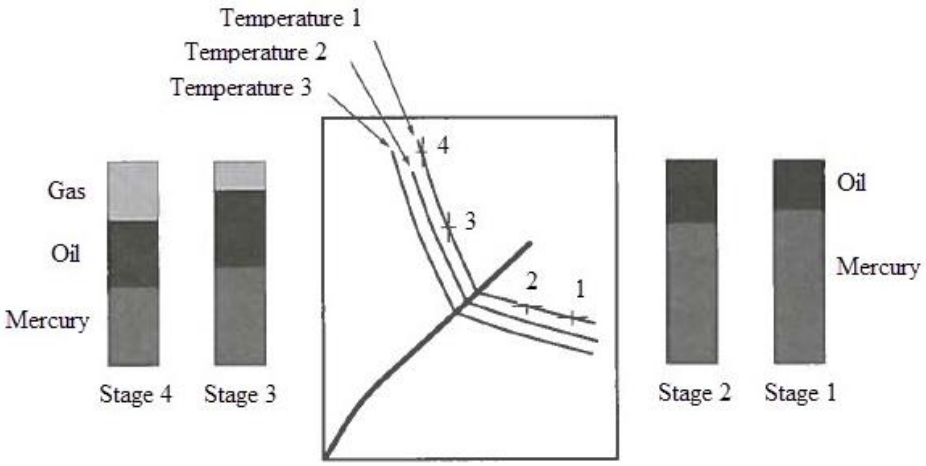

Figure 5.1.1.2: Stages involved in a CME experiment. Sample is initially at high pressure at stage 1, before pressure is reduced below the bubblepoint. The centre plot illustrates how pressure (x-axis) vs. volume (y-axis) is recorded and the discontinuity which equals the bubblepoint pressure (Carlson, 2006).

Table 5.1.1.3 – Constant mass expansion results (Ravnås and Skog, 2012; Nielsen, Winsnes and Bjørsvik, 2013)

Sample	Reservoir temperature (°C)	P_{bp} (bar)	Isothermal compressibility at P_{bp} (bar^{-1})	Viscosity at P_{bp} (cp)
Recombination	82.9	146.5	2.045E-04	0.463
PT-2550	82.9	172.3	2.290E-04	0.520

Differential liberation:

DL experiments are performed in order to approximate the depletion process in an oil reservoir and provide suitable PVT data to calculate reservoir performance (Whitson and Brulé, 2000). Figure 5.1.1.3 illustrates how the DL experiment is conducted. A sample is initially brought to its bubblepoint pressure at reservoir temperature to ensure single phase. The volume and density of the sample is recorded at the bubblepoint pressure before pressure is decreased in specified increments. Evolved gas is removed at every pressure increment (Figure 5.1.1.3) and measured together with volume of the remaining oil in the cell. Because gas is removed at every pressure increment the DL experiment is more prone to experimental error than a CME experiment which is easier to run. The final stage of this experiment is at standard conditions. The experimental results from a DL experiment is a stepwise and path dependent process which leads to variations in the obtained results based on the pressure decrements utilized (Whitson and Brulé, 2000; Carlson, 2006).

The summarized results of the DL experiment on fluid samples from Jette are listed in Figure 5.1.1.4.

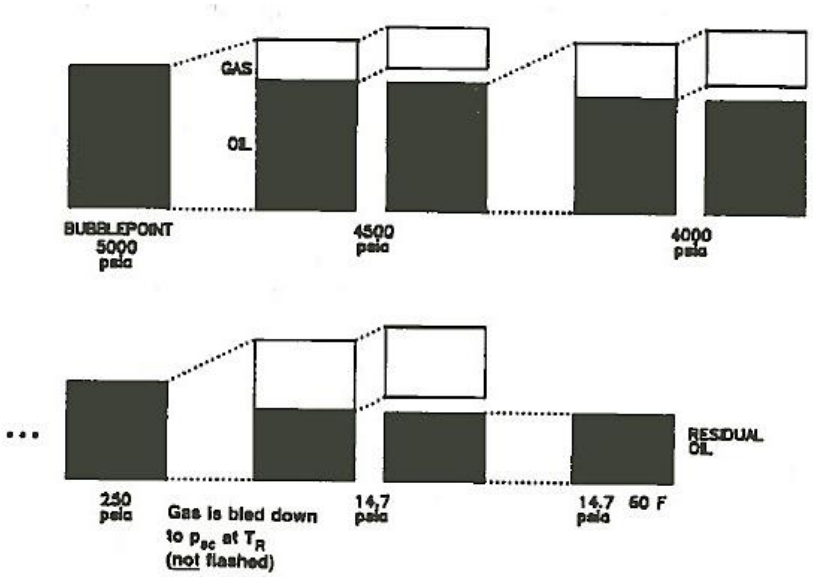

Figure 5.1.1.3: Workflow followed during a DL experiment. Gas is bled off at every pressure increment before reaching standard conditions (Whitson and Brulé, 2000).

Table 5.1.1.4 – Differential liberation results (Ravnås and Skog, 2012; Nielsen, Winsnes and Bjørsvik, 2013)

Sample	GOR (Sm^3/Sm^3)	B_o at P_{bp} (m^3/Sm^3)	Density of residual oil (kg/m^3)	Molecular weight of residual oil	Calculated density at P_{bp} (kg/m^3)
Recombination	122.7	1.4312	843.8	205.1	699.7
PT-2550	126.7	1.4284	844.8	206.4	687.9

Fluid model 1 and fluid model 2 were both created in PVTsim. They were entered and characterized as plus fraction fluids with compositions given in Table 5.1.1.5. The experiments mentioned above was simulated for both fluids using the SRK Peneloux EOS (described in Chapter 5.1.2). The fluid models had to be tuned slightly to establish match. PVTsim performs regression analysis by changing a set of fluid parameters. In this case the molecular weight, critical temperature, critical pressure and acentric factor of the plus fraction components were allowed to be tuned in order for a match to be obtained between the EOS model and the experiments. A discussion of the resulting match is given in Chapter 5.1.3.

Table 5.1.1.5 – Composition of reservoir fluids used for fluid model 1 and fluid model 2 (Ravnås and Skog, 2012; Nielsen, Winsnes and Bjørsvik, 2013)

Components	Fluid model 1 (mole %)	Fluid model 2 (mole %)
Nitrogen	0.999	0.624
Carbon dioxide	0.160	0.201
Hydrogen sulphide	0.000	0.000
Methane	30.912	35.956
Ethane	7.881	8.239
Propane	7.596	6.523
iso-Butane	1.493	1.176
n-Butane	3.883	3.086
Neopentane	0.025	0.032
iso-Pentane	1.530	1.193
n-Pentane	2.224	1.735
Hexanes	2.821	2.294
Heptanes	4.323	3.864
Octanes	4.964	4.584
Nonanes	3.371	3.107
Decanes plus (C10+)	27.818	27.386
Sum	100.000	100.000

Fluid models created in PVTsim are expressed in terms of composition whilst the Jette reservoir model uses a black oil fluid formulation. Hence, an export of PVT behavior to ECLIPSE 100 format was needed. During export it is vital to specify the pressure range in the PVT tables wide enough to cover all pressures encountered during simulation. If not, the model will extrapolate from the last points in the PVT table and this will introduce errors because fluid behavior does not exhibit a linear behavior. Initial pressure in the Jette reservoir model is 195.9 bar at the WOC and because there are no injection wells at Jette it was decided that it was sufficient with a pressure range from 25 to 250 bar in the exported PVT tables. A temperature gradient of 3.5 $^{\circ}$C/100m (Det norske oljeselskap ASA, 2011b) was used to estimate R_{so} as a function of depth (Table 5.1.1.6). Fluid properties of both fluid models after

export to ECLIPSE 100 are summarized in Table 5.1.1.7. Water have been modeled similarly for the entire Jette field using a salt concentration of 60,000 ppm.

Exported fluid models were entered in ECLIPSE 100 as tables under the keywords PVTO, PVDG and PVTW. PVTO is used for live oils and the input table lists oil formation volume factor, R_{so} and oil viscosity as function of pressure. PVDG is used for dry gases, gas with no vaporized oil, and has gas formation volume factor and gas viscosity as function of pressure in the input table. It is important that the entered tables in ECLIPSE 100 are smooth in order to reduce numerical issues when the simulator calculates derivatives from values in the tables. One table is needed for each fluid model in the reservoir model (ECLIPSE Reference Manual, 2012). PVTNUM was used to divide the Jette dynamic reservoir model in two fluid systems according to the sealing fault added in Chapter 7.3.1 and what was discussed in Chapter 5.1. The PVT zonation is illustrated in Figure 5.1.1.4.

Table 5.1.1.6 – Solution gas-oil ratio as a function of depth for the new fluid models

Depth (mTVD MSL)	Fluid model 1 R_{so} (Sm^3/Sm^3)	Fluid model 2 R_{so} (Sm^3/Sm^3)
2000.0	132.7	142.3
2015.7	128.4	136.9
2031.3	124.3	131.8
2047.0	120.2	126.9
2062.7	116.3	122.3
2078.3	112.5	117.8
2091.0	109.4	114.4
2094.0	108.7	113.6

Table 5.1.1.7 – Fluid parameters for the two created fluid models

	Fluid model 1	Fluid model 2	
Reference Pressure	195.9	195.9	bara @ WOC
Reservoir Temperature	82.9	82.9	°C
Bubblepoint Pressure	141.4	175.3	bara
R_{so} (@ref.pressure)	109.4	114.4	Sm^3/Sm^3
Salinity	60,000	60,000	mg/l
Oil Density	840.6	801.3	kg/Sm^3
Water Density	1,041	1,041	kg/Sm^3
Gas Density	1.169	1.079	kg/Sm^3
B_o (@ref.pressure)	1.354	1.354	rm^3/Sm^3
μ_o (@ref.pressure)	0.520	0.524	cP

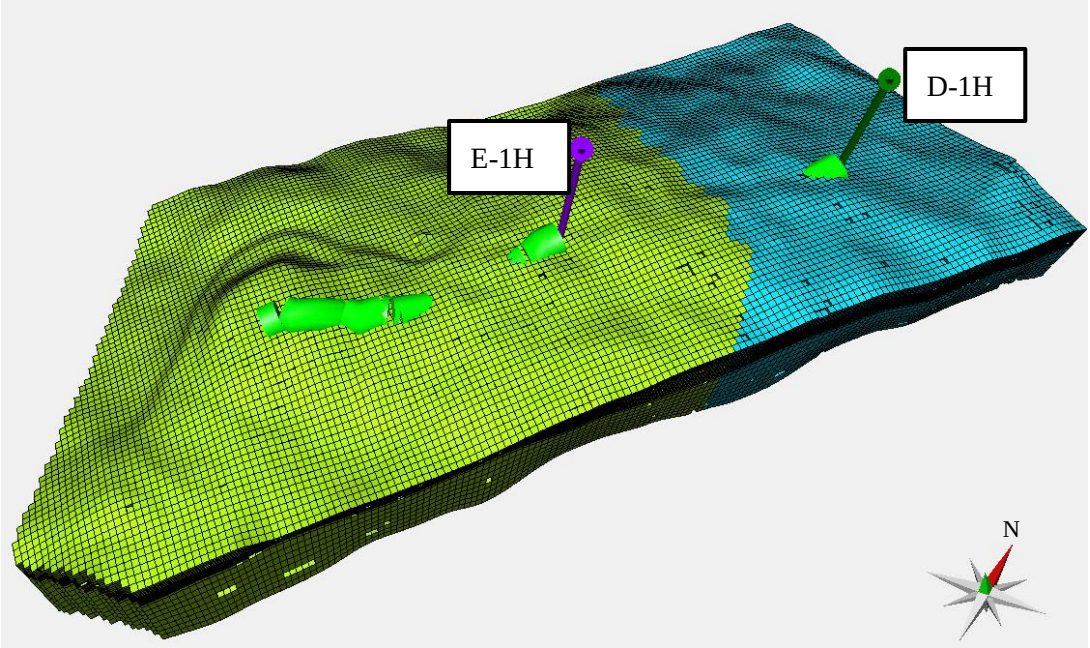

Figure 5.1.1.4: PVT zonation in the Jette dynamic reservoir model. Fluid model 1 is located to the south (green) and fluid model 2 (blue) to the north. A sealing fault separates the two fluid systems.

5.1.2 SRK PENELOUX

An EOS is an analytical expression relating pressure, temperature and volume for pure components or mixtures of components. The Soave-Redlich-Kwong (SRK) EOS is perhaps the most commonly used EOS to represent hydrocarbon reservoir fluids. The SRK EOS belongs to the van der Waals family of EOS models and is given in Equation 5.1.2.1 (Dandekar, 2006). P expresses pressure, T the temperature, V the molar volume, R the gas constant and a and b are equation of state parameters (PVTsim Help, 2013).

$$P = \frac{RT}{(V-b)} - \frac{a\alpha}{V(V+b)} \qquad \text{Equation 5.1.2.1}$$

Equation 5.1.2.2 expresses α which is a dimensionless parameter incorporating the acentric factor, ω, and reduced temperature, T_r. A correlation parameter, m, is used with the acentric factor and is expressed by Equation 5.1.2.3.

$$\alpha = (1 + m(1 - T_r^{0.5}))^2 \qquad \text{Equation 5.1.2.2}$$

$$m = 0.480 + 1.574\omega - 0.176\omega^2 \qquad \text{Equation 5.1.2.3}$$

The SRK EOS is in its simplest form (Equation 5.1.2.1) defined for pure components. When critical point constraints are imposed to pure components a and b can be defined as given in

Equation 5.1.2.4 and Equation 5.1.2.5 respectively. T_c and P_c is critical temperature and critical pressure respectively while Ωa and Ω_b are constants of 0.42727 and 0.08664 respectively (Dandekar, 2006; PVTsim Help, 2013). Values for pure components are found from physical tables.

$$a = \Omega_a \frac{R^2 T_c^2}{P_c} \quad \text{Equation 5.1.2.4}$$

$$b = \Omega_b \frac{R^2 T_c^2}{P_c} \quad \text{Equation 5.1.2.5}$$

Since reservoir fluids consist of several components it is necessary to extend the EOS described above to consider mixtures. This is performed by employing mixing rules such as Equation 5.1.2.6 and Equation 5.1.2.7. Pure component values for *a*, *b* and α are calculated before mixing. Subscript m denotes mixed values, Z_i and Z_j the mole fraction of component i and j, k_{ij} the binary interaction parameter and a_i and a_j the constant *a* for component i and j (Dandekar, 2006). Normally some tuning is needed to adjust the EOS to model mixtures sufficiently and the binary interaction parameters are usually adjusted for this purpose.

$$(a\alpha)_m = \sum_{i=1}^{n}\sum_{j=1}^{n} Z_i Z_j \left(a_i a_j \alpha_i \alpha_j\right)^{0.5} (1 - k_{ij}) \quad \text{Equation 5.1.2.6}$$

$$b_m = \sum_{i=1}^{n} Z_i b_i \quad \text{Equation 5.1.2.7}$$

The SRK Peneloux EOS, used to create fluid models, is similar to the SRK EOS except that it uses a volume correction. Equation 5.1.2.8 gives the SRK Peneloux EOS, with the only difference from Equation 5.1.2.1 being $\tilde{V}$ and $\tilde{b}$. Expressions for $\tilde{V}$ and $\tilde{b}$ are given in Equation 5.1.2.9 and Equation 5.1.2.10 respectively. The *c* parameter is the volume translation parameter and is a function of temperature, pressure and the acentric factor (PVTsim Help, 2013). It is commonly better to use the SRK Peneloux for mixtures with lumped or plus fraction components since they imply larger volume corrections.

$$P = \frac{RT}{(V - b)} - \frac{a\alpha}{\tilde{V}\left(\tilde{V} + \tilde{b}\right)} \quad \text{Equation 5.1.2.8}$$

$$\tilde{V} = V + c \quad \text{Equation 5.1.2.9}$$

$$\tilde{b} = b + c \quad \text{Equation 5.1.2.10}$$

5.1.3 QUALITY CONTROL OF FLUID MODELS

Because an analytical EOS model (SRK Peneloux) is used to express the physical behavior of the reservoir fluids it is necessary to quality control the tuned EOS model in order to ensure that it is capable of representing the measured laboratory experiments within acceptable tolerance. The EOS model in PVTsim was tuned towards all available laboratory experiments in order to match data as accurate as possible. The quality of the match is assessed below.

Both fluid models match bubblepoint pressure measured from laboratory. Comparison of measured bubblepoint pressure and calculated bubblepoint pressure from the EOS models are given in Table 5.1.3.1. Fluid model 1 has somewhat higher deviation from the measured bubblepoint than fluid model 2. However, an error of 3.4% is considered acceptable.

Table 5.1.3.1 – Comparison of bubblepoint pressure obtained from laboratory measurements and EOS models

	Fluid model 1	Fluid model 2
Measured P_{bp} (bar)	146.4	172.3
Calculated P_{bp} from EOS model (bar)	141.43	175.26
Error (%)	-3.39	1.72

Figure 5.1.3.1 compares the calculated formation volume factor of oil in the EOS model with experimental data obtained from laboratory measurements. It is evident that fluid model 2 shows the best match and that fluid model 1 is estimated somewhat too high. This corresponds well with what was mentioned above regarding bubblepoint pressures of the two models. From calculations it is known that the error between measured and calculated behavior of the oil formation volume factor is less than 2.5% for fluid model 1 and less than 0.6% for fluid model 2. This is sufficiently accurate for modeling purposes. The entire calculation of matching error is given in Appendix D.

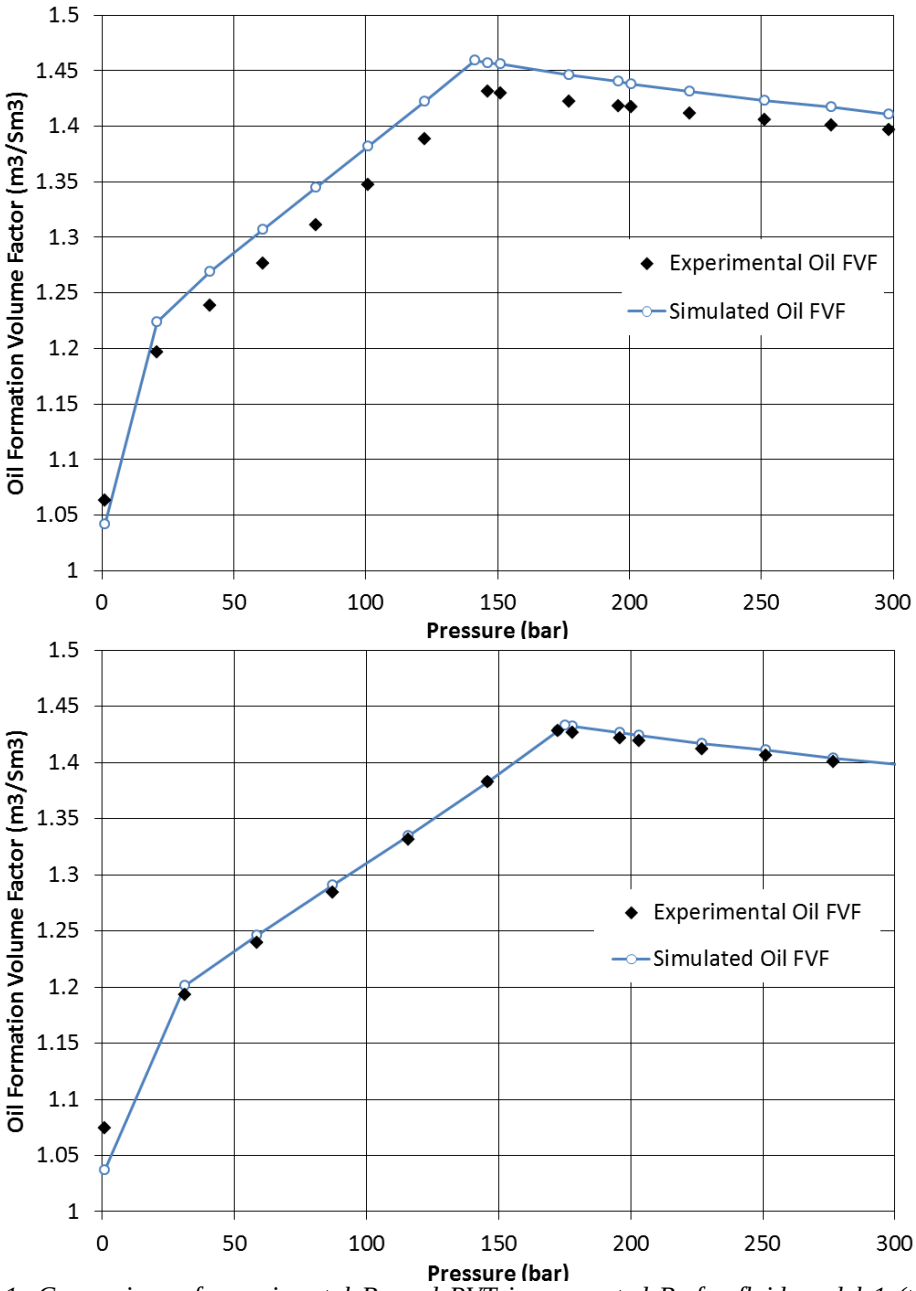

Figure 5.1.3.1: Comparison of experimental B_o and PVTsim computed B_o for fluid model 1 (top) and fluid model 2 (bottom).

A comparison of the match between measured and calculated R_{so} is illustrated in Figure 5.1.3.2. This also indicates that fluid model 1 has the largest error, and that the error is positive which leads to too high gas content in the oil. This corresponds with the overestimated oil formation volume factor of fluid model 1 (Figure 5.1.3.1 top), since higher values of the oil formation volume factor is associated with oils consisting of more gas. Fluid model 1 has an error of 5.13% in R_{so} at the bubblepoint pressure and is slightly increasing as pressure is lowered. It must be noted that the reservoir pressure in the area with Fluid model 1 is not expected to fall below bubblepoint pressure according to the BHP history illustrated in

Figure 6.3.1 for well 25/8-E-1 H. The pressure in Figure 6.3.1 is measured at 1,864 mTVD MSL and the hydraulic pressure gradient down to reservoir depth needs to be accounted for. Fluid model 2 has an error of 3.31% at the bubblepoint pressure. Both fluid models are considered to match measured experimental data for R_{so} sufficiently. However, it is considered that it might be too much gas in the system when the model is initialized.

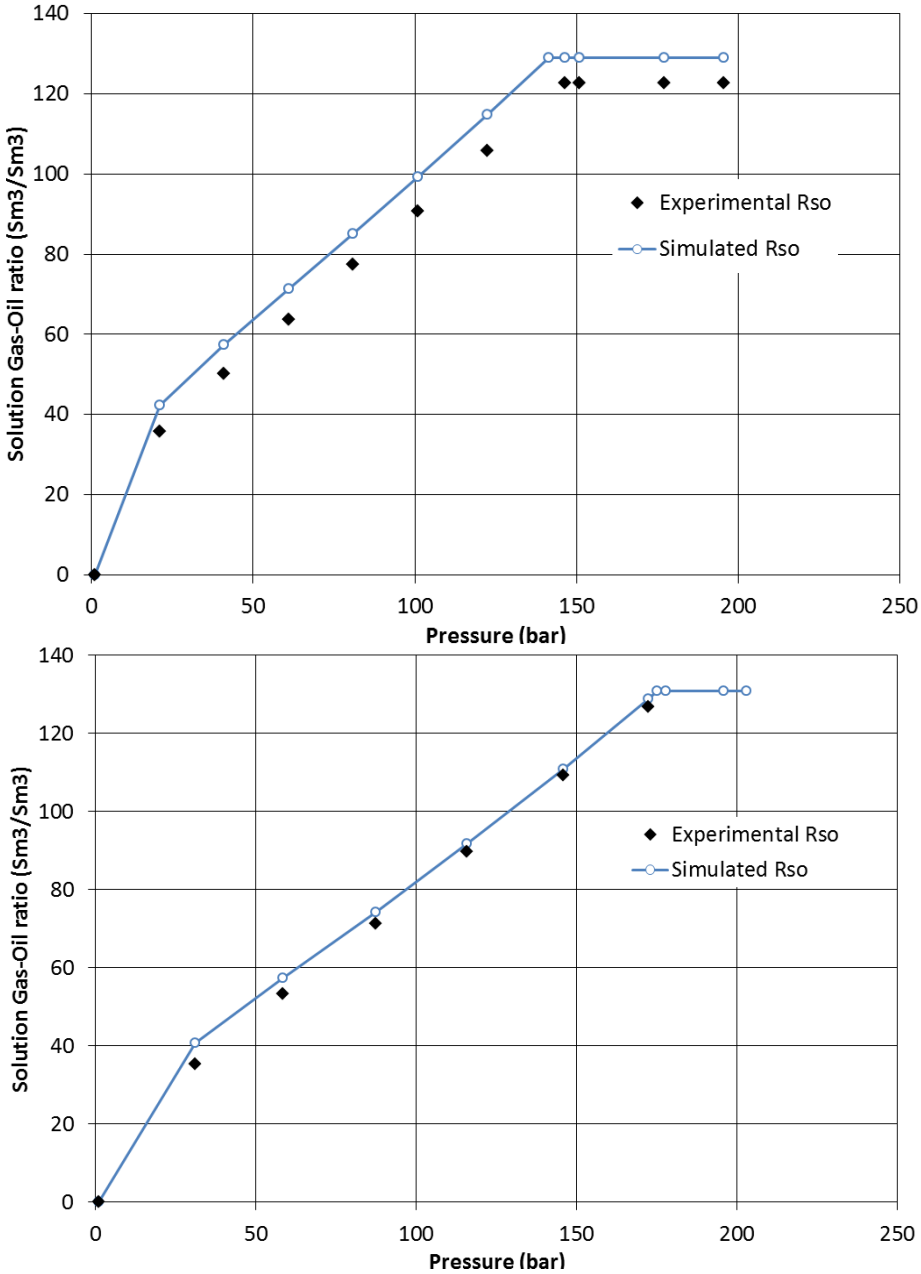

Figure 5.1.3.2: Comparison of experimental R_{so} and PVTsim computed R_{so} for fluid model 1 (top) and fluid model 2 (bottom).

Other important parameters to match besides oil formation volume factor and R_{so} include oil viscosity, oil density and gas formation volume factor. Appendix D gives a comparison of measured experimental data and data calculated from the fluid models for these properties

together with calculated error. The errors calculated for these properties are within acceptable limits and suggest that both fluid models are representative of the fluid samples taken at Jette.

Figure 5.1.3.3 illustrates the calculated phase envelopes from the created fluid models. Phase envelopes are consistent with the specified compositions in Table 5.1.1.5 because fluid model 1 is lower than fluid model 2. This is because the phase envelope of fluids with an increasing amount of heavy components are shifted down and to the right. From compositions it is seen that fluid model 2 contains approximately 5 mole% more methane, in addition to smaller amounts of other light hydrocarbon components, than fluid model 1. This verifies that the created fluid models are reasonable.

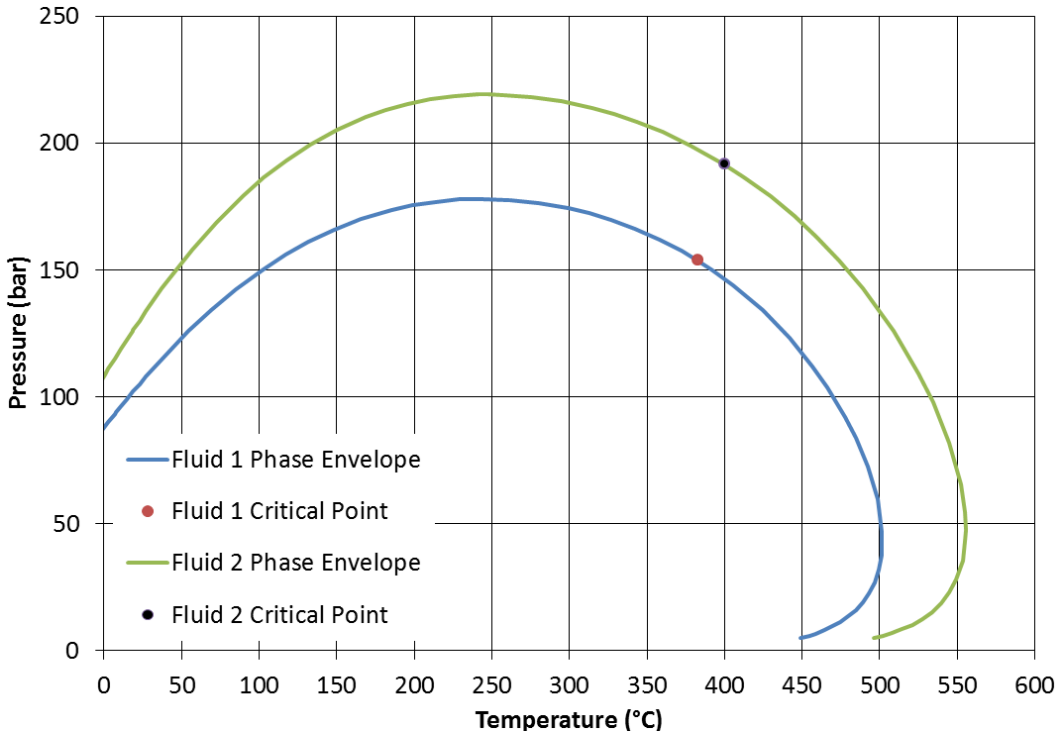

Figure 5.1.3.3: Calculated phase envelopes of fluid model 1 and fluid model 2 from tuned EOS model (SRK Peneloux).

New fluid models imply changes to the volume vs. pressure relationship for fluids in a simulation model. Hence, a new fluid model or division of one fluid model into two or more will affect calculation of fluids in place. Because of this the newly created fluid models as discussed here will lead to new volumes of oil, gas and water in the Jette dynamic reservoir model as listed in Table 5.1.3.2. The change in STOIIP is -1.76% which is well within the 20% uncertainty of STOIIP described in Chapter 4.2.1. The reduction in oil is explained by the oil formation volume factor in fluid model 1 being higher than that of the previous fluid model.

Table 5.1.3.2 – Difference in volumes of fluid in place in the Jette dynamic reservoir model due to change of fluid models			
	Oil (Sm^3)	Gas (Sm^3)	Water (Sm^3)
Old fluid model (1 fluid system)	6,226,452	746,433,954	195,871,118,695
New fluid model (2 fluid systems)	6,116,582	717,381,872	195,872,912,232
Error (%)	-1.76	-3.89	9.15E-04

5.2 WELL SPECIFICATIONS

It is important that wells in the Jette dynamic reservoir model are located correctly and with the same properties as the drilled wells if the reservoir behavior is to be replicated realistically. All available well and completion data should be used to validate wells in the reservoir model. Log data from wells can be used to verify model properties if the grid blocks where wells are located match properties measured from logs. The validation of wells in the Jette reservoir model is described below.

5.2.1 WELL LOCATION AND COMPLETION

The best way to ensure that wells in a reservoir simulation model is located correctly is to compare the coordinates in the model with those measured from a well deviation survey. Petrel was used to compare coordinates between the model and deviation surveys since the deviation survey together with the correct completion range had been loaded into the software when the geological model was built. In order to compare location and completion specifications the Jette dynamic reservoir model was imported into Petrel such that the model coordinates was loaded into the same coordinate system. Figure 5.2.1.1 illustrates a comparison of the well trajectory in the Jette dynamic reservoir model and the deviation survey for both wells. It is seen from Figure 5.2.1.1 that both wells in the Jette dynamic reservoir model, D-1H and E-1H, match the coordinates from their respective deviation survey. The reason why the well trajectory from the deviation survey starts before the well trajectory from the Jette dynamic reservoir model is because the modeled wells have only coordinates defined within the reservoir model itself, hence the well trajectory before the first connection in the reservoir model is assumed vertical. However, this is not a problem because it is only in the reservoir we are interested in validating well locations. From Figure 5.2.1.1 it

is obvious that wells in the model does not have a continuous well trajectory such as the well trajectories from the deviation surveys. This is because wells in the reservoir model are connected to the center of the grid blocks they encounter along their supplied trajectory, resulting in a stair step feature such as that seen in Figure 5.2.1.1. The stair step feature follows the deviation survey closely and model wells are considered to be located correctly in the model. Even though wells in the reservoir model are located correctly according to the well deviation surveys, there is still some associated uncertainty in the deviation survey. This may be up to a few meters.

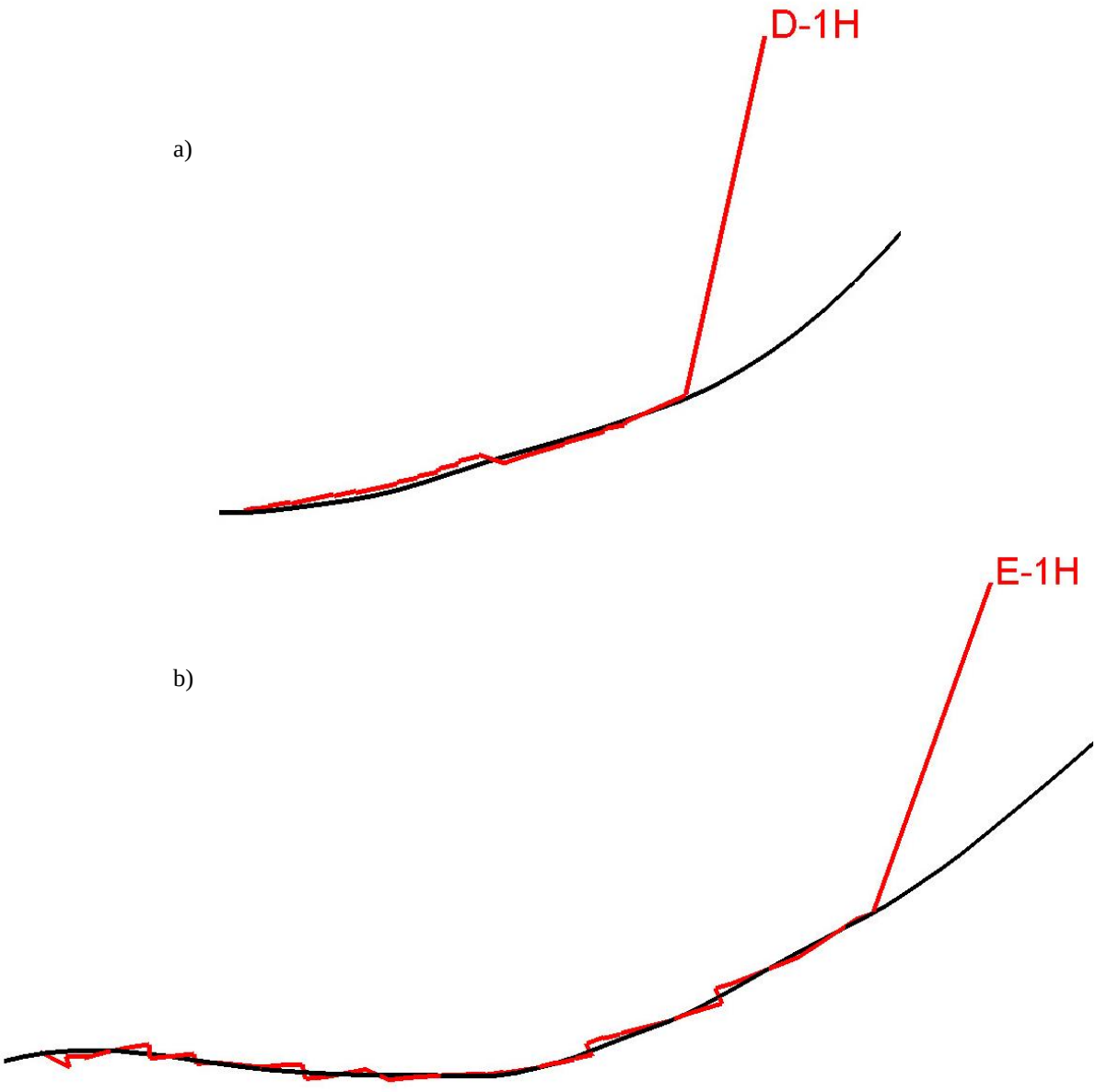

Figure 5.2.1.1: Comparison of well trajectory from well deviation surveys (black) and the Jette dynamic reservoir model (red) for well D-1H, a), and E-1H, b). The vertical section of the model wells connects with the first connection in the reservoir model. A stair step feature is seen because of the well trajectory from the reservoir model is based on the connections with grid blocks.

Validation of well and completion properties were performed based on well and completion schematics available from planning and drilling of well 25/8-D-1 AH T3 and 25/8-E-1 H. The utilized well and completion schematics are attached in Appendix B. It was noticed that well D-1H had a perforation diameter of 7.5″ in the reservoir model. Completion schematics indicated that 8.5″ was the correct perforation diameter for well D-1H and this was quickly corrected in Petrel using the completion manager (Det norske oljeselskap ASA, 2013b). A change in perforation diameter affects the calculation of connection factors performed by Petrel when wells are exported to the grid. Further details about how connection factors are calculated is given in Chapter 5.3.1. New connection factors for well D-1H was exported from Petrel and added to the Jette dynamic reservoir model in order to represent completions correctly. Table 5.2.1.1 summarizes the completion specifications of wells in the Jette dynamic reservoir model. A slight mismatch is seen in the model where well E-1H has end of completion at 4,354 m MD RKB when it should actually be at 4,384 m MD RKB. However, this mismatch of 30 meters in completion length at the end of the string is not believed to affect well behavior because the reservoir quality at this location is poor and considered non-pay. This can be seen in Figure 5.2.1.2 where an extraction from the well log is illustrated. From the above mentioned it is concluded that the location and completions of wells in the Jette dynamic reservoir model are representative of the actual wells drilled at Jette.

Finally, the datum depth had to be changed because the current setting was that calculated BHP was given at the depth of the first completion. If the calculated BHP in the model is to be compared with the pressure measured at the gauges the datum depth must be the same. Hence, the datum depth was changed to 1,622 m TVD MSL and 1,864 m TVD MSL for well D-1H and E-1H respectively.

Table 5.2.1.1 – Completion specifications of wells in the Jette dynamic reservoir model

Well	*Perforation diameter (in)*	*Start of completion (m MD RKB)*	*End of completion (m MD RKB)*	*Length of completion (m)*	*Datum Depth (m TVD MSL)*
D-1H	8.5″	2,419	2,977	558	1,622
E-1H	9.5″	3,163	4,354	1,191	1,864

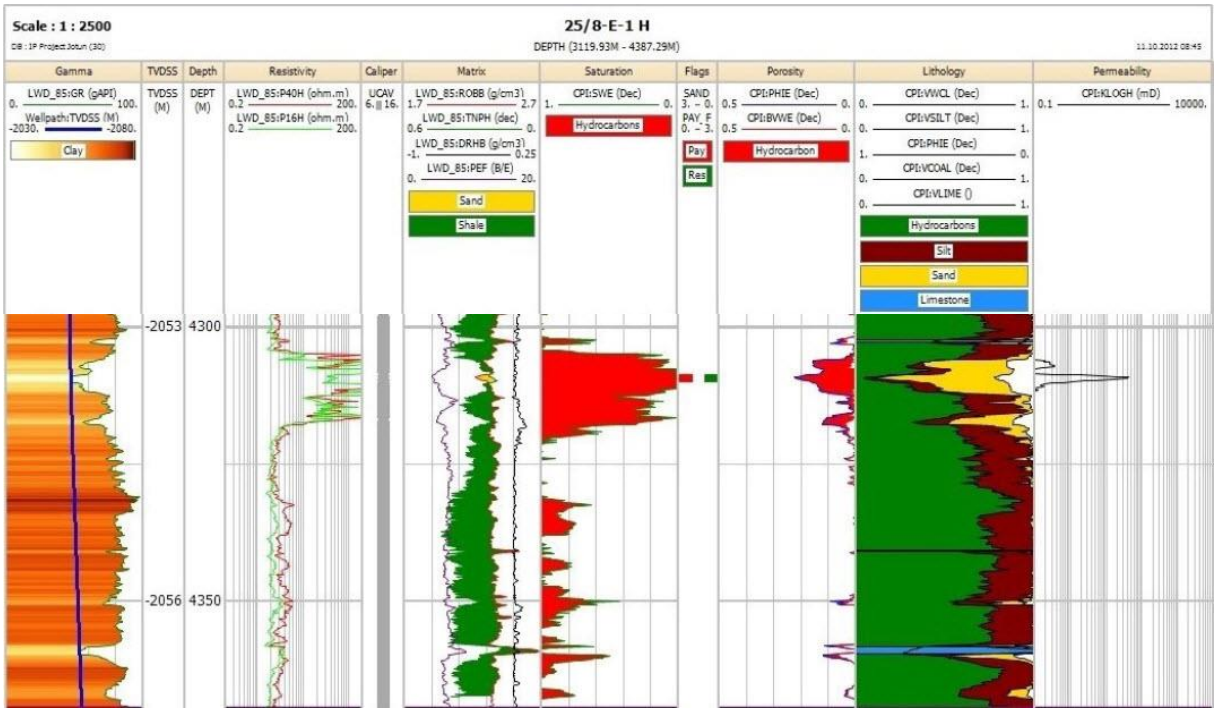

Figure 5.2.1.2: Extraction from the 25/8-E-1 H well log indicating that the reservoir quality between 4,354 m MD RKB and 4,384 m MD RKB is poor (Det norske oljeselskap ASA, 2013e).

5.2.2 COMPARING WELL LOGS WITH MODEL PROPERTIES

Log data from drilled wells at Jette gives important information about the reservoir and how it should be modeled. The properties in the Jette dynamic reservoir model should in principle be similar to those measured by logs along well trajectories to ensure a realistic reservoir model. However, logs will never match perfectly with properties from the reservoir model due to differences in scale. Hence, model properties will usually be an average of several log readings for the interval represented by the grid blocks. Due to this logs should be compared qualitatively against model properties rather than quantitatively.

Several wells are drilled at Jette and Figure 5.2.2.1 gives an overview of wells with available log data for comparison with properties in the reservoir model. Available log data includes porosity, water saturation and permeability. It must be noted that logs from the wells at Jette have not been calibrated with core samples (no core samples collected at Jette) and that there are major uncertainties related to the interpreted log data. Even though log data are uncertain they will still give a good indication of the possible property values along well trajectories.

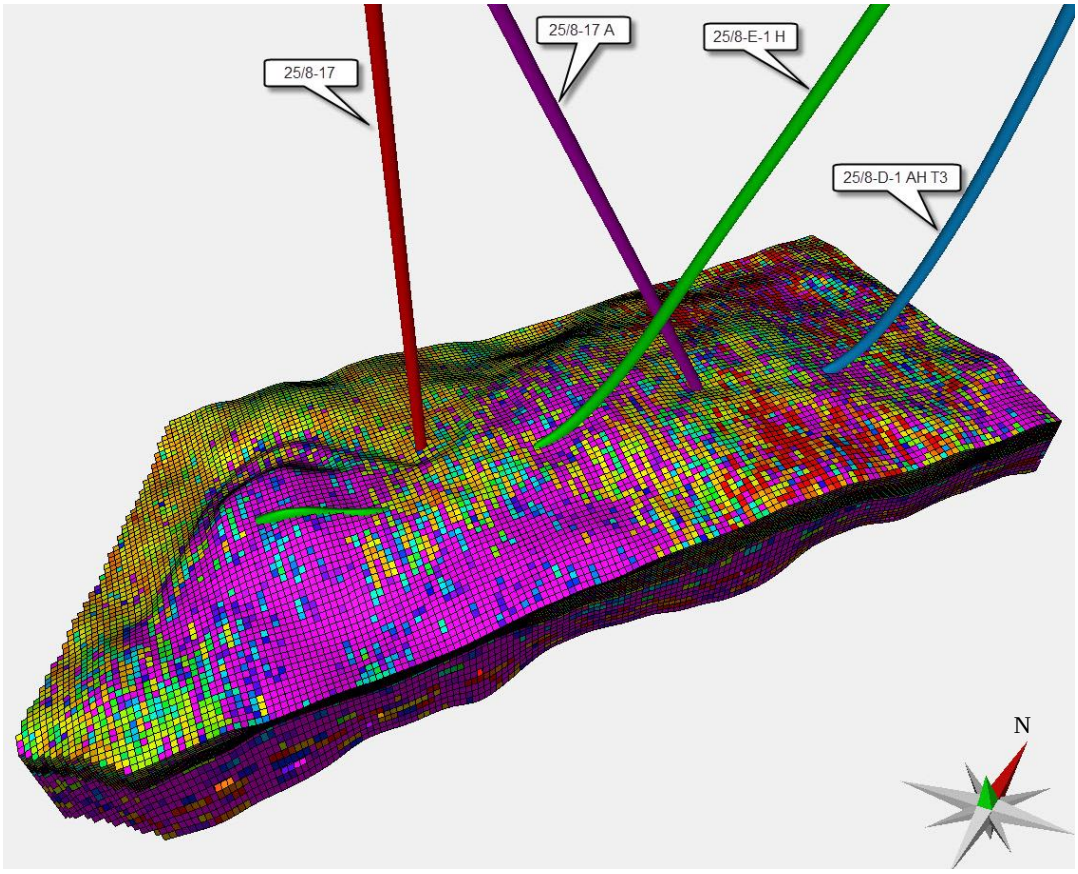

Figure 5.2.2.1: Overview of wells used for comparison of log data with model properties along well trajectories.

When the geological model was first populated it was constrained from log data of all available wells. This way the log data was honored in the reservoir model, but because the reservoir model was upscaled prior to history matching it was necessary to check if the log data was still honored in the model. From the available log data, water saturation and porosity is the most important measurements to match. This is because there are too much uncertainty related to permeability because no core samples have been taken in order to establish good correlations. Also, the permeability from logs does not represent the permeability anisotropy that was a result of upscaling the horizontal and vertical directions with different algorithms. Hence, permeabilities in the reservoir model will not be directly comparable with the logged permeability values.

A comparison of log and model for porosity and water saturation is given in Figure 5.2.2.2 and Figure 5.2.2.3, for well 25/8-E-1 H and 25/8-D-1 AH T3 respectively. Porosity and water saturation from the Jette dynamic reservoir model match the logged data sufficiently. It is seen from Figure 5.2.2.2 and Figure 5.2.2.3 that there is a difference in scale, as mentioned above, such that model properties represent an average log value in areas where values of the log data fluctuates. Comparison of log and model properties for wells 25/8-17

and 25/8-17 A is given in Appendix E. The match between log and model properties are equally good as that illustrated for the two producing wells in Figure 5.2.2.2 and Figure 5.2.2.3. Comparison of log and model permeability is also given for all four wells in Appendix E.

No major differences between log data and data along well trajectories in the Jette dynamic reservoir model has been observed. Hence, it is concluded that the reservoir properties after upscaling still represent log data accurately and that the current properties in the Jette dynamic reservoir model form a geologically consistent starting point for history matching.

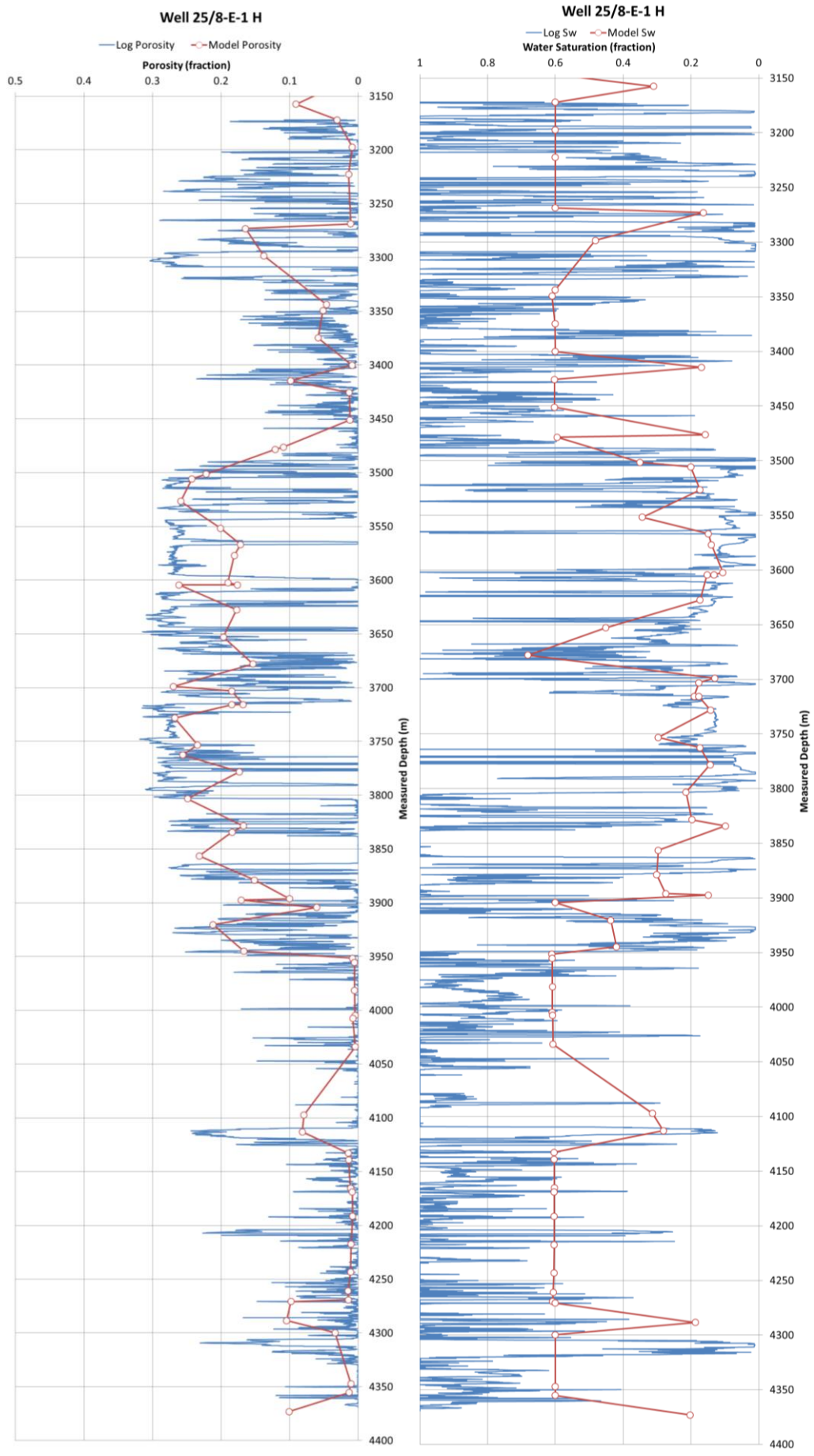

Figure 5.2.2.2: Comparison of model and log for porosity and water saturation along well 25/8-E-1 H.

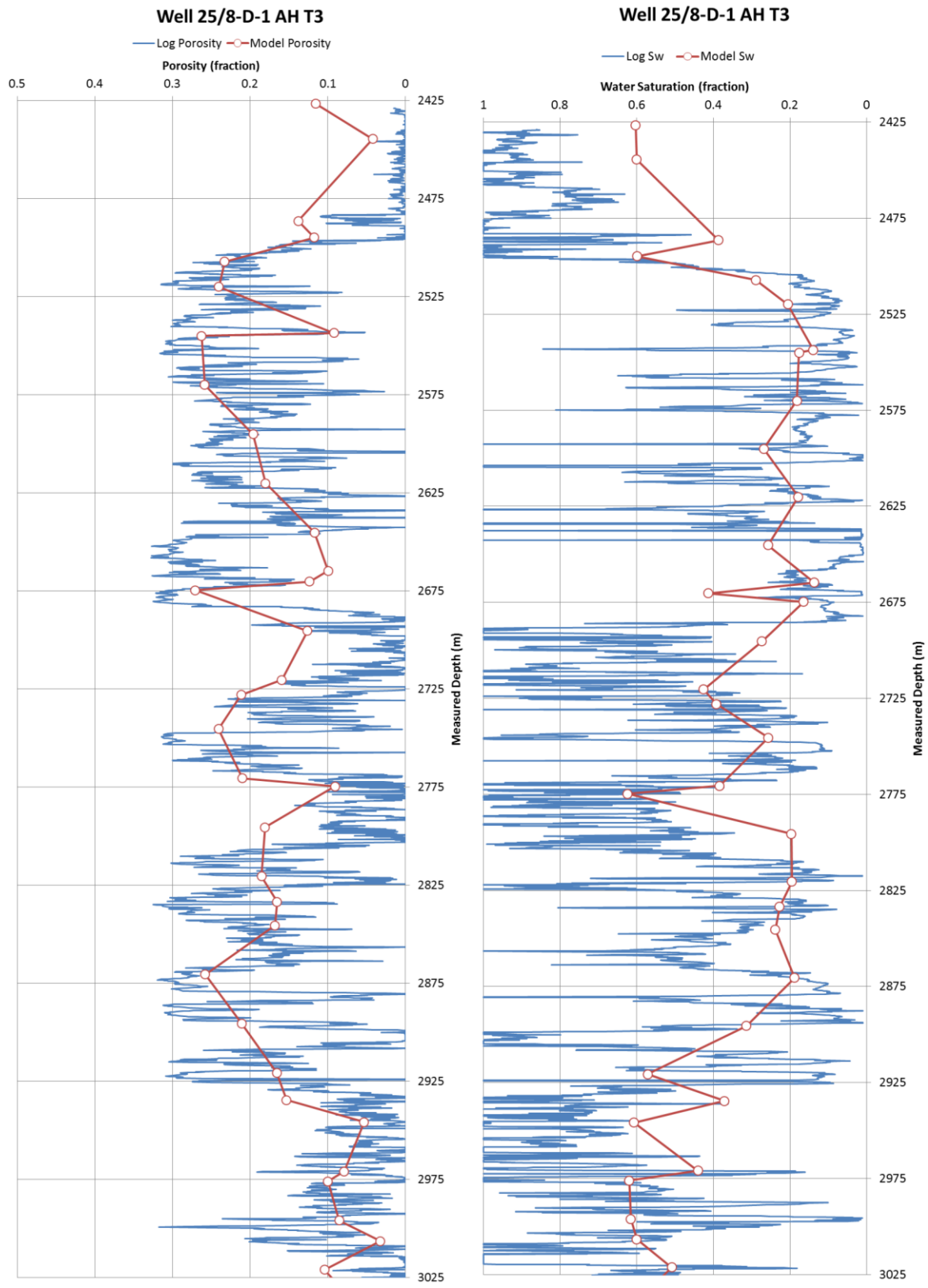

Figure 5.2.2.3: Comparison of log and model for porosity and water saturation along well 25/8-D-1 AH T3.

5.3 VERTICAL FLOW PERFORMANCE OF WELLS

A reservoir management modeling system can be thought of as four interacting subsystems. The four subsystems are represented by the reservoir model, well model, wellbore model and surface model as illustrated in Figure 5.3.1 (Fanchi, 2006). The models listed above need not all be included in a reservoir simulation study, but the standard is to include at least the reservoir model and the well model. The reservoir model represents fluid dynamics within the porous system which constitutes the reservoir, while the well model represents extraction of fluids (or injection of fluids) from the reservoir model. However, the well model does not account for fluid flow in the wellbore from the reservoir to the surface (Fanchi, 2006). The well model can be considered as a sink or source term in the reservoir simulator. To represent flow from the reservoir to the surface it is necessary to add a wellbore model. The wellbore model is a multivariable table relating wellhead pressure with flow rate, water cut, GOR and other flow related parameters. This multivariable table is commonly known as a vertical flow performance (VFP) table when input to reservoir simulators and is usually calculated in a separate program.

In wells with artificial lift such as at Jette, it is of interest to include VFP-tables to represent flow between the reservoir and surface in order to assess and optimize the effect from artificial lift. Also, adding VFP-tables will allow for history matching of one additional parameter, namely THP, and as mentioned in Chapter 2.3.2 this will establish greater confidence to the final history match. The Jette dynamic reservoir model which was received by Det norske already included VFP-tables for both wells, D-1H and E-1H. However, these needed to be changed because they were calculated using the old fluid system. The change of fluid models from subdivision of the reservoir and creation of two fluid systems (described in Chapter 5.1) dictates that new VFP-tables are needed in order to model fluid flow from the reservoir to the surface. This is because fluid flow in the wellbore is a strong function of fluid properties. The process of creating two VFP-tables to represent flow from the reservoir to the surface for well D-1H and E-1H is described in Chapter 5.3.1.

The created VFP-tables will be used in order to constrain the reservoir model with THP during prediction of reservoir performance. It is common to perform predictions constrained by THP because this value is almost constant and can easily be controlled by valves at the wellhead or by changing conditions in the separator. Also, it will be possible to perform simulations with variations in gas lift injection rate to evaluate the performance of wells.

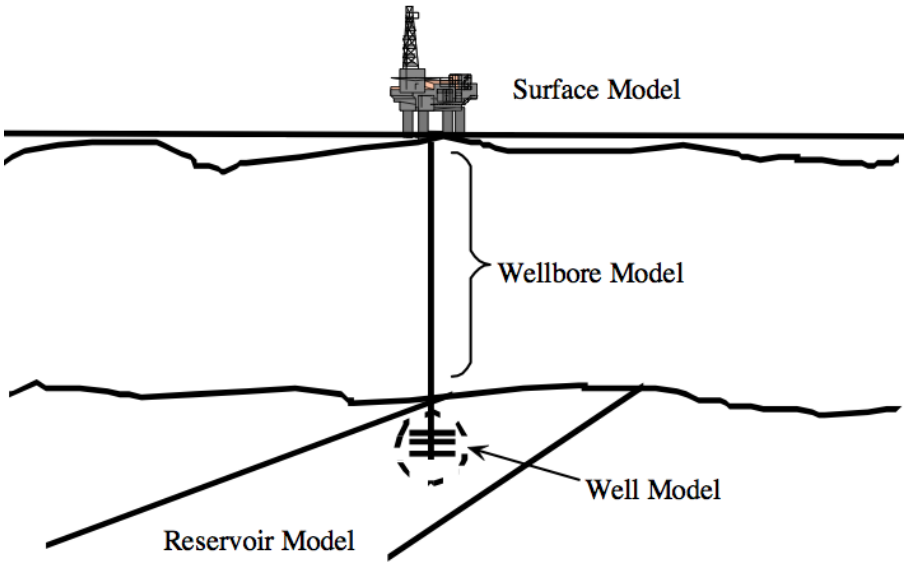

Figure 5.3.1: Different subsystems incorporated in reservoir management modeling. All subsystems are integrated in most commercially available simulators (Fanchi, 2006).

5.*3.1* *CREATING NEW LIFT CURVES*

VFP-tables for well D-1H and E-1H in the Jette dynamic reservoir model were created in WellFlo which is a commercially available software from Weatherford. The input in WellFlo is based on previous work performed by Weatherford Petroleum Consultants AS for Det norske and was edited in order to be entered into the Jette dynamic reservoir model.

The deliverability of a producing well is determined from an IPR and a tubing performance curve (TPC). A TPC expresses the pressure loss required to lift the fluid in the tubing from the reservoir to the surface. The TPC can for instance be specified for a given wellhead pressure and will then give the required BHP for various oil production rates. Such a TPC is only valid for the wellhead pressure which it was calculated for and a new curve should be calculated for every new wellhead pressure condition (Whitson and Golan, 1996). Several parameters such as, liquid rate, GOR, water cut and artificial lift affect the calculation of the TPC and one TPC should be calculated for every value of these parameters. A collection of several TPCs is what establishes the VFP-tables that are used in the reservoir simulator. The TPC itself is calculated from empirical correlations within software packages such as WellFlo or Prosper. Figure 5.3.1.1 illustrates a set of TPCs calculated for various wellhead pressures, P_{wh}, with all other parameters constant. The crossing between the TPC and the IPR represents the natural flow rate for the given operating conditions.

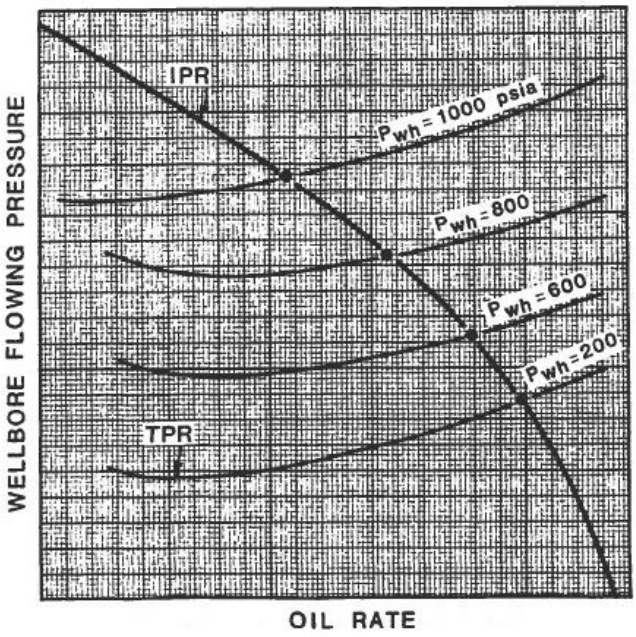

Figure 5.3.1.1: TPCs for various wellhead pressures plotted together with an IPR to establish the point of natural flow where the curves intersect (Whitson and Golan, 1996).

The IPR of the Jette dynamic reservoir model is calculated by ECLIPSE 100. When wells are coupled with the reservoir they connect with all grid blocks along their trajectory. An IPR for each connection is established and the total flow rate from a well model is the sum of flow rates from the individual connections. The IPR used in ECLIPSE 100 is given from Equation 5.3.1.1. Where $q_{p,j}$ is the production rate of phase p from connection j, $M_{p,j}$ the mobility of the phase in the connection, P_j the connection pressure, P_w pressure in the well and H_{wj} the well pressure head between the connection and the BHP datum depth. T_{wj} is the connection transmissibility factor given in Equation 5.3.1.2. It depends on the geometry of the connecting grid block, wellbore radius and rock permeability. The connection transmissibility factor is automatically calculated when exporting wells from Petrel (ECLIPSE Technical Description, 2012). For further description of how ECLIPSE 100 calculates IPR the reader is advised to look up Chapter 79 of the ECLIPSE Technical Description (2012).

$$q_{p,j} = T_{wj} M_{p,j} (P_j - P_w - H_{wj}) \qquad \text{Equation 5.3.1.1}$$

$$T_{wj} = \frac{c\theta Kh}{\ln\left({}^{r_o}/_{r_w}\right) + S} \qquad \text{Equation 5.3.1.2}$$

Modeling of VFP-tables in WellFlo requires specific information about flow correlation, well trajectory, installed equipment, fluid properties and any artificial lift if applicable. The WellFlo model provided by Weatherford Petroleum Consultants AS included everything

except for the fluid models. Table 5.3.1.1 summarizes information entered in the WellFlo model regarding flow correlation and artificial lift. The wellbore deviation in the model is taken from deviation surveys which results in the same well trajectories as those in the Petrel model described in Chapter 5.2. Well profiles are illustrated in Figure 5.3.1.2.

Table 5.3.1.1 – Gas lift information entered in the WellFlo model		
Flow Correlation:	-	OLGA Steady State
Artificial Lift:	-	Continuous Gas Lift
Depth of Gas Lift Valve (GLV)	-	D-1H: 1,617 m MD RKB E-1H: 1,636 m MD RKB
Operating Pressure GLV	-	D-1H: 92 bar E-1H: 92 bar
Injection Gas Gravity	-	D-1H: 0.84 specific gravity E-1H: 0.84 specific gravity

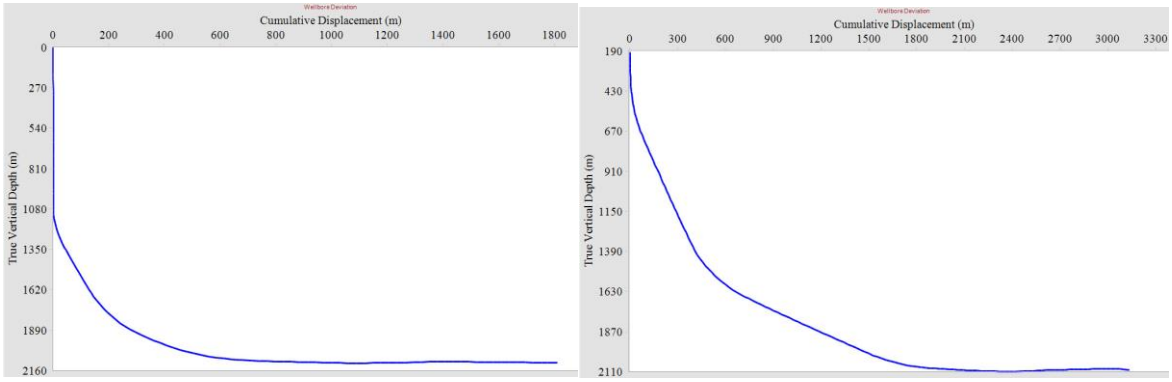

Figure 5.3.1.2: Well profile for well D-1H (left) and E-1H (right). True vertical depth refers to RKB which is 40m above MSL.

It was not possible to enter fluid models from PVTsim directly into WellFlo. Hence, the fluid models created in Chapter 5.1.1 had to be entered manually in WellFlo and laboratory experiments were matched using various correlations for the black oil parameters. The correlations used to model fluids are summarized in Table 5.3.1.2. It was established a good match in behavior of both fluid models, with a root mean square (RMS) error of 3.89% and 4.36% for well E-1H and D-1H respectively.

Table 5.3.1.2 – Correlations used to calculate black oil fluid parameters		
	D-1H	E-1H
P_b, R_{so} and B_o Correlation:	Glaso	Petrosky Frashad
Oil Viscosity Correlation:	ASTM Beggs	ASTM Beggs
Gas Viscosity Correlation:	Carr	Carr

VFP-tables were exported from the WellFlo models in ECLIPSE 100 format in order to be used in the Jette dynamic reservoir model. They were entered using the VFPPROD keyword in ECLIPSE 100. Simple hydrostatic corrections are performed by ECLIPSE 100 to correct for differences in datum depth between the VFP-tables and the wells. During export of VFP-tables it was necessary to specify values for flow properties such as liquid rate, GOR, THP, water cut and gas lift injection rate. A TPC will be calculated and tabulated for every value entered for these properties. During simulation ECLIPSE 100 will look up the TPC that corresponds with the flow dynamics of the well. Hence, it is important that values entered for the various flow properties to cover all conditions which can occur during a simulation run. Because a discrete number of TPCs are calculated ECLIPSE 100 will interpolate between curves if it is not possible to look up the exact value in the VFP-table. If flow properties are encountered outside the given range in the VFP-tables ECLIPSE 100 will extrapolate to find a value, resulting in errors since the behavior of TPCs is highly non-linear. The entry values selected in the exported VFP-tables for Jette are listed in Table 5.3.1.3. A wide range is given to ensure that values outside the range will not be encountered by the simulation model. The density of values around the common operating conditions are higher in order to ensure low interpolation errors when ECLIPSE 100 looks up values during simulation.

Table 5.3.1.3 – Specified values in calculated VFP-tables

Liquid Rate (Sm^3)	Gas Lift Injection Rate (Sm^3)	GOR (Sm^3/Sm^3)	THP (bar)	Water Cut (fraction)
10	0.0	100	10	0.0
50	30,000	110	20	0.1
100	60,000	120	30	0.2
150	100,000	150	40	0.3
200	150,000	200	50	0.5
300	200,000	300	75	0.7
500		400		0.9
1,000				0.99
1,500				
2,000				
3,000				
4,000				

5.4 MODEL INITIALIZATION

Initialization is the process of establishing a correct fluid and pressure distribution within the reservoir model. The initialization of the Jette dynamic reservoir model was described in Chapter 4.2.1. The quality of the initialization applied to the Jette dynamic reservoir model will be discussed below.

The Jette dynamic reservoir model was initialized from a WOC located at 2,091 mTVD MSL with a datum pressure of 195.9 bar. The depth of the WOC and datum depth are based on MDT measurements from well 25/8-17 and 25/8-D-1 H in October 2009 and May 2012 respectively. A pressure versus depth profile for both wells are shown in Figure 5.4.1. The pressure distribution established in the reservoir should equal the pressures measured with MDTs. However, the pressure distribution in the Jette dynamic reservoir model plotted in Figure 5.4.1 is seen to deviate from measurements in well 25/8-D-1 H by 1 bar and from well 25/8-17 by 2.5 bar. The location of the wells can be seen in Figure 5.1.1. The 1 to 2 bar difference in pressure measurements of well 25/8-17 and 25/8-D-1 H is believed to be caused by production at Jotun between October 2009 and May 2012 when the MDT surveys were obtained. Because of the compartmentalization of the reservoir, discussed in Chapter 5.1, it is uncertain if well 25/8-17 has experienced the 1 to 2 bar depletion due to production at Jotun since it is uncertain if these are in hydraulic communication.

Figure 5.4.1 contains pressure versus depth for all wells, including 25/8-17 and 25/8-17 A for observation, in the Jette dynamic reservoir model. Figure 5.4.1 indicates that the Jette dynamic reservoir model has been initialized with pressures too low compared with the MDT surveys. However, the gradients used during initialization of pressure shows a good match with the gradients obtained from the MDT surveys. The Jette dynamic reservoir model has been initialized using the same settings for the whole reservoir. Because of the compartmentalization introduced in Chapter 5.1 it might be more correct to initialize the model using two regions, similar to the fluid zonation (Figure 5.1.1.4) established in Chapter 5.1.1. This way Jette south would be modeled to match the pressure distribution indicated from the MDT in well 25/8-17 while Jette north would be initialized according to the MDT in well 25/8-D-1 H. A pressure increase of 2.5 bar at Jette south and 1 bar at Jette north would be needed to obtain a perfect initialization of pressure distribution in the Jette dynamic reservoir model. However, the pressure distribution obtained from the current initialization will not be changed because the operator of Jette, Det norske, has recommended the current settings for initialization. Even if the pressure distribution in the Jette dynamic reservoir model had been changed in order to match the MDT surveys by increasing pressure it would not change the response of the model significantly, due to a maximum change in pressure of 2.5 bar.

The best way to validate initialization of pressure in the Jette dynamic reservoir model would have been to run the model from the date of the first MDT survey and force the simulator to print pressure in wells at the date of consecutive MDT surveys. In the time

between MDT surveys production from Jotun would be represented by a ”dummy-well” in the Jette dynamic reservoir model. This way it would have been possible to check if the pressure difference between well 25/8-17 and 25/8-D-1 H is caused by depletion from Jotun. And if a good match was obtained the model could have been simulated until the starting date of Jette (20.05.2013) to obtain the correct initialization pressure. Unfortunately it has not been time to perform this process but it is recommended to conduct such simulations as part of further work.

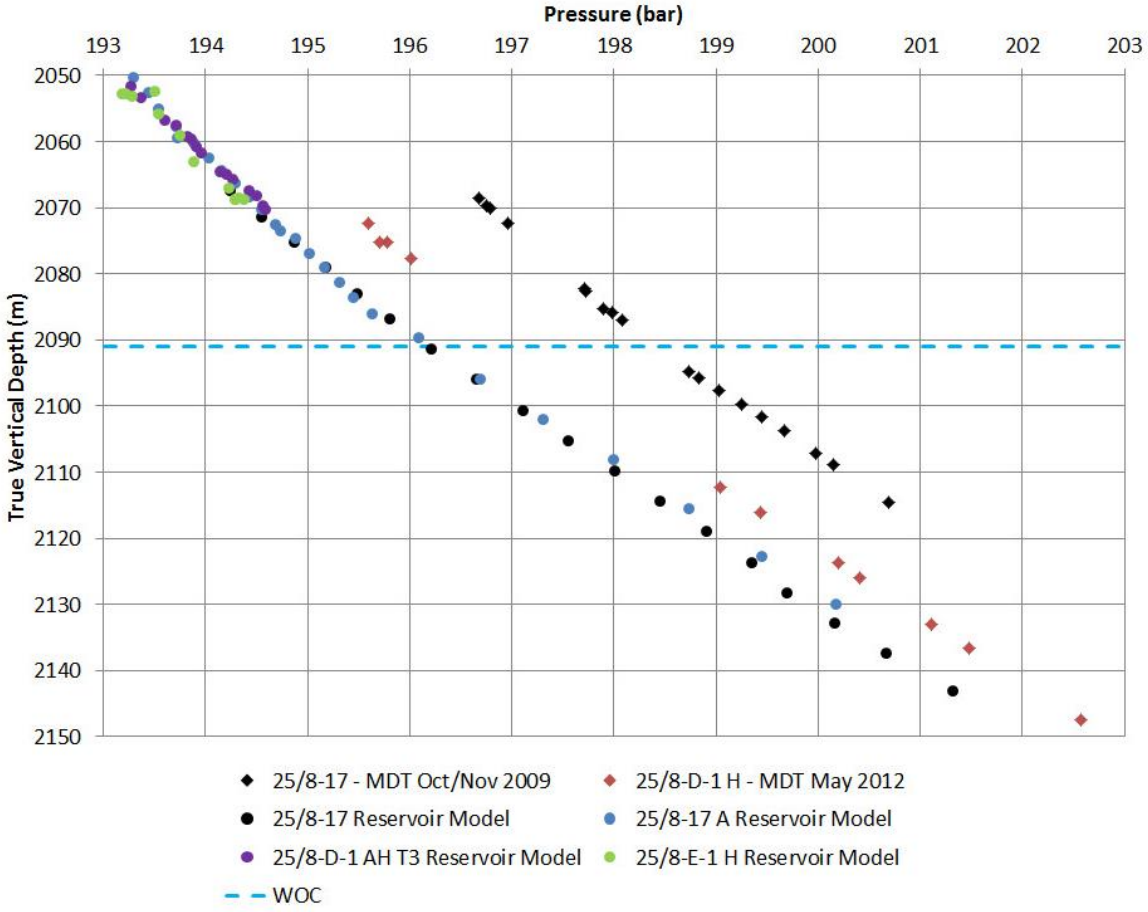

Figure 5.4.1: Pressure profiles obtained from MDT surveys in well 25/8-17 and 25/8-D-1 H together with pressure profiles from wells in the Jette dynamic reservoir model at the 20th of May 2013.

Saturation distribution in the Jette dynamic reservoir model is based on static gravity capillary pressure equilibrium. This method calculates grid block saturation based on the capillary pressure curve derived from a Leverett J-function (Chapter 4.2.1). Capillary pressures in the reservoir model are calculated from a known fluid contact using gradients and an average saturation is assigned to grid blocks. A final check to see if the reservoir has been initialized properly is to run the model with no wells. A model initialized from a static gravity capillary pressure equilibrium is expected not to show any variation in saturations or pressures when

running without any production or injection wells. If there are any saturation changes within the model this may indicate problems with the initialization (Lorentzen, 2013).

The Jette dynamic reservoir model was simulated without any wells from 20th of May 2013 until 1st of September 2013. A map of the saturation difference during the run was created in order to identify saturation changes. The difference in oil saturation for the Jette dynamic reservoir model in the period between 20th of May 2013 and 1st of September 2013 is illustrated in Figure 5.4.2 (Lorentzen, 2013).

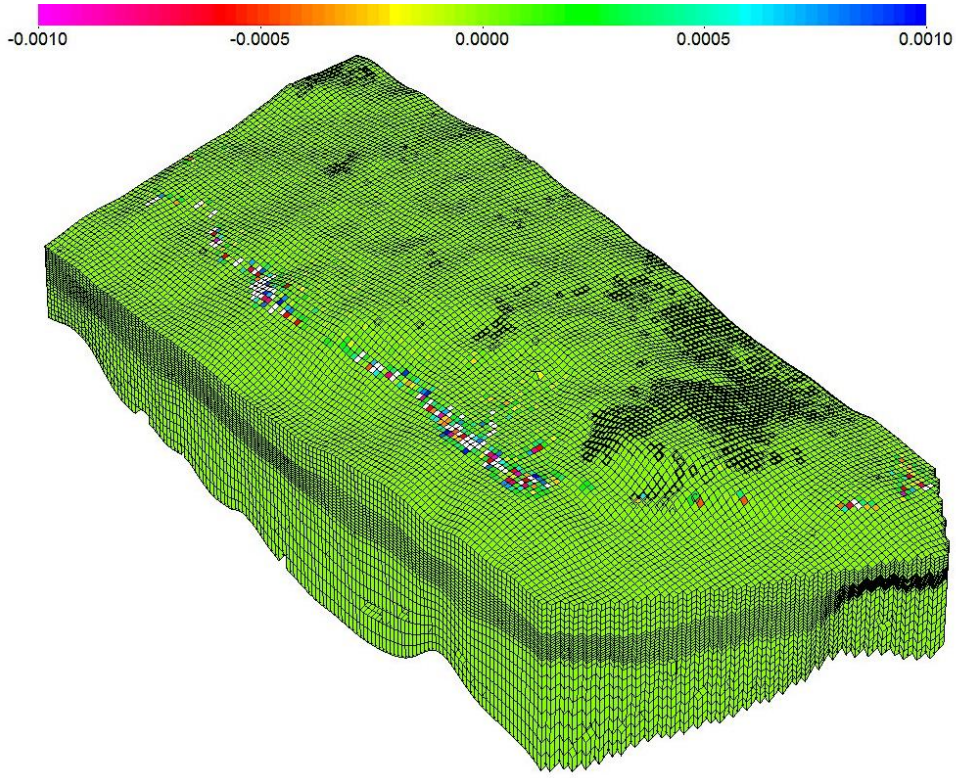

Figure 5.4.2: Difference in oil saturation between 20th of May 2013 and 1st of September 2013 when running the Jette dynamic reservoir model without any production from wells (Lorentzen, 2013).

Difference in oil saturation ($\Delta S_o = S_o(20.05.13) - S_o(01.09.13)$) would result in zero if the model was perfectly initialized from static gravity capillary pressure equilibrium because an equilibrium between gravity and capillary pressure implies no fluid flow within the model. However, as seen in Figure 5.4.2 there are several non-zero grid blocks close to the WOC in the Jette dynamic reservoir model. Grid blocks shown in white are outside the scale (-0.001 to 0.001) and indicates the largest saturation changes. The largest saturation changes are in the range of 0.1 which are well above what would have been expected for a static system in equilibrium (Lorentzen, 2013).

To investigate and explain the phenomenon of changing saturations along the WOC two small two-dimensional grids cut from the Jette dynamic reservoir model has been used. It was observed that most grid blocks along the WOC were tilted such that grid blocks are having significant parts above and below the WOC. Because of this, initialization becomes difficult since the averaging of saturation and pressure assigns only one value for each grid block. Considering a tilted grid block with its center close to the WOC and approximately half the block size on either side of the contact. When saturation and pressure is assigned this block will be somewhat below the WOC and have high water saturation and low capillary pressure. The neighbor of this block will experience being completely above the WOC which will result in low water saturation and high capillary pressure. Originating from this situation is a pressure discontinuity. This discontinuity will result in flow within the reservoir to obtain a stable pressure equilibrium. Hence, the saturation change observed along the WOC (Lorentzen, 2013).

This phenomenon may be hard to account for but can be alleviated by having a higher grid resolution. Another method may be to initialize the reservoir by subdividing grid blocks into smaller parts when averaging values of pressure and saturation within each grid block to establish a more accurate distribution (Lorentzen, 2013).

To illustrate the phenomenon of change in water saturation along the WOC two small two-dimensional grids cut from the Jette dynamic reservoir model has been used. The intention is to illustrate the effect of tilted grid blocks along fluid contacts and that change in saturation occur due to small discontinuities in pressure and saturation, arising from assignment of wrong grid block values. Figure 5.4.3 a) illustrates the model with tilted grid blocks and an indication of WOC at initial conditions. Figure 5.4.3 b) calculates the resulting change in oil saturation between 20th of May 2013 and 1st of September 2013. It is clearly seen that the tilted blocks experience saturation changes close to the WOC. White grid blocks are outside the scale, indicating the most severe saturation changes (Lorentzen, 2013).

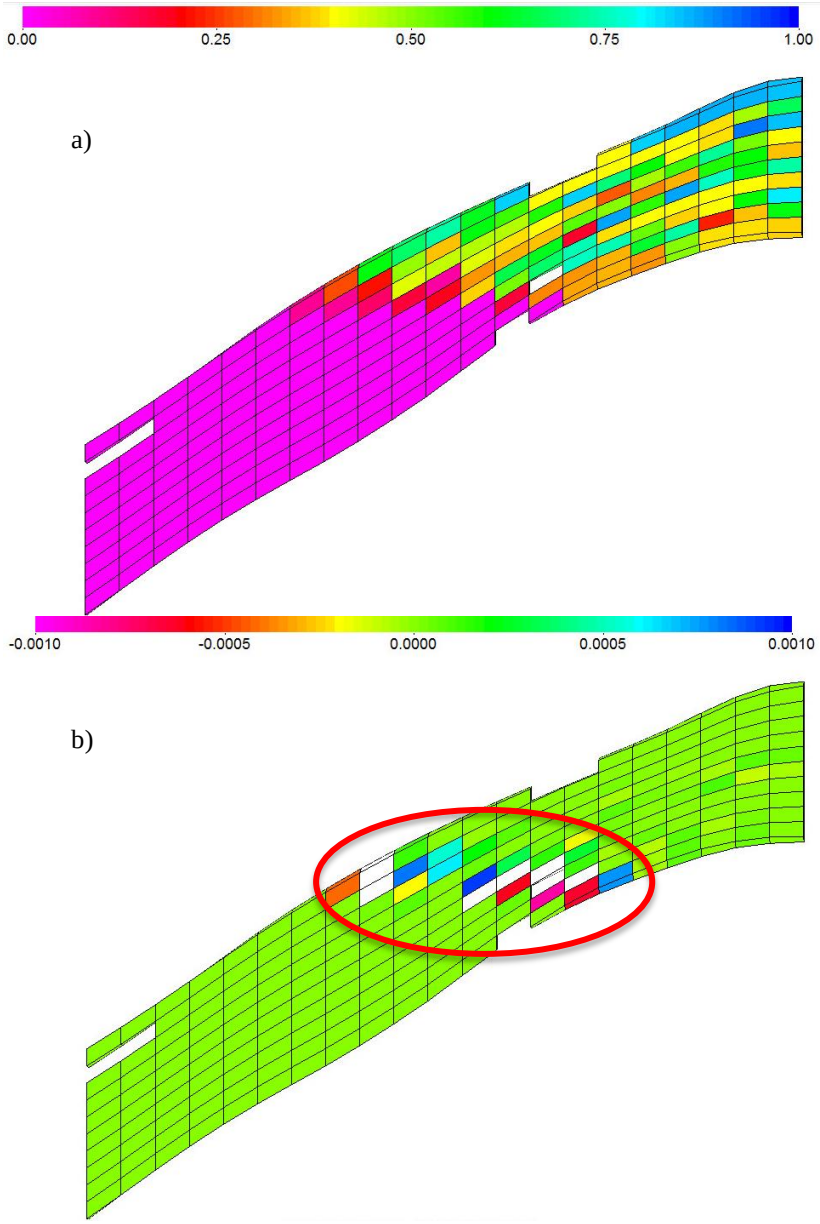

Figure 5.4.3: Two-dimensional model with WOC and tilted grid blocks, a) shows initial oil saturation and b) shows ΔS_o from 20.05.13 to 01.09.13 (Lorentzen, 2013).

To prove that the saturation changes are due to tilted grid blocks at the WOC a two-dimensional model with horizontal grid blocks and the WOC located approximately at the interface between grid blocks were cut from the grid. The initial oil saturation from this model is illustrated in Figure 5.4.4 a) where a distinct WOC is seen. When running this model without any production the resulting change in oil saturation is zero, illustrated in Figure 5.4.4 b). This indicates that saturation changes in the model when running without any production most likely arises from having tilted grid blocks along the WOC (Lorentzen, 2013). Because saturation changes in the Jette dynamic reservoir model are small (most changes are below 0.001) and constrained to an area close to the WOC it is considered not to affect the modeling of Jette. The small changes in oil saturation happens early in the simulation in order to instill

equilibrium in the fluid distribution along the WOC. After this equilibrium is reached the Jette dynamic reservoir model does not experience any changes in saturation. Hence, the Jette dynamic reservoir model is initialized sufficiently accurate.

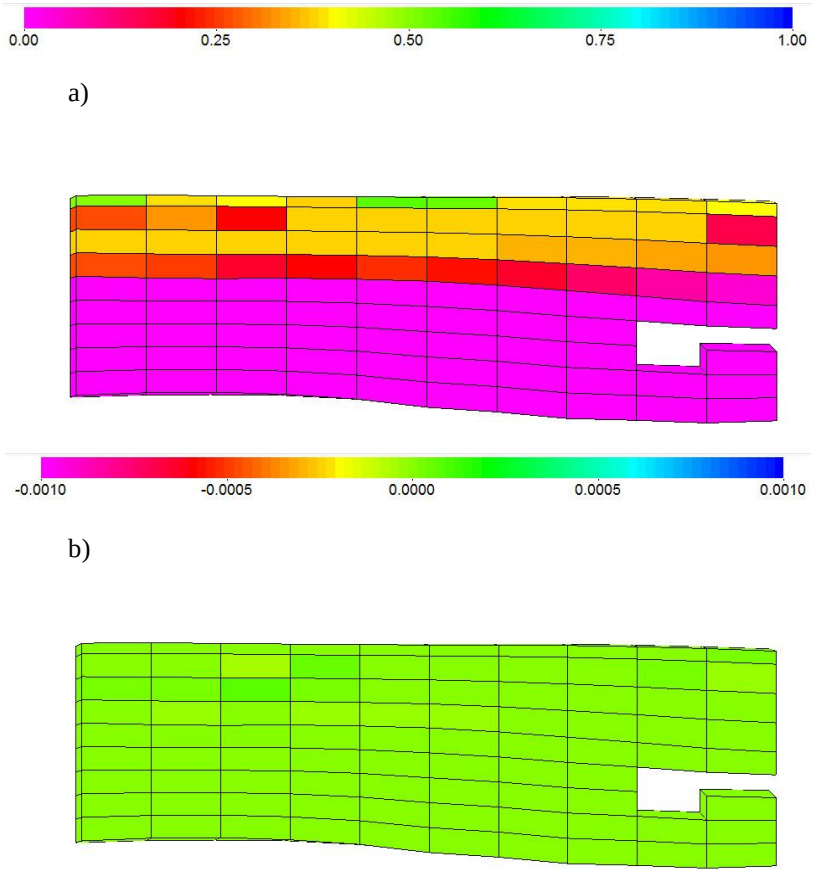

Figure 5.4.4: Two-dimensional model with WOC and horizontal grid blocks, a) shows initial oil saturation and b) shows ΔS_o from 20.05.13 to 01.09.13 (Lorentzen, 2013).

6 HISTORICAL PERFORMANCE DATA FROM JETTE

History matching of a reservoir simulation model requires historical data describing reservoir performance. This performance data will be compared with the response of the reservoir model. It was mentioned in Chapter 2.3.2 that the quality of a history match is directly proportional to the amount and quality of the historical performance data, and that matching multiple parameters will increase confidence of the matched model. Ensuring that historical performance data are representative of the actual field is key if a good history match is to be obtained, hence much effort has been focused at selecting the correct historical performance data from Jette to use during history matching. The data selected to represent reservoir performance at Jette will be described thoroughly throughout this chapter.

6.1 JETTE ALLOCATION

In Chapter 3 it was described that Jette produces from two subsea wells with commingled production tied back to Jotun B, operated by ExxonMobil. A consequence of this is that back-allocation of production needs to be performed in order to obtain individual well performance data to use during history matching. This introduces some uncertainty to the individual well performance data as allocated rates not necessarily represents the true production from wells 25/8-D-1 AH T3 and 25/8-E-1 H, herof denoted D-1H and E-1H respectively. Allocation of production between wells at Jette has been performed by Weatherford Petroleum Consultants AS, and was available through their Intelligent Daily Operations software (I-DO^{TM}). A description of how the allocation at Jette is performed is given below.

In order to perform allocation of production between wells it is necessary to acquire multi rate tests from wells on a regular basis. The main reason for regularly acquiring rate tests is that reservoir conditions change with time. Several well tests have been performed at Jette, the dates of all well tests used for allocation are summarized in Table 6.1.1. As seen from Table 6.1.1 there are only a few well tests available for well D-1H resulting in higher uncertainty in the allocated production between 20th of May 2013 and the first well test 20th of October 2013.

Table 6.1.1 – Overview of well tests used in back allocation of production at Jette

D-1H (dd.mm.yyyy hh:mm)	E-1H (dd.mm.yyyy hh:mm)
20.10.2013 10:30	05.07.2013 18:00
21.10.2013 00:00	17.08.2013 04:00
21.12.2013 05:30	17.10.2013 08:00
21.12.2013 16:15	18.10.2013 06:00
22.12.2013 05:00	18.12.2013 16:20
	18.12.2013 21:00
	19.12.2013 07:20

For each rate test a relationship between a given parameter and production rate is established. Production at Jette is expressed from a relationship with the BHP since this parameter is measured from gauges installed downhole in both wells. This inflow performance relationship (IPR) is then used to calculate a theoretical flow rate of oil for both wells (Q_{OD}^{T} and Q_{OE}^{T}). Ideally the sum of the theoretical flow rates from D-1H and E-1H should equal the measured oil rate at the MPFM topside Jotun. To account for mismatch between theoretical and measured oil rates a daily allocation factor (DAF) is calculated to obtain the final allocated oil rate for both wells (Equation 6.1.2). The DAF is calculated from Equation 6.1.1, best practice is to keep DAF between 0.95 and 1.05. However, with gas lift at Jette it is difficult to keep within this limit. Once allocated oil rates are obtained these will be used to calculate allocated gas and water rates based on measurements of GOR and water cut from previous tests (Lysne, Nakken, Totland et al., 2013). A schematic of the allocation process is illustrated in Figure 6.1.1.

$$DAF = \frac{Q_O^F}{Q_{OD}^T + Q_{OE}^T} \qquad \text{Equation 6.1.1}$$

$$Q_O^A = Q_O^T \cdot DAF \qquad \text{Equation 6.1.2}$$

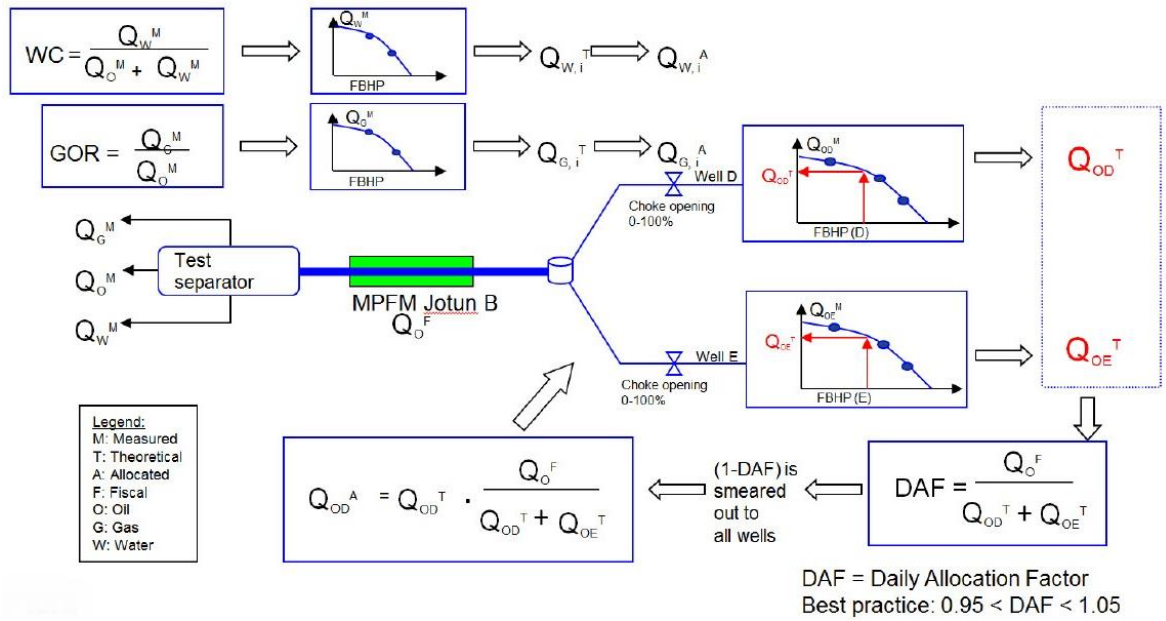

Figure 6.1.1: Allocation theory (Lysne, Nakken, Totland et al., 2013).

There is an issue affecting the credibility of the allocated rates, namely that the comingled production from Jette is not measured fiscally at the separator. This is due to Jette producing together with wells from Jotun to the same separator. The current agreement with ExxonMobil is that oil produced from Jette is given by difference. Effectively this means that Jette produces what is left at the separator after ExxonMobil has allocated what belongs to the Jotun wells. This issue was adressed and from the 7th of December 2013 until the 6th of January 2014 Jette was allowed to produce to the test separator at Jotun A without interference from production at Jotun. This period accurately represents the production from Jette and is used for comparison with selected production performance data used for history matching, presented in the next subchapter.

6.2 PRODUCTION PERFORMANCE DATA

Production performance data have been scrutinized to ensure that the selected data represents the correct production from Jette. The presented performance data is what will be used during history matching of the Jette dynamic reservoir model. Production of oil, gas and water is based on back allocation performed by Weatherford Petroleum Consultants AS (mentioned above) and can be seen in Figure 6.2.1 through Figure 6.2.8. A summary of available performance data to use during history matching is listed in Table 6.2.1. Well test measurements are plotted together with the allocated production for comparison. Production

measured when Jette produced to the test separator without interference from Jotun wells is also plotted. The reason for plotting measured rates at the test separator between 7th of December and 6th of January is to reduce uncertainty in the production performance data as these rates represent an accurate production from Jette. Production performance data used for history matching is specified for the period between 20th of May 2013 and 1st of March 2014.

Table 6.2.1 – Available performance data from Jette

- Allocated production rates
  - Oil
  - Water
- Field rates
  - Gas
  - Liquid
- Cumulative production
  - Oil
  - Water
  - Gas
- Pressures (@ gauges)
  - BHP
  - THP
- Measurements at test separator
  - Oil rate
  - Water rate
  - Gas rate
  - Liquid rate
  - GOR
  - WC
- Other Measurements
  - Gas lift injection rate
  - Well test data

Figure 6.2.1 illustrates the historical oil rate on a level of field and individual wells. The field oil rate corresponds well with rates measured from the test separator and is believed to accurately represent oil production from Jette.

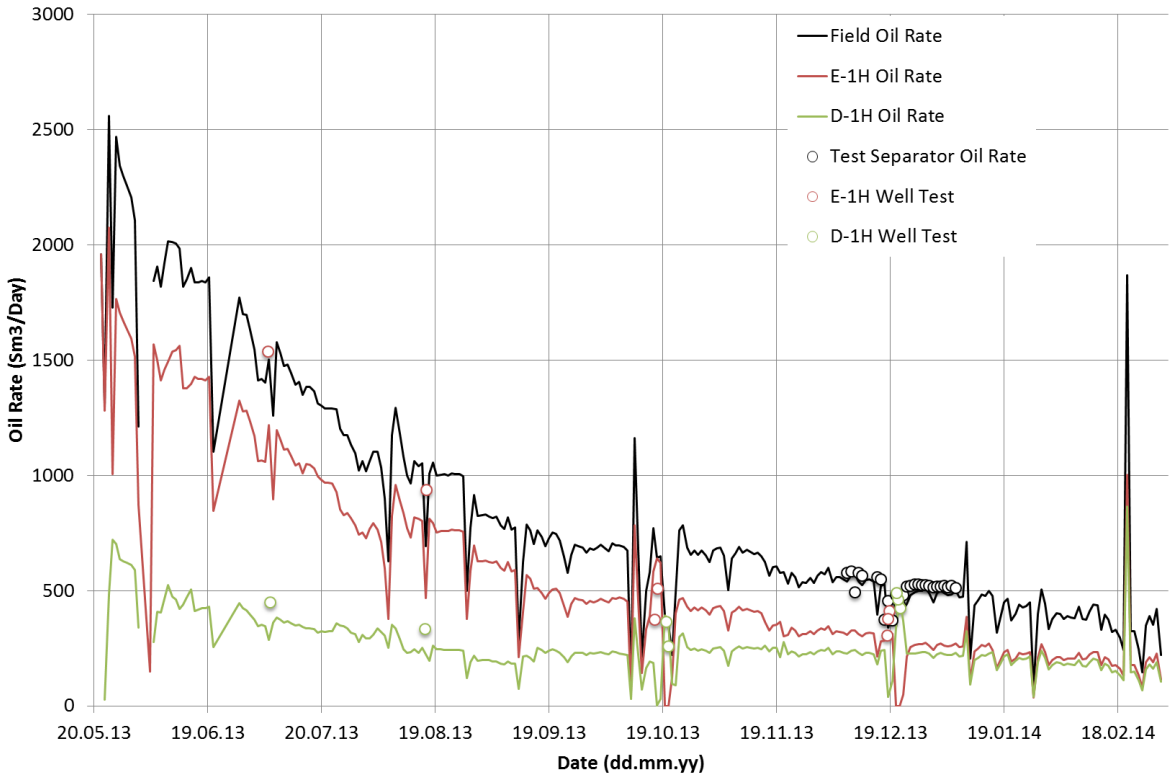

Figure 6.2.1: Historical oil production rate for the Jette field and individual wells, D-1H and E-1H, between 20.05.2013 and 01.03.2014. Measurements from well tests and test separator are included to establish confidence in data.

In Figure 6.2.2 it can be seen that there is a slight deviation between the allocated water rates and the measured water rate from the test separator. Most confidence is given the measured rate from the test separator. The allocated rates are based on well tests, plotted as points in Figure 6.2.2, and shows that especially the allocated E-1H rate is too low compared with measured points.

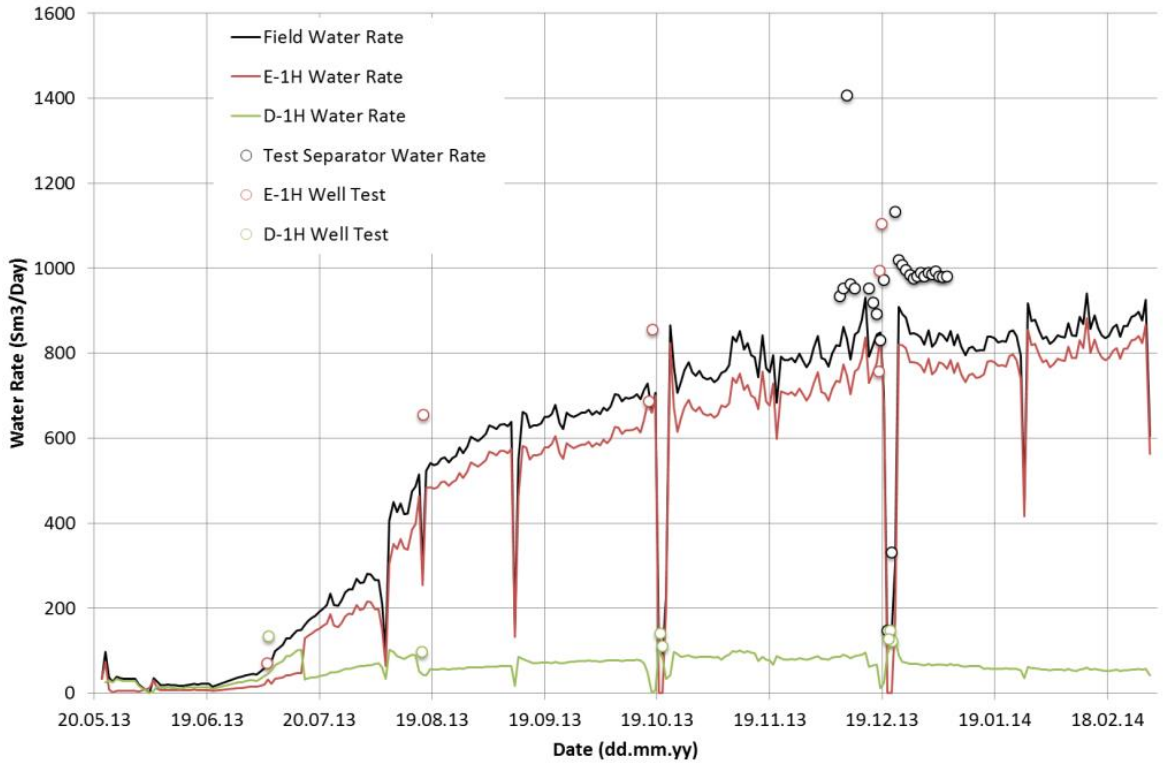

Figure 6.2.2: Historical water production rate for the Jette field and individual wells, D-1H and E-1H, between 20.05.2013 and 01.03.2014. Measurements from well tests and test separator are included for comparison.

The performance data representing gas production rate has only been aquired on a field level, illustrated in Figure 6.2.3. Uncertainty with regards to the fluid systems, as dicussed in Chapter 5.1, has made the process of allocating gas between wells especially difficult as it is believed that two different fluids are being produced. As seen from Figure 6.2.3 there is some mismatch between the allocated gas production and measured gas production at the test separator. Again, most confidence is given to measurements from the test separator as the GOR used when allocating gas to Jette is assumed too low. Gas lift gas has been subtracted from the total gas rate such that data represent net gas production rate (Figure 6.2.3).

The same mismatch in performance data can be seen when plotting GOR (Figure 6.2.4). This clearly indicates that the fluid system contains too little solution gas. The test separator suggest a possible GOR in the range between 100 – 125 $Sm3/Sm^3$, consistent with changes made to the fluid model in Chapter 5.1.

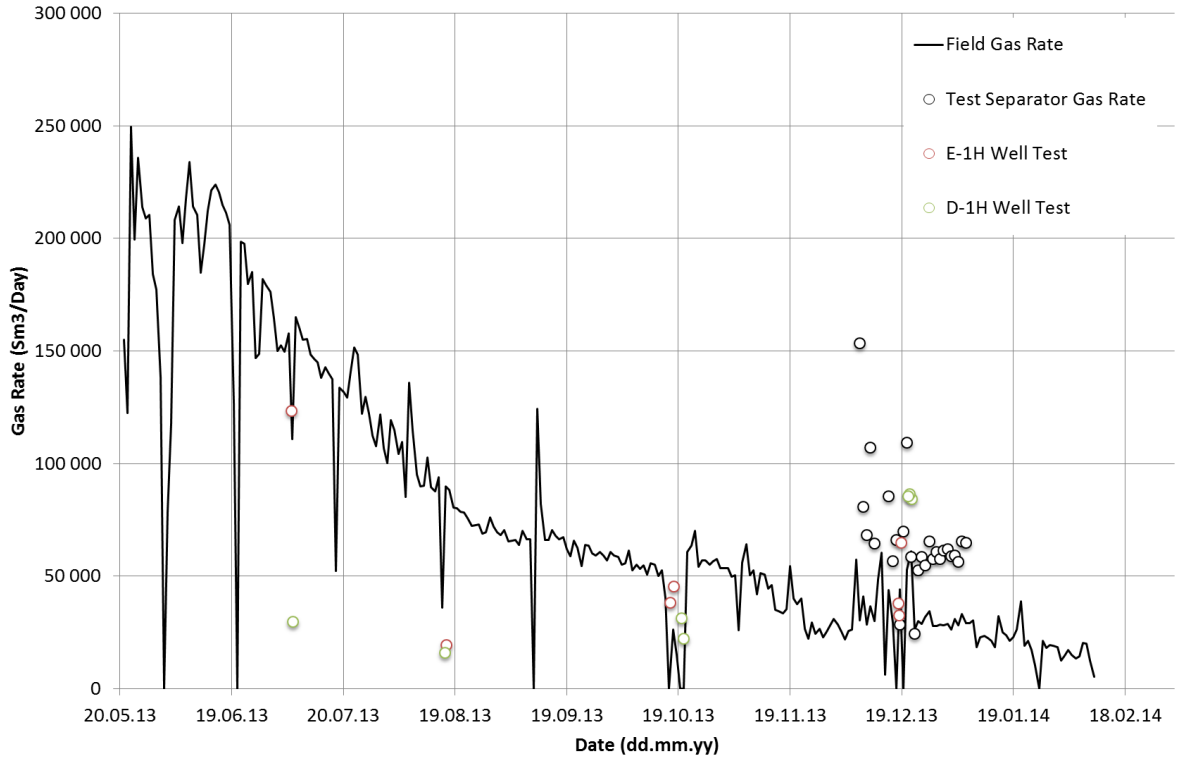

Figure 6.2.3: Historical gas production rate for the Jette field between 20.05.2013 and 10.02.2014. Measurements from individual well tests and test separator are included for comparison.

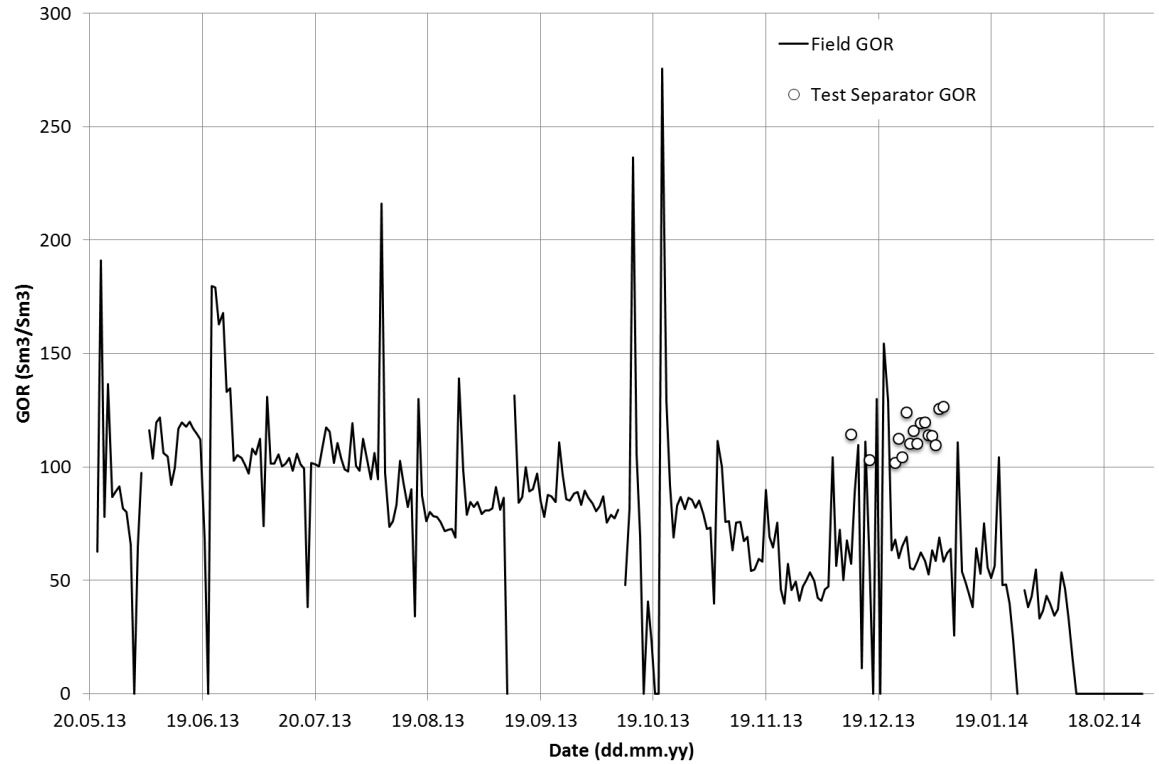

Figure 6.2.4: Historical gas-oil ratio produced at the Jette field between 20.05.2013 and 10.02.2014. Measurements from test separator are included for comparison.

Cumulative production of oil, water and gas is illustrated in Figure 6.2.5. The final produced volumes of all phases on the 1st of March 2014 is tabulated in Table 6.2.2. As discussed

above, volumes of produced water and gas are probably too low due to the difference between allocation and measurements from the test separator in december. Numbers in Table 6.2.2 are simple summation of the production rates given in Figure 6.2.1, Figure 6.2.2 and Figure 6.2.3.

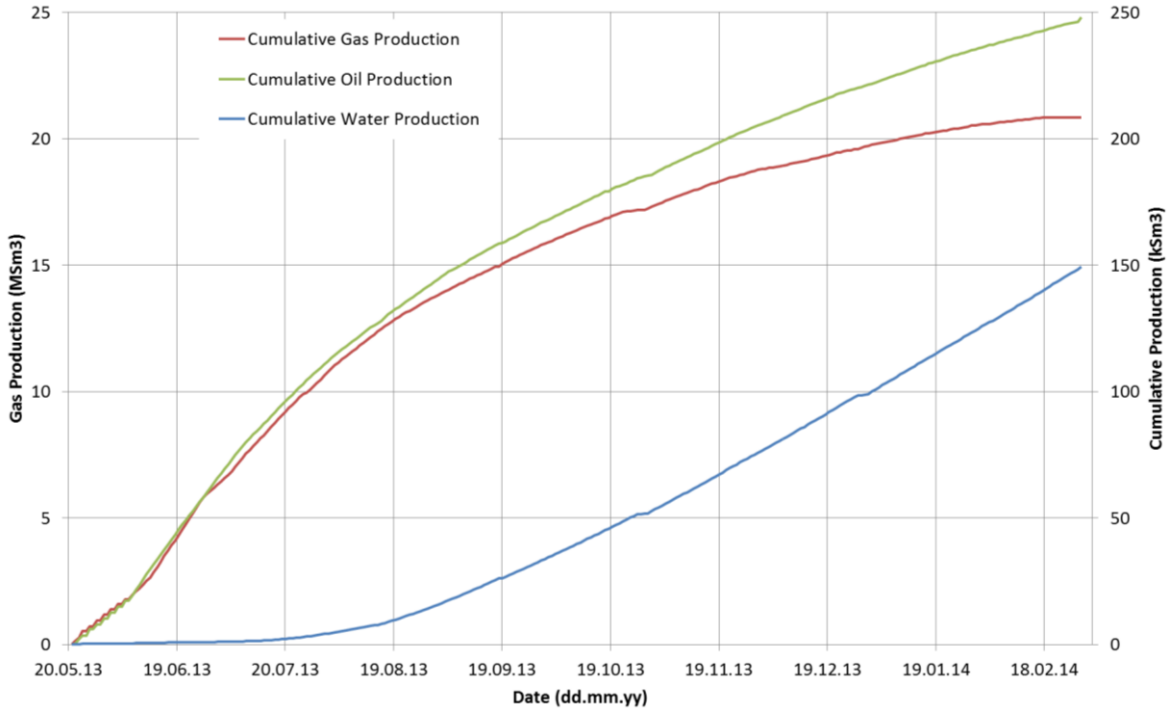

Figure 6.2.5: Cumulative production of oil, gas and water from 20.05.2013 to 01.03.2014.

Table 6.2.2 – Cumulative production of oil, gas and water on 01.03.2014

	Cumulative Production (Sm^3)
Oil	250,800
Gas	21,023,660
Water	155,482

Even though allocated water rate was different from measurements at the test separator there are measurements of total liquid rate at field level which corresponds with test separator measurements (Figure 6.2.6). The total liquid rate is taken from measurements at the MPFM and is considered less uncertain than the allocated liquid rate in Figure 6.2.6. The difference between allocated liquid rate and MPFM liquid rate corresponds well with the difference between allocated water rate and test separator water rate (Figure 6.2.2). Since oil and liquid rate both match test separator measurements it is believed that the most realistic water rate should be the difference when subtracting oil rate from the liquid rate. However, this only applies to water rate at a field level because the additional water would need to be allocated

between wells. If a water rate similar to that required to match total liquid rate is to be used, cumulative water production given in Table 6.2.2 should be somewhat higher.

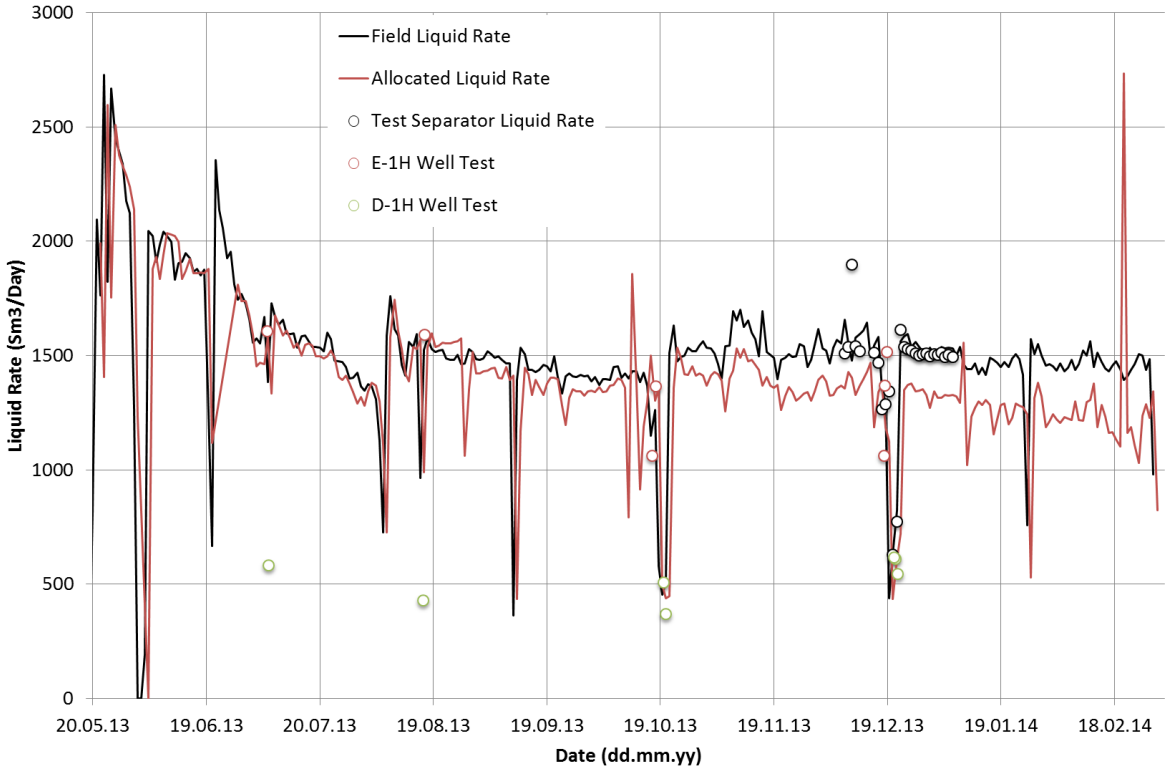

Figure 6.2.6: Historical liquid production rate for the Jette field between 20.05.2013 and 01.03.2014. Measurements from individual well tests and test separator are included for comparison.

Measurements of water cut at the test separator compared with water cut calculated from the allocated oil and water rate is illustrated in Figure 6.2.7. The measurements correspond surprisingly well given given the discrepancy in water rate mentioned above. However, the difference is probably smeared because the calculation takes oil rate into account, hence the difference is not dependent on the water rate alone. Water cut is important in order to assess the performance of wells when history matching because it gives the relationship between production of water and oil together with a clear indication of water breakthrough at an individual well level.

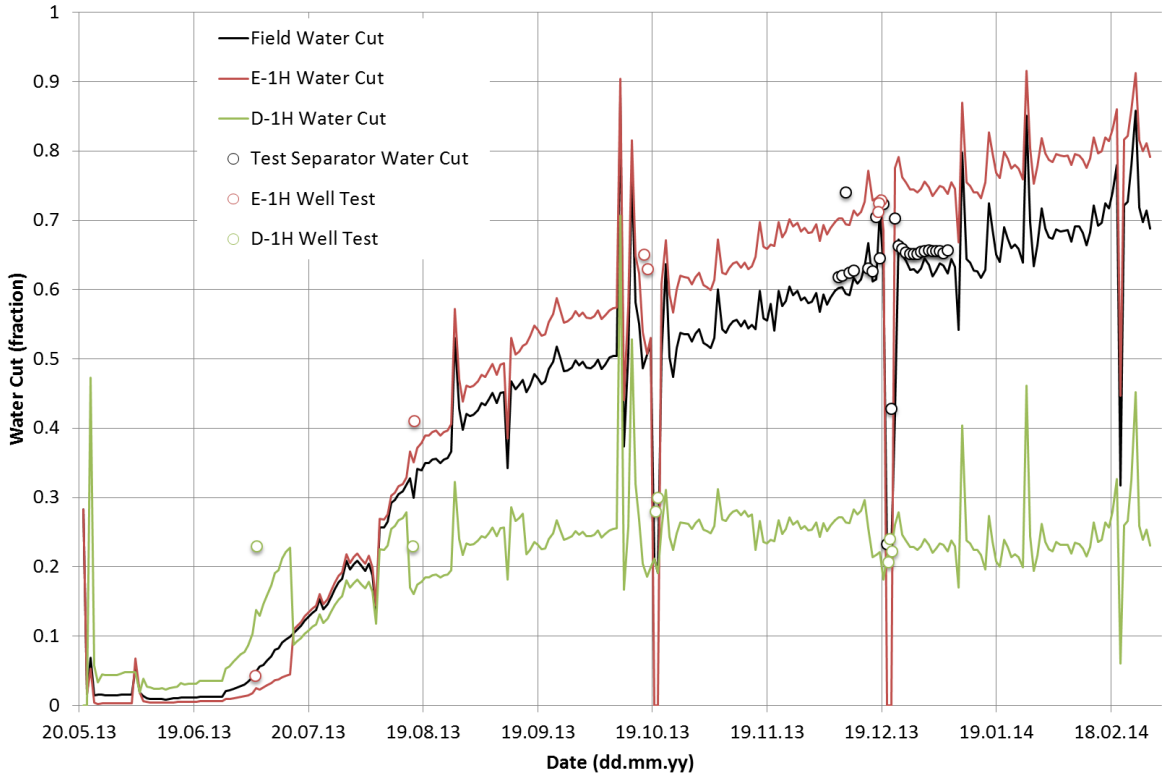

Figure 6.2.7: Historical water cut for the Jette field and individual wells, D-1H and E-1H, between 20.05.2013 and 01.03.2014. Measurements from well tests and test separator are included for comparison.

Gas lift injection rate is measured and illustrated in Figure 6.2.8. Performance data of gas lift injection rate will be used in order to calculate vertical flow performance of wells during simulation. By including VFP-tables in ECLIPSE 100 and using historical gas lift we can calculate the THP which in turn will be compared with historical data describing THP measured at the wellhead.

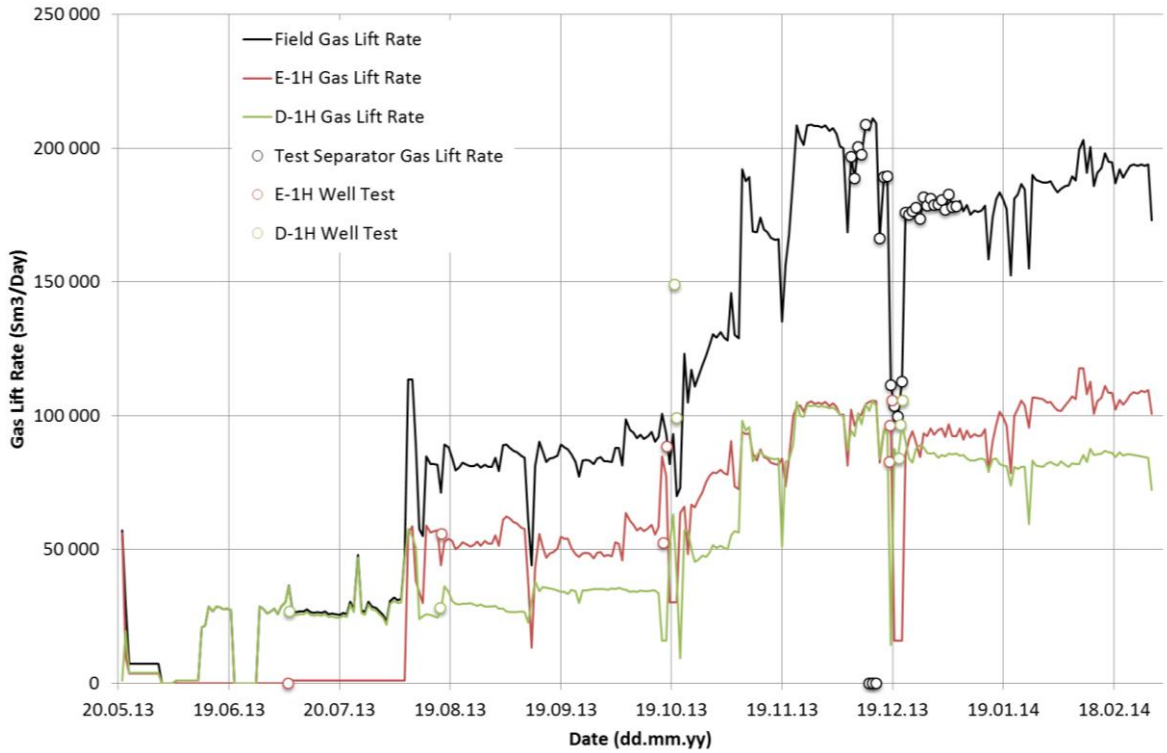

Figure 6.2.8: Historical gas lift injection rate for the Jette field and individual wells, D-1H and E-1H, between 20.05.2013 and 01.03.2014. Measurements from individual well tests and test separator are included for comparison.

6.3 PRESSURE DATA

Pressure in both wells are continuously measured from gauges. BHP and THP is illustrated in Figure 6.3.1. THP is measured upstream of the subsea choke at the well head. From Figure 6.3.1 it is evident that the difference in THP between wells are small, which is to be expected since the wells have a commingled production stream from the PLEM about 100 metres away from wellheads. BHP is measured from gauges installed downhole at a depth of 1,623 mTVD MSL and 1,864 mTVD MSL, in well D-1H and E-1H respectively. The location of both BHP gauges are some distance above the reservoir section and care needs to be taken to specify the correct datum for well pressures in the simulator if the BHP performance data is to be used as comparison against the simulation model to establish a pressure match.

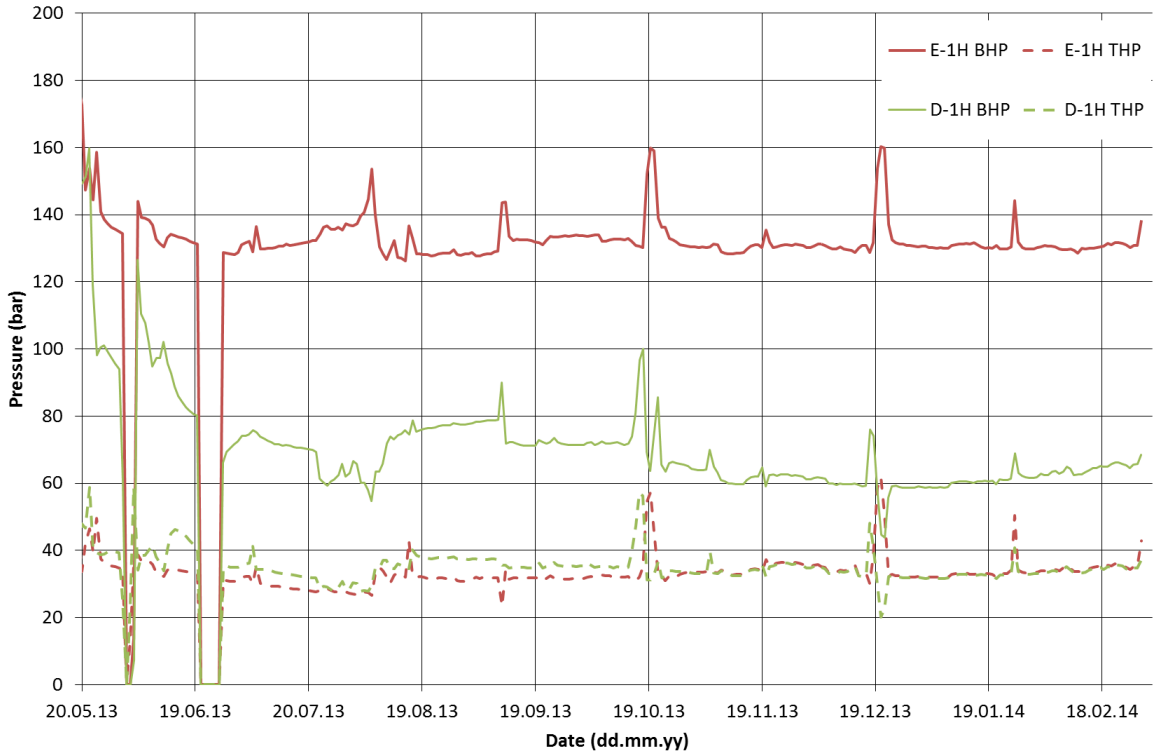

Figure 6.3.1: BHP and THP performance of well E-1H and D-1H measured at gauges in the period between 20.05.2013 and 01.03.2014.

It can be seen from Figure 6.3.1 that BHP in well D-1H indicate a higher degree of depletion and less, or no, aquifer pressure support compared to well E-1H. This supports the theory of compartmentalization and different fluid regions in the Jette field presented in the previous chapter. Note that BHP and THP measurements in june where the value is zero represents erroneous measurements at pressure gauges and should be neglected.

6.4 PREPARATION OF SIMULATION INPUT

The presented performance data from Jette had to be prepared in order to be used for simulations. A description of how history matching is performed using ECLIPSE 100 was given in Chapter 2.8. Historical performance data was organized as tables in a simple text file and imported to Petrel. Petrel allows import of all data types compatible with the WCONHIST keyword used to enter historical data in ECLIPSE 100. The rationale behind an import of data into Petrel is that ECLIPSE 100 requires specification of the WCONHIST keyword at every timestep a new historical data point is added. Petrel can automatically export the historical data to ECLIPSE 100 format such that there is no need to manually

create all the WCONHIST keywords and add historical data. Obviously much time is saved and the possibility of entering wrong data is reduced.

The available historical performance data is added on a daily basis, meaning that a new historical data point is added every day in the history match period between 20th of May 2013 and 1st of March 2014. Historical performance data in the Jette dynamic reservoir model includes oil production rate, water production rate, gas lift injection rate, BHP and THP for both wells in addition to field gas production rate and field liquid production rate. Because all this data is entered in the WCONHIST keyword the model performance can easily be compared with historical performance in a post-processing software. When entering data it was necessary to remove a few data points due to erroneous measurements at the downhole pressure gauges. Data points which have been removed are 01.06.2013 to 04.06.2013 and 21.06.2013 to 27.06.2013, they can be seen as zero values in Figure 6.3.1. Input of historical performance data to the Jette dynamic reservoir model is constructed such that WCONHIST specifies the model to be constrained from oil rate. However this can easily be changed to any of the other historical data types entered in the WCONHIST keyword if needed.

An alternative file for input of historical performance data was also created. This file was specified to constrain the Jette dynamic reservoir model from THP. However, ECLIPSE 100 does not allow the model to be constrained by historical THP in the WCONHIST keyword. Hence, the historical THP data had to be entered using the WCONPROD keyword which is normally used to set operating conditions during prediction mode. As long as the entered data in the WCONPROD keyword are from the historical period the simulation run will be considered to be in history mode.

6.5 COMPARING THE INITIAL MODEL WITH HISTORICAL PERFORMANCE

Once historical data describing reservoir performance at Jette had been selected and prepared for input to the simulator it was of interest to run the Jette dynamic reservoir model and compare it with the historical performance data. From such a simulation it was possible to assess how well the simulation model matched the historical performance data and at the same time obtain indications of what changes were needed to better model the Jette reservoir. The Jette dynamic reservoir model, as described in Chapter 4, was simulated constrained by oil rate given in Figure 6.2.1.

Figure 6.5.1 and Figure 6.5.2 illustrate the production of oil and water calculated from the model for well D-1H and E-1H respectively and how it compares to historical performance data. Well D-1H is able to produce the constraining oil rate but is experiencing a major mismatch for water rate. From Figure 6.5.1 we see that D-1H does not produce any water at all, hence the model is too optimistic in the area around D-1H. This is also seen from Figure 6.5.5 where the calculated BHP is too high, indicating that only a small drawdown is needed in order to meet with the constraining oil production rate. If a history match is to be obtained a mechanism of how water is produced in D-1H will need to be found. It is possible that if BHP in D-1H is lowered closer to the observed pressure it will help increase water production as a higher pressure gradient is established.

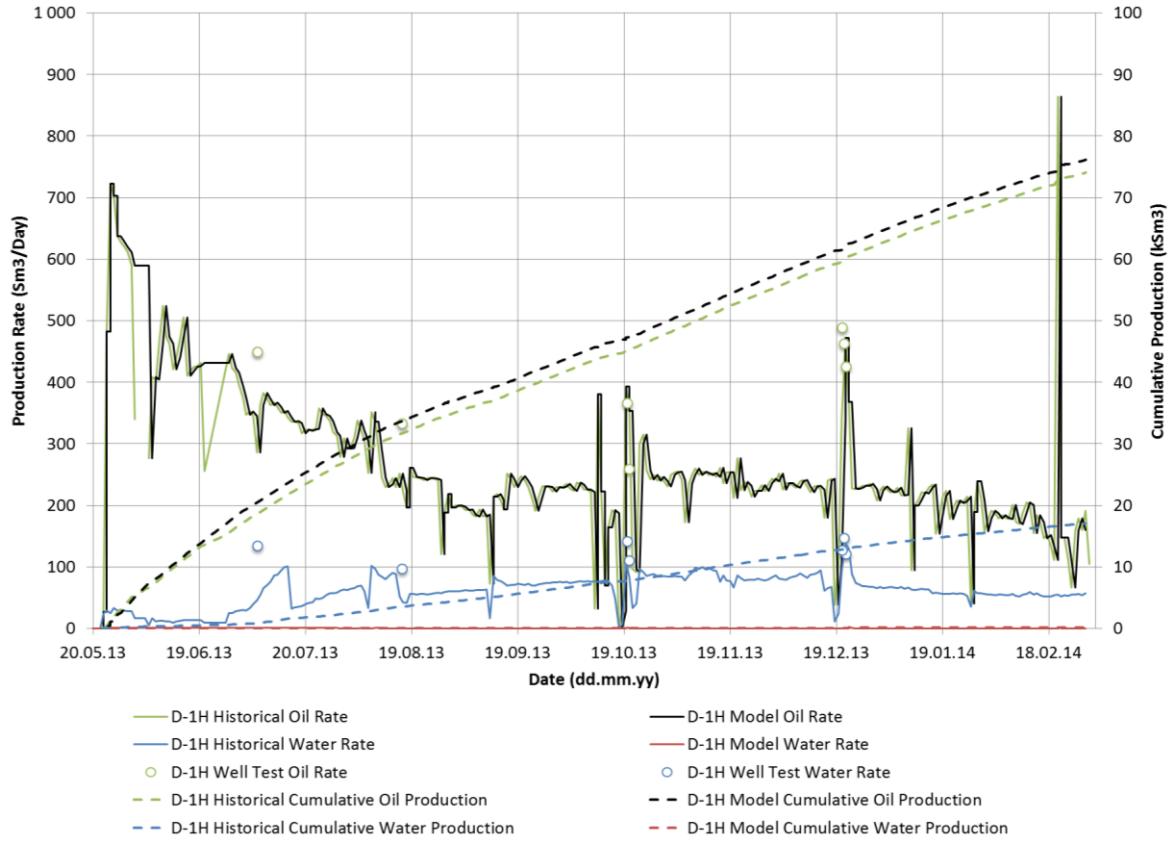

Figure 6.5.1: Comparison of oil and water production between historical performance data and the Jette dynamic reservoir model for well D-1H.

Well E-1H is having problems producing the constraining oil rate (Figure 6.5.2) due to low BHP (Figure 6.5.5). There is restricted flow of oil around E-1H leading to the lower BHP limit (1 atm) being reached between june and august 2013. It is believed that evolution of free gas around E-1H caused by reservoir pressures below the bubblepoint pressure is affecting the low BHP. Due to this it is expected that the BHP calculated in the model after implementing

the updated fluid model (Chapter 5.1) will increase due to the new fluid having a much lower bubblepoint pressure (141.3 bar) compared to the old (170.9 bar).

Water production from E-1H is experiencing a good match until mid august except for a too steep production right after breakthrough. After mid august the water production is too low and the trend is decreasing rather than increasing as the historical performance data indicates. Attention will need to be focused at increasing late time water production.

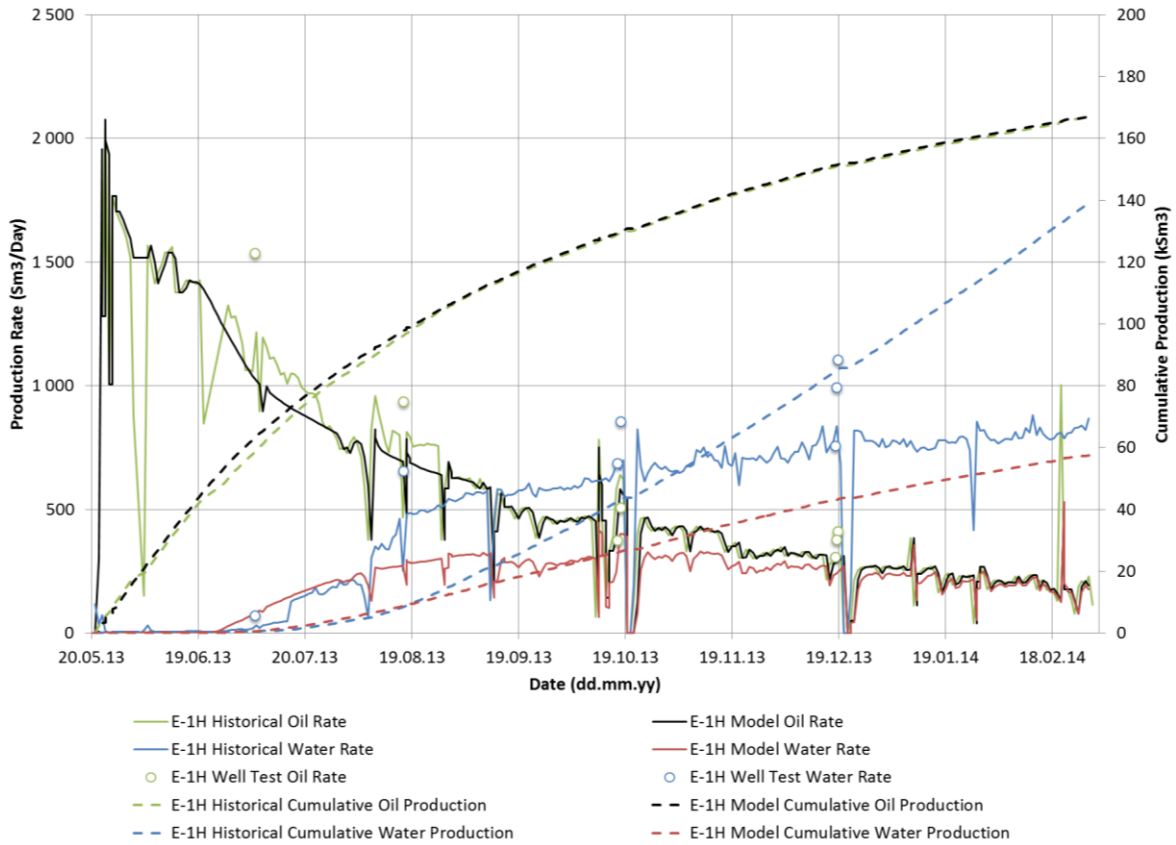

Figure 6.5.2: Comparison of oil and water production between historical performance data and the Jette dynamic reservoir model for well E-1H.

Because of D-1H not producing any water and E-1H struggling to meet constraining oil rate and producing too little water from mid august the resulting liquid rate (Figure 6.5.3) is too low. This is an indication of the model having problems producing the required volumes and that permeability might be too low, especially around E-1H due to the low BHP.

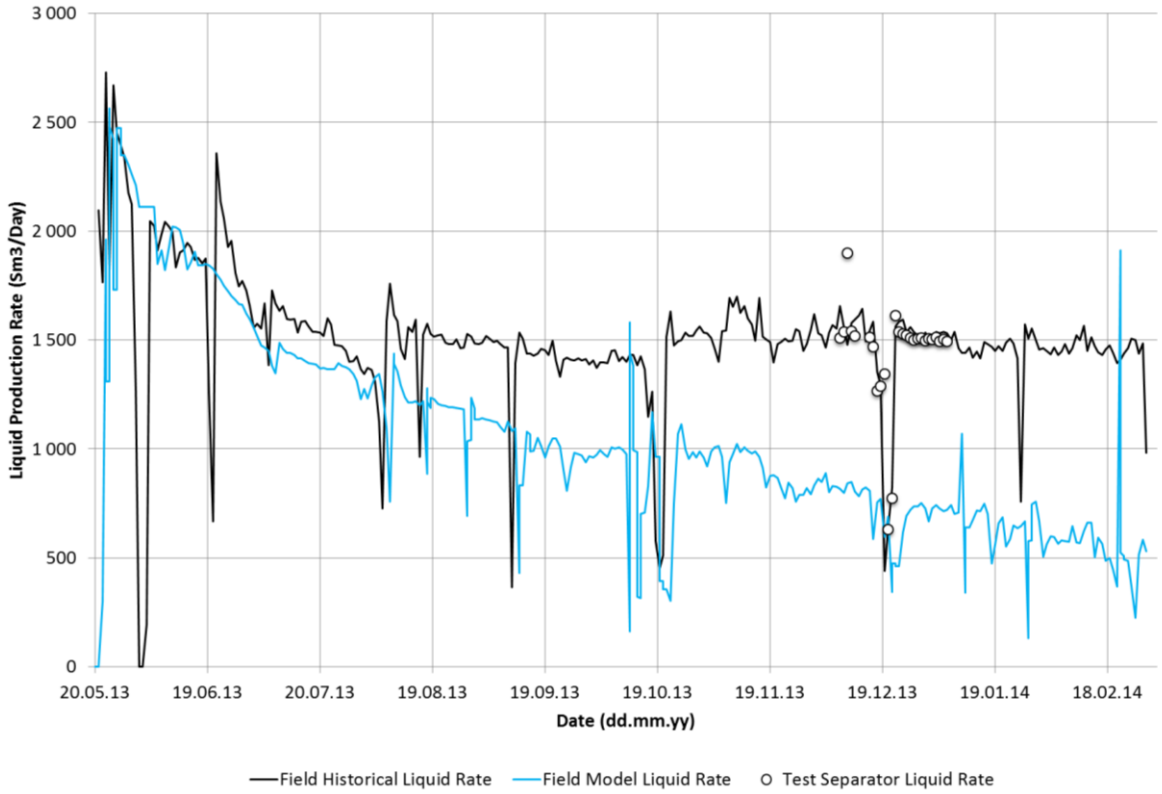

Figure 6.5.3: Comparison of liquid production rate between historical performance data and the Jette dynamic reservoir model on a field level.

The calculated gas production from the model, illustrated in Figure 6.5.4, shows a good match towards measurements obtained from the test separator in december. The fluid model has a solution gas-oil ratio around 120 Sm^3/Sm^3 (specified to vary with depth as in Table 4.2.2.1) which corresponds well with separator measurements.

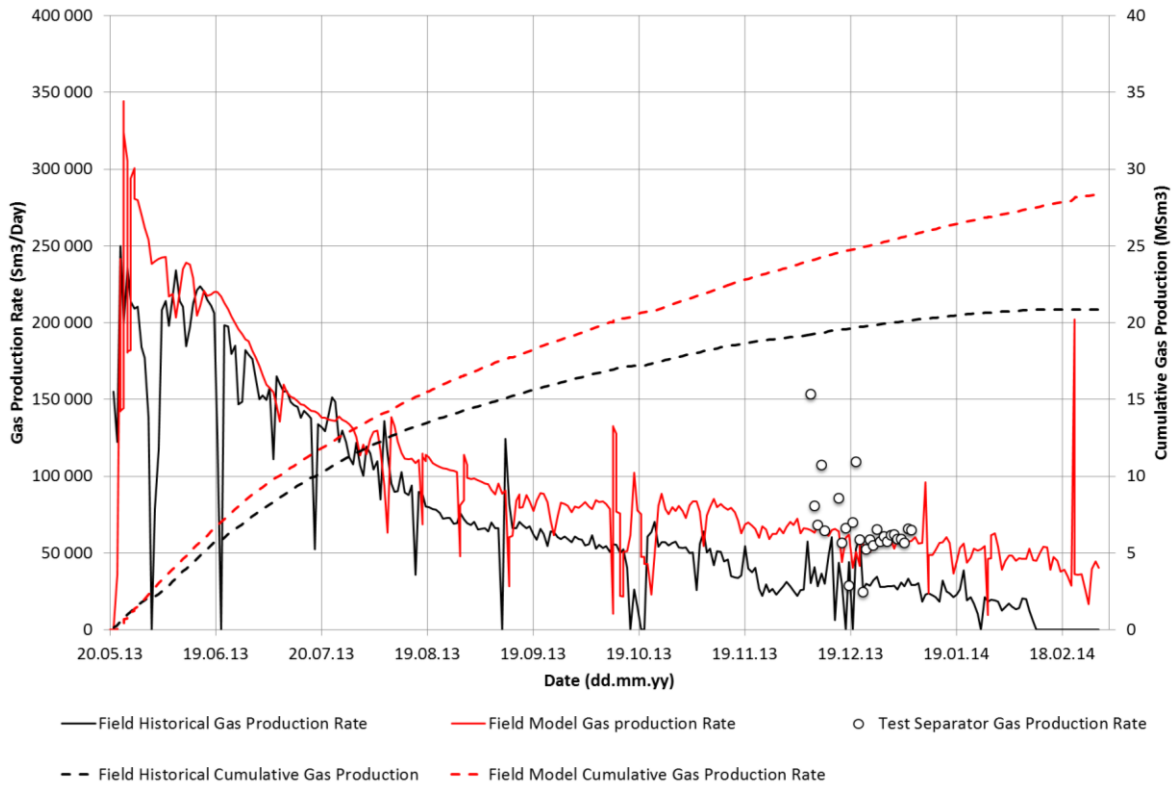

Figure 6.5.4: Comparison of gas production between historical performance data and the Jette dynamic reservoir model on a field level.

Table 6.5.1. compares the cumulative production of all phases from the Jette dynamic reservoir model with those from the historical performance data. Oil production is closely matched as this is what constrains the model. Water production is too low as discussed above and is one of the primary parameters that will need to be matched. Even though gas production is too high this value might represent the gas production at Jette more accurately than the allocated gas rate since measurements at the test separator in december were closely matched.

Table 6.5.1 – Comparison of cumulative production 01.03.2014

	Historical Performance Data	Jette Dynamic Reservoir Model
Cumulative Oil Production (Sm^3)	250,800	243,238
Error (%)	n/a	- 3.01
Cumulative Water Production (Sm^3)	155,482	57,710
Error (%)	n/a	- 62.88
Cumulative Gas Production (Sm^3)	21,023,660	28,384,530
Error (%)	n/a	35.01

Comparison of THP is not included since calculated BHP's for D-1H and E-1H in Figure 6.5.5 is not even close to a match. Also, calculation of THP in E-1H results in non-physical values because it would require a negative pressure at the wellhead to produce anything from a well with BHP of 1 atm.

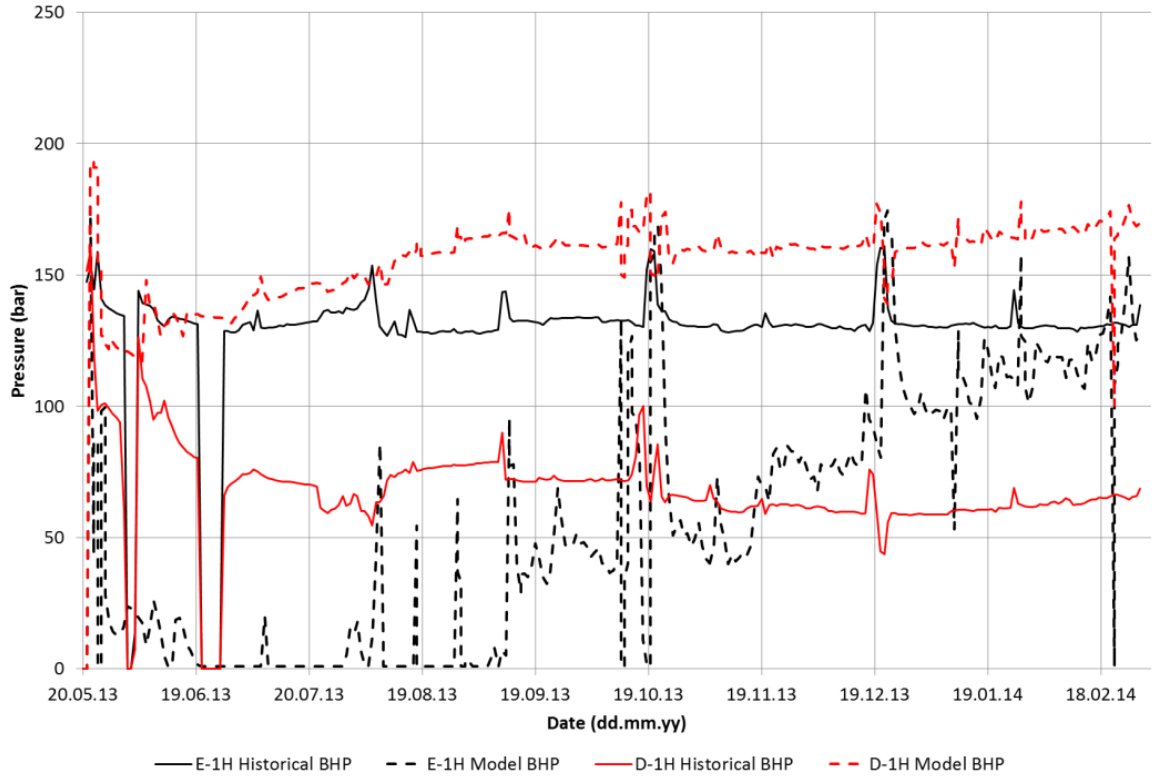

Figure 6.5.5: Comparison of BHP and THP between historical performance data and the Jette dynamic reservoir model for well D-1H and E-1H.

7 HISTORY MATCHING THE JETTE RESERVOIR MODEL

The Jette dynamic reservoir model presented in Chapter 4 has been history matched in order to represent the reservoir performance from Jette. A variety of perturbations were needed in order to obtain a reasonable history match and much effort has been focused at only making realistic changes to the Jette dynamic reservoir model. This chapter will describe the process of history matching and the necessary perturbations required to obtain a history match of the Jette dynamic reservoir model.

7.1 APPROACH TO HISTORY MATCHING

Before history matching a dynamic reservoir model it will be wise to work out a set of study objectives and select what history matching method to apply. Two available history matching methods were described in Chapter 2.5 and Chapter 2.6. In the history matching of the Jette dynamic reservoir model it was selected to perform manual history matching. Hence, perturbations have been made in a trial and error fashion. Even though perturbations to the model were made in a trial and error fashion it was decided that the perturbations was not to be made randomly but rather according to geologic understanding and knowledge of the Jette reservoir, obtained from various sources such as logs, reports, well tests and other reservoir studies.

It was selected that the approach presented in Table 2.5.2.1 should be followed when making perturbations to the model in order to obtain a history match. This table suggests a method to perturb the model in the most geologically sound manner. As a result, most changes to the model during history matching has been applied globally or to individual layers.

There has not been specified any matching criterias by Det norske of which the Jette dynamic reservoir model must meet with in order to be considered a valid match. It has been entirely up to the author to decide what is required in order to consider the Jette dynamic reservoir model successfully history matched. It was decided to focus on matching trend, hence no explicit limit in terms of maximum error and mismatch was set.

It was determined to constrain the Jette dynamic reservoir model from allocated oil rates during history matching. This is, as described in Chapter 2.3.1, the most commonly used

constraint during history matching because it is important to account for the most valuable fluid. Because allocated oil rate will be used to constrain the Jette dynamic reservoir model the objective will be to match other historical performance data such as water production, gas production, BHP and THP. Obviously, the objective will be to match as much of the available historical performance data, presented in Chapter 6, as possible in order to increase confidence of the obtained history matched model. Because the Jette dynamic reservoir model only has two wells the main focus will be on matching individual well behavior rather than field behavior.

After a history match has been obtained for the Jette dynamic reservoir model constrained by allocated oil rate the model will be constrained from THP in order for it to be verified. THP is measured at the wellhead in both wells and measurements are considered to be more confident than the allocated oil rates. Hence, a good match with historical performance data when running on THP will help validate the obtained history match of the Jette dynamic reservoir model.

7.2 SELECTION OF HISTORY MATCHING PARAMETERS

The selection of which parameters to perturb in the Jette dynamic reservoir model in order to obtain a history match has been based on uncertainty related to the parameter in addition to the effect related with a change to this parameter. Hence, if a parameter has a high degree of uncertainty but a neglible effect on model response the parameter will not be considered a history matching parameter. This is because focus has been to only perturb parameters governing the response required to obtain a history match. Also, effort was focused at obtaining a history match with the least possible amount of perturbations.

Most history matching parameters are selected based on information from various reports written by Det norske. Simulations of the Jette dynamic reservoir model has also been used to select history matching parameters. The selected history matching parameters, based on initial screening and sensitivity studies, are listed in Table 7.2.1. There are several uncertain parameters in the Jette dynamic reservoir model which are not listed in Table 7.2.1. The main reason for not selecting these as history matching parameters are because they only have a limited effect on the model response. Chapter 7.3 will describe how the Jette dynamic reservoir has been perturbed in order to obtain a history match using the history matching parameters in Table 7.2.1.

Table 7.2.1 – History matching parameters for the Jette dynamic reservoir model

• Permeability
  ○ Anisotropy
  ○ Flow Barriers
  ○ Max value
• Aquifer
  ○ Connectivity
  ○ Size and extent
• Faulting
  ○ Compartmentalization

7.3 HISTORY MATCHING PROCEDURE

The perturbations made during history matching are based on extensive studies of the Jette reservoir from all available data sources. It has been the focus to obtain as much knowledge as possible about the governing processes of reservoir behavior in order to make the most geologically sound perturbations during matching. Hence, perturbations are based on intuition and a hypothesis describing the processes most likely taking place within the reservoir. There have been several hypothesises seeking to explain reservoir behavior at Jette. However, they were all updated in the course of history matching to reflect the latest knowledge obtained of the reservoir. The history matched model is based on a hypothesis stating that the reservoir is compartmentalized with faults and vertical flow barriers resulting in no communication between well 25/8-E-1H and 25/8-D-1 AH T3. Also, well 25/8-E-1H produce with high water cut due to coning and pressure support from the close by aquifer while well 25/8-D-1 AH T3 is assumed to have no aquifer support which leads to depletion in the area of the reservoir where it is located. Finally, fluid sampling has suggested several fluid systems within the reservoir, resulting in a theory that well 25/8-E-1H produces undersaturated oil while well 25/8-D-1 AH T3 produces at pressures below the bubblepoint pressure with evolution of free gas.

Some changes have been performed on the Jette dynamic reservoir model prior to history matching. This includes all changes made during validation of input data in Chapter 5. These changes were performed in order to ensure that the model is characterized realistically and can be seen as the first step in obtaining a history matched model. It was described in Chapter 2.2 that a reservoir model should incorporate the best available static and dynamic data prior to the history matching and validation of all input will increase chances of obtaining a realistic history match. The data which was altered in Chapter 5 is not considered

history matching parameters because they are static parameters which should not be altered once they have been properly characterized. Hence, Chapter 5 was an important step before making all history matching changes presented in this chapter.

The history matched model is a result of several hundred simulation runs. Initially, only one parameter were perturbed between simulation runs in order to isolate the effect from the given change of each parameter. However, as the understanding of reservoir behavior was improved several parameters were perturbed together to get a combined effect. Required perturbations in order to obtain the history matched model will be presented below.

7.3.1 Faults and Flow Barriers

Faults and flow barriers have been added to the Jette dynamic reservoir model in order to reflect the compartmentalization which have been suggested from pressure buildup (PBU) tests, well logs and fluid samples. Response from PBU tests in well 25/8-D-1 AH T3 and well 25/8-E-1 H are illustrated in Figure 7.3.1.1 and Figure 7.3.1.2 respectively. Figure 7.3.1.1 indicates that well 25/8-D-1 AH T3 experiences depletion of the reservoir. This suggests compartmentalization of the Jette reservoir due to a decreasing reservoir pressure between consecutive PBU tests. Well 25/8-E-1 H on the other hand has close to identical response from consecutive PBU tests which is an indication of pressure support from the aquifer. Also, the recorded pressure in well 25/8-D-1 AH T3 indicating that there is no communication between wells.

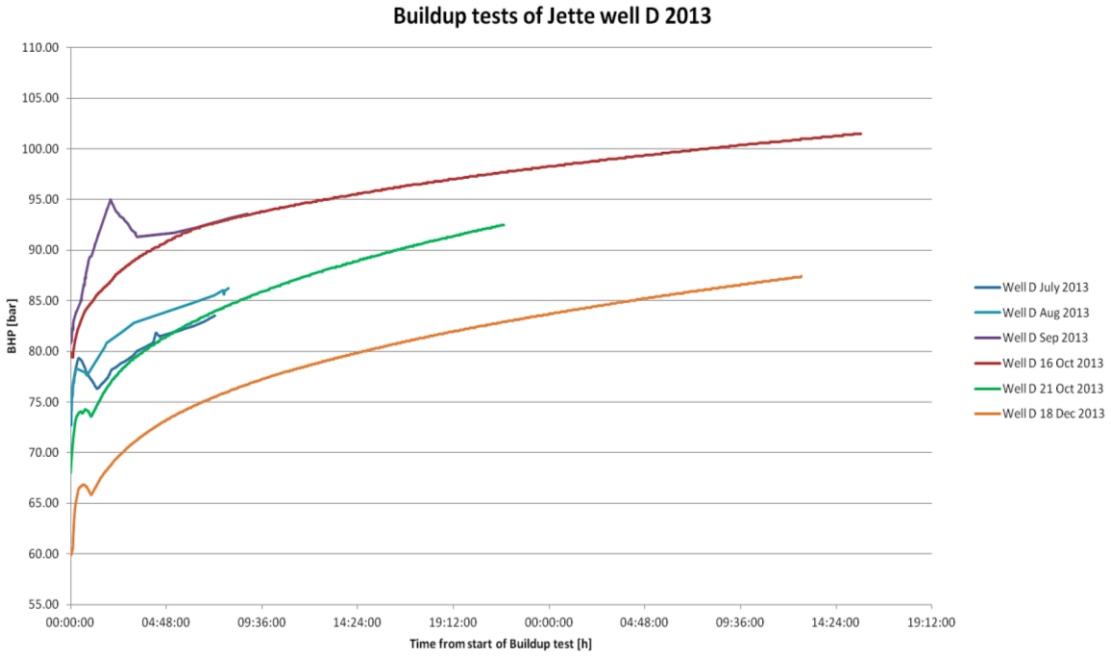

Figure 7.3.1.1: Pressure buildup tests in well 25/8-D-1 AH T3. Response indicates depletion (Lysne, 2014).

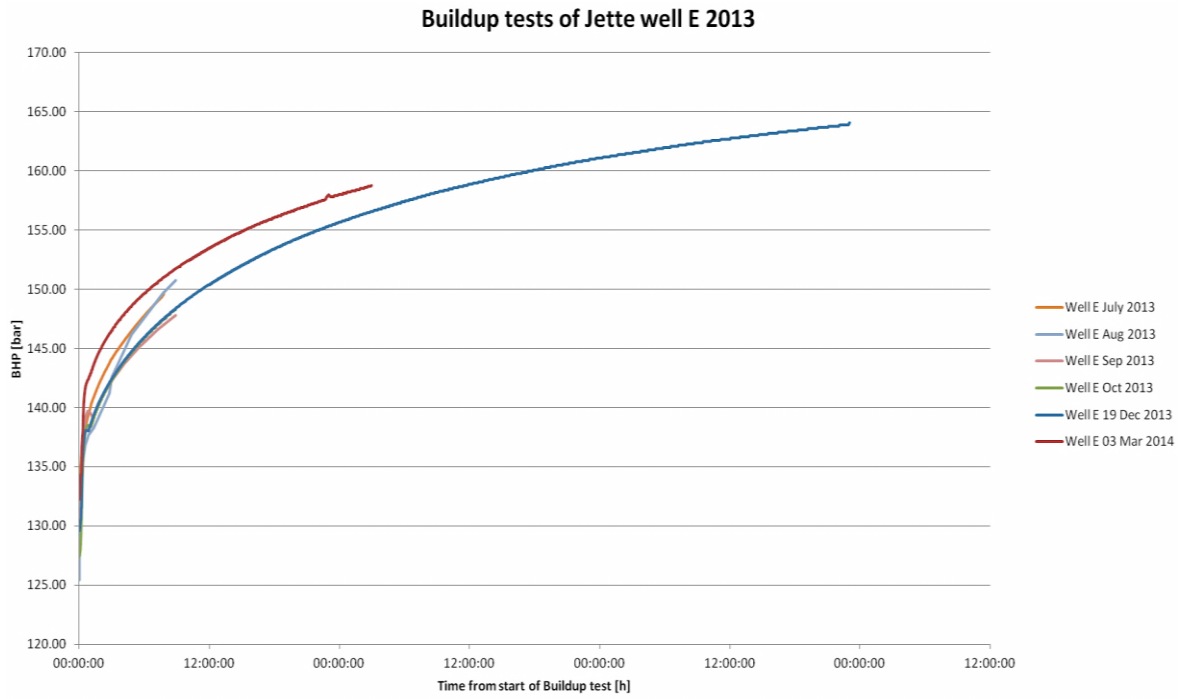

Figure 7.3.1.2: Pressure buildup tests in well 25/8-E-1 H. Response indicates pressure support (Lysne, 2014).

Two sealing faults were added to the Jette dynamic reservoir model, illustrated in Figure 7.3.1.3. One of the reasons for adding two sealing faults was to be able to initialize the Jette dynamic reservoir model with two fluid systems as described in Chapter 5.1. In order to initialize the reservoir model with more than one fluid system it is required by ECLIPSE 100 that the two fluid systems are not to be in connection. The sealing faults acts like a no flow boundary which results in no pressure communication between well 25/8-D-1 AH T3 and 25/8-E-1 H. Faults are based entirely on fault polygons and fault surfaces found in the geomodel of Jette, created by Det norske. The faults have previously been indicated in Figure 3.4.2 but was not added in the model due to the uncertainty of their existence. However, gained understanding of the reservoir has led to believe that these faults should be included in the Jette dynamic reservoir model in order to account for compartmentalization and multiple fluid systems. The two sealing faults illustrated in Figure 7.3.1.3 were exported from the geomodel of Jette using Petrel 2012.2 and added to the Jette dynamic reservoir model in ECLIPSE 100 with the keyword FAULT. Fault transmissibility was set to zero.

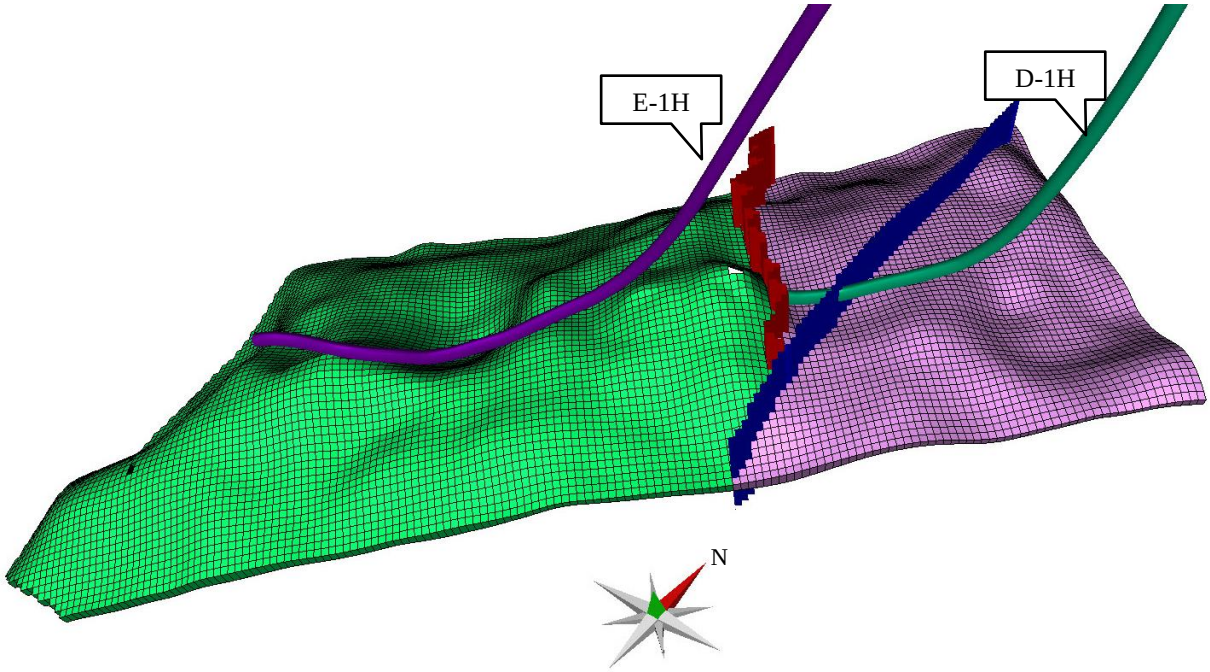

Figure 7.3.1.3: Location of the two sealing faults added to the Jette dynamic reservoir model. The sealing faults ensure that the model is initialized with two fluid systems and that there is no communication between wells.

An alteration in aquifer connectivity was performed in order to accommodate for the depletion process indicated by PBU in the northern area around well 25/8-D-1 AH T3. The result was that the aquifer connecting with the northern segment (purple area in Figure 7.3.1.3) in the Jette dynamic reservoir model was removed. An implication of this was a reduction in aquifer size as the aquifer was now only connected to half the western flank of the Jette dynamic reservoir model as illustrated by the blue grid blocks in Figure 7.3.1.4. Information about aquifer properties after history matching is given in Table 7.3.1.1.

Table 7.3.1.1 – Aquifer properties in the history matched model

Aquifer size	100 GSm^3		
Aquifer Permeability	1,000 mD		
Aquifer Depth	2,095 m TVD MSL		
	I1-I2	*J1-J2*	*K1-K2*
Aquifer Connections	33 - 122	1 - 1	1 - 25

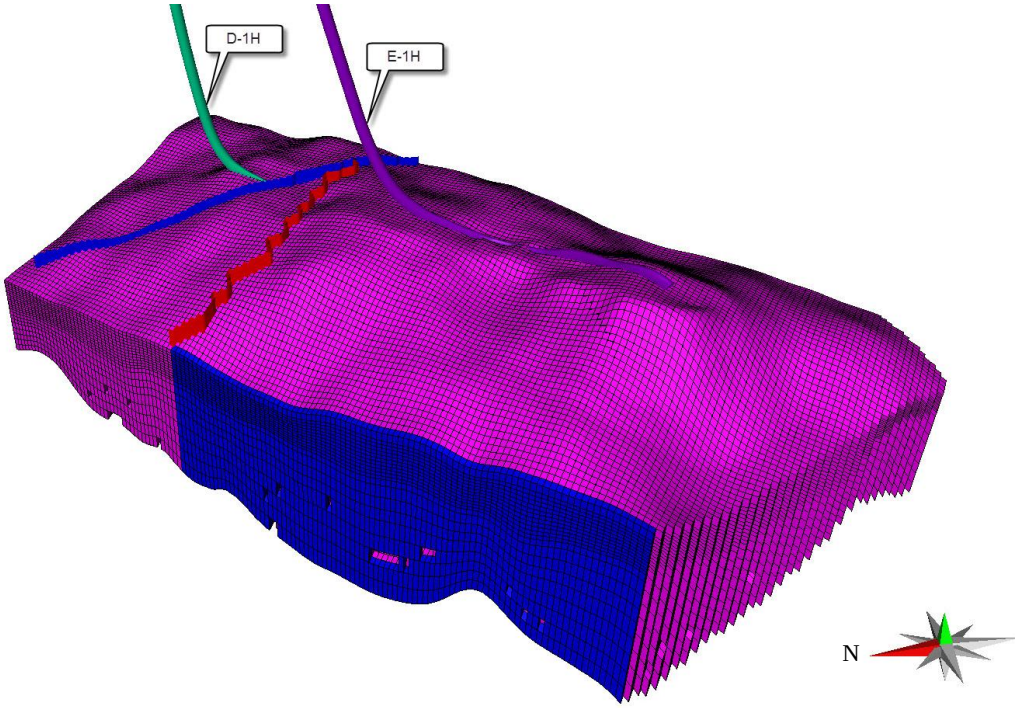

Figure 7.3.1.4: Aquifer connections with the Jette dynamic reservoir model after history matching are shown in blue. Faults are included to illustrate the area where aquifer connectivity has been removed.

Several possible vertical flow barriers were observed from well logs in vertical wells 25/8-17, 25/8-17 A and the pilot well 25/8-D-1 H (Figure 3.4.1). The vertical flow barriers are represented by black shale layers or calcite stringers, described in Chapter 3.3. However, the extent of these shales and calcite stringers were unknown. Simulations with sealing layers in the northern area around well 25/8-D-1 AH T3 in the Jette dynamic reservoir model gave good response. Three sealing layers were added to the Jette dynamic reservoir model in order to represent the three reservoir sands located in the Z2 zone of the Jette reservoir. Figure 7.3.1.5 illustrates the log response from well 25/8-D-1 H used to justify addition of the three sealing layers in the northern area. The location of well 25/8-D-1 H can be seen from Figure 5.1.1 and Figure 7.3.1.7, just north of 25/8-D-1 AH T3. The three sealing layers were entered in the Jette dynamic reservoir model by multiplying the vertical transmissibility with zero using the MULTZ keyword in ECLIPSE 100. Hence, there will be no flow between the layer specified with MULTZ and the adjacent layer in positive vertical direction. MULTZ was added to layers 5, 10 and 14 in the Jette dynamic reservoir model, meaning that there is no flow between layer 5 and 6, layer 10 and 11 or layer 14 and 15. Comparison of log data from well 25/8-17 A with location of the vertical flow barriers in the model indicate a good match and increases confidence to the addition of these sealing layers. The log used for comparison is given in Figure 7.3.1.6. A complete overview of faults and vertical flow barriers added to the history matched model is illustrated in Figure 7.3.1.7.

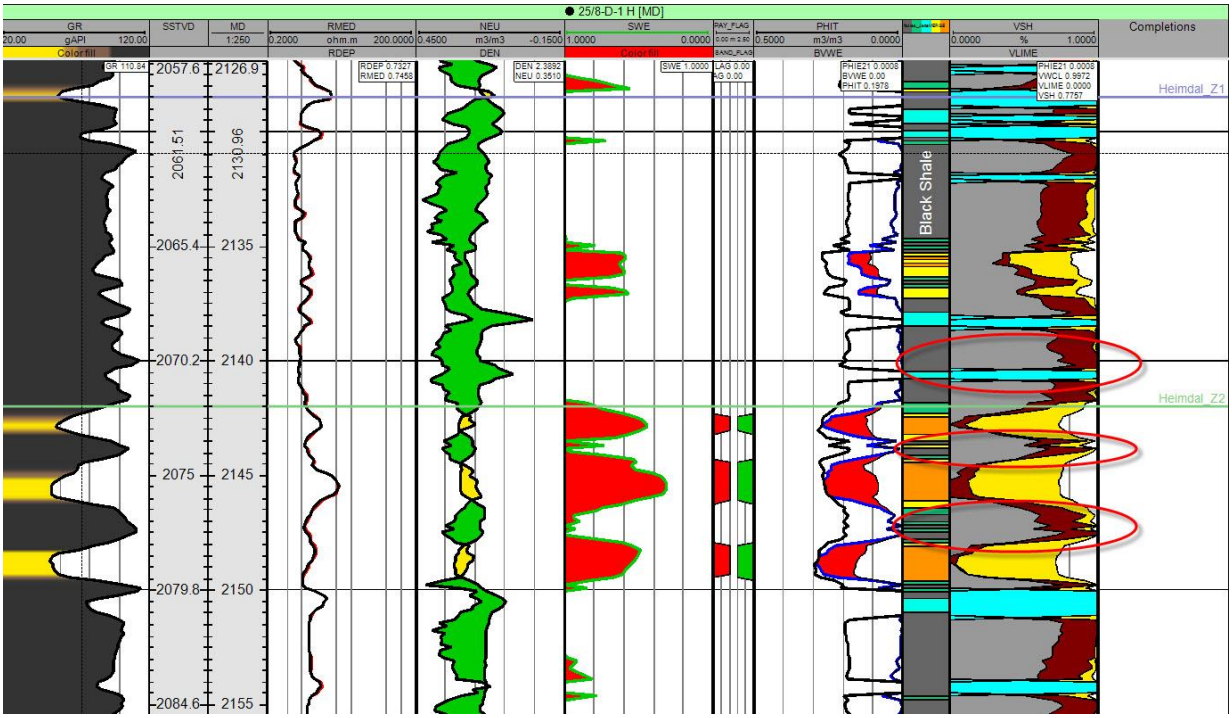

Figure 7.3.1.5: Log from well 25/8-D-1 H. Red circles indicate which vertical barriers have been replicated in the history match of the Jette dynamic reservoir model.

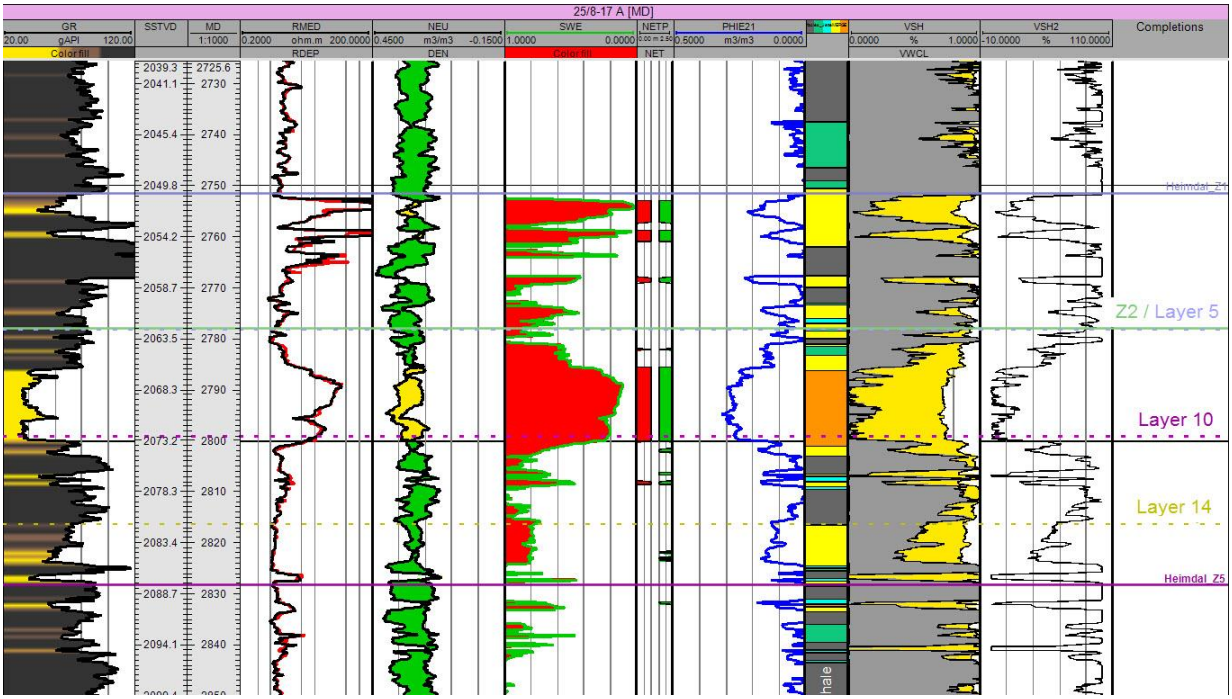

Figure 7.3.1.6: Log from well 25/8-17 A. The location of the sealing layers (5, 10 and 14) are plotted on the log for comparison with logged data and confirms that they are located in areas of low reservoir quality.

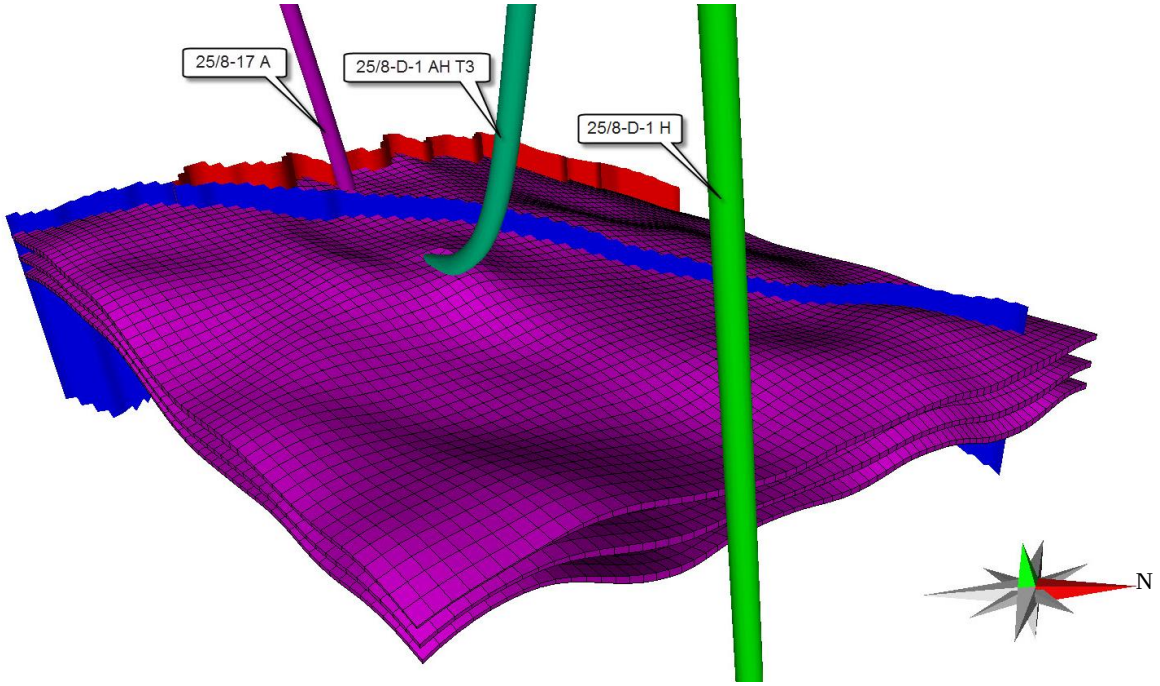

Figure 7.3.1.7: Faults and vertical flow barriers added to the history matched model. Faults are shown in blue and red while vertical flow barriers are in purple. The vertical flow barriers are layers 5, 10 and 14 in the Jette dynamic reservoir model.

Addition of vertical flow barriers in the northern part of the Jette reservoir promotes horizontal and linear flow indicated by PBU tests. This is discussed further in Chapter 7.3.2.

7.3.2 PERMEABILITY MODIFICATIONS

Permeability has been the main history matching parameter during matching of the Jette dynamic reservoir model. The uncertainty in permeability is rather high considering that permeability is based on a porosity/permeability transform defined from cores taken at Jotun and that the porosity log has not been calibrated with any cores from Jette. The Jette dynamic reservoir model was also upscaled adding even more uncertainty to the populated permeability. Hence, permeability has been modified without too many restrictions. The restrictions which have been followed are from direct measurements such as PBU tests and early MDT in well 25/8-17.

PBU tests performed at Weatherford Petroleum Consultants AS has concluded that both wells at Jette experience linear flow regimes. The PBU test from 27th of April 2014 in well D-1H is illustrated in Figure 7.3.2.1 with a pressure derivative matched with a half slope, indicating linear flow. The same response was seen in well E-1H. Hence, permeability modifications have been performed such that wells produce mainly along the Y-direction,

perpendicular to wells, in the Jette dynamic reservoir model. Linear flow was also promoted by the addition of sealing layers in Chapter 7.3.1.

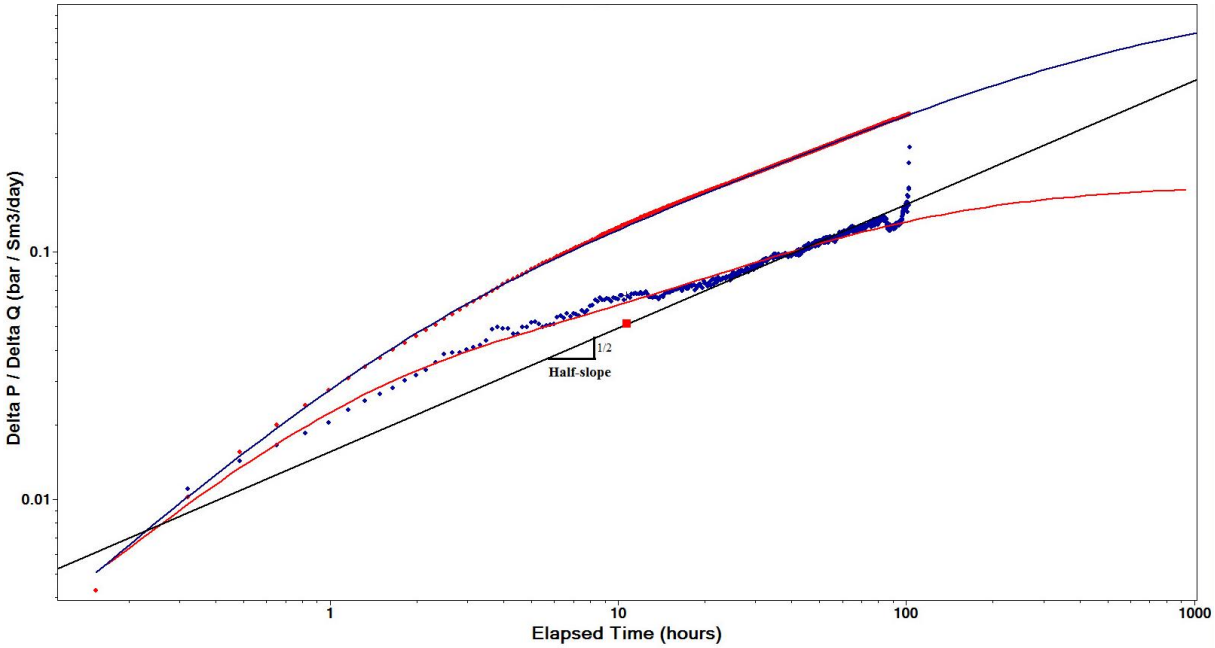

Figure 7.3.2.1: PBU test from well D-1H plotted in a log-log plot for pressure derivative (blue points) and ΔP (red points). The pressure derivative is fitted with a half slope line indicating linear flow (Dahle, 2014[1]).

The maximum value for permeability in the Jette dynamic reservoir model was reduced from 4,500 mD to 2,000 mD based on results from simulations and experience from well tests indicating much lower permeabilities than was first expected by Det norske when setting 4,500 mD as the maximum permeability. It has later been confirmed by Det norske that the initial estimates of permeability have been too high which works in favor for the new maximum value of 2,000 mD. However, the maximum measured mobility from MDT runs in well 25/8-17 has indicated a permeabilty of approximately 472 mD derived from multiplying the measured mobility of 945 mD/cP with a viscosity of 0.5 cP for the reservoir oil (Det norske oljeselskap ASA, 2010). Even though this value is lower it is expected that the maximum permeability is higher since this sample only represents a small fraction of the total reservoir sands.

Because of the sealing fault separating the Jette dynamic reservoir model in two it was possible to split the model in two during history matching in order to save time. This way a match was obtained for the individual wells. The model was split in a southern part and northern part, corresponding to the area represented by fluid model 1 and fluid model 2 in Figure 5.1.1.4 respectively. In order to obtain a match it was necessary to introduce further

[1] Unpublished results from J. E. Dahle. 2014. Trondheim: Weatherford Petroleum Consultants AS.

permeability anisotropy. The permeability was specified along all principle axes (X, Y and Z) in order to promote linear flow. Previous permeability anisotropy in the upscaled model only considered horizontal and vertical permeability due to different algorithms used during upscaling.

E-1H experiences linear flow and coning from the close by aquifer. Numerous simulations with variations in permeability has been performed in order to end up with a history match. The approach has been to modify permeability with multipliers, first on a global level before focusing on single layers. It has been difficult to represent the coning behavior in such a coarsely gridded reservoir model as the Jette dynamic reservoir model. The final permeability modifications used in the history matched model are listed in Table 7.3.2.1. In the match it is assumed that well E-1H produces mainly from the Z2 sand.

Table 7.3.2.1 – Permeability modifications used in the history matched model for the southern area around well E-1H

Parameter	Action	Value	Layer
PERMX	Multiplication	0.25	1 - 5
PERMY	Multiplication	0.25	1 - 5
	Multiplication	2	6 - 10
	Multiplication	5	11 - 16
PERMZ	Multiplication	0.25	1 – 5
	Multiplication	5	6 – 16
	Addition	1 mD	6 – 16

Because vertical flow barriers were added to the northern part of the reservoir where well D-1H is located, the flow is predominantly within the sand layer where the well is completed. This implies that performance of well D-1H is governed by the flow in layer 6 to 10 since all producing well connections are located in between the vertical flow barriers added in layer 5 and layer 10. The well connections were originally located outside these layers as well but they were changed to represent findings from studies performed by Weatherford Petroleum Consultants AS. The change in well connections for well D-1H will be described further in Chapter 7.3.3.

Most of the permeability modifications around well D-1H has been performed in order to represent the linear flow regime interpreted from the PBU test illustrated in Figure 7.3.2.1. However, the main challenge was to understand how water moves and is produced in the northern part of the Jette reservoir considering that the initial model did not produce any water at all (Figure 6.5.1). The mechanism governing water production in the history matched model is based on the uncertainty with regards to faulting, sandstone injection and slumping

which governs vertical flow (Det norske oljeselskap ASA, 2011b). Hence, the solution was to add vertical permeability along the northern fault introduced in Chapter 7.3.1.3. 500 mD was added to vertical permeability for all grid blocks adjacent to the fault. The vertical permeability along the fault can be thought of as a combined feature caused by the fault itself together with sandstone injections. The result is that water is allowed to flow vertically along the fault and enter into the producing layers (6 to 10) as illustrated in Figure 7.3.2.2. Once the mechanism for production of water in well D-1H was addressed, focus was on finding corrections to permeability in order to improve match. Several permeability modifications were made to the northern part of the Jette reservoir in order to end up with a history match. The final set of permeability modifications was obtained from numerous simulations and is listed in Table 7.3.2.2.

Because most permeability modifications were performed in layer 6 to layer 10 there are some uncertainties regarding how well the layers above and below represent the reservoir as these layers does not significantly affect D-1H performance. The only effect from layers below the producing sand is some vertical flow across pinched out grid blocks, corresponding to sandstone injections.

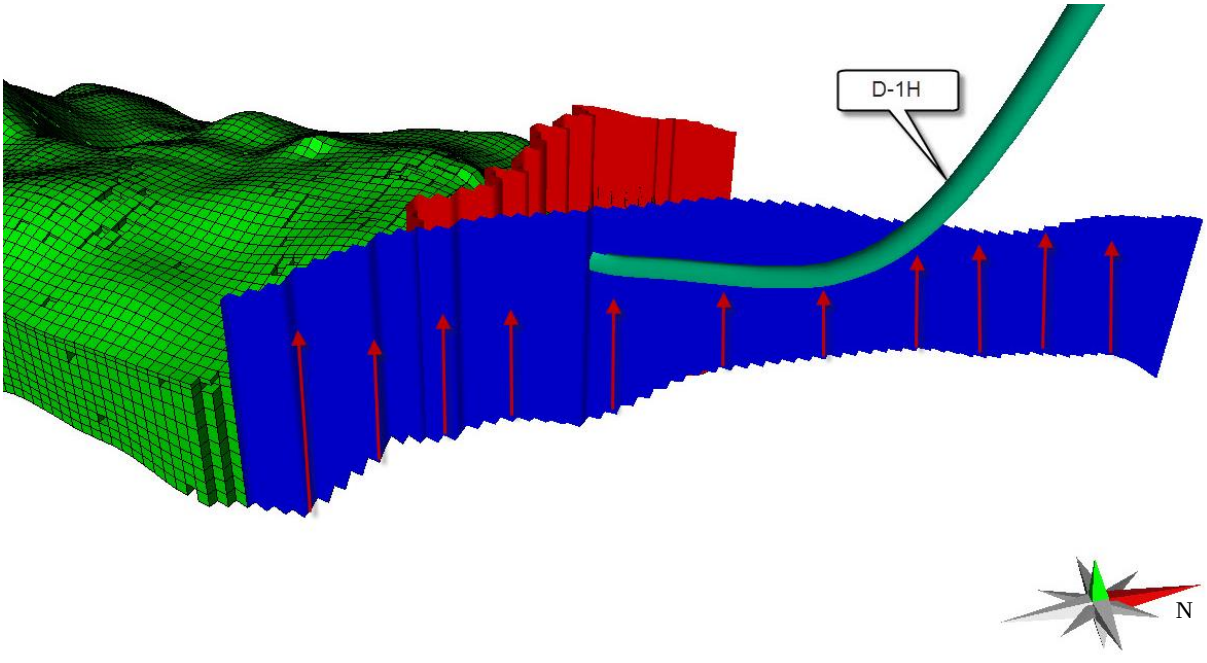

Figure 7.3.2.2: Vertical flow (red arrows) along the northern fault in the Jette dynamic reservoir model introduced by adding 500 mD vertical permeability to grid blocks adjacent to the fault. Vertical flow of water close to the fault provides a mechanism for water production in well D-1H.

Table 7.3.2.2 – Permeability modifications used in the history matched model for the northern area around well D-1H

Parameter	Action	Value	Layer
PERMX	Multiplication	0.1	1 - 25
PERMY	Addition	5 mD	6 - 16
	Multiplication	10	6
	Multiplication	8	7
	Multiplication	12	8
	Multiplication	15	9 - 10
PERMZ	Addition	2 mD	6 – 17
	Multiplication	5	6 – 17

It would be interesting to perform a well test using the history matched Jette dynamic reservoir model in order to compare the permeability measured from previous well tests with the permeabilities in the model. However, this has not been conducted because it is difficult to interpret results from a numerical simulation using analytical equations in PTA. In stead an average of the permeabilities in the drainage area from well E-1H, thought to represent the area tested in PTA, has been compared with well test results. Figure 7.3.2.3 illustrates the drainage area used when averaging model permeabilities for well E-1H. The figure also illustrates the main direction of flow. It is assumed that a geometric average of the average directional permeabilities in the horizontal direction is the best value for comparison with well test permeability. The calculated average of horizontal permeability around well E-1H is 191.20 mD which is considerably higher than 27.5 mD obtained from the well test in October 2013 (Lysne, Nakken, Totland et al., 2013). However, the area used to find an average model permeability may not be representative of the investigated area from the well test. Hence, the two values may not be directly comparable.

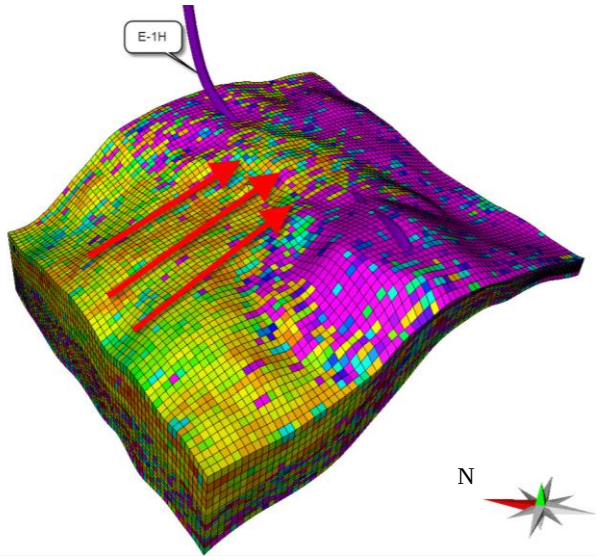

Figure 7.3.2.3: Area used to calculate an average horizontal permeability around well E-1H for comparison with well test results. Red arrows indicate the main direction of flow in the reservoir model.

All modifications to permeability were performed using Petrel 2012.2 such that updated well connections could be exported for both wells upon completion of the history matched model.

7.3.3 WELL COMPLETIONS

The location and completion range of well D-1H and E-1H in the Jette dynamic reservoir model was verified in Chapter 5.2.1 according to specifications given in drilling reports. However, it was seen when comparing the initial model with historical performance data that well D-1H produces optimistic rates with too high BHP (Figure 6.5.5). Because of this it was necessary to look closer at the completion range of well D-1H. Studies performed at Weatherford Petroleum Consultants AS had indicated a possibility of plugged sand screens in well D-1H (Lysne, Nakken, Totland et al., 2013). This led to believe that connections in the Jette dynamic reservoir model which represents the plugged sand screens should be removed from the model, resulting in shorter well completion. A reduction in completion length will result in lower well productivity and a better match towards historical performance data.

Plugged sand screens is believed to be caused by trouble during setting of sand screens since several tight spots were experienced. The well was originally drilled to a depth of 3,535 m MD RKB, but due to a restriction at 2,977 m MD RKB it was not possible to complete the well further. Due to several tight spots during setting of sand screens the swell packers were exposed to low solids oil based mud (LSOBM) for 5.7 days which would result in swell packers expanding up to 8.3″. A consequence of expanding swell packers are pack off in annulus due to pressure restrictions over swell packers. The hypothesis proposed by Weatherford Petroleum Consultants AS suggests that sand screens are plugged due to a combination of debris from pack off and LSOBM fluid loss material, such as $CaCO_3$. The pack off and plugging of sand screens is believed to be below the swell packer located at 2,535 m MD RKB. This is at the depth of the first encountered tight spot and it is reasonable that the swell packer, located at the same depth, seals off the entire well portion below this point (Lysne, Nakken, Totland et al., 2013). This in combination with plugged sand screens formed the basis for removing all completions in the Jette dynamic reservoir model below 2,535 m MD RKB. There is still some uncertainty related to what interval well D-1H produces from and it would therefore be helpful if PLT-data was aquired such that relative productivity along the well could be determined.

The new completion specifications of well D-1H are given in Table 7.3.3.1. A reduction in D-1H well length of 442 metres gave a very good response in the history matched model. The completion manager in Petrel was used to perform the changes and new connections for well D-1H could easily be exported into the correct ECLIPSE 100 format. Figure 7.3.3.1 illustrates the completion specifications before and after history matching. After reducing the completion range well D-1H no longer crosses the fault and produces from a smaller reservoir compartment then what it did before the given changes were applied.

Table 7.3.3.1 – Completion specifications of well D-1H before and after history matching

	Start of completion (m MD RKB)	End of completion (m MD RKB)	Length of completion (m)
D-1H (before history matching)	2,419	2,977	558
D-1H (after history matching)	2,419	2,535	116

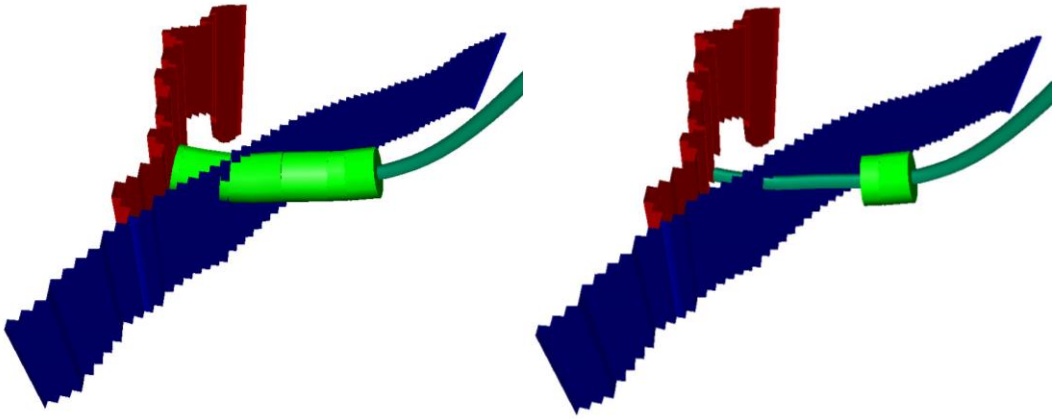

Figure 7.3.3.1: Completion specifications for well D-1H before history matching (left) and after history matching (right) together with the two faults added in Chapter 7.3.1. The light green sylinder encompassing the welltrack represents completions.

Both wells, D-1H and E-1H, experienced too high BHP when compared with historical performance data after changes described in Chapter 7.3 had been applied. To adjust BHP in order to match recorded data a multiplier was added to well indices using WPIMULT in ECLIPSE 100. It is common for horizontal wells to have unrealistically high well indices due to ECLIPSE 100 assuming all well connections to penetrate the full length of grid blocks. This is not always the case since a well may only cut through a small portion of the grid block. Hence, well indices often needs to be reduced for horizontal wells (Gilman and Ozgen, 2013). Several simulation runs were performed to optimize the selected value of WPIMULT for each well. The WPIMULT value was selected as 0.25 for well E-1H and 0.15 for well D-1H and applies to all connections in respective wells.

7.4 SUMMARY OF HISTORY MATCH

The changes performed to the Jette dynamic reservoir model in order to obtain the history matched model will be summarized briefly in the following points and includes changes made to the model during validation of input data:

- Creation and implementation of two new fluid models (Chapter 5.1).
- Changed perforation diameter in well D-1H to 8.5″ (old: 7.5″).
- Creation and implementation of new VFP-tables for well E-1H and D-1H.
- Addition of two sealing faults, separating the Jette dynamic reservoir model in south and north. E-1H is located in the southern area and D-1H in the northern area.
- Addition of three vertical flow barriers representing black shales and calcite stringers in the northern area.
- Removal of aquifer support in the northern area.
- Various permeability modifications to promote linear flow for both wells in addition to water coning in well E-1H.
- Maximum value of permeability set to 2,000 mD (old: 4,500 mD).
- Addition of vertical permeability along the northernmost fault in order to promote water production in well D-1H.
- Reduction in completion range for well D-1H due to plugging of sand screens below the swell packer located at 2,535 m MD RKB.
- Multiplier used to tune well indices. A value of 0.25 for E-1H and 0.15 for D-1H was specified with WPIMULT.

8 RESULTS FROM HISTORY MATCHING

The history matching process of the Jette dynamic reservoir model, described in Chapter 7, resulted in a single history matched model. This model is constrained from historical oil rate in order to account for production of the most valuable fluid. The history matched model has also been simulated constrained by THP. The reason for this is to assess uncertainty and elaborate further on the quality of the history matched model. It is also of interest to use the history matched model constrained by THP during prediction of reservoir performance, as it is common practice to specify the THP in prediction mode. This will be discussed further in Chapter 9. Results from the history matched model constrained by historical oil rate will be presented in Chapter 8.1 through Chapter 8.4. The history matched model of the Jette dynamic reservoir model will be referred to as the history matched model in the presentation of results while the initial model used during the beginning of history matching will be referred to as the non-matched model.

8.1 OIL PRODUCTION

Oil production rate and cumulative oil production from the history matched model is presented on a field level in Figure 8.1.1. The response of the non-matched reservoir model has also been included in Figure 8.1.1 in order to observe the improved response of the Jette dynamic reservoir model after history matching.

From Figure 8.1.1 it is seen that the history matched model follows the historical oil rate closely. This is to be expected since the history matched model is constrained from oil rate. There was a slight mismatch in oil production in the non-matched model, but this has been corrected during history matching and the Jette dynamic reservoir model is now capable of producing the correct volumes of oil. Oil production rate and cumulative volumes produced for well E-1H and well D-1H are illustrated in Figure 8.1.2 and Figure 8.1.3 respectively. Cumulative oil produced at the 1st of March 2014, the end of history matching, is compared with historical data in Table 8.1.1 for the field and individual wells. The mismatch between historical production and production from the history matched model is neglible.

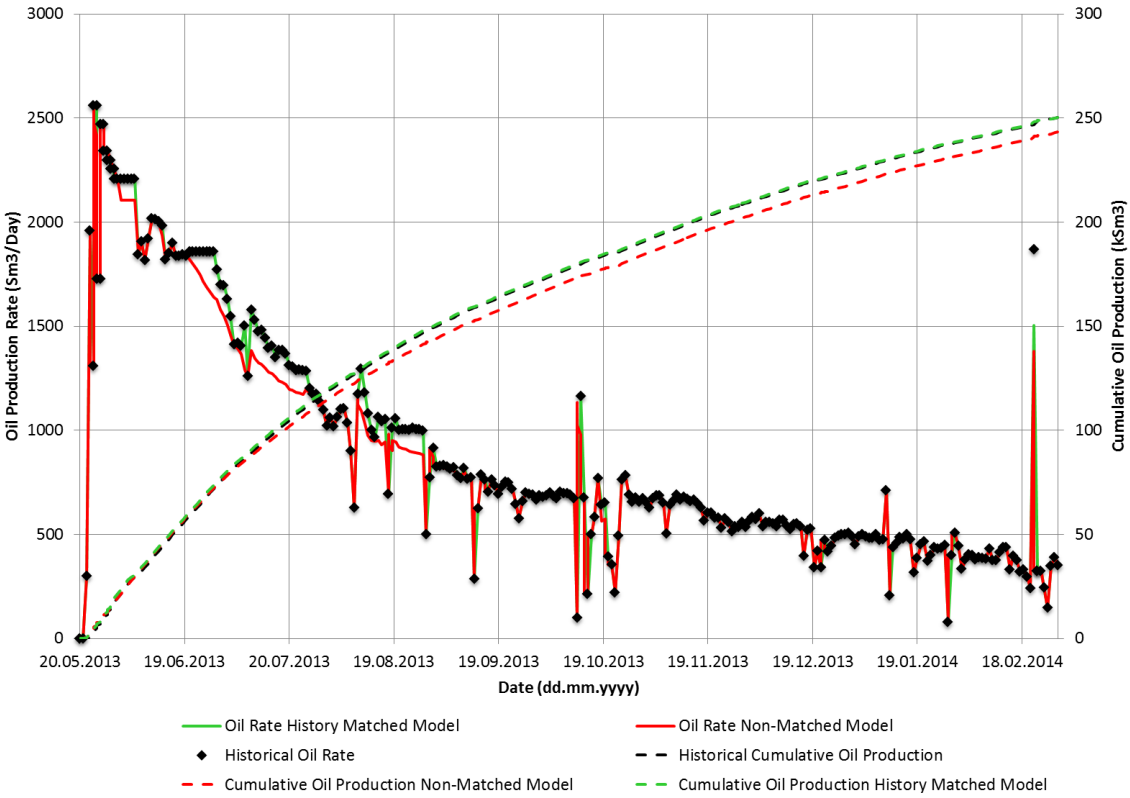

Figure 8.1.1: Field oil production in the history matched model and non-matched model together with historical oil production between 20.05.2013 and 01.03.2014.

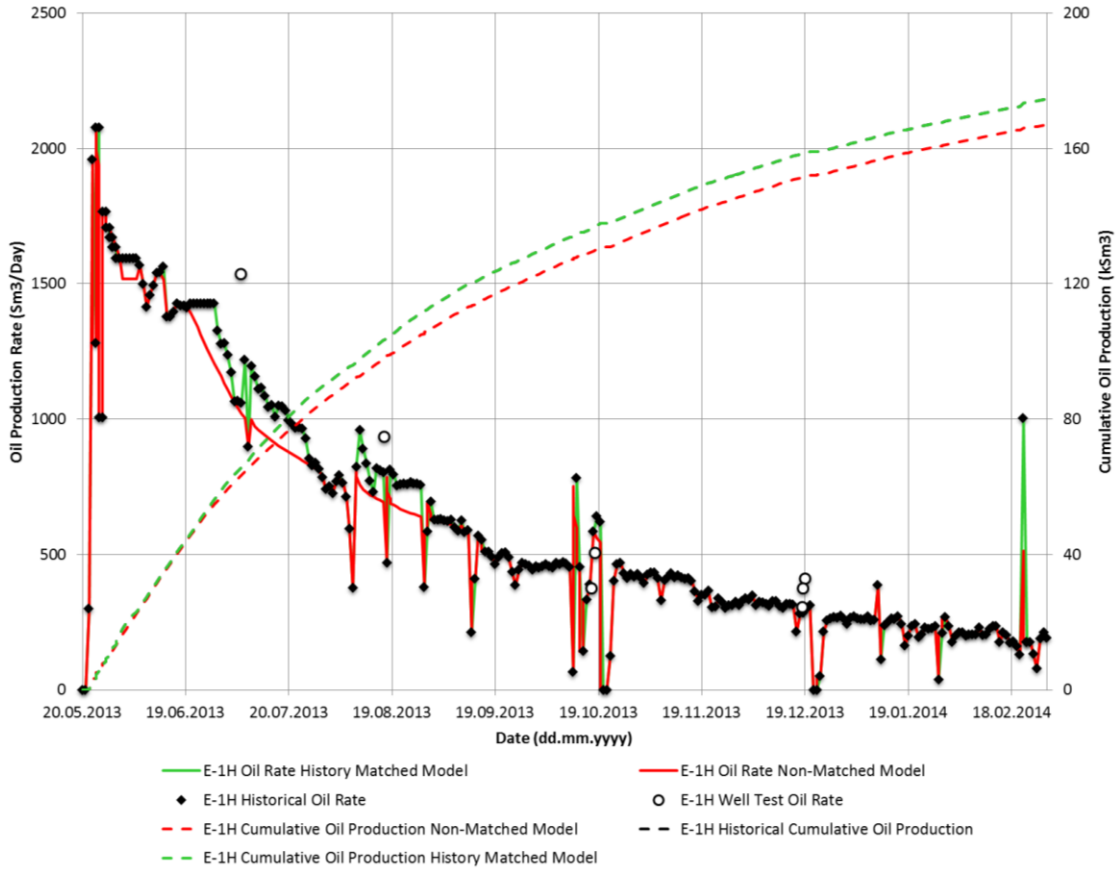

Figure 8.1.2: Oil production in the history matched model and non-matched model together with historical oil production in well D-1H between 20.05.2013 and 01.03.2014.

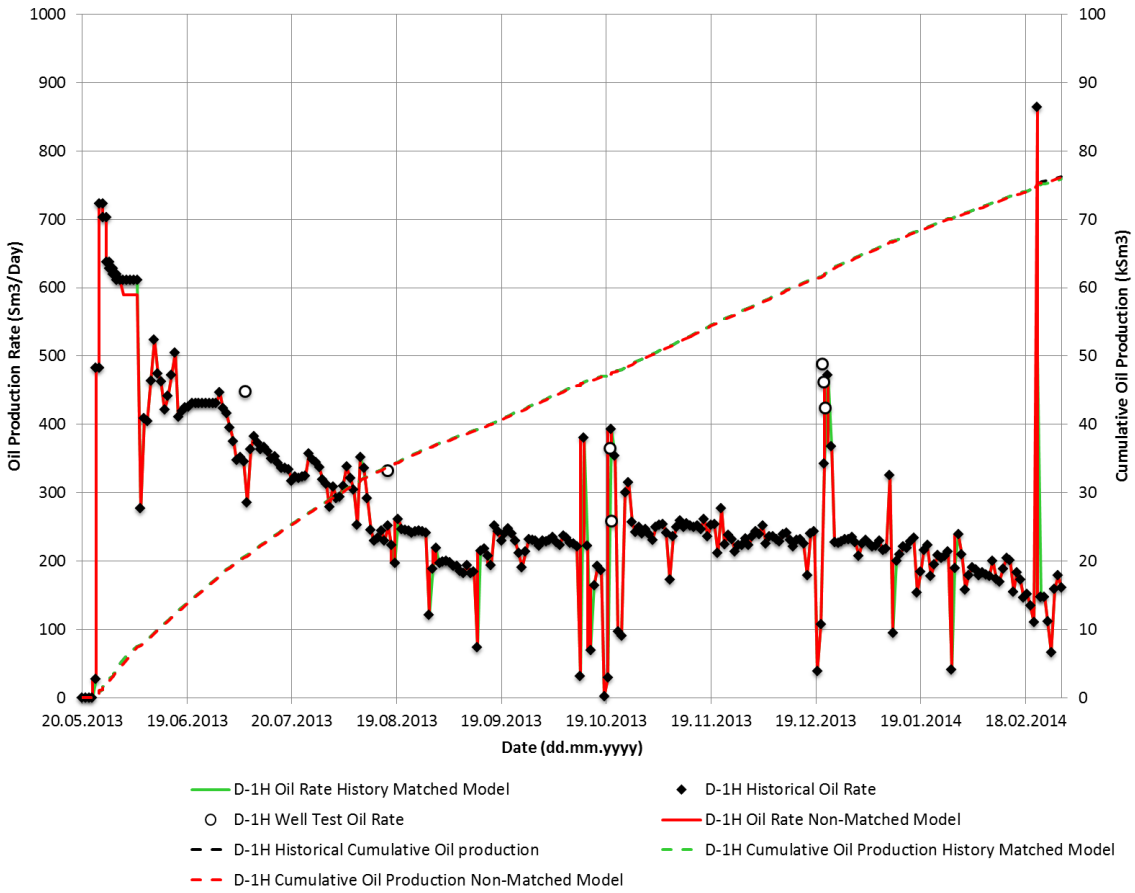

Figure 8.1.3: Oil production in the history matched model and non-matched model together with historical oil production in well D-1H between 20.05.2013 and 01.03.2014.

Table 8.1.1 – Comparison of cumulative oil production 01.03.2014			
	Field	D-1H	E-1H
Historical Cumulative Oil Production (Sm^3)	250,800	76,245	174,554
Cumulative Oil Production History Matched Model (Sm^3)	250,436	75,881	174,554
Error (%)	- 0.14	- 0.47	0.00

8.2 WATER PRODUCTION

Water production in the history matched model is illustrated in Figure 8.2.1 for the field and in Figure 8.2.2 and Figure 8.2.3 for well E-1H and well D-1H respectively. When looking at the field water production rate in Figure 8.2.1 it is evident that there is some mismatch between the history matched model and the historical production data. However, a good match is experienced before early september. From september the history matched model produces too little water compared with historical data, and from november the model also experience a deteriorating trend where the water production rate is declining rather than increasing. This is an indication that the model does not fully capture the processes taking

place within the reservoir. Note that the historical water rate in Figure 8.2.1 which has been used for matching not necessarily represents the correct historical water rate, as was discussed in Chapter 6.2. The water rate measured at the test separator represents the correct water rate and indicates a higher historical water production than the historical water rate. Unfortunately the test separator only measures water production between 7th of December and 6th of January, but it is believed that the correct historical water rate is somewhat higher than that used for history matching. If this is the case, the deviation between the history matched water production and the actual water production will be higher. Hence, the match is worse.

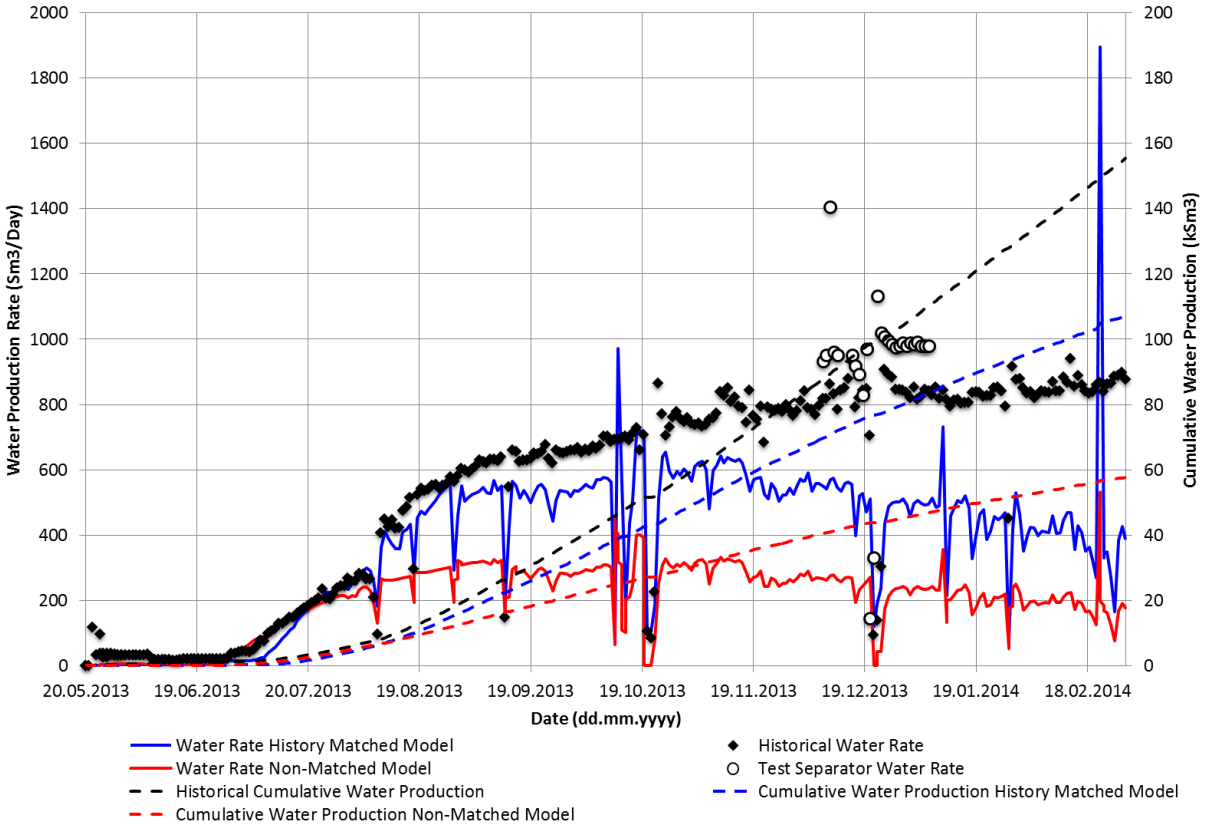

Figure 8.2.1: Field water production in the history matched model and non-matched model together with historical water production between 20.05.2013 and 01.03.2014.

Looking at Figure 8.2.2 and Figure 8.2.3 it is obvious that the mismatch in water production is caused mainly by well E-1H. However, the early water production in well E-1H is matched and the timing of water breakthrough is very close with the actual water breakthrough. The match is very close with the historical production from 20th of May until 1st of September, from which on the match deteriorates. The water production of the history matched model has been improved compared with the non-matched model but still produces with the same trend where water production declines from 15th of November. Well tests performed in well E-1H indicates higher water rates than that which has been allocated to be the historical water rate,

similar to test separator measurements in Figure 8.2.1. A reason why well tests may overestimate the water production rate is that the well produces alone, rather than commingled with D-1H during the test. This way the production from well E-1H will not be affected by having commingled production with D-1H. Hence, conditions for production are improved during the well test.

Figure 8.2.3 indicates that well D-1H matches water production rate from the 17th of July 2013 and through the rest of the history matching period until 1st of March 2014. However, the early breakthrough and water production has not been matched. This is not believed to be a concern since early water production rates in well D-1H are highly uncertain due to problems with back-allocation. The history matched water rate fluctuates more than the history but this is believed to be caused by fluctuations in the historical oil rate which the model has been constrained from. Water production in the history matched model has been improved dramatically from the non-matched model which did not produce water at all.

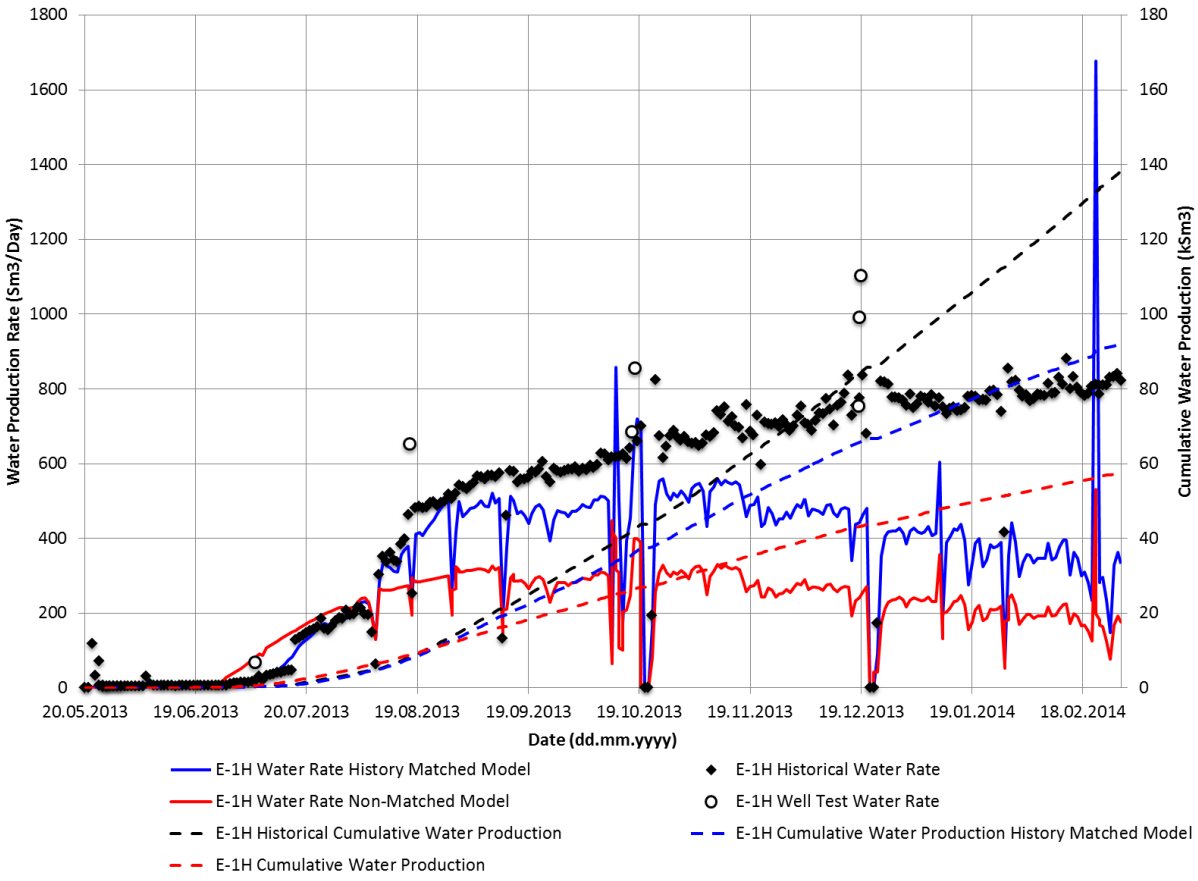

Figure 8.2.2: Water production in the history matched model and non-matched model together with historical water production in well E-1H between 20.05.2013 and 01.03.2014.

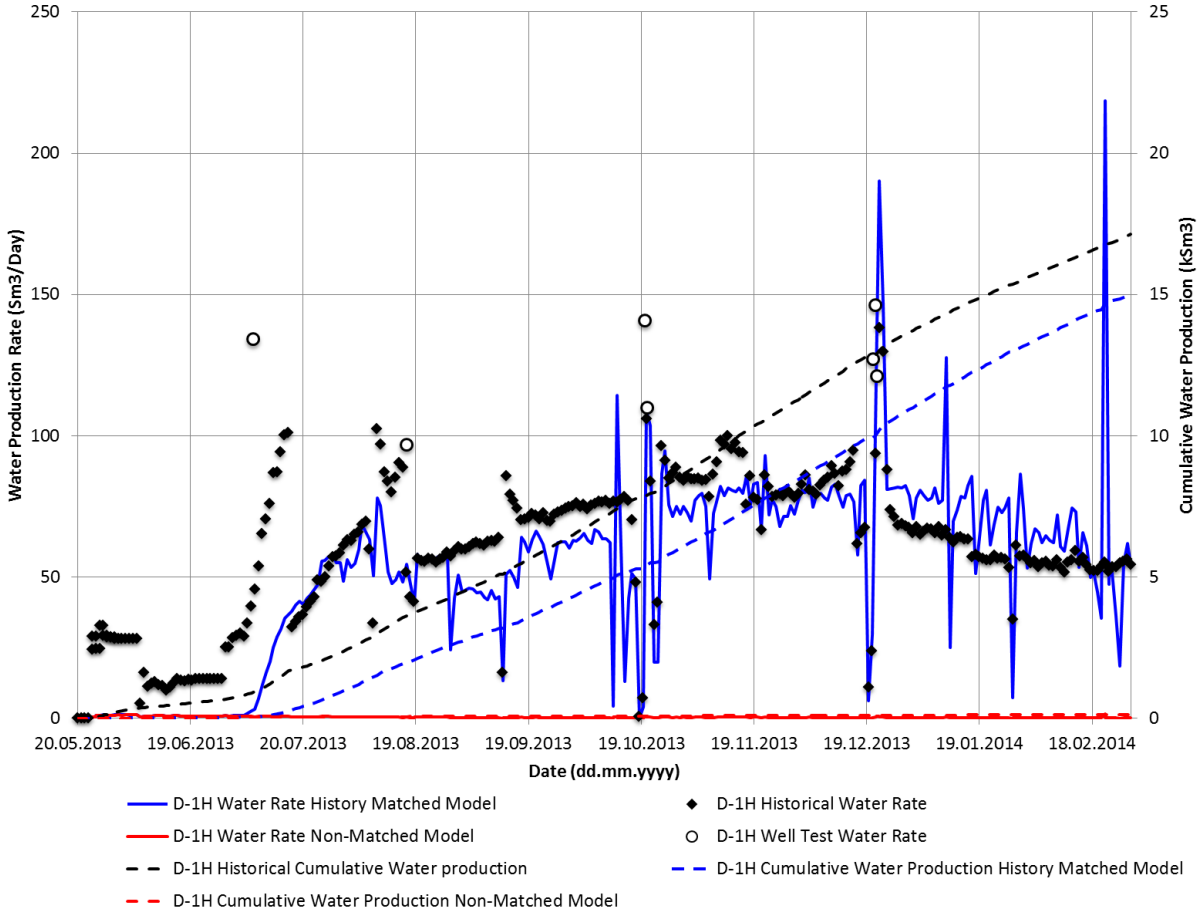

Figure 8.2.3: Water production in the history matched model and non-matched model together with historical water production in well D-1H between 20.05.2013 and 01.03.2014.

A comparison of the cumulative water production at the 1st of March 2014 between the history matched model and the historical water production is given in Table 8.2.1. The cumulative water production on a field level shows a negative error of 31.03% which is high. This error is, as discussed above, caused mainly by well E-1H not being able to follow the trend in water production rate properly. Well D-1H experiene a negative error of 12.38% in cumulative water production. This error is due to the delayed water breakthrough and problems matching early water production.

Table 8.2.1 – Comparison of cumulative water production 01.03.2014

	Field	D-1H	E-1H
Historical Cumulative Water Production (Sm^3)	155,482	17,124	138,358
Cumulative Water Production History Matched Model (Sm^3)	107,234	15,004	92,230
Error (%)	- 31.03	- 12.38	- 33.34

Figure 8.2.4 illustrates water cut in well E-1H and D-1H. D-1H has an overall good match while the match in E-1H deteriorates from 10th of September 2013. However, the history

matched model has significantly improved water production in E-1H. Figure 8.2.5 illustrates liquid production rate, oil plus water, for the field. The liquid production rate in the history matched model has a slight mismatch due to the low water production rate in well E-1H. The mismatch in liquid rate is in its entirety caused by too little water because well E-1H and D-1H both produces the correct historical oil rates (Figure 8.1.2 and Figure 8.1.3).

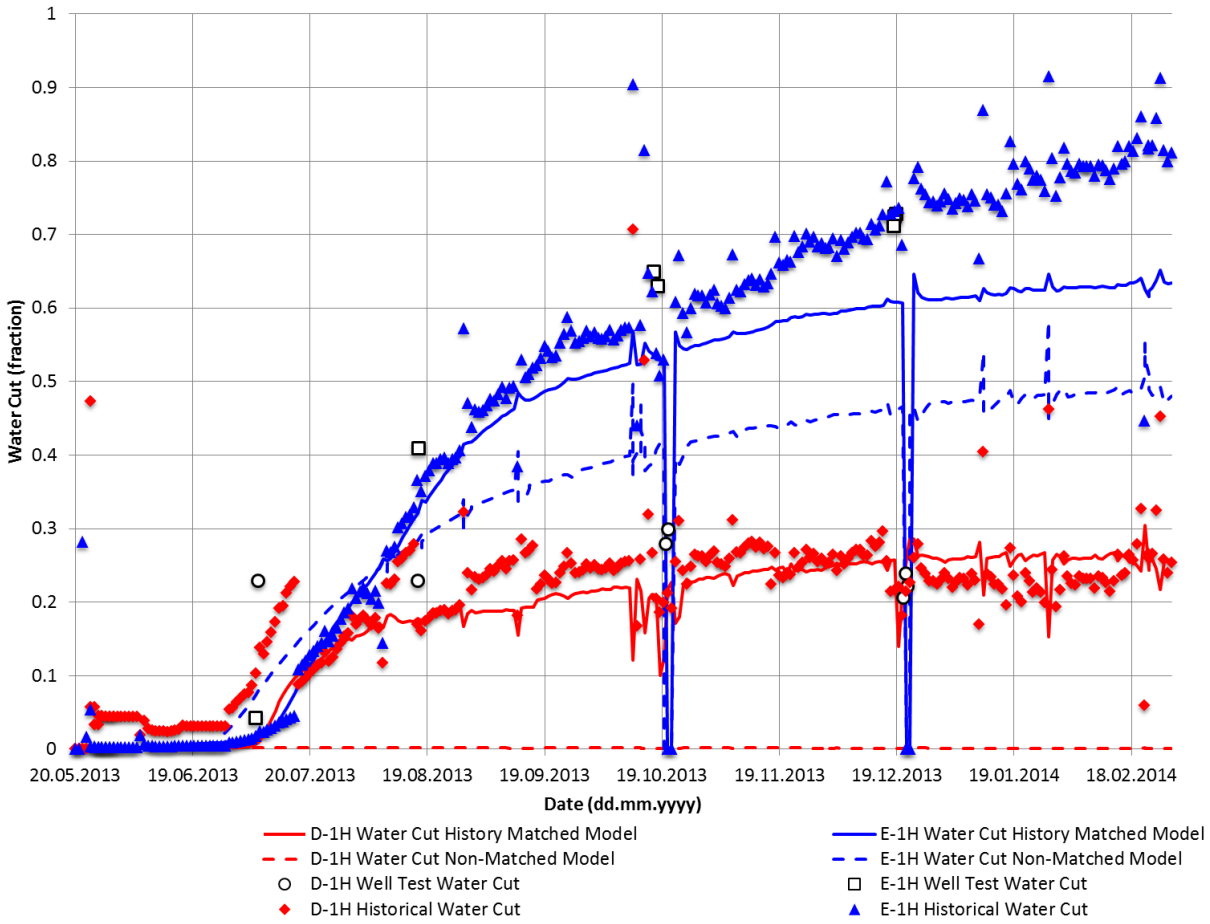

Figure 8.2.4: Water cut in the history matched model and non-matched model together with historical water cut for well D-1H and E-1H between 20.05.2013 and 01.03.2014.

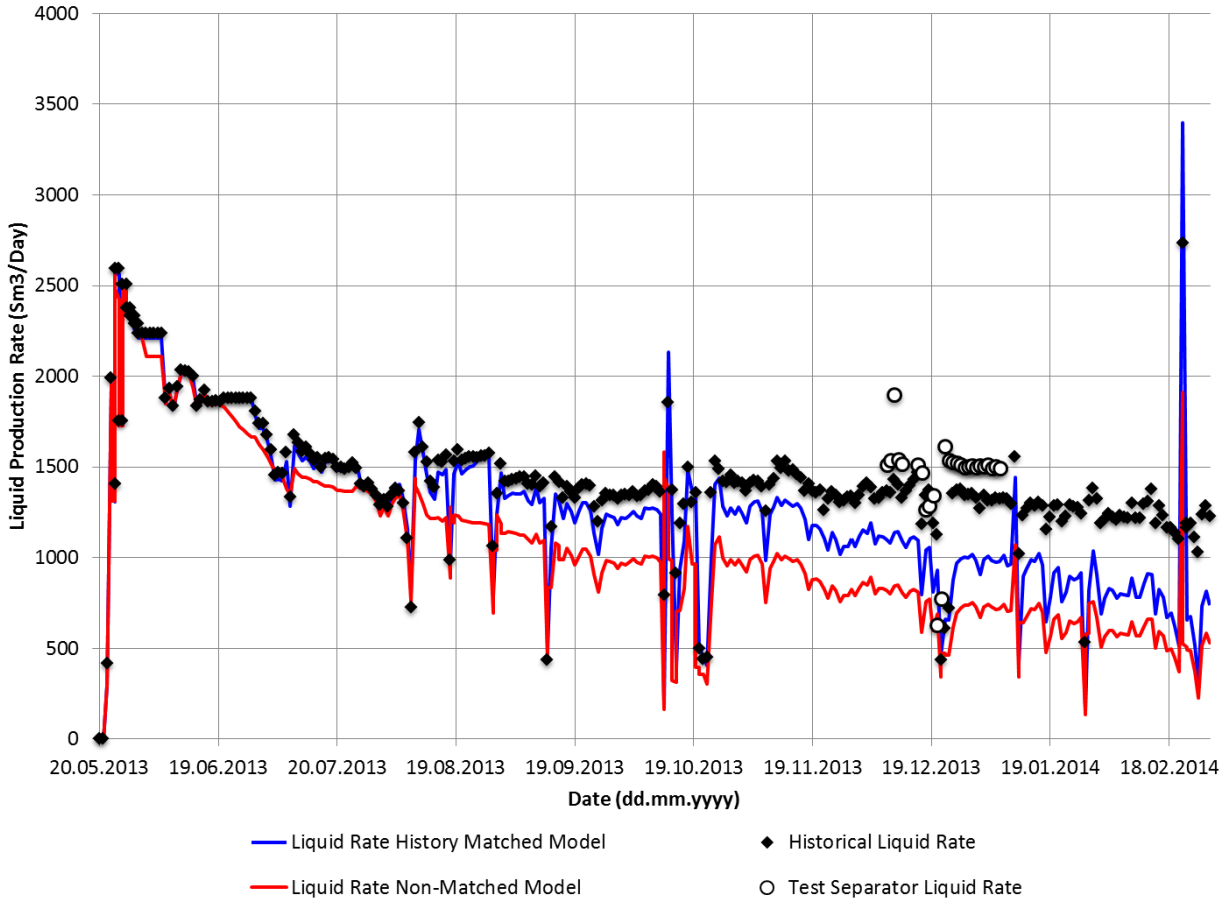

Figure 8.2.5: Field liquid production rate for the history matched model and non-matched model together with historical liquid rate between 20.05.2013 and 01.03.2014.

8.3 GAS PRODUCTION

The history matched gas production rate illustrated in Figure 8.3.1 indicates a rather large discrepancy with the historical gas production rate. This was expected as the historical gas production data described in Chapter 6.2 is too low due to back-allocation being performed using the wrong fluid data. The measurements with highest confidence is taken at the test separator in the period between 7th of December 2013 and 6th of January 2014 and is what have indicated that gas production should be higher than that which has been allocated. Figure 8.3.1 illustrates a good match between the history matched model and measurements of gas production at the test separator. Hence, it is believed that the gas production rate from the history matched model represents a more realistic production than the allocated historical gas production. The cumulative gas production of the history matched model is compared with historical gas production data in Table 8.3.1. An error of 42.04% between the two models is obtained at 1st of March 2014.

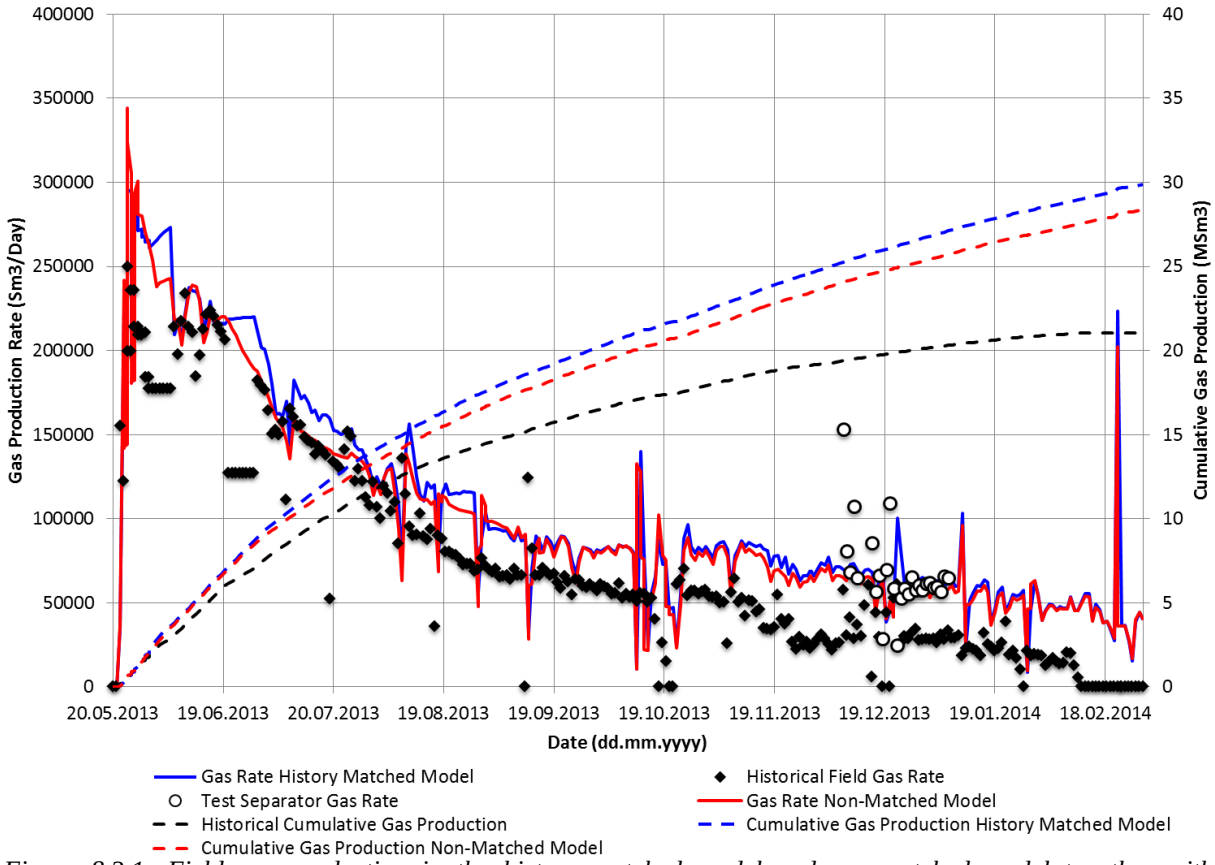

Figure 8.3.1: Field gas production in the history matched model and non-matched model together with historical gas production between 20.05.2013 and 01.03.2014.

Table 8.3.1 – Comparison of cumulative gas production 01.03.2014	
	Field
Historical Cumulative Gas Production (Sm^3)	21,023,660
Cumulative Gas Production History Matched Model (Sm^3)	29,863,520
Error (%)	42.04

Figure 8.3.2 illustrates the resulting GOR. Once again, most confidence is given measurements at the test separator and the history matched model is seen to match these measurements accurately. Also, the GOR in the history matched model is more or less constant compared with the historical GOR which is declining. This decline in GOR is not realistic as GOR should increase due to gas coming out of solution with the oil when the reservoir is depleted below bubblepoint pressure.

There is not observed much difference between the non-matched model and the history matched model in gas production (Figure 8.3.1) and GOR (Figure 8.3.2). Even though new fluid models were created in Chapter 5.1 the GOR was not altered significantly. Hence, only a small difference in gas production.

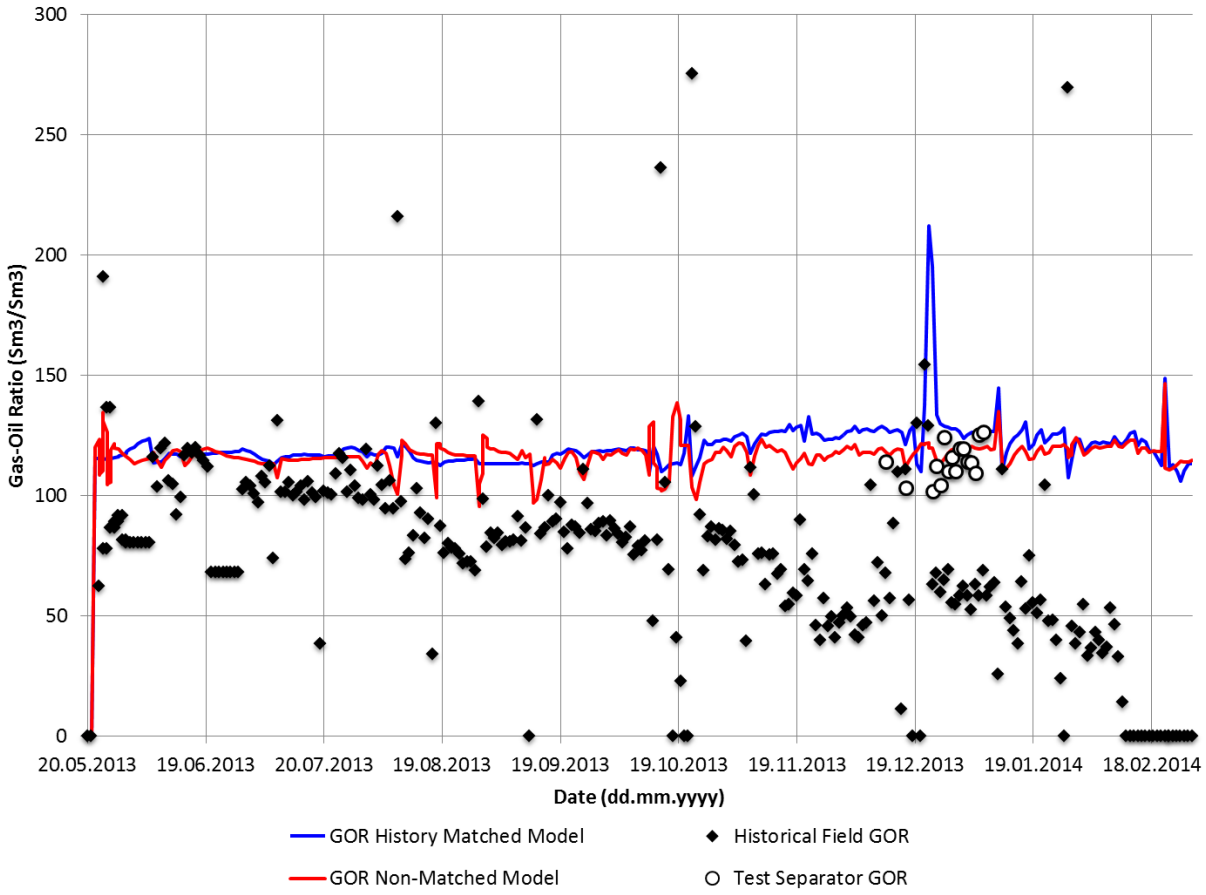

Figure 8.3.2: GOR in the history matched model and non-matched model together with historical GOR between 20.05.2013 and 01.03.2014.

8.4 PRESSURE MATCH

Figure 8.4.1 and Figure 8.4.2 illustrates the obtained pressure match of BHP and THP in well E-1H and D-1H respectively. Well E-1H experiences a good match in both BHP and THP from 20th of May 2013 until 15th of November 2013. After 15th of November 2013 the match deteriorates as the BHP increases. This happens at the same time as the water production trend in well E-1H starts to decline, such that the model gradually produces too little water. When seen together this implies that there may be too much oil in the model because the historical oil rate which constrains the model can easily be met with a gradually lower drawdown. A consequence of an increase in BHP is lower drawdown which in turn leads to less water production. Hence, it is believed that if the BHP had been lowered to match the recorded BHP values the water production rate in well E-1H would have been matched more closely with history and the trend of increasing water. This has been investigated when the history matched model were simulated constrained from THP and is presented in Chapter 8.5.

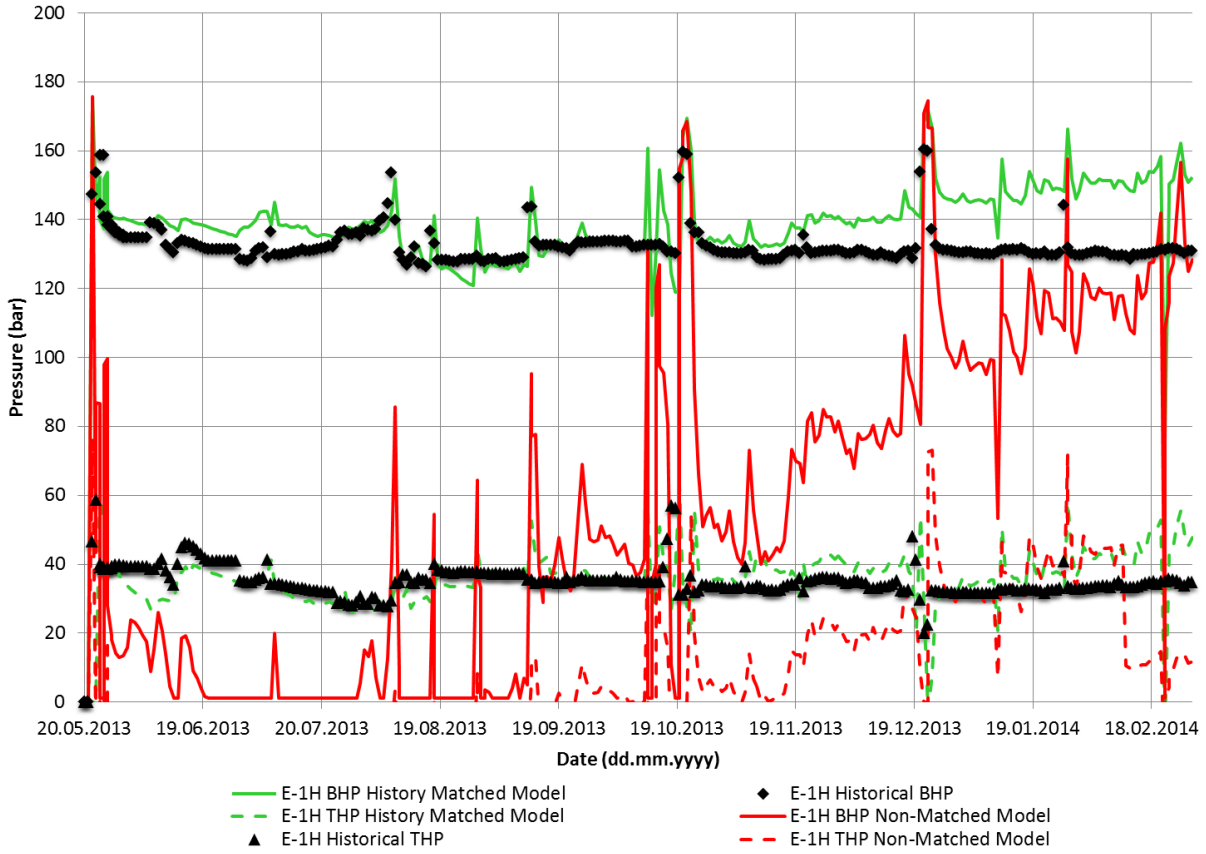

Figure 8.4.1: BHP and THP in the history matched model and non-matched model together with historical BHP and THP in well E-1H between 20.05.2013 and 01.03.2014.

The BHP and THP in the history matched model has been improved dramatically when compared with the non-matched model. A comparison of the measured BHP and THP with the history matched model at 1st of March 2014 is given in Table 8.4.1. There is more error in the THP, probably due to a combination of mismatch in flow rates and minor errors in the VFP-tables supplied to the simulator.

Table 8.4.1 – Comparison of history matched and historical pressures for well E-1H 01.03.2014

	BHP	THP
Recorded Pressure at Gauge (bar)	130.9	35.2
History Matched Model (bar)	152.2	58.3
Error (%)	16.27	65.62

BHP and THP is closely matched in well D-1H (Figure 8.4.2) except for a small deviation in THP at the end of the history matching period. This corresponds to the time where well D-1H produces slightly too much water. However, if there is too much water in the wellbore it should result in an overestimate of the pressure gradient and a lower THP than the measured historical value. Hence, the mismatch is believed to be due to minor errors in the VFP-table of well D-1H. Table 8.4.2 summarizes the error in BHP and THP at the 1st of March 2014. Even

though there is a 37.06% error in THP and 9.11% error in BHP it is important to look at the trend which has been matched closely for both THP and BHP through most of the history matching period.

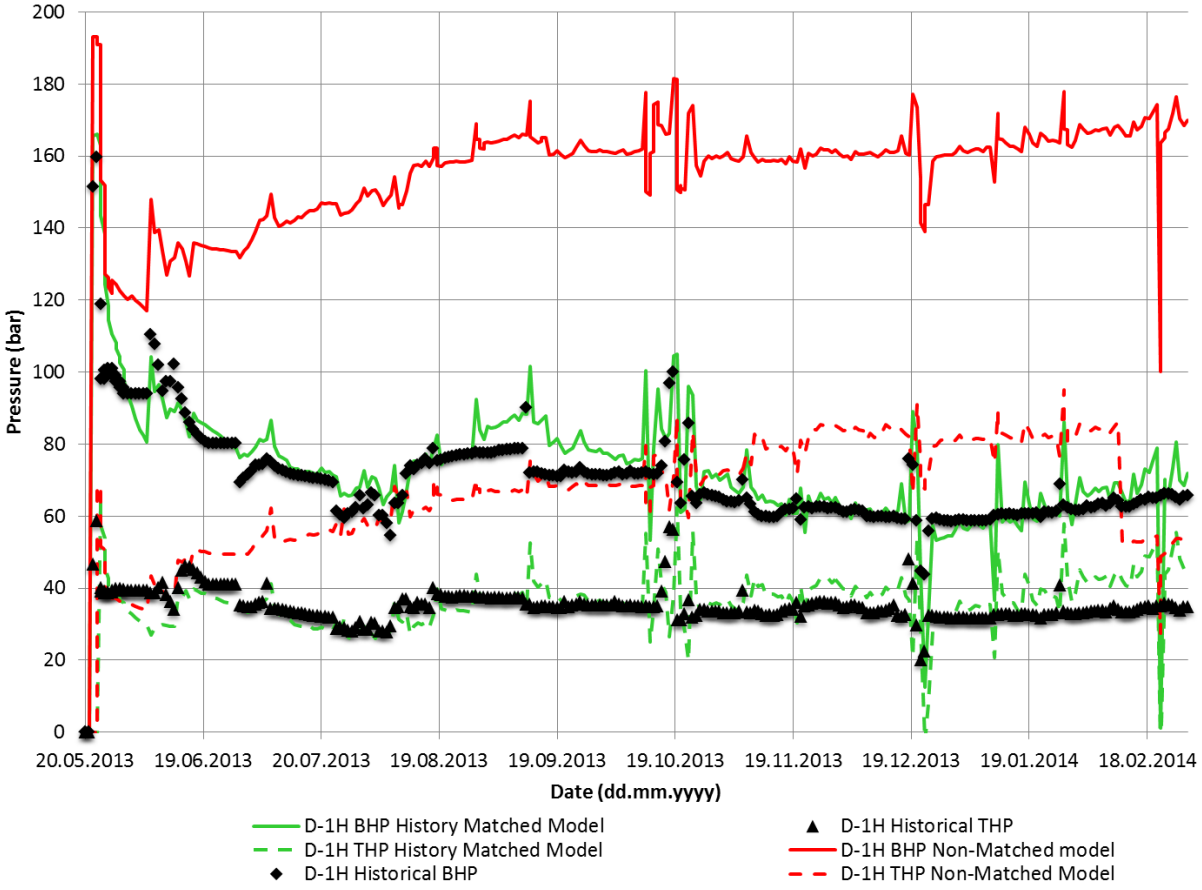

Figure 8.4.2: BHP and THP in the history matched model and non-matched model together with historical BHP and THP in well D-1H between 20.05.2013 and 01.03.2014.

Table 8.4.2 – Comparison of history matched and historical pressures for well D-1H 01.03.2014		
	BHP	THP
Recorded Pressure at Gauge (bar)	65.8	34.8
History Matched Model (bar)	71.8	47.7
Error (%)	9.11	37.06

8.5 MATCH FROM THP CONSTRAINT

An alternative simulation run of the history matched model was performed where the model was constrained from recorded THP rather than allocated oil rate. When the history matched model is constrained from THP it will calculate the rate of all phases and BHP resulting from the given THP and gas lift rate. Figure 8.5.1 and Figure 8.5.2 illustrates THP and BHP in well E-1H and D-1H respectively. The calculated BHP deviates slightly for both wells. However,

the trend of the calculated BHP in well E-1H (Figure 8.5.1) follows the history closely with a negative error of only 6.34% at 1st of March 2014. The trend in calculated BHP in well D-1H (Figure 8.5.2) is also very good but experiences a slightly higher error in BHP at 1st of March 2014 with a negative error of 13.07%. There is much reason to believe that some of the error in the calculated BHP is caused by small errors in the VFP-tables of wells. One indication which points in the direction of trouble with the VFP-tables are the periods where the wells have been shut in because it cannot flow at the given conditions. Where this happen is indicated in Figure 8.5.1 and Figure 8.5.2 by red circles. The phenomenon is associated with well tests where the wells have already been shut in or where gas lift rates are very low.

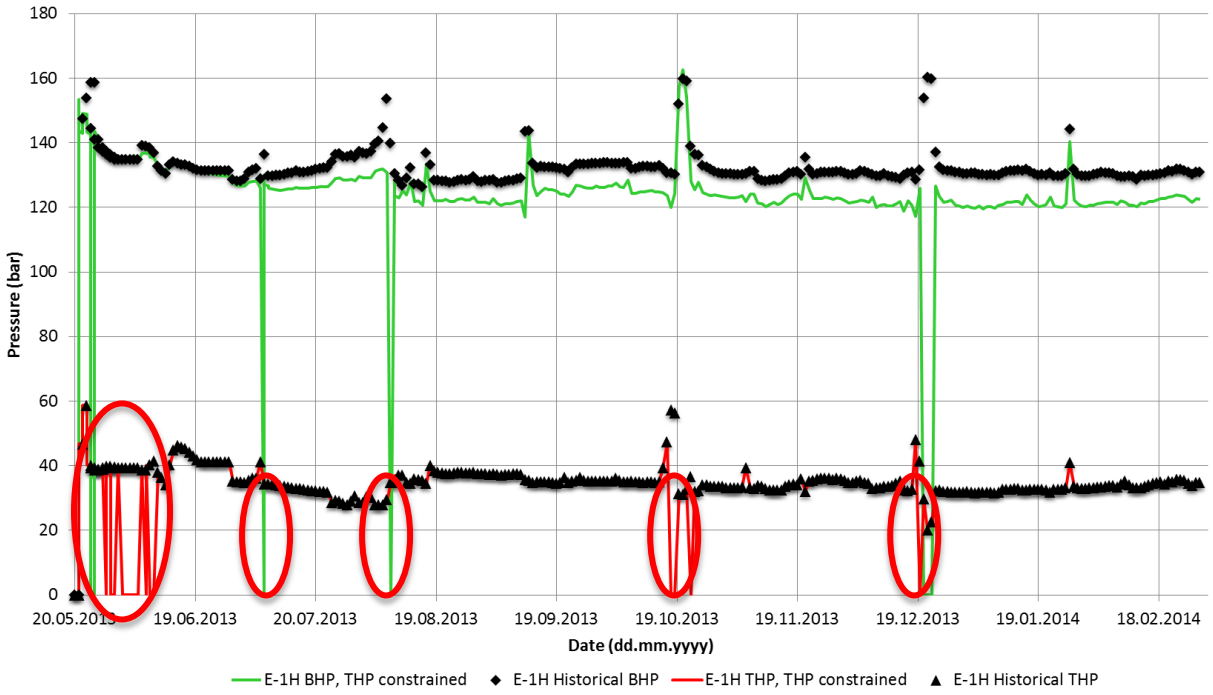

Figure 8.5.1: BHP and THP for well E-1H in the history matched model when constrained from THP during simulation. Red circles indicate the times when the well has been shut in because of it not being able to flow at the given conditions.

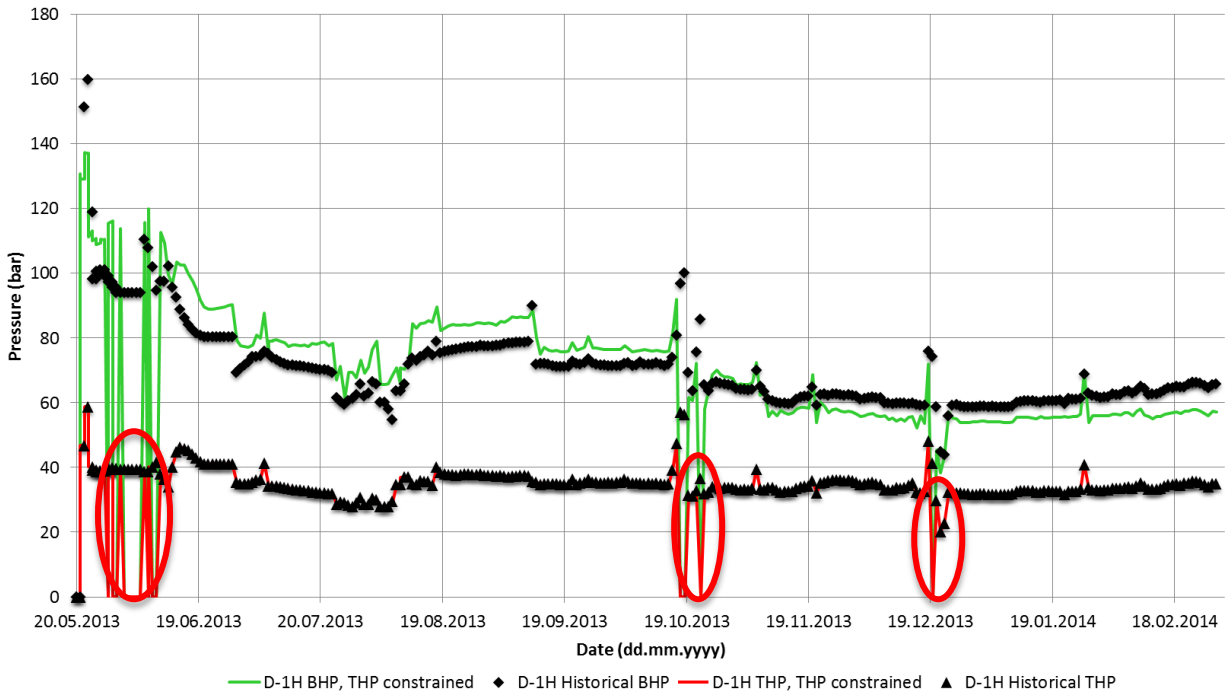

Figure 8.5.2: BHP and THP for well D-1H in the history matched model when constrained from THP during simulation. Red circles indicate the times when the well has been shut in because of it not being able to flow at the given conditions.

Table 8.5.1 – Comparison of BHP at 01.03.2014 when the history matched model is constrained by THP

	E-1H	D-1H
Recorded Pressure at Gauge (bar)	130.9	65.8
History Matched Model (bar)	122.6	57.2
Error (%)	- 6.34	- 13.07

The resulting oil and water production when the model has been constrained by THP is illustrated in Figure 8.5.3 and Figure 8.5.4 for well E-1H and D-1H respectively. Well E-1H experiences a good match in water production rate. Comparison of water production when the model was constrained from allocated oil rate (Figure 8.2.2) shows that the model now follows the trend spot on, with an exception of too early water breakthrough. However, the oil rate is now overestimated due to the reduction in BHP resulting from the model being constrained by THP. This confirms the theory from Chapter 8.4 that there might be too much oil in the area around well E-1H. Also, the model is capable of producing the correct amount of water when the BHP is closer to the recorded BHP. The model overestimates cumulative oil production in well E-1H by 16.4% and water production by 5.68%. Oil rate in the history matched model at 1st of March 2014 is 389 Sm^3/day compared with 191 Sm^3/day which is the the recorded oil rate at this date. Hence, the oil production rate is overestimated by 103.6% at the end of history mode.

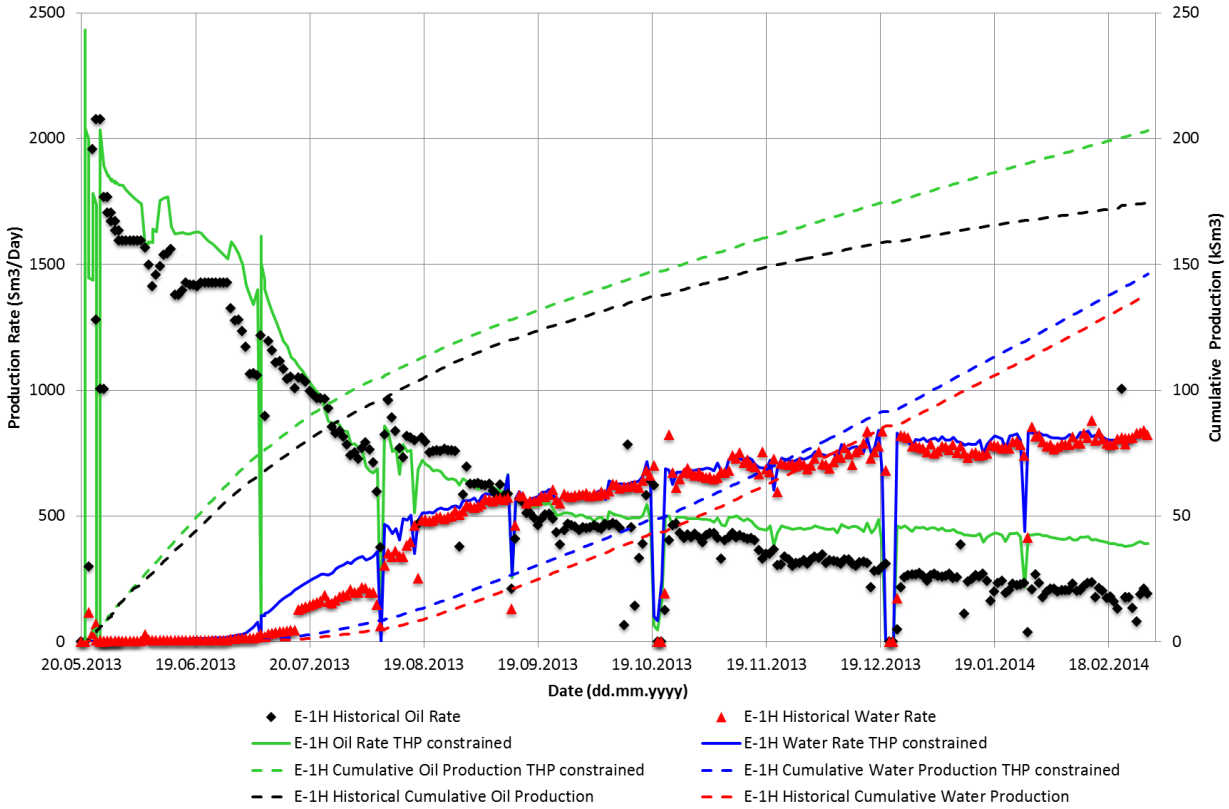

Figure 8.5.3: Oil production and water production for well E-1H in the history matched model when constrained from THP during simulation.

Table 8.5.2 – Comparison of cumulative production 01.03.2014 for well E-1H when the history matched model is constrained by THP		
	Oil	Water
Historical Cumulative Production (Sm^3)	174,554	138,358
Cumulative Production History Matched Model (Sm^3)	203,185	146,227
Error (%)	16.4	5.68

The behavior of well D-1H when running the history matched model constrained by THP is similar to the behavior when it was constrained by allocated oil rate. Hence, validating the match. This is seen when comparing Figure 8.5.4 with Figure 8.1.3 and Figure 8.2.3. The water production experiences a negative error of 8.81%, slightly less than in the model constrained by allocated oil rate, whilst the error in oil production is 0.76%.

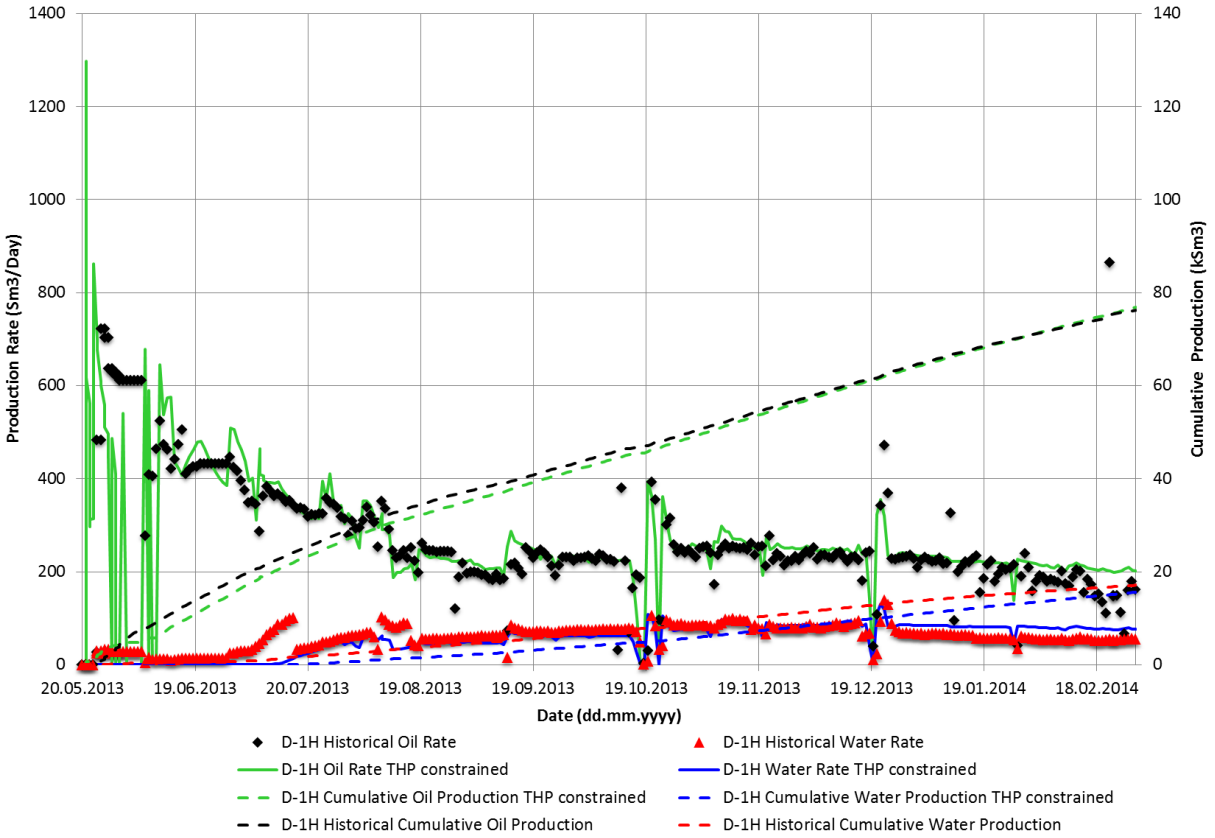

Figure 8.5.4: Oil production and water production for well D-1H in the history matched model when constrained from THP during simulation.

Table 8.5.3 – Comparison of cumulative production 01.03.2014 for well D-1H when the history matched model is constrained by THP		
	Oil	Water
Historical Cumulative Production (Sm^3)	76,245	17,124
Cumulative Production History Matched Model (Sm^3)	76,824	15,614
Error (%)	0.76	- 8.81

Further results from the history matched model when constrained from THP is given in Appendix F. This includes gas production, liquid production and water cut.

8.6 SENSITIVITY IN STOIIP

From the presented results it is believed that the history matched model contains too much oil and that this is what causes well E-1H to experience mismatch in water production and BHP after 15th of November 2013 when the history matched model is constrained by allocated oil rate. Based on this it was decided to run a few simulations with sensitivity to the STOIIP to investigate if this would improve match. Because well D-1H is considered successfully history matched sensitivity in STOIIP has only been applied to the southern part of the Jette

reservoir corresponding to the area of fluid model 1 (Figure 5.1.1.4). STOIIP was reduced by applying a pore volume multiplier of 0.9 and 0.95 to form two simulations for sensitivity. Figure 8.6.1 illustrates the results. It is seen that a reduction in STOIIP leads to a worse history match. However, it is still believed that there is too much oil in the model close to well E-1H. It is possible that a reduction in STOIIP for smaller areas of the Jette dynamic reservoir model will be more effective and establish a better representation of late time oil production than the applied sensitivity runs. However, locating and altering STOIIP in areas which governs late time oil production is a challenging process and only one of several hypothesises explaining the observed mismatch in well E-1H of the history matched model.

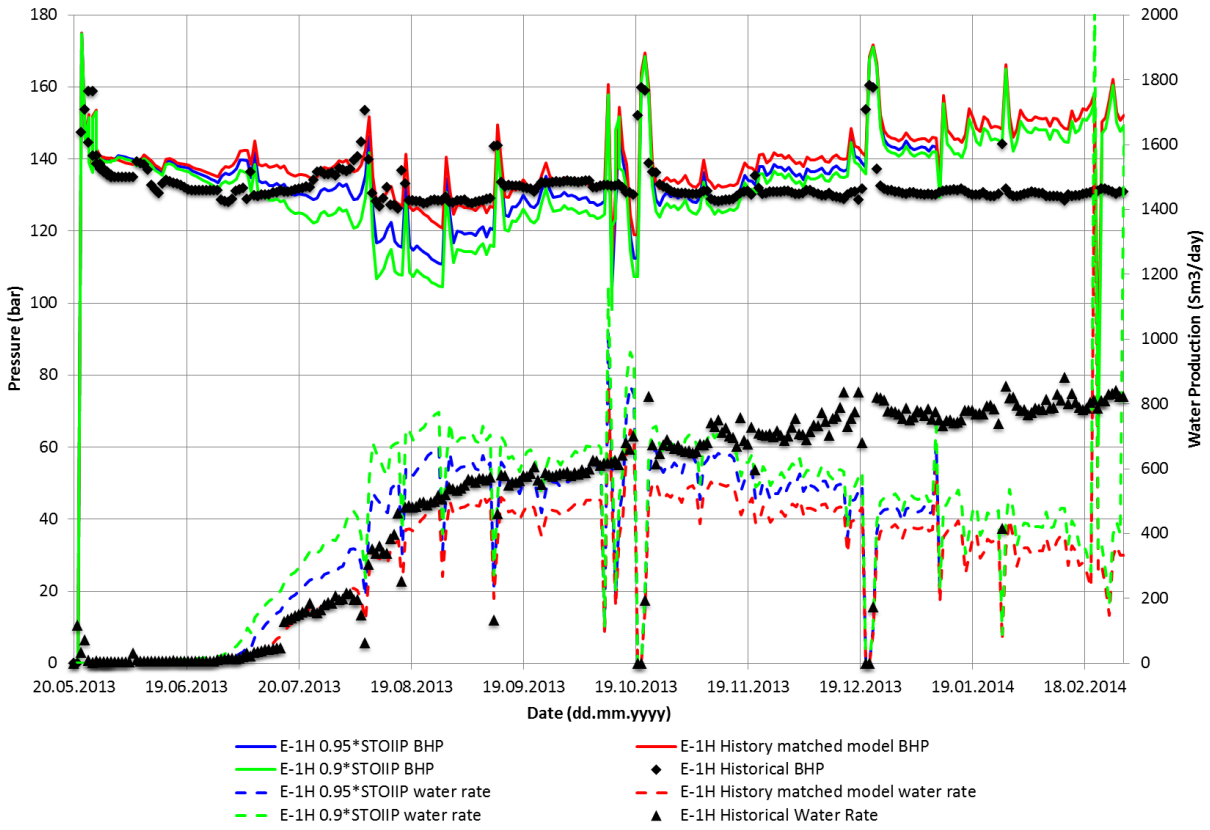

Figure 8.6.1: BHP and water rate for well E-1H in the history matched model constrained by allocated oil rate with sensitivity in STOIIP. STOIIP is reduced with a pore volume multiplier of 0.95 and 0.9.

9 FORECASTING JETTE RESERVOIR PERFORMANCE

The objective of history matching is to provide a model capable of predicting future reservoir performance under various operational scenarios and guide reservoir management decisions for optimization of production. Reservoir performance from Jette has been predicted using the history matched model and will be discussed below.

9.1 SETTING UP FOR PRODUCTION FORECAST AT JETTE

Reservoir performance forecasting has been performed using the history matched Jette dynamic reservoir model described in Chapter 7 and Chapter 8. It was decided to use the history matched model which had been constrained by THP during the history mode for predictions. The response of this model is described in Chapter 8.5 and Appendix F. The reason for choosing this model for predictions rather than the history matched model constrained by allocated oil rate is that the most common procedure is to specify wells to operate at a given THP during predictions. This was described in more detail in Chapter 2.9. Also, running the model constrained from measured pressures are considered less uncertain than running the model constrained from an allocated rate. Choosing this model and operating wells at a given THP during prediction of reservoir performance will allow us to avoid a seam effect when moving from history mode to prediction mode. A disadvantage of using the history matched model constrained from THP is that it overpredicts oil in well E-1H (Figure 8.5.3). However, water production and pressures are more realistic in this model. Also, if the history matched model constrained from allocated oil rate had been chosen we would need to set an unrealistic operating pressure during predictions in order to avoid seam effects. This is due to the pressure mismatch at the end of the history mode in the history matched model constrained from allocated oil rate.

The history matched Jette dynamic reservoir model was set up for predictions using a restart in the ECLIPSE 100 simulator. A restart allows the user to start a simulation run from any of the previously written restart files. The prediction model was specified to start simulation at the 1st of March 2014 (end of history mode) in order to avoid having to simulate the historical period. Hence, reducing the simulation time of predictions since there will be no changes in model performance before 1st of March 2014. The model used for predictions was

specified to run until 1st of January 2020, similar to the period used in previous predictions performed by Det norske.

It was necessary to define a basecase in order to compare the incremental change in production with varying operational constraints. The basecase was selected as a ”do-nothing” case where the model performance was predicted using the existing operational conditions at the end of the historical period. It was specified to operate at the last measured THP from the historical data. The gas lift rate used in the basecase was selected as the average gas lift rate from the two first weeks in March 2014, 80,000 Sm^3/day and 100,000 Sm^3/day for well D-1H and E-1H respectively.

Gas lift rate was chosen as the main variable to be changed between the various prediction scenarios. Performing workovers, infill drilling or secondary recovery planning during predictions at Jette was simply not realistic because of the enormeous expenses this would pose to the owners of such a marginal field as Jette. Hence, it was decided to look at how various gas lift rates affect the forecasted reservoir performance. Three prediction scenarios were selected in addition to the basecase, resulting in a total of four scenarios. All scenarios are constrained by THP during simulation and with gas lift rate as the only parameter changed. Details about the scenarios used to forecast reservoir performance are given in Table 9.1.1.

Table 9.1.1 – Overview of scenarios used to forecast reservoir performance at Jette

			THP Constraint		Gas Lift Rate	
Scenario #	Description	Prediction Period	D-1H (bar)	E-1H (bar)	D-1H (Sm^3/day)	E-1H (Sm^3/day)
1	Basecase	01.03.2014 – 01.01.2020	34.83	35.21	80,000	100,000
2	Optimum Gas Lift Rate	01.03.2014 – 01.01.2020	34.83	35.21	90,000	110,000
3	Reduced Gas Lift Rate	01.03.2014 – 01.01.2020	34.83	35.21	50,000	50,000
4	No Gas Lift	01.03.2014 – 01.01.2020	34.83	35.21	0	0

Prediction scenario number two uses the optimum gas lift injection rate. The optimum gas lift rate was selected based on a gas lift optimization study performed by Krogstad and Barbier (2014) at Weatherford Petroleum Consultants AS. Figure 9.1.1 illustrates gas lift sensitivity for well D-1H and E-1H when producing together. It was concluded that the optimum gas lift rate is 200,000 Sm^3/Day in total when both wells produce together, with a distribution of 45% (90,000 Sm^3/day) in well D-1H and 55% (110,000 Sm^3/day) in well E-1H (Krogstad and Barbier, 2014). The remaining prediction scenarios, number three and number four,

investigate the effect of reducing gas lift rate for each well to 50,000 Sm^3/day and to stop gas lift injection completely.

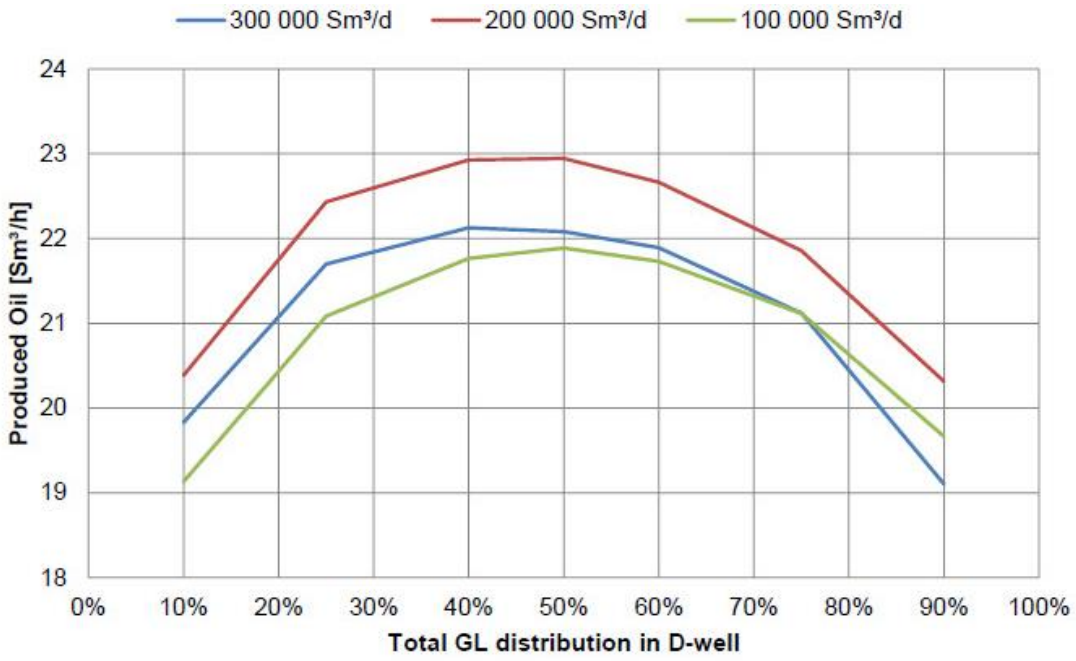

Figure 9.1.1: Sensitivity in total gas lift rate and distribution of gas lift between well D-1H and well E-1H when producing together. Optimum oil production is obtained for a total gas lift rate of 200,000 Sm^3/day with 45% distributed in well D-1H and 55% distributed in well E-1H (Krogstad and Barbier, 2014).

Predictions are performed without any considerations regarding economics. Hence, the model will not be restricted by an economic rate. Also, the cost of gas lift is not considered when comparing production between the various scenarios used for prediction of reservoir performance. Finally, predictions have been performed without consideration of well regularity. As a consequence, wells are assumed to produce 100% of the simulation time without any halts in production. This makes predictions optimistic since wells are regularly shut in to perform well tests or to resolve problems.

9.2 PRODUCTION FORECAST RESULTS

Predicted oil rate and cumulative oil production for all scenarios are illustrated in Figure 9.2.1. It is obvious that the choice of gas lift rate affects the predicted reservoir performance and that the reservoir is unable to produce without gas lift as indicated by the response from scenario #4. Gas lift rates used in the different scenarios are given in Table 9.1.1. From Figure 9.2.1 it is observed that scenario #2 with an optimum gas lift rate produces slightly better than

the basecase (scenario #1). An incremental increase in oil production of 1.08% is obtained if the gas lift rate is changed to the optimum gas lift rate indicated by Krogstad and Barbier (2014). With the increased oil production obtained from switching gas lift rate also comes an increased water production (Figure 9.2.2). The increase in water production is more pronounced than the increase in oil production. An overview of predicted oil production and predicted water production is given in Table 9.2.1 and Table 9.2.2 respectively.

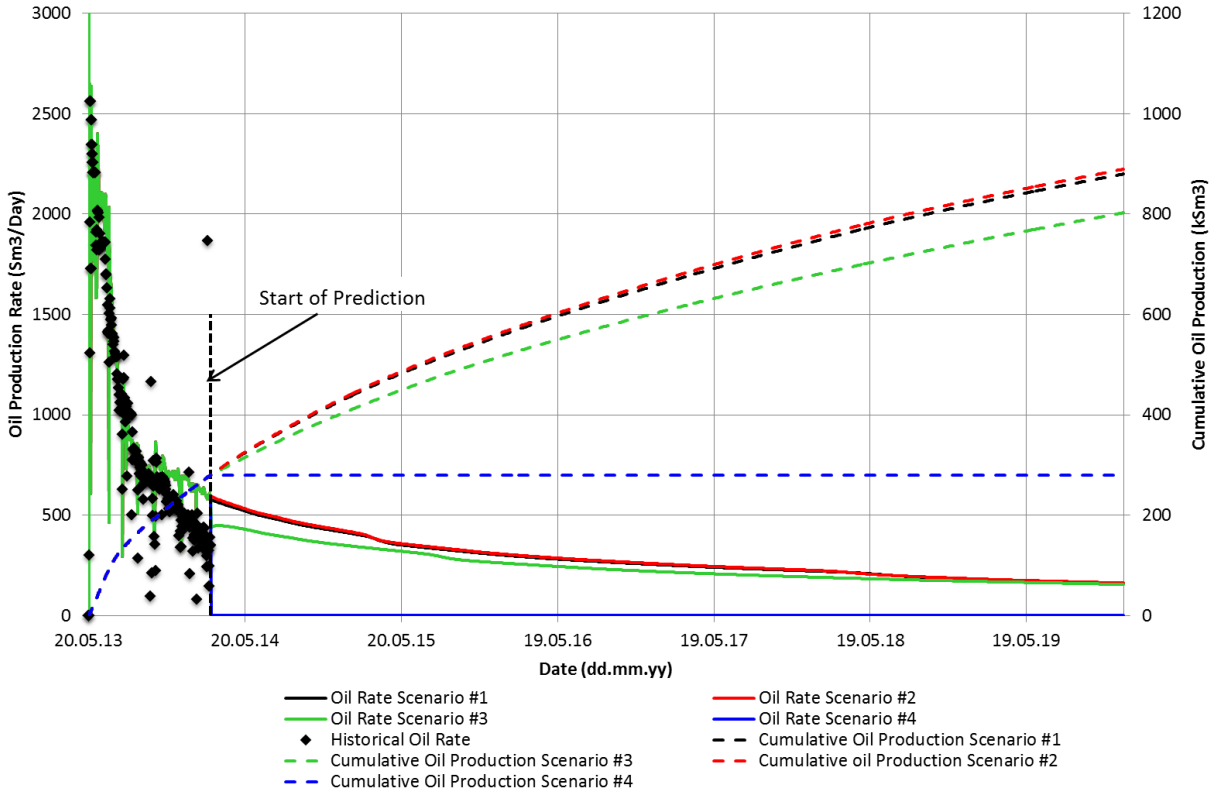

Figure 9.2.1: Predicted oil rate and cumulative oil production for the Jette field in the period 01.03.2014 to 01.01.2020.

Scenario #3 experience a dramatic reduction in oil rate due to a lower gas lift rate when compared to the basecase and scenario #2. It is also seen that scenario #3 causes a discontinuity (seam effect) when moving from history mode to prediction mode. This is caused by a severe alteration in operating conditions for wells due to the total gas lift being reduced from 200,000 Sm^3/day to 100,000 Sm^3/day. Hence, the seam effect is caused by the newly imposed operating conditions rather than problems with the model, as discussed in Chapter 2.9. This is also supported by the basecase and scenario #2 having a smooth transition from history mode to prediction mode.

Table 9.2.1 – Predicted oil production 01.01.2020		
Scenario #	Cumulative Oil Production (Sm^3)	Incremental Increase in Oil Production* (%)
1	879,709	n/a
2	889,247	1.08
3	802,441	- 8.78
4	280,010	- 68.17
* Compared with basecase (Scenario #1)		

Further results from prediction of reservoir performance are given in Appendix G.

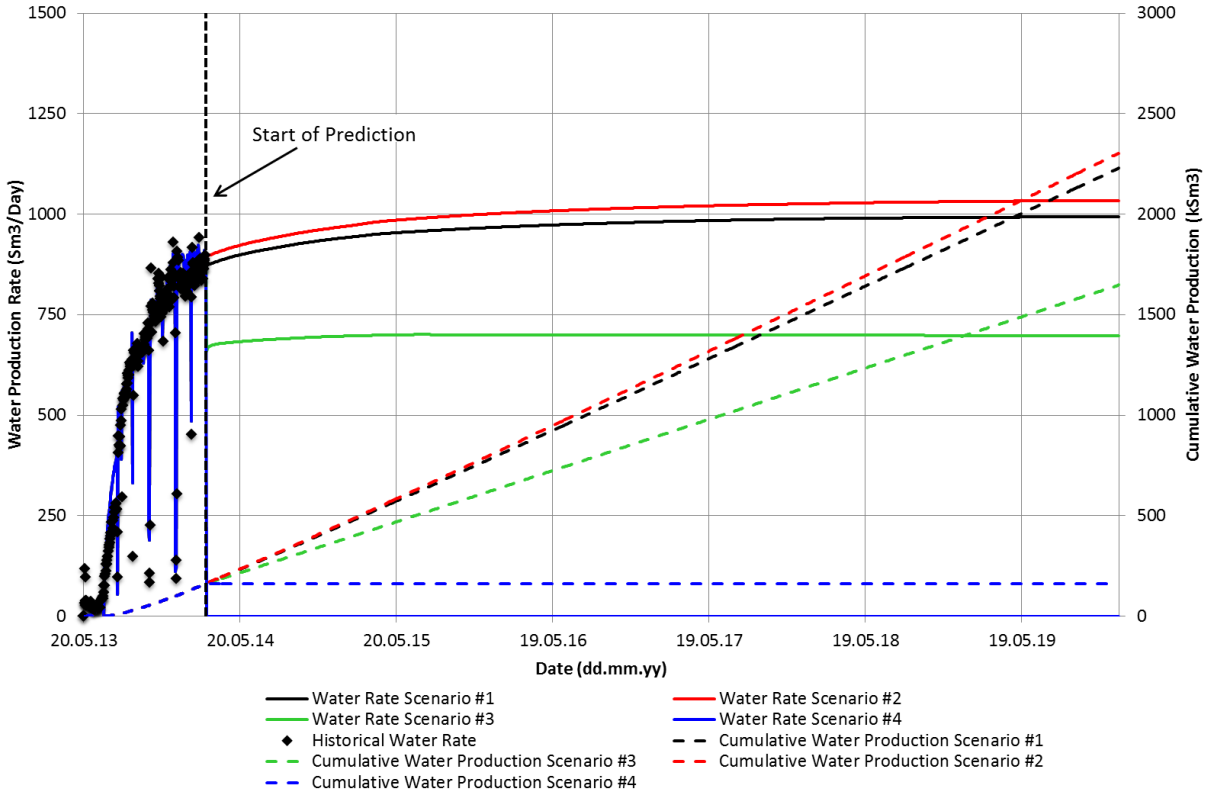

Figure 9.2.2: Predicted water rate and cumulative water production for the Jette field in the period 01.03.2014 to 01.01.2020.

Table 9.2.2 – Predicted water production 01.01.2020	
Scenario #	Cumulative Water Production (Sm^3)
1	2,229,629
2	2,304,040
3	1,647,853
4	161,842

It is important to note that predicted oil production from the history matched model is overestimated, mainly caused by well E-1H. Chapter 8.5 discusses this issue and it is also seen in Figure 9.2.1 that the oil rate is higher than the historical rate at the start of prediction. To underscore this point historical oil rate from 01.03.2014 to 05.05.2014 has been plotted together with predicted oil rate for comparison in Figure 9.2.3. At 01.04.2014, one month into

prediction mode, predicted oil rate was 556 Sm^3/day while the historical oil rate was measured to be 360 Sm^3/day, an overestimate of 54.4% in prediction scenario #1. The overestimate in oil production would have been slightly less if a well efficiency factor had been included in the predictions to account for well regularity.

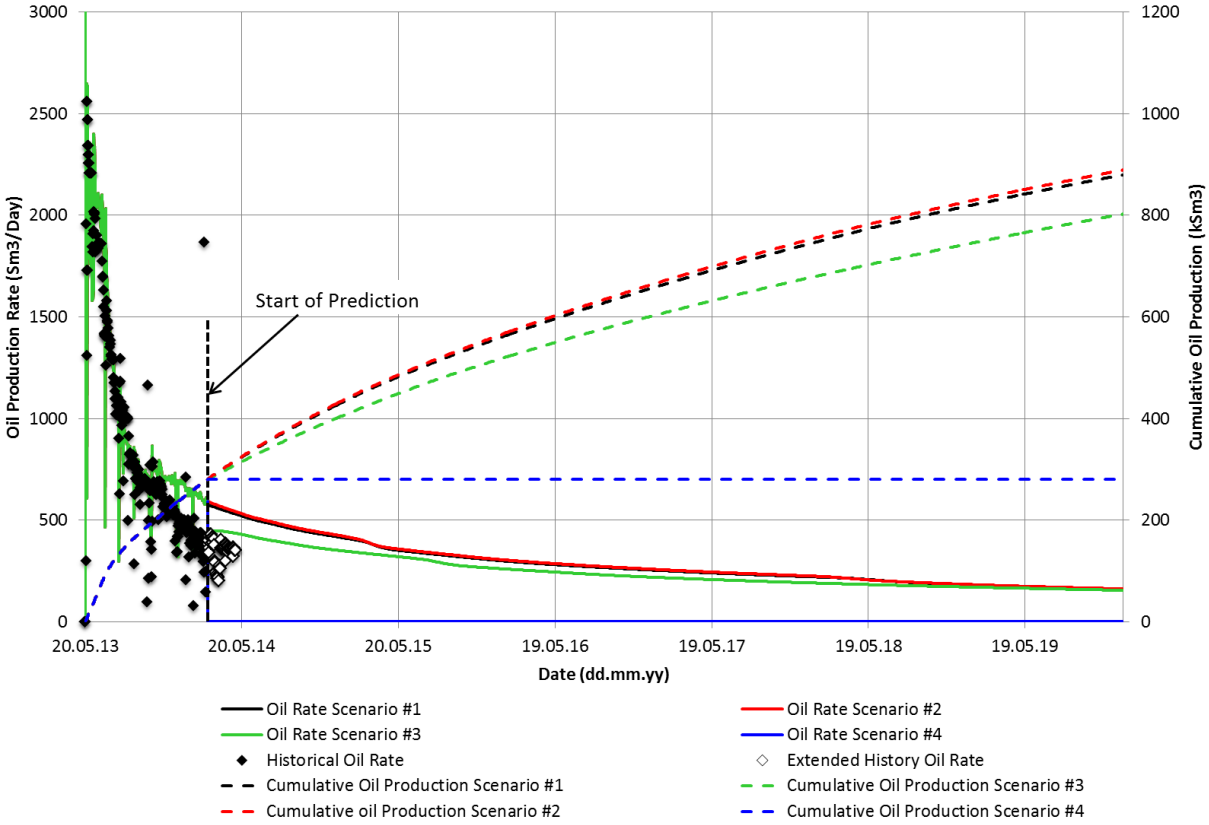

Figure 9.2.3: Predicted oil rate and cumulative oil production for the Jette field in the period 01.03.2014 to 01.01.2020. Historical oil rate available after start of prediction has been added for comparison with predicted oil rate.

10 DISCUSSION

A history match of the Jette dynamic reservoir model was obtained by making perturbations in a trial and error fashion. However, all perturbations have been made in accordance with geologic understanding and available information from Jette as described in Chapter 7. It is believed that all changes made to the Jette dynamic reservoir model are realistic, or at least possible, and that the obtained history match represent the reservoir behavior at Jette with more realism than the initial non-matched model. However, there is still some discrepancy between performance of the history matched model and the historical data describing reservoir performance at Jette which will have to be elaborated.

It is especially important to realize that the obtained history match of the Jette dynamic reservoir model is only one of several possible solutions, because of the non-unique nature of history matching problems. Hence, several equiprobable history matched models may be obtained in addition to the history match presented in this Master's thesis. Even though the obtained match is believed to improve understanding of the reservoir and model the governing reservoir mechanisms more correctly, it might be wise to obtain several history matched models of Jette in the future. Having several equiprobable history matched models is useful when predicting reservoir performance where one is interested in assessing uncertainty and form estimates of P10, P50 and P90 for capital investments.

There has been much uncertainty surrounding historical performance data from Jette which the history matched model has been matched with. It is believed that production from Jette has been erroneously allocated by ExxonMobil because of the mismatch in production when Jette was allowed to produce to the test separator alone. Hence, it is possible that the Jette dynamic reservoir model should have been history matched towards slightly different rates, most likely higher than those used in the history matched model. If it is concluded that historical rates are false, they should be updated in the Jette dynamic reservoir model such that the history match can be adjusted to match the new production data, believed to be more correct than the old.

The Jette dynamic reservoir model is deemed successfully history matched even though there still exist some mismatch when comparing model performance with historical performance data. It is particularly difficult to obtain a good history match for reservoir models which have a stochastic property distribution, such as that in the Jette dynamic

reservoir model. This is because stochastic models are highly heterogeneous and not capable of modeling more homogeneous sands and continuous channels that might be present in the reservoir. However, it is uncertain if a better history match could have been obtained with a deterministic property distribution in the Jette dynamic reservoir model. The distribution of sands at Jette is probably more homogeneous than what have been modeled in the stochastic Jette dynamic reservoir model and it is possible that populating the model again, not necessarily with a stochastic distribution, will provide an alternative history match.

It is mainly well E-1H which experience mismatch in the history matched model. Well E-1H has problems with water production and increasing BHP after 15th of November 2013 when constrained from allocated oil rate. This is believed to be due to an overestimate of oil in the Jette dynamic reservoir model. A specification of too low residual oil saturation is of course also possible since this value is based on SCAL from Jotun and therefore highly uncertain. Sensitivity to STOIIP in the area around well E-1H was applied in Chapter 8.6 but did not improve results in the history matched model. This sensitivity was applied on the entire region and it is believed that reduction of oil in a given area of the Jette dynamic reservoir model might improve the response. It is a possibility that the fluid model in the region with well E-1H is wrong and that a higher formation volume factor would give a better result, because this would reduce the amount of oil produced at surface conditions.

Initialization of fluids in the Jette dynamic reservoir model is also based on SCAL from Jotun, and it is possible that the distribution have been wrong and that it would be possible to obtain a better history match if fluids were distributed differently from a new initialization.

Relative permeability can be questioned in the history matched model as a single set of relative permeability curves have been used to model two different fluid systems. In addition, relative permeability curves are based on tests performed with core samples and fluids from Jotun. Hence, a high degree of uncertainty is related to relative permeability, and an alteration of the curves might improve water production in well E-1H. Previous attempts to improve water production in well E-1H with high permeable channels between the well and aquifer were not successful, which leads to believe that an alteration in relative permeability is needed in order to improve match. The fluid present in the region around well D-1H is more similar to the fluid at Jotun and this region would probably require less alterations in relative permeability than the region around well E-1H.

Due to the linear flow behavior present at Jette and in the Jette dynamic reservoir model it is not believed to be any significant grid orientational effects. There might be some

numerical dispersion present, causing smearing of the saturation front and problems when modeling water coning close to well E-1H. There is a good chance that a finer grid could reduce numerical dispersion and improve the ability to model water coning in well E-1H to obtain a better match. However, downscaling the grid would most likely lead to convergence issues when running the model because of too large throughput ratios in the grid blocks close to the well.

All perturbations required to obtain the history matched model was described and justified in Chapter 7. However, the completion length of well D-1H in the history matched model is still uncertain. One of the reasons for this is that well test analysis has problems obtaining linear flow with such a short well. On the other hand, well test analysis does not consider permeability anisotropy in the same way as what has been introduced in the history matched model. In the Jette dynamic reservoir model it is permeability anisotropy which allows linear flow. Well test analysis is able to obtain a good match for linear flow when the reservoir around D-1H is modeled as a channel. This result supports the obtained history match with D-1H being completed down to 2,535 m MD RKB. Hence, there is a possibility that well completion should be reduced as done in the history matched model. It would probably be possible to obtain a history match without a reduction in completion length as well. However, this would require alterations in the thickness of the sand D-1H produces from such that similar depletion could be obtained. It is unfortunate that such a large uncertainty in producing length of D-1H exist, because knowing the exact length would condition the history match and reduce number of possible solutions (reduce uncertainty). Obtaining information about the relative productivity of zones in the well from a PLT would greatly benefit the history match.

Because this Master's thesis has been performed by the author alone, perturbations to the model has been based solely on one's intuition and interpretation of various reports and previous reservoir studies. It is believed that an even better history match would have been obtained if the history matching had been conducted in a multidisciplinary team. Confidence of perturbing certain parameters would most likely have been higher because there would be experts backing up changes related to their domain of expertise.

Simple predictions were conducted with the history matched model. Oil production were overestimated due to well E-1H, as mentioned in Chapter 9.2. The overestimate would have been less if the BHP in the model had been higher, closer to recorded data, and it is possible that this could have been achieved with a slight alteration to VFP-tables by including lift gas with higher specific gravity. Previous predictions of oil production at Jette have been

even more optimistic than the predictions presented in this Master's thesis. The latest estimate of technical reserves at Jette, amount of oil which will be produced, was estimated to be 1.039 MSm^3 (Det norske oljeselskap ASA, 2013a). The basecase prediction presented in Chapter 9.2 yields a cumulative oil production of 0.879 MSm^3, a 15.4% reduction from previous estimates by Det norske. Predicted oil should have been even lower because of well E-1H overestimating production, compared with historical data. Hence, the trend in predicted production of oil is declining as new information about the reservoir is obtained and incorporated into the Jette dynamic reservoir model.

Even though the work in this Master's thesis has resulted in a successfully history matched Jette dynamic reservoir model there will always be room for improvements to the model. Also, new production data will be available which needs to be incorporated into the model together with other information obtained during the lifetime of the field. Hence, history matching will never obtain a perfect match and should be seen as a continuous process.

11 CONCLUSION

From results presented in Chapter 8 it is concluded that history matching of the Jette dynamic reservoir model has been performed successfully. The history matched model represents a non-unique solution and is believed to model reservoir behavior at Jette with greater confidence and accuracy than the initial model before history matching was capable of. The increased realism and understanding of the Jette dynamic reservoir model will be valuable when performing reservoir studies in the future which will help guide reservoir management decisions.

Additional conclusions from history matching of the Jette dynamic reservoir model are:

- Uncertainty from back-allocation of production at Jette is inherent in the history matched Jette dynamic reservoir model. Higher confidence in back-allocation of production and historical performance data at Jette will yield higher confidence to the history matched model.
- The Jette reservoir is compartmentalized and consist of several fluid systems.
- Oil is produced mainly from the Z2 zone in both wells, D-1H and E-1H.
- It is likely that water production in well E-1H is caused by water coning from the close by aquifer. The history matched Jette dynamic reservoir model is not able to fully capture water coning at Jette.
- Well D-1H has no pressure support from the aquifer.
- Vertical communication along the northernmost fault in the model represents the mechanism for water production in well D-1H. Water is allowed to flow vertically close to the fault from the underlying water zone in order to enter the producing layer where it will be produced.
- The STOIIP in the Jette dynamic reservoir model is likely too high in the southern area close to well E-1H.
- Production forecasting indicate that production at Jette is sensitive to gas lift rate and unable to produce without artificial lift. An increase in gas lift rate yields higher oil production.
- Recoverable reserves at Jette have been reduced compared with previous estimates calculated by Det norske.

12 FURTHER WORK

Recommendations for further work with Jette can be split in two categories, continuation and further work based on the current history matched model and creation of several other equiprobable history matched models of the Jette reservoir. Each category will list several points with recommendations for further work below.

Further work with current history matched model:

- Continue the history matching to obtain an even better match. Incorporate new production data to keep the history matched model updated.
- Utilize AHM software in order to improve the current history match and perform sensitity analysis to various parameters.
- Create a network model to represent commingled production from the PLEM to Jotun B. This will help minimize uncertainties because the Jette dynamic reservoir model will be matched with more measured data, such as the pressure topside Jotun B.
- Use the history matched model to investigate actions for improving oil recovery, such as sidetracking of current wells and infill drilling.
- Convert the history matched model into a 2-dimensional fine grid model capable of modeling water coning in well 25/8-E-1 H. Tuning and matching of such a model will yield valuable information on how to update the 3-dimensional Jette dynamic reservoir model in order to improve the history match.
- Perform decline curve analysis to obtain a prediction of reservoir performance and an estimate of recoverable reserves which can be used for comparison with predicted performance from the history matched Jette dynamic reservoir model.
- Perform studies with material balance calculations to assess volumetrics in the reservoir and determine compartmentalization and aquifer influx. The obtained information can be used to update and validate the history matched Jette dynamic reservoir model.

Creation of equiprobable history matched models:

- Utilize AHM software in conjuction with manual history matching on the initial Jette dynamic reservoir model to obtain several equiprobable history matched models. The

set of equiprobable history matched models will be used to predict reservoir performance and to provide estimates of P10, P50 and P90 for any capital investments in the field.

- Create new realizations of the Jette dynamic reservoir model which will then be history matched. This requires facies and properties, such as porosity and permeability, to be repopulated in the model, in addition to an update of the current initialization. New realizations allows the possibility of creating a deterministic model rather than a stochastic model which the current model is, and might improve reservoir characterization.

13 NOMENCLATURE

Symbol	*Description*	*Unit*
B_o	Oil formation volume factor	m^3/Sm^3
c	Volume translation parameter in SRK Peneloux	-
c_i	Calculated model response	-
c_t	Total compressibility	bar^{-1}
h	Height	m
H_{fwl}	Height above free water level	m
H_{wj}	Well pressure head between grid block j and datum depth	m
k_h	Horizontal permeability	mD
k_{HDT}	Permeability for facies HDT	mD
$k_{i,j}$	Binary interaction parameter between component i and j	-
k_{LDT}	Permeability for facies LDT	mD
k_{max}	Maximum permeability	mD
k_{rg}	Gas relative permeability	-
k_{rog}	Oil-gas relative permeability	-
k_{row}	Oil-water relative permeability	-
k_{rw}	Water relative permeability	-
$k_{shale,Calcite,E\text{-}seq}$	Permeability for facies Shale, Calcite and E-Sequence	mD
k_v	Vertical permeability	mD
$M_{p,j}$	Mobility of phase *p* in grid block *j*	mD/cP
OF	Objective function	-
o_i	Observed model response	-
P(r,t)	Pressure at specified radius and time	bar
P_{bp}	Bubblepoint pressure	bar
P_c	Capillary pressure	bar
P_c	Critical pressure	bar
P_{cow}	Oil-water capillary pressure	bar
PCW	Scaled maximum capillary pressure	bar
P_i	Initial reservoir pressure	bar
P_j	Pressure in grid block *j*	bar

P_w	Pressure in the well	bar
P_{wh}	Wellhead pressure	bar
q	Flow rate	Sm^3/day
Q_{OD}^T	Theoretical flow rate of well 25/8-D-1 AH T3	Sm^3/day
Q_{OE}^T	Theoretical flow rate of well 25/8-E-1 H	Sm^3/day
$q_{p,j}$	Production rate of phase p from grid block j	Sm^3/day
r	Perturbation parameter used in the Probability Perturbation approach	-
r_w	Wellbore radius	m
R	Universal gas constant (8.3145)	J/K· mol
r_{inv}	Radius of investigation	ft
r_o	Peacemans wellblock-equivalent pressure radius	ft
R_{so}	Solution gas-oil ratio	Sm^3/Sm^3
S	Skin	-
S_o	Oil Saturation	-
S_{wirr}	Irreducible water saturation	-
SWJ	Water saturation from Leverett J-function	-
SWL	Scaled connate water saturation	-
SWN	Normalized water saturation	-
t	Production time	hr
T	Temperature	K
T_c	Critical temperature	K
T_r	Reduced temperature	-
T_{wj}	Connection transmissibility factor	mD· m
V	Molar volume	m^3/mol
W_i	Weighting factor for data point *i*	-
Z_i	Mole fraction of component i	-
α	Dimensionless parameter in SRK Peneloux	-
ΔS_o	Change in oil saturation	-
Δt_s	Shut-in time when buildup pressure and grid block pressure should be compared	hr
θ	Contact angle	°
μ	Viscosity	cP

σ	Interfacial tension	N/m
φ	Porosity	-
φ_e	Effective porosity	-
ω	Acentric factor	-
Ω_a	EOS constant (0.42727)	-
Ω_b	EOS constant (0.08664)	-

14 ABBREVIATIONS

Abbreviation	*Description*
AHM	Assisted History Matching
BHP	Bottomhole Pressure
CCE	Constant Composition Expansion
CME	Constant Mass Expansion
CVD	Constant Volume Depletion
DAF	Daily Allocation Factor
DL	Differential Liberation
EOS	Equation Of State
FPSO	Floating Production Storage and Offloading vessel
FVF	Formation Volume Factor
GLV	Gas Lift Valve
GOC	Gas-Oil Contact
GOR	Gas-Oil Ratio
HDT	High Density Turbidite
I-DO™	Intelligent Daily Operations
ICD	Inflow Control Device
ID	Inner Diameter
IMPES	IMplicit Pressure Explicit Saturation
IPR	Inflow Performance Relationship
LDT	Low Density Turbidite
LSOBM	Low Solid Oil Based Mud
MD	Measured Depth
MDT	Modular formation Dynamics Tester
MSL	Mean Sea Level
NCS	Norwegian Continental Shelf
NTNU	Norwegian University of Science and Technology
PBU	Pressure Buildup
PDO	Plan for Development and Operations
PI	Productivity Index

PLEM	Pipeline End Manifold
PLT	Production Logging Tool
PTA	Pressure-Transient Analysis
PVT	Pressure, Volume, Temperature
RFT	Repeat Formation Test
RKB	Rotary Kelly Bushing
RMS	Root Mean Square
SCAL	Special Core Analysis
SDU	Subsea Distribution Unit
SSTVD	Sub Surface True Vertical Depth
STOIIP	Stock Tank Oil Initially In Place
TD	Target Depth
THP	Tubing Head Pressure
TPC	Tubing Performance Curve
TVD	True Vertical Depth
VFP	Vertical Flow Performance
WC	Water Cut
WOC	Water-Oil Contact
WOR	Water-Oil Ratio

15 BIBLIOGRAPHY

Baker, R. O., Chugh, S., Mcburney, C. and Mckishnie, R. 2006. History Matching Standards; Quality Control and Risk Analysis for Simulation. Paper PETSOC 2006-129 presented at the Petroleum Society's 7th Canadian International Petroleum Conference, Calgary, Alberta, Canada, 13 – 15 June. http://dx.doi.org/10.2118/2006-129

Caers, J. 2005. *Petroleum Geostatistics*. Richardson, Texas, SPE.

Carlson, M. R. 2006. *Practical Reservoir Simulation*. Tulsa, Oklahoma: PennWell Corporation.

Dandekar, A. Y. 2006. *Petroleum reservoir rock and fluid properties*. Boca Raton, Florida: CRC Press, Taylor & Francis Group.

Det norske oljeselskap ASA. 2010. *Final Well Report Well 25/8-17 Jetta PL 027D – Section A Geology*; EI-DENOR-G-1022.

Det norske oljeselskap ASA. 2011a. *Plan for utbygging og drift av Jette*.

Det norske oljeselskap ASA. 2011b. *Jetta DG2 G&G Evaluation Report*; JE-DENOR-G-1035.

Det norske oljeselskap ASA. 2011c. *Jetta Reservoir Engineering Report*; JE-DENOR-X-1011.

Det norske oljeselskap ASA. 2013a. *Jette - Long range reservoir management plan*; JT02-DN-X-TA-0001.

Det norske oljeselskap ASA. 2013b. *Final Well Report – Section B Drilling and Well Operations Jette Wells 25/8-U-25, 25/8-D-1 H, 25/8-D-1 AH*; JE-DENOR-D-1382.

Det norske oljeselskap ASA. 2013c. *Final Well Report – Section B Drilling and Well Operations Jette Well 25/8-E-1 H*; JE-DENOR-D-1383.

Det norske oljeselskap ASA. 2013d. *Final Well Report – 25/8-U-25, 25/8-D-1 H, -AH, -AH T2 & -AH T3 Jette Sør – Section A Geology*; JE-DENOR-G-1058.

Det norske oljeselskap ASA. 2013e. *Final Well Report – 25/8-E-1 H Jette Nord – Section A Geology*; JE-DENOR-G-1059.

Det norske oljeselskap ASA. 2014. Production data from fields of Det norske, http://www.detnor.no/var-virksomhet/produksjon/ (accessed 26.05.2014).

ECLIPSE Reference Manual, Version 2012.2 User Manual. 2012. Schlumberger.

ECLIPSE Technical Description, Version 2012.2 User Manual. 2012. Schlumberger.

Ertekin, T., Abou-Kassem, J.H. and King, G.R. 2001. *Basic Applied Reservoir Simulation*, Vol. 7. Richardson, Texas: Textbook Series, SPE.

Fanchi, J.R. 2006. *Principles of Applied Reservoir Simulation*, third edition. Burlington, Massachusetts: Gulf Professional Publishing/Elsevier.

Gilman, J. R. and Ozgen, C. 2013. *Reservoir Simulation: History Matching and Forecasting*. Richardson, Texas, SPE.

Krogstad, M.K. and Barbier, J. C. 2014. *Jette Production Opimization and Well Intervention Study – Phase 2: OLGA Modeling of Gas Lift Sensitivities*. Weatherford Petroleum Consultants AS; Report No. WPC100185/01/2014.

Lorentzen, K. 2013. Dynamic Reservoir Modeling of Jette – Upscaling for Enhanced Model Performance. Project Report, Norwegian University of Science and Technology (NTNU), Trondheim, Norway (December 2013).

Lysne, D. 2014. *Sammenligning av buildup tester på Jette fra juli 2013 til mars 2014*. Internal presentation at Det norske, Trondheim, Norway, April 2014.

Lysne, D., Nakken E. I., Totland, N. et al. 2013. *Jette Production Optimization and Well Intervention Study*. Weatherford Petroleum Consultants AS; Report No. WPC100179/2013/01.

Mattax, C. C. and Dalton, R. L. 1990. *Reservoir Simulation*, Vol. 13. Richardson, Texas, USA: Monograph Series, SPE.

Nielsen, B., Winsnes, Ø., and Bjørsvik, H. August 2013. *Physical Recombination and PVT Analysis of Separator Samples from Wells 25/8-D-1 AHT3 and 25/8-E-1 H, Jette*. Weatherford Laboratories.

PVTsim Help, Version 21.0.0 Method Documentation. 2013. Calsep A/S.

Rajvanshi, A. K., Meyling, R. G. and Danny ten Haaf, 2012. Instilling Realism in Production Forecasting: Dos and Don'ts. Paper SPE-155443-MS presented at the SPE Annual Technical Conference and Exhibition, San Antonio, Texas, USA, 8 – 10 October. http://dx.doi.org/10.2118/155443-MS

Ravnås, A. and Skog, Ø. September 2012. *PVT Analysis of MDT Oil Samples from Well 25/8-D-1 H, Jette Observation*. Weatherford Laboratories.

Rwechungura, R., Dadashpour, M. and Kleppe, J. 2011. Advanced History Matching Techniques Reviewed. Paper SPE-142497-MS presented at the SPE Middle East Oil and Gas Show and Conference, Manama, Bahrain, 25 – 28 September. http://dx.doi.org/10.2118/142497-MS

Saleri, N. G., Toronyi, R. M. and Snyder, D. E. 1992. Data and Data Hierarchy. *Journal of Petroleum Technology* 44 (12): 1286 – 1293. Paper SPE-21369-PA. http://dx.doi.org/10.2118/21369-PA

Sandvik, S. L. and Ravnås, A. March 2010. *PVT Analysis of MDT Oil Samples from 25/8-17, Jetta*. Weatherford Laboratories.

Sandø, I. A., Munkvold, O.P. and Elde, R. 2009. *4D Geophysical Data*. Printed in GeoExPro Vol. 6, No. 5. http://www.geoexpro.com/articles/2009/05/4d-geophysical-data (accessed 24.03.2014).

Schlumberger. 2013. ECLIPSE Core Simulator, http://www.software.slb.com/Store/Core-Simulator--A1EC-P1_0 (accessed 16.09.13).

Whitson, C. H. and Brulé, M. R. 2000. *Phase Behavior*, Vol. 20. Richardson, Texas, USA: Monograph Series, SPE.

Whitson, C. H. and Golan, M. 1996. *Well Performance*, Second Edition. Trondheim, Norway: Tapir.

APPENDIX A

ECLIPSE 100 DESCRIPTION

Simulation of the Jette dynamic reservoir model is performed using the ECLIPSE 100 commerical reservoir simulator provided by Schlumberger. ECLIPSE 100 is a fully-implicit, three phase, three dimensional general purpose black oil simulator with gas condensate options. The ECLIPSE 100 black oil simulator is considered the industry standard for conducting reservoir simulations (Schlumberger, 2013). Some of the model features available in ECLIPSE 100 are listed in Table A.1. In addition to the features listed in Table A.1 ECLIPSE 100 contains multiple special extensions such as Polymer, Multi Segment Well and Coal Bed Methane options to mention but a few (Lorentzen, 2013).

Table A.1 – ECLIPSE 100 features (Schlumberger, 2013)

- Variety of grid geometry options such as corner point, block-centered and radial
- Able to model all recovery mechanisms
- Possibility of subdivision of reservoir into regions of different rock/fluid properties
- Local grid refinements
- Both dual porosity and dual permeability formulation option for fractured reservoirs
- Fault modeling with non-neighboring connections
- Numerical and analytical aquifer modeling
- Miscible flood modeling for three components
- Non-darcy flow
- Tracer, brine and API tracking
- Rock compaction
- Hysteresis
- Network modeling

ECLIPSE 100 uses the fully-implicit method by default. This provides stability over long timesteps and the non-linear equations are solved precisely to reduce residuals to within a very fine tolerance. Non-linear equations are solved by use of Newton's method while the linear equations are solved by use of nested factorization accelerated by orthomin. Implicit pressure explicit saturation (IMPES) and semi-implicit methods are also available in the simulator but due to restrictions in stability care should be taken before applying any one of them (ECLIPSE Technical Description, 2012). By default flow equations are set up using a five-point finite difference scheme, but ECLIPSE 100 offers the possibility of using a nine-point finite difference scheme to alleviate grid orientation effects in displacement processes of adverse mobility ratios. The ECLIPSE 100 simulator provides a wide range of features and special extensions (Lorentzen, 2013). Also, ECLIPSE 100 can be used together with Petrel (a shared earth software) which provides the user great flexibility when modifying and updating the reservoir model in a simulation study.

APPENDIX B

COMPLETION SCHEMATIC & COMPLETION STRING DESIGN:

25/8-D-1 AH T3

25/8-E-1 H

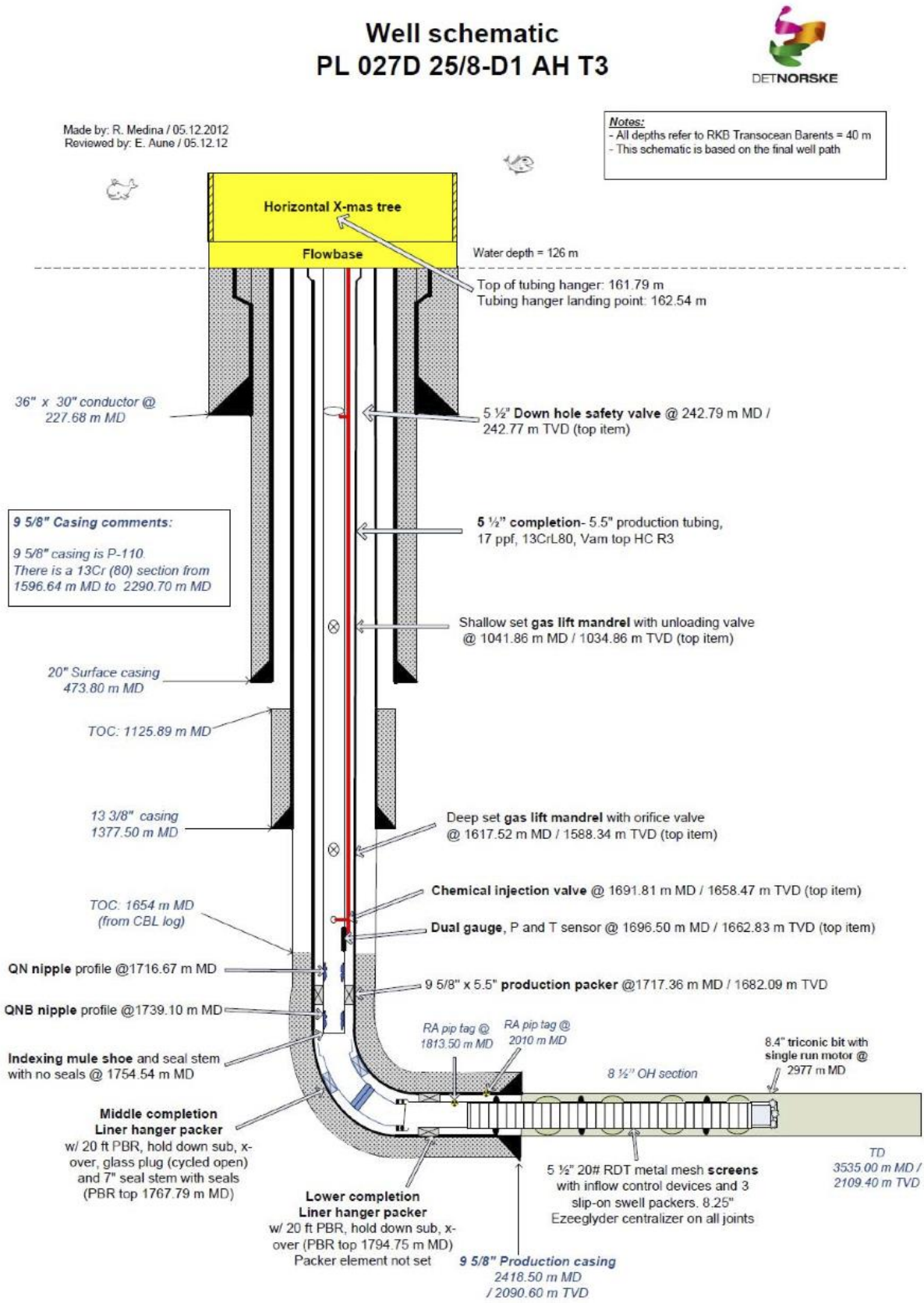

Picture taken from: Det norske oljeselskap ASA. 2013b

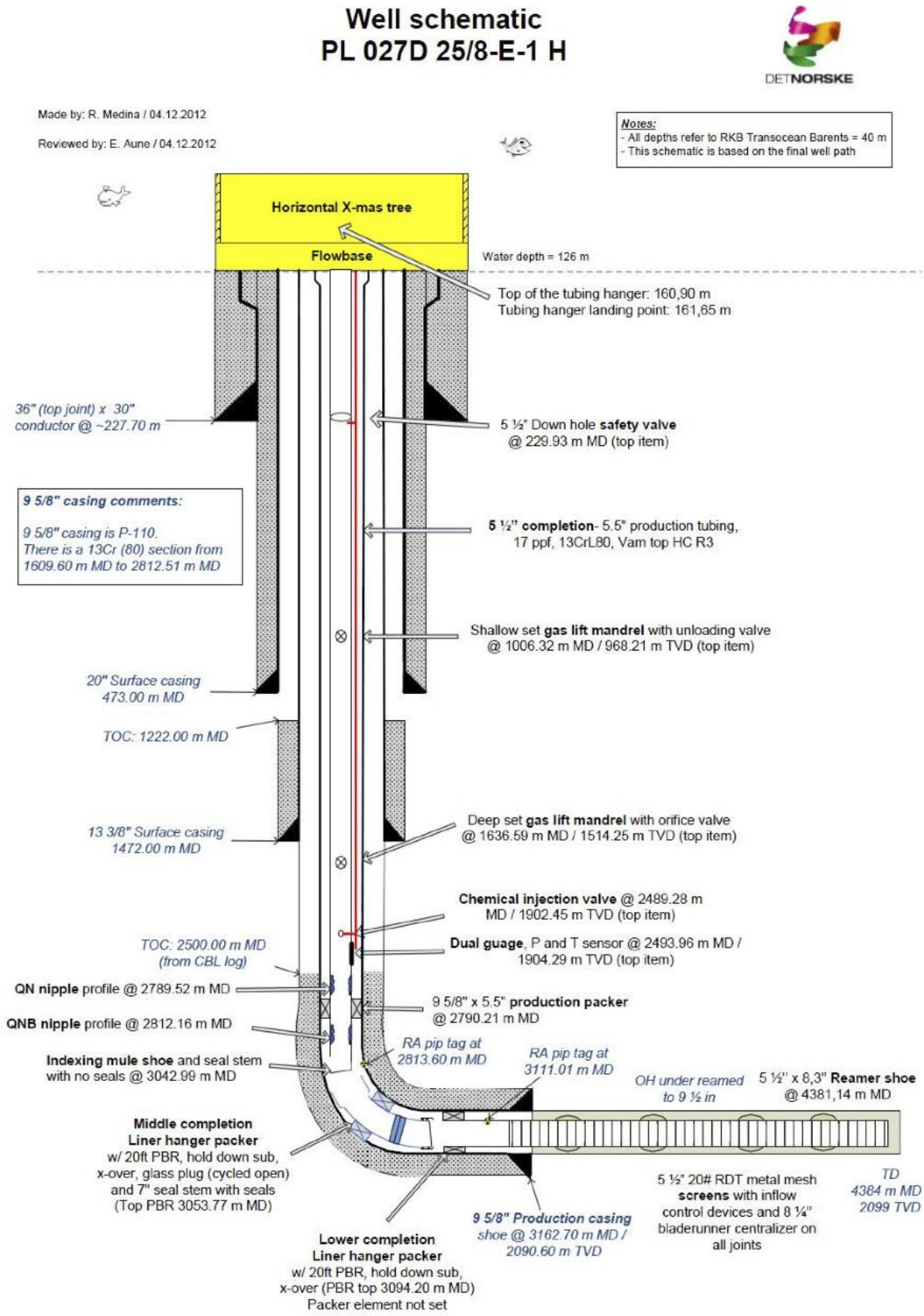

Picture taken from: Det norske oljeselskap ASA. 2013c

Jette

25/8-D-1 AH (25/8-D-1 AH T3)

Compl.: 1.00 **Tub.Inst.Date:** 19.11.2012

Rig: Transocean Barents **Status:** Oil Producer

Existing

Wellbore schematic for 25/8-D-1 AH T3

Remark: All pup joints and tubing are provided by Vallourec unless stated otherwise

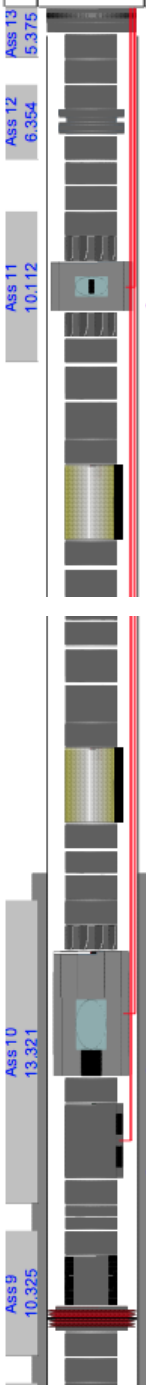

Ass	Symbol	Symbol Extra Info	Fo	MD [RKB] Top [m]	TVD [RKB] [m]	Length [m]	ID [inch]	Drift ID [inch]	Max OD [inch]	Description
				161.790	161.789	1.980	4.795	4.767	18.498	Tubing Hanger
				163.770	163.769	3.395	4.811	4.767	5.978	5.5" Pup Joint
				167.165	167.164	1.500	4.811	4.767	5.500	5.5" Pup Joint
				168.665	168.664	2.889	4.811	4.767	5.978	5.5" handling Pup Joint
				171.554	171.553	1.575	4.790	4.665	8.250	Bumper wire anchor sub
				173.129	173.128	1.890	4.811	4.767	5.978	5.5" Pup Joint
				175.019	175.017	62.944	4.811	4.767	5.500	5.5" production Tubing
				237.963	237.952	2.992	4.811	4.767	5.978	5.5" handling Pup Joint
				240.955	240.943	1.834	4.790	4.665	8.250	Splice sub above DHSV
				242.789	242.777	2.211	4.578	4.453	7.755	5.5" Optimax WSP-7.5 Tubing Retrievable Safety Valve
		Control Line: Dual Control Line 2x1/4" 0.049WT								
				245.000	244.987	1.073	4.790	4.767	8.250	Splice Sub below DHSV
				246.073	246.060	2.002	4.811	4.767	5.500	5.5" Pup Joint
				248.075	248.061	790.883	4.811	4.767	5.500	5.5" production Tubing
				1038.958	1032.028	2.902	4.811	4.767	5.500	5.5" Pup Joint
				1041.860	1034.863	3.341	4.698	4.653	8.000	5.5" DVX gas lift mandrel w/orifice valve
				1041.860		*0.575*			*1.500*	*Unloading Valve, RH-2Q w/RK-2 latch, 24/64" choke*
				1045.201	1038.126	2.003	4.811	4.767	5.500	5.5" Pup Joint
				1047.204	1040.083	458.662	4.811	4.767	5.500	5.5" production tubing
				1505.866	1482.078	5.762	4.811	4.767	5.500	5.5" Pup Joint
				1511.628	1487.575	102.995	4.811	4.767	5.500	5.5" production tubing
				1614.623	1585.586	2.900	4.811	4.767	5.500	5.5" Pup Joint
				1617.523	1588.338	3.346	4.698	4.767	8.000	5.5" DVX gas lift mandrel w/orifice valve
				1617.523		*0.568*			*1.500*	*Gas lift valve, RO-2Q w/RK-2 latch, 32/64" choke*
				1620.869	1591.514	1.898	4.811	4.767	5.500	5.5" Pup Joint
				1622.767	1593.315	64.577	4.811	4.767	5.500	5.5" production tubing
				1687.344	1654.307	2.887	4.811	4.767	5.500	5.5" handling Pup Joint
				1690.231	1657.002	1.577	4.790	4.665	8.250	Splice sub, above CIM
				1691.808	1658.472	2.770	4.698	4.653	8.000	5.5" chemical injection mandrel w/ shear open valve
				1691.808		*1.000*				*Chemical injection valve, RDDK-2AQ w/RKP-2 latch, 6.22 mm choke*
		Control Line: Chemical 3/8" 0.065 WT		*1691.808*		*1.000*				*Inline check valve, CCCI, 0.188" choke*
				1694.578	1661.050	1.919	4.811	4.767	5.500	5.5" Pup Joint
				1696.497	1662.834	2.256	4.798	4.767	7.000	Gauge mandrel
		Control Line: Electrical 1/4"		*1696.497*		*1.000*				*NPQG-EE Dual Tubing / Annulus Gauge*
				1698.753	1664.929	1.912	4.811	4.767	5.500	5.5" Pup Joint
				1700.665	1666.701	13.119	4.811	4.767	5.500	5.5" production tubing
				1713.784	1678.805	2.885	4.811	4.767	5.500	5.5" handling Pup Joint
				1716.669	1681.453	0.690	4.313	4.188	6.033	4.313" QN Nipple Top No-Go
				1717.359	1682.085	4.739	4.650	4.525	8.310	9.625 x 5.5 OptiPkr with Hydrostatic Module
				1722.098	1686.424	2.011	4.811	4.767	5.500	5.5" pup joint
				1724.109	1688.261	12.981	4.811	4.767	5.978	5.5" production tubing

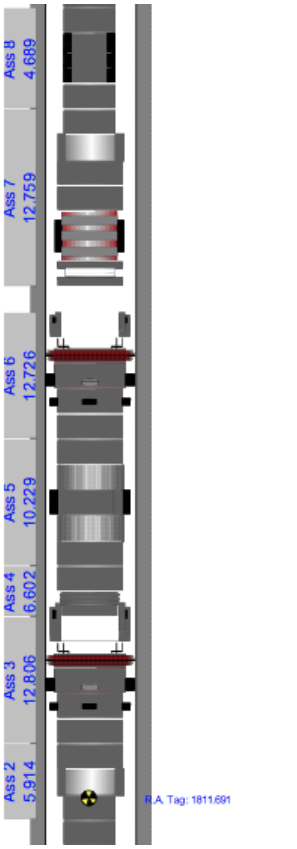

1737.090	1700.066	2.011	4.811	4.767	5.500	5.5" handling pup joint
1739.101	1701.887	0.685	4.244	4.119	6.033	4.313" QNB Nipple Bottom No-Go
1739.786	1702.506	1.993	4.811	4.767	5.500	5.5" Pup Joint
1741.779	1704.307	1.936	4.811	4.767	5.500	5.5" handling pup joint
1743.715	1706.055	0.791	4.811	4.767	7.050	X-over 5.5" x 7"
1744.506	1706.768	2.924	6.059	6.000	7.640	7" pup joint
1747.430	1709.403	4.999	6.059	6.000	7.717	Pup Joint x-over 7" 32# VAM Top HC x New vam
1752.429	1713.897	1.256	6.083	6.000	7.500	Seal stem
1753.685	1715.024	0.853	6.125	6.000	7.354	Indexing mule shoe
1754.538	1715.789	13.250				
1767.790	1727.626	6.383	7.502	7.375	8.300	7.5in ID liner hanger PBR 20 ft
1774.173	1733.296	1.295	6.080	6.000	8.290	9 5/8 x 7 Liner Top Packer
1775.468	1734.443	1.830	6.090	6.000	8.330	9 5/8 x 7 Liner Hanger
1777.298	1736.064	1.225	6.079	6.000	8.300	Hold Down Sub
1778.523	1737.149	1.993	6.094	6.000	6.980	7" Pup Joint
1780.516	1738.911	2.995	6.094	6.000	7.640	7" handling pup joint
1783.511	1741.556	0.699	6.094	6.000	7.000	X-Over
1784.210	1742.173	4.120	5.750	5.704	8.270	TCO Glas Plug TDP-3
1788.330	1745.804	0.405	6.094	6.000	7.000	X-Over
1788.735	1746.161	2.010	6.094	6.000	7.640	7" Pup Joint
1790.745	1747.929	2.295	6.020	6.000	7.736	7" handnling pup joint
1793.040	1749.946	4.307	6.114	5.844	8.250	Seal stem
1794.750	1751.447	6.405	7.502	7.375	8.300	7.5in ID liner hanger PBR 20 ft
1801.155	1757.058	1.360	6.080	6.000	8.290	9 5/8 x 7 Liner Top Packer
1802.515	1758.246	1.765	6.090	6.000	8.330	9 5/8 x 7 Liner Hanger
1804.280	1759.786	1.243	6.079	6.000	8.300	Hold Down Sub
1805.523	1760.870	2.033	6.059	6.000	6.980	7" Pup Joint
1807.556	1762.640	3.047	6.059	6.000	7.718	7" handling pup joint
1810.603	1765.288	0.818	4.811	4.767	7.752	X-Over 7" x 5.5"
1811.421	1765.998	2.049	4.811	4.767	6.013	5.5" Pup Joint
1813.470	1767.775	3.000	4.811	4.767	5.978	5.5" Pup Joint

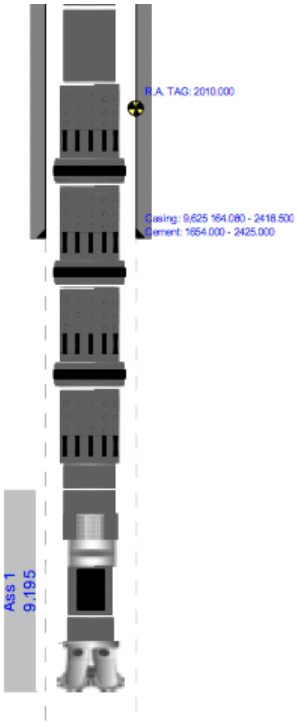

1816.470	1770.371	122.163	4.811	4.767	5.978	5.5" Blank Pipe
1938.633	1868.733	202.898	4.715	4.653	6.550	5.5" RDT ICD metal mesh screen with centralizer
2141.531	1993.890	12.024	4.778	4.653	8.000	5.5" RDT Mesh screen ICD with swell packer
2153.555	2000.024	380.640	4.715	4.653	6.550	5.5" RDT ICD metal mesh screen with centralizer
2534.195	2085.037	11.944	4.778	4.653	8.000	5.5" RDT Mesh screen ICD with swell packer
2546.139	2085.596	263.420	4.715	4.653	6.550	5.5" RDT ICD metal mesh screen with centralizer
2809.559	2096.201	11.852	4.778	4.653	8.000	5.5" RDT Mesh screen ICD with swell packer
2821.411	2096.136	141.591	4.715	4.653	6.550	5.5" RDT ICD metal mesh screen with centralizer
2963.002	2094.267	3.000	4.811	4.767	5.978	5.5" spacer pup joint
2966.002	2094.155	2.890	4.811	4.767	5.978	5.5" handling pup joint
2968.892	2094.039	0.605	1.500	1.375	5.978	X-over
2969.497	2094.014	0.640	1.500	1.375	4.750	Rupture Disc Valve Sub
2970.137	2093.987	4.570			4.750	SingleRUN Motor, 4.75", 5:5 Lobe, 3 Stage
2974.707	2093.779	0.250			6.000	6" bit sub
2974.957	2093.767	0.240			8.500	Drill bit 8.5" Model: RC347

Picture taken from Det norske oljeselskap ASA. 2013b

Jette

25/8-E-1 H (25/8-E-1 H)

Compl.: 1.00 **Tub.Inst.Date:** 04.11.2012

Rig: Transocean Barents **Status:** Oil Producer

Existing

25/8-E-1 H

Remark: Pup joints and tubings provided by Vallourec unless stated otherwise

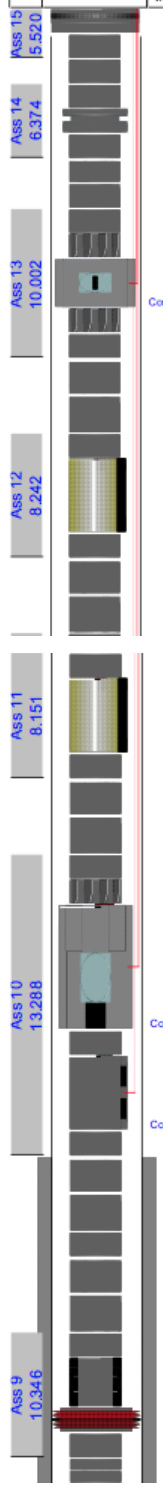

Ass	Symbol	Symbol Extra Info	Fo	MD [RKB] Top [m]	TVD [RKB] [m]	Length [m]	ID [inch]	Drift ID [inch]	Max OD [inch]	Description
				160.900	160.894	1.970	4.795	4.767	18.498	Tubing Hanger
				162.870	162.864	3.550	4.811	4.767	5.978	5 1/2" pup joint
				166.420	166.414	1.401	4.811	4.767	5.978	5 1/2" pup joint
				167.821	167.814	2.913	4.811	4.767	5.978	51/2" handling pup joint
				170.734	170.727	1.575	4.790	4.767	8.250	Bumper wire anchor sub
				172.309	172.302	1.886	4.811	4.767	5.978	5 1/2" pup joint
				174.195	174.188	50.907	4.811	4.767	5.978	5 1/2" production tubing
				225.102	225.090	2.996	4.811	4.767	5.978	5 1/2" handling pup joint
				228.098	228.086	1.834	4.790	4.767	8.250	Splice sub above DHSV
				229.932	229.920	2.211	4.578	4.453	7.755	5.5" Optimax WSP-7.5 Tubing Retrievable Safety Valve
		Control Line: Dual Control Line 2x1/4" 0.049WT		232.143	232.130	1.070	4.790	4.767	8.250	Splice Sub below DHSV
				233.213	233.200	1.891	4.811	4.767	5.978	5 1/2" pup joint
				235.104	235.091	768.328	4.811	4.767	5.978	5 1/2" production tubing
				1003.432	965.594	2.886	4.811	4.767	5.978	5 1/2" handling pup joint
				1006.318	968.206	3.345	4.698	4.653	8.000	5.5" DVX gas lift mandrel w/unloading valve
				1006.318		*0.575*			*1.500*	*Unloading Valve, RH-2Q w/RK-2 latch, 24/64" choke*
				1009.663	971.234	2.011	4.811	4.767	5.978	5 1/2" pup joint
				1011.674	973.054	622.022	4.811	4.767	5.978	5 1/2" production tubing
				1633.696	1512.211	2.892	4.811	4.767	5.978	5 1/2" handling pup joint
				1636.588	1514.250	3.344	4.698	4.653	8.000	5.5" DVX gas lift mandrel w/orifice valve
				1636.588		*0.568*			*1.500*	*Gas lift valve, RO-2Q w/RK-2 latch, 32/64" choke*
				1639.932	1516.598	1.915	4.811	4.767	5.978	5 1/2" pup joint
				1641.847	1517.937	842.973	4.811	4.767	5.978	5 1/2" production tubing
				2484.820	1900.701	2.879	4.811	4.767	5.978	5 1/2" handling pup joint
				2487.699	1901.832	1.580	4.790	4.767	8.250	Splice sub, above CIM
				2489.279	1902.453	2.770	4.698	4.653	8.000	5.5" chemical injection mandrel w/ shear open valve
				2489.279		*1.000*				*Inline check valve, CCCI, 0.188" choke*
		Control Line: Chemical 3/8" 0.065 WT		*2489.279*		*1.000*				*Chemical injection valve, RDDK-2AQ w/RKP-2 latch, 6.22 mm choke*
				2492.049	1903.540	1.908	4.811	4.767	5.978	5 1/2" pup joint
				2493.957	1904.289	2.259	4.798	4.767	7.000	Gauge mandrel
		Control Line: Electrical 1/4"		*2493.957*		*1.000*				*NPQG-EE Dual Tubing / Annulus Gauge*
				2496.216	1905.176	1.892	4.811	4.767	5.978	5 1/2" pup joint
				2498.108	1905.919	179.086	4.811	4.767	5.978	5 1/2" production tubing
				2677.194	1976.316	5.757	4.811	4.767	5.978	5 1/2" pup joint 13 Cr (80)
				2682.951	1978.583	103.676	4.811	4.767	5.978	5 1/2" production tubing
				2786.627	2017.632	2.896	4.811	4.767	5.978	5 1/2" handling pup joint
				2789.523	2018.603	0.690	4.313	4.188	6.033	4.313" QN Nipple Top No-Go
				2790.213	2018.833	4.739	4.650	4.525	8.310	9.625 x 5.5 OptiPkr with Hydrostatic Module
				2794.952	2020.400	2.021	4.811	4.767	5.978	5 1/2" pup joint
				2796.973	2021.062	13.195	4.811	4.767	5.978	5 1/2" production tubing

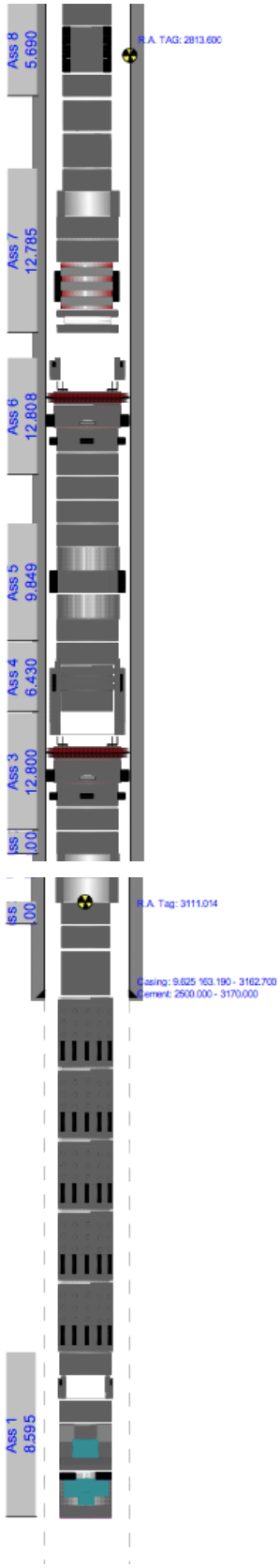

2810.168	2025.308	2.995	4.811	4.767	5.978	5 1/2" handling pup joint
2813.163	2026.257	0.685	4.244	4.119	6.033	4.313" QNB Nipple Bottom No-Go
2813.848	2026.473	2.010	4.811	4.767	5.978	5 1/2" pup joint
2815.858	2027.106	214.342	4.811	4.767	5.978	5 1/2" production tubing
3030.200	2076.868	1.934	4.811	4.767	5.978	5 1/2" handling pup joint
3032.134	2077.135	0.813	4.811	4.767	7.050	X-over 5.5" x 7"
3032.947	2077.245	2.923	6.059	6.000	7.717	7" pup joint
3035.870	2077.636	5.006	6.059	6.000	7.717	Pup joint x-over
3040.876	2078.279	1.256	6.083	6.000	7.500	Seal stem
3042.132	2078.436	0.853	6.125	6.000	7.354	Indexing mule shoe
3042.985	2078.541	10.810				
3053.770	2079.788	6.394	7.502	7.375	8.300	7.5in ID liner hanger PBR 20 ft
3060.164	2080.481	1.295	6.080	6.000	8.290	9 5/8 x 7 Liner Top Packer
3061.459	2080.621	1.828	6.090	6.000	8.330	9 5/8 x 7 Liner Hanger
3063.287	2080.819	1.245	6.079	6.000	8.300	Hold Down Sub
3064.532	2080.953	2.046	6.059	6.000	7.717	7" pup joint
3066.578	2081.175	1.938	6.059	6.000	7.717	7" spacer pup joint
3068.516	2081.384	12.218	6.059	6.000	7.717	7" blank pipe
3080.734	2082.703	3.000	6.059	6.000	7.717	7" handling pup joint
3083.734	2083.027	0.404	6.094	6.000	7.000	X-Over
3084.138	2083.070	4.119	5.750	5.704	8.270	TCO Glas Plug TDP-3
3088.257	2083.514	0.405	6.094	6.000	7.000	X-Over
3088.662	2083.558	1.921	6.059	6.000	7.717	7" pup joint
3090.583	2083.765	5.010	6.059	6.000	7.717	7" handling pup joint
3095.593	2084.305	1.420	6.114	5.844	8.250	Seal stem
3094.200	2084.155	6.405	7.502	7.375	8.300	7.5in ID liner hanger PBR 20 ft
3100.605	2084.848	1.290	6.080	6.000	8.290	9 5/8 x 7 Liner Top Packer
3101.895	2084.987	1.825	6.090	6.000	8.330	9 5/8 x 7 Liner Hanger
3103.720	2085.185	1.245	6.079	6.000	8.300	Hold Down Sub
3104.965	2085.319	2.035	6.059	6.000	7.717	7" pup joint
3107.000	2085.539	3.000	6.059	6.000	7.717	7" handling pup joint
3110.000	2085.864	0.914	4.811	4.767	7.752	X-over 7" x 5.5"
3110.914	2085.962	3.000	4.715	4.653	6.071	5 1/2" pup joint
3113.914	2086.284	6.070	4.715	4.653	6.071	5 1/2" spacer pup joint
3119.984	2086.918	37.961	4.715	4.653	6.071	5 1/2" blank pipe
3157.945	2090.264	214.652	4.715	4.653	6.550	5.5" RDT ICD metal mesh screen with centralizer
3372.597	2101.981	250.000	4.715	4.653	6.550	5.5" RDT ICD metal mesh screen with centralizer
3622.597	2108.903	250.000	4.715	4.653	6.550	5.5" RDT ICD metal mesh screen with centralizer
3872.597	2101.065	250.000	4.715	4.653	6.550	5.5" RDT ICD metal mesh screen with centralizer
4122.597	2095.699	250.000	4.715	4.653	6.550	5.5" RDT ICD metal mesh screen with centralizer
4372.597	2097.945	3.060	4.715	4.653	6.071	5 1/2" handling pup joint
4375.657	2098.216	1.290	4.000	3.997	6.070	4" ID Polished Bore Receptacle
4376.947	2098.333	3.060	4.715	4.653	6.071	5 1/2" spacer pup joint
4380.007	2098.616	0.515	4.673	4.653	6.079	5 1/2" Float collar
4380.522	2098.664	0.670	4.715	4.653	8.300	5 1/2" Pen-O-trator reamer shoe

Picture taken from Det norske oljeselskap ASA. 2013c

APPENDIX C

SATURATION TABLE SCALING

Saturation table scaling is enabled in ECLIPSE 100 by the ENDSCALE keyword. It provides a mechanism for redefining values for connate, critical and maximum saturations in saturation tables describing flow in the reservoir (ECLIPSE Technical Description, 2012). Application of the saturation table scaling is useful in reservoirs with variation in either connate, critical or maximum saturation for either one or more of the phases present. Saturation table scaling is usually performed with a two-point transformation, meaning that two saturation values from the table are moved to new positions. In the Jette dynamic reservoir model saturation table scaling is performed on both saturation and capillary pressure. New endpoint values are defined for all grid blocks (Lorentzen, 2013).

Scaling of saturation functions

Endpoints taken from the saturation table are referred to as unscaled saturation endpoints. By supplying new endpoint values for grid blocks needed to be scaled ECLIPSE 100 will calculate new saturation values for table look-up using a linear transformation (Equation C.1). These new saturation look-up values are used when values of relative permeability or capillary pressure need to be looked up from tables at a particular saturation (Lorentzen, 2013).

$$S'_w = S_{wco} + \frac{(SW - SWCO)(S_{wmax} - S_{wco})}{SWU - SWCO} \qquad \text{Equation C.1}$$

SW is the grid block water saturation, SWCO the scaled connate water saturation, SWU the scaled maximum water saturation. The corresponding unscaled connate water saturation is S_{wco} and maximum water saturation S_{wmax}. S_w' is the value of saturation used for look-up in the capillary pressure or relative permeability table. Figure C.1 illustrates an example of endpoint scaling where a grid block has been scaled with SWCO and SWU. The figure also illustrates how a saturation value SW in the grid block is transformed into a look-up value, Sw', in the saturation table (Lorentzen, 2013).

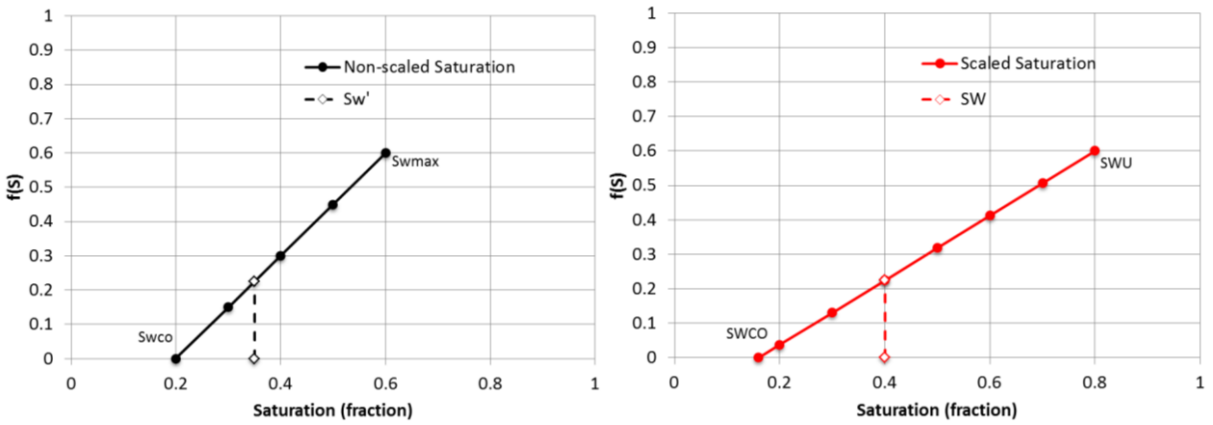

Figure C.1: Unscaled saturation function to the left and scaled saturation function to the right. SW is the grid block saturation and Sw' is the corresponding saturation table look-up value.

Scaling of maximum capillary pressure

The maximum capillary pressure can be scaled on a grid block by grid block basis. The scaled maximum capillary pressure is entered for all grid blocks by use of the PCW or PCG keyword in ECLIPSE 100 for oil-water and oil-gas capillary pressure respectively. The scaled capillary pressure is then calculated from Equation C.2 (Lorentzen, 2013).

$$P_c = P_{ct}\frac{PCW}{P_{cm}} \qquad \text{Equation C.2}$$

PCW is the scaled maximum capillary pressure value, P_{cm} the maximum capillary pressure from the table, P_{ct} the capillary pressure from the table at given saturation and P_c the scaled capillary pressure at a given saturation (Lorentzen, 2013).

APPENDIX D

FLUID MODEL VERIFICATION

This appendix presents illustrations and calculations of the difference between experimental and simulated fluid behavior for fluid model 1 and fluid model 2. The purpose of this appendix is to supply additional verification of the created fluid models described in Chapter 5.1. The following figures compare experimental fluid behavior with that calculated from the created EOS models. Properties include gas formation volume factor, B_g, oil density and oil viscosity.

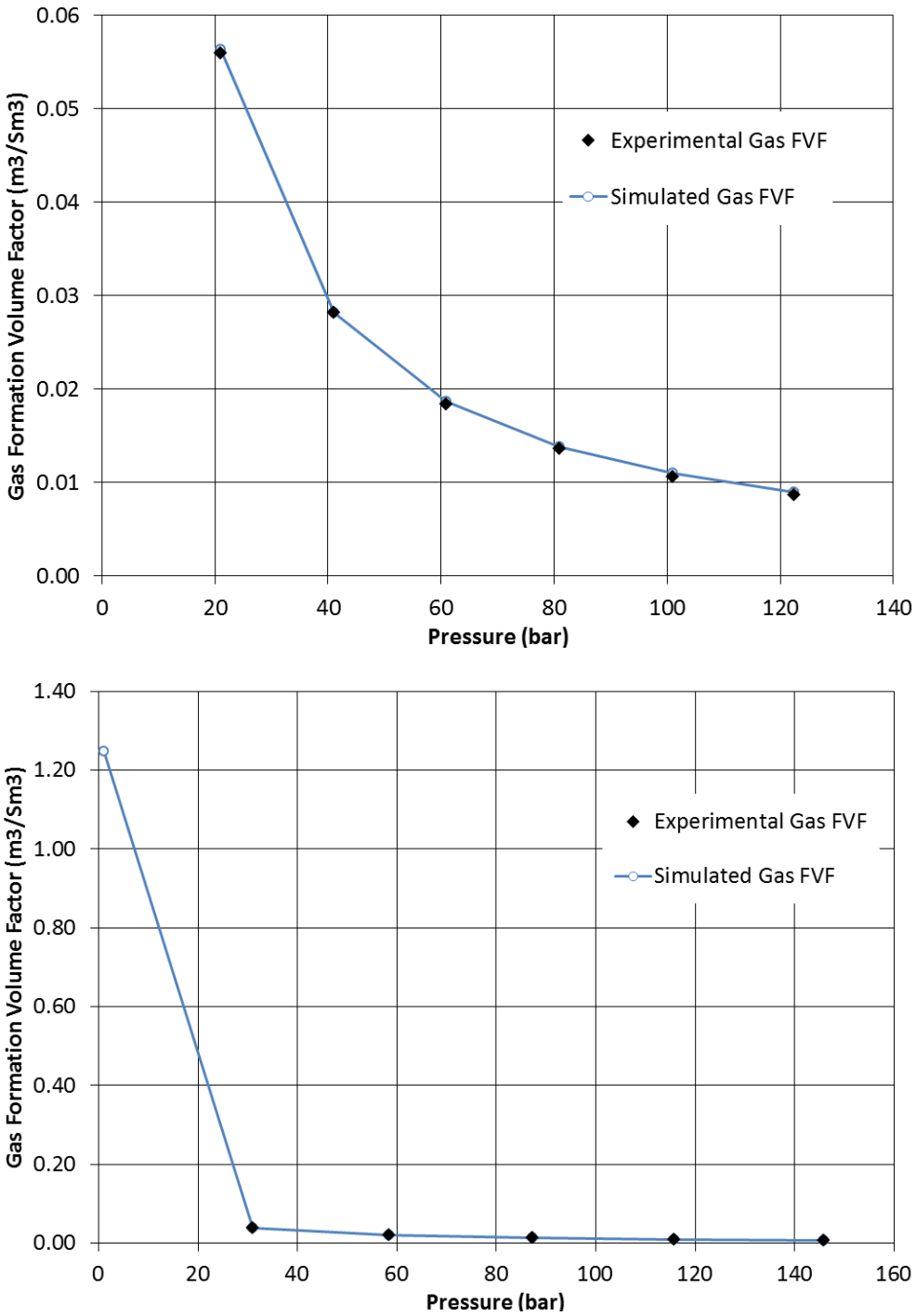

Figure D.1: Comparison of experimental gas B_g and PVTsim computed B_g for fluid model 1 (top) and fluid model 2 (bottom).

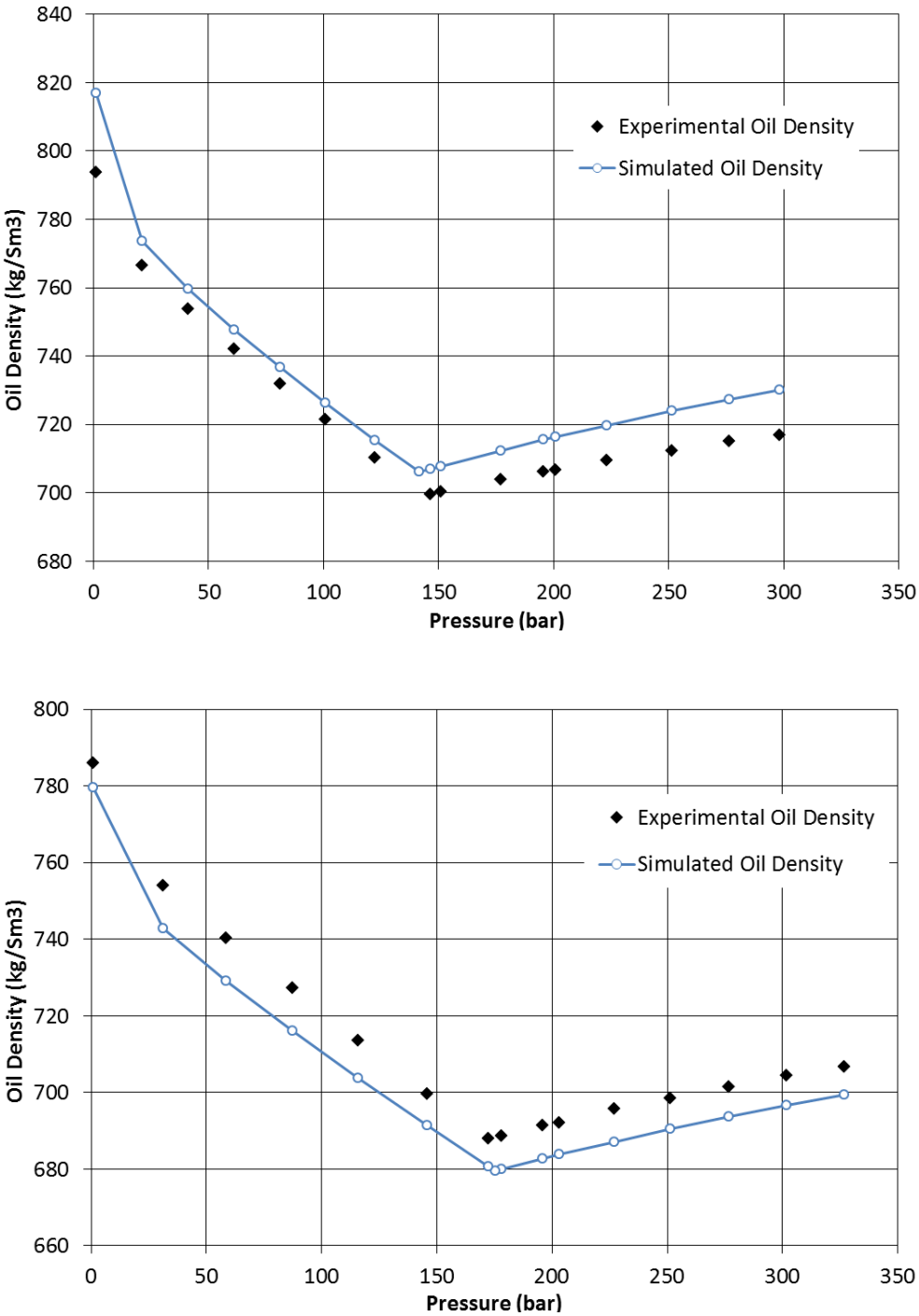

Figure D.2: Comparison of experimental oil density and PVTsim computed oil density for fluid model 1 (top) and fluid model 2 (bottom).

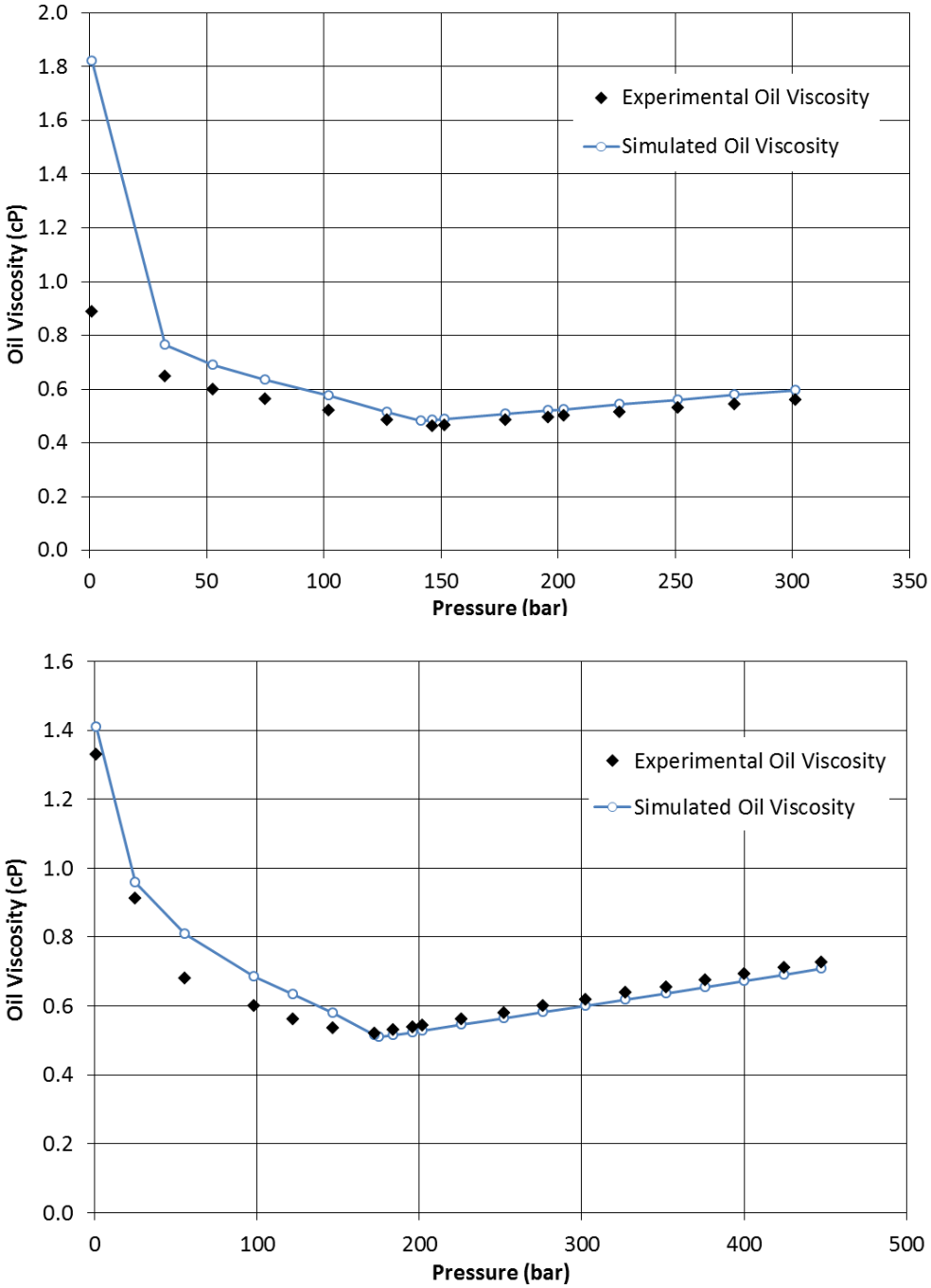

Figure D.3: Comparison of experimental oil viscosity and PVTsim computed oil viscosity for fluid model 1 (top) and fluid model 2 (bottom).

The error between experimental and calculated fluid behavior in PVTsim for B_o, R_{so}, B_g, oil density and oil viscosity for fluid model 1 and fluid model 2 have been calculated and is given in the following tables.

Table D.1 – Comparison of experimental and PVTsim calculated B_o for fluid model 1

Pressure (bar)	Experimental B_o (m^3/Sm^3)	PVTsim calculated B_o (m^3/Sm^3)	Error (%)
298.3	1.3968	1.411	1.016
276.5	1.4006	1.417	1.170
251.4	1.4058	1.423	1.223
223	1.4116	1.431	1.374
200.8	1.4171	1.438	1.474
195.7	1.4182	1.44	1.537
177.2	1.4226	1.446	1.644
151	1.43	1.456	1.818
146.4	1.4312	1.457	1.802
122.5	1.3881	1.422	2.442
101	1.3474	1.382	2.567
81	1.3112	1.345	2.577
61	1.2764	1.307	2.397
41	1.2387	1.269	2.446
21	1.1969	1.224	2.264
1.01	1.0631	1.042	-1.984

Table D.2 – Comparison of experimental and PVTsim calculated B_o for fluid model 2

Pressure (bar)	Experimental B_o (m^3/Sm^3)	PVTsim calculated B_o (m^3/Sm^3)	Error (%)
326.8	1.3902	1.392	0.129
301.9	1.395	1.398	0.215
276.6	1.4009	1.404	0.221
251.3	1.4066	1.411	0.312
227	1.4122	1.417	0.339
203.1	1.4195	1.424	0.317
195.8	1.4214	1.427	0.393
177.9	1.4267	1.432	0.371
172.3	1.4284	1.428	-0.028
145.8	1.3827	1.383	0.021
115.8	1.3313	1.335	0.277
87.3	1.2841	1.291	0.537
58.5	1.2397	1.246	0.508
31.1	1.1932	1.201	0.653
1.01	1.0748	1.037	-3.516

Table D.3 – Comparison of experimental and PVTsim calculated R_{so} for fluid model 1

Pressure (bar)	Experimental R_{so} (Sm^3/Sm^3)	PVTsim calculated R_{so} (Sm^3/Sm^3)	Error (%)
146.4	122.7	129	5.134
122.5	105.8	114.8	8.506
101	90.7	99.2	9.371
81	77.4	85.1	9.948
61	63.8	71.3	11.755
41	50.3	57.5	14.314
21	35.8	42.4	18.435
1.01	0	0	0

Table D.4 – Comparison of experimental and PVTsim calculated R_{so} for fluid model 2

Pressure (bar)	Experimental R_{so} (Sm^3/Sm^3)	PVTsim calculated R_{so} (Sm^3/Sm^3)	Error (%)
172.3	126.7	128.8	1.657
145.8	109.3	110.9	1.463
115.8	89.6	91.7	2.343
87.3	71.4	74.3	4.061
58.5	53.4	57.3	7.303
31.1	35.4	40.8	15.254
1.01	0	0	0

Table D.5 – Comparison of experimental and PVTsim calculated B_g for fluid model 1

Pressure (bar)	Experimental B_g (m^3/Sm^3)	PVTsim calculated B_g (m^3/Sm^3)	Error (%)
122.5	8.65E-03	8.92E-03	3.132
101	1.06E-02	1.09E-02	3.018
81	1.36E-02	1.38E-02	1.323
61	1.83E-02	1.86E-02	1.584
41	2.81E-02	2.82E-02	0.320
21	5.59E-02	5.63E-02	0.769

Table D.6 – Comparison of experimental and PVTsim calculated B_g for fluid model 2

Pressure (bar)	Experimental B_g (m^3/Sm^3)	PVTsim calculated B_g (m^3/Sm^3)	Error (%)
145.8	7.27E-03	7.45E-03	2.489
115.8	9.29E-03	9.47E-03	1.926
87.3	1.24E-02	1.28E-02	2.983
58.5	1.98E-02	1.95E-02	-1.515
31.1	3.85E-02	3.77E-02	-2

Table D.7 – Comparison of experimental and PVTsim calculated oil density, ρ_o, for fluid model 1

Pressure (bar)	Experimental ρ_o (kg^3/m^3)	PVTsim calculated ρ_o (kg/m^3)	Error (%)
298.3	716.9	730.2	1.855
276.5	715	727.3	1.720
251.4	712.3	723.9	1.629
223	709.4	719.7	1.452
200.8	706.6	716.3	1.373
195.7	706.1	715.5	1.331
177.2	703.9	712.4	1.208
151	700.3	707.8	1.071
146.4	699.7	707	1.043
122.5	710.3	715.3	0.704
101	721.5	726.2	0.651
81	732	736.8	0.656
61	742	747.8	0.782
41	753.8	759.7	0.783
21	766.6	773.7	0.926
1.01	793.7	816.9	2.923

Table D.8 – Comparison of experimental and PVTsim calculated oil density, ρ_o, for fluid model 2

Pressure (bar)	Experimental ρ_o (kg^3/m^3)	PVTsim calculated ρ_o (kg/m^3)	Error (%)
326.8	706.8	699.5	-1.033
301.9	704.4	696.6	-1.107
276.6	701.4	693.6	-1.112
251.3	698.6	690.4	-1.174
227	695.8	687.1	-1.250
203.1	692.2	683.8	-1.214
195.8	691.3	682.7	-1.244
177.9	688.7	680	-1.263
172.3	687.9	680.7	-1.047
145.8	699.6	691.3	-1.186
115.8	713.6	703.7	-1.387
87.3	727.3	716	-1.554
58.5	740.2	729	-1.513
31.1	754	742.8	-1.485
1.01	786	779.5	-0.827

Table D.9 – Comparison of experimental and PVTsim calculated oil viscosity, μ_o, for fluid model 1

Pressure (bar)	Experimental μ_o (cp)	PVTsim calculated μ_o (cp)	Error (%)
301.4	0.559	0.597	6.798
275.4	0.543	0.578	6.446
251.2	0.529	0.56	5.860
226.4	0.514	0.542	5.447
202.4	0.5	0.525	5.000
195.7	0.495	0.52	5.051
177.6	0.484	0.507	4.752
151.6	0.467	0.488	4.497
146.5	0.463	0.484	4.536
127.2	0.485	0.514	5.979
102	0.522	0.575	10.153
75	0.563	0.634	12.611
52.8	0.598	0.69	15.385
32.2	0.647	0.763	17.929
1.01	0.888	1.821	105.068

Table D.10 – Comparison of experimental and PVTsim calculated oil viscosity, μ_o, for fluid model 2

Pressure (bar)	Experimental μ_o (cp)	PVTsim calculated μ_o (cp)	Error (%)
447.7	0.726	0.708	-2.479
425	0.71	0.691	-2.676
400	0.693	0.673	-2.886
376	0.674	0.655	-2.819
352	0.655	0.637	-2.748
327	0.639	0.619	-3.130
302.4	0.618	0.601	-2.751
276.5	0.6	0.582	-3.000
252	0.58	0.564	-2.759
226	0.562	0.545	-3.025
202	0.542	0.528	-2.583
195.8	0.538	0.523	-2.788
184	0.53	0.515	-2.830
172.3	0.52	0.515	-0.962
146.8	0.536	0.578	7.836
122.3	0.562	0.633	12.633
98	0.599	0.685	14.357
55.5	0.68	0.809	18.971
25	0.911	0.958	5.159
1.01	1.33	1.408	5.865

APPENDIX E

COMPARISON OF LOG DATA WITH MODEL PROPERTIES:

Porosity

Water Saturation

Permeability

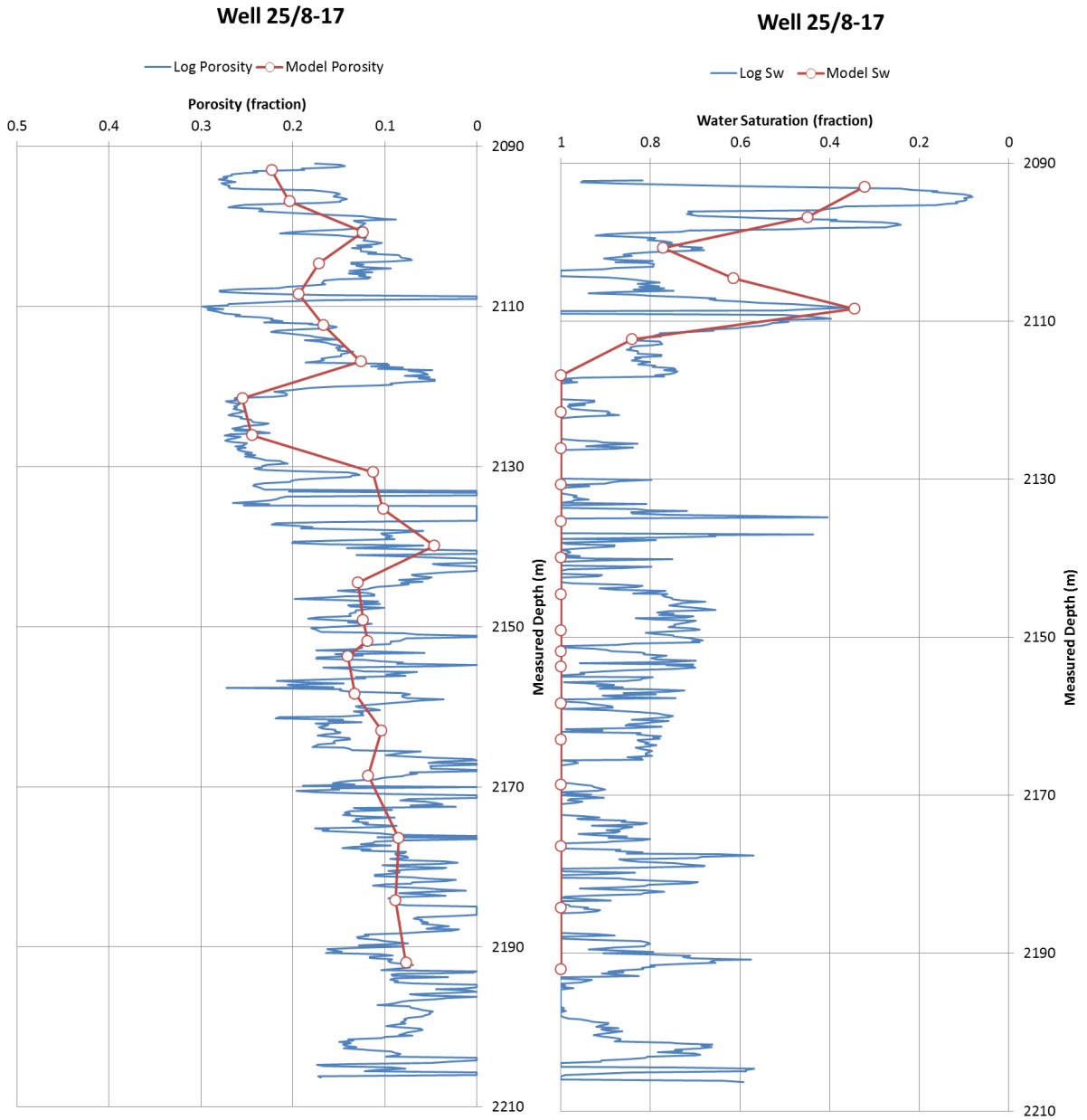

Figure E.1: Comparison of model and log for porosity and water saturation along well 25/8-17. Mismatch in water saturation is caused by the model assuming 100% water saturation below the water-oil contact.

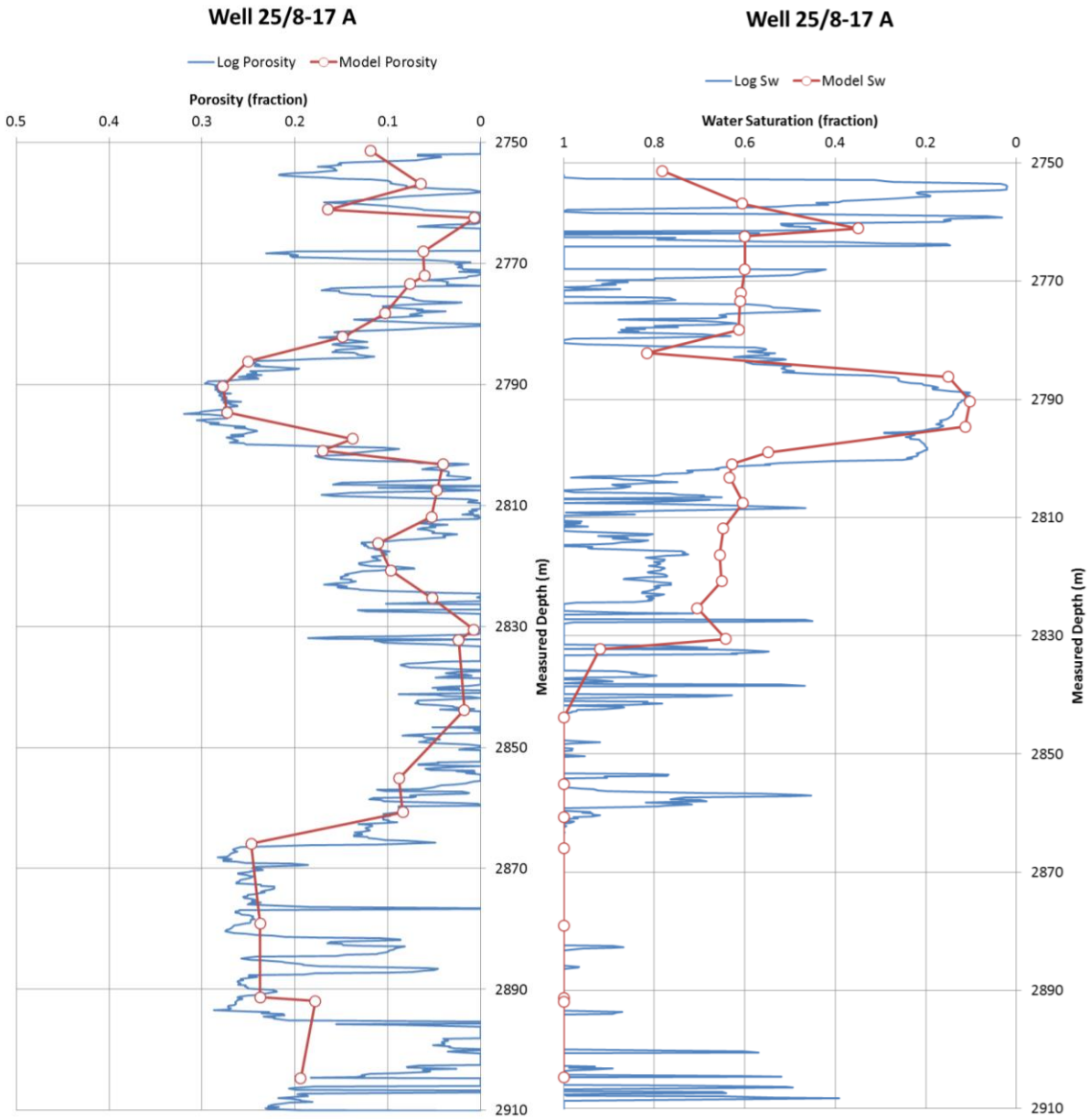

Figure E.2: Comparison of model and log for porosity and water saturation along well 25/8-17 A. Mismatch in water saturation is caused by the model assuming 100% water saturation below the water-oil contact.

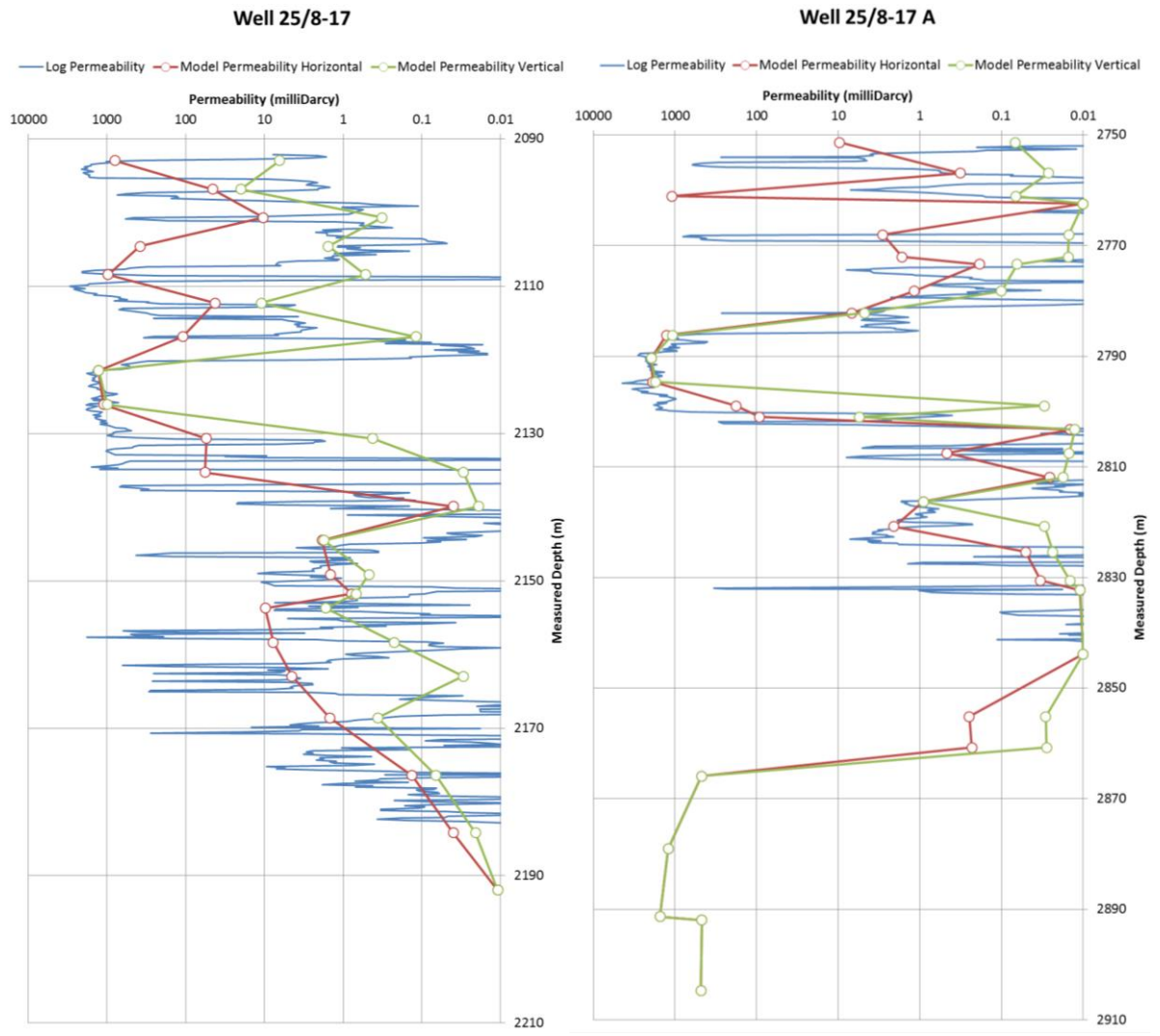

Figure E.3: Comparison of permeability between model and log along well 25/8-17 and 25/8-17 A. The reservoir model has permeability anisotropy represented by vertical and horizontal permeability while the log only measures one averaged value of permeability.

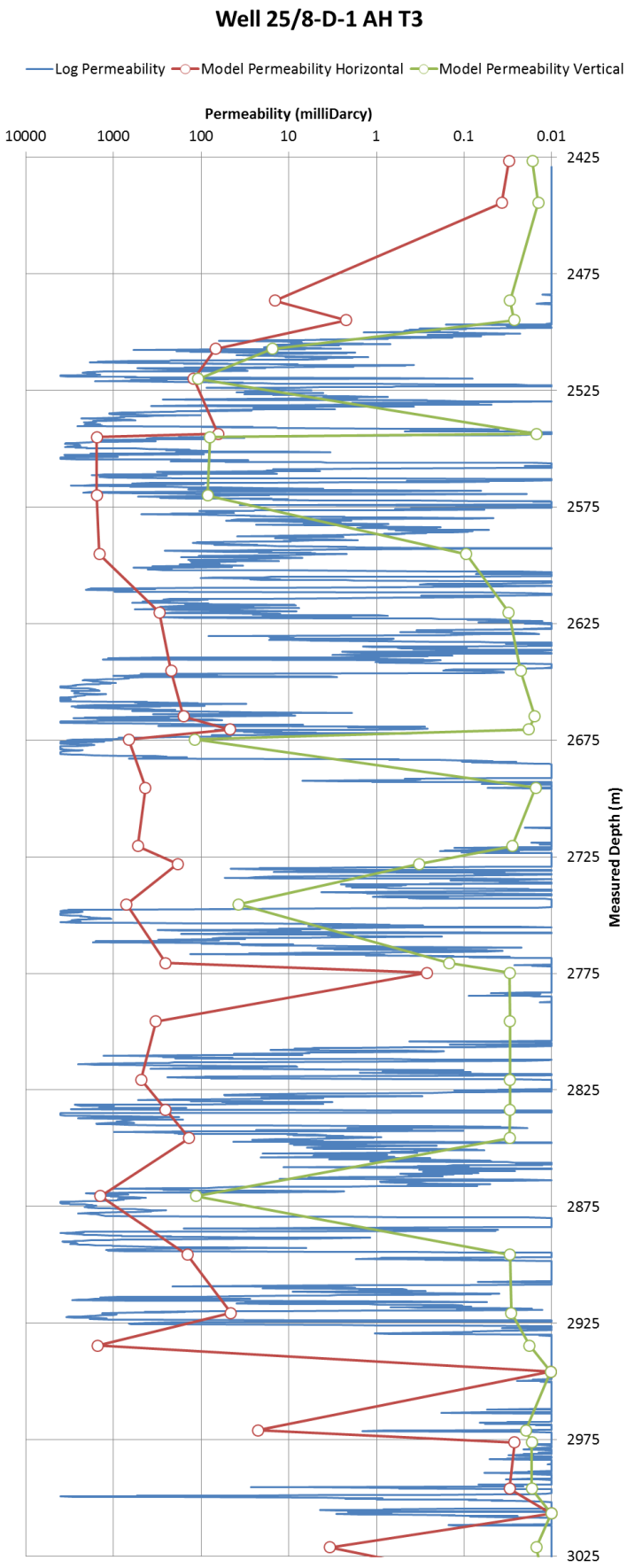

Figure E.4: Comparison of permeability between model and log along well 25/8-D-1 AH T3. The reservoir model has permeability anisotropy represented by vertical and horizontal permeability while the log only measures one averaged value of permeability.

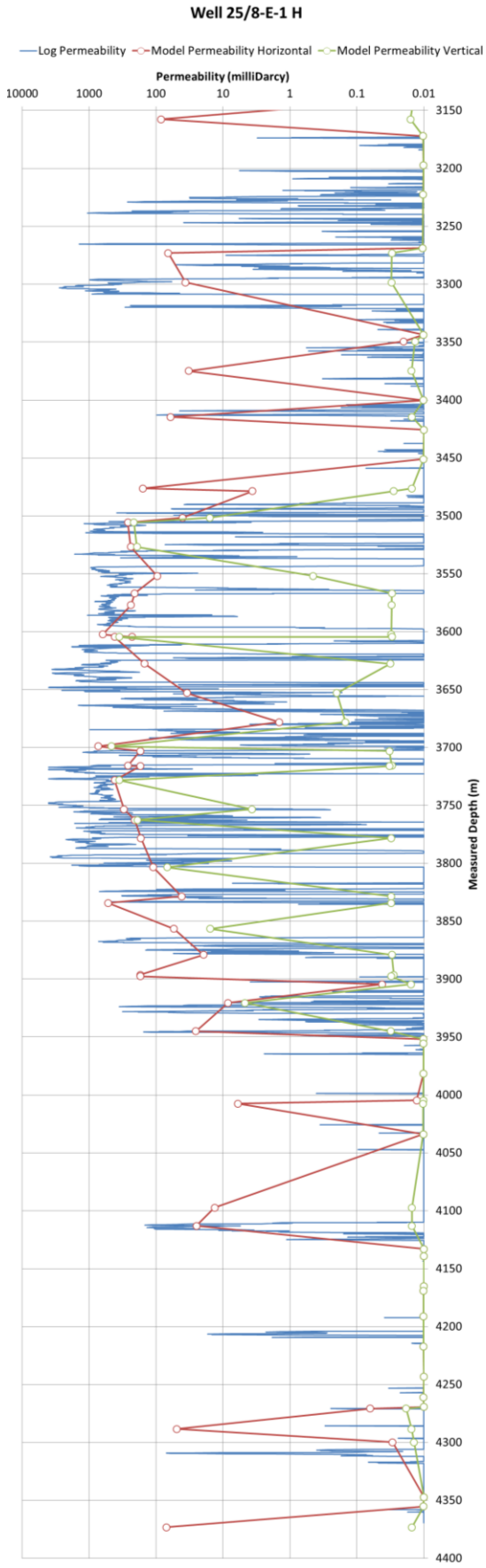

Figure E.5: Comparison of permeability between model and log along well 25/8-E-1 H. The reservoir model has permeability anisotropy represented by vertical and horizontal permeability while the log only measures one averaged value of permeability.

APPENDIX F

RESULTS FROM HISTORY MATCHED MODEL CONSTRAINED BY THP

This appendix presents additional results from the history matched model constrained by THP, as discussed in Chapter 8.5. All results are presented on a field level.

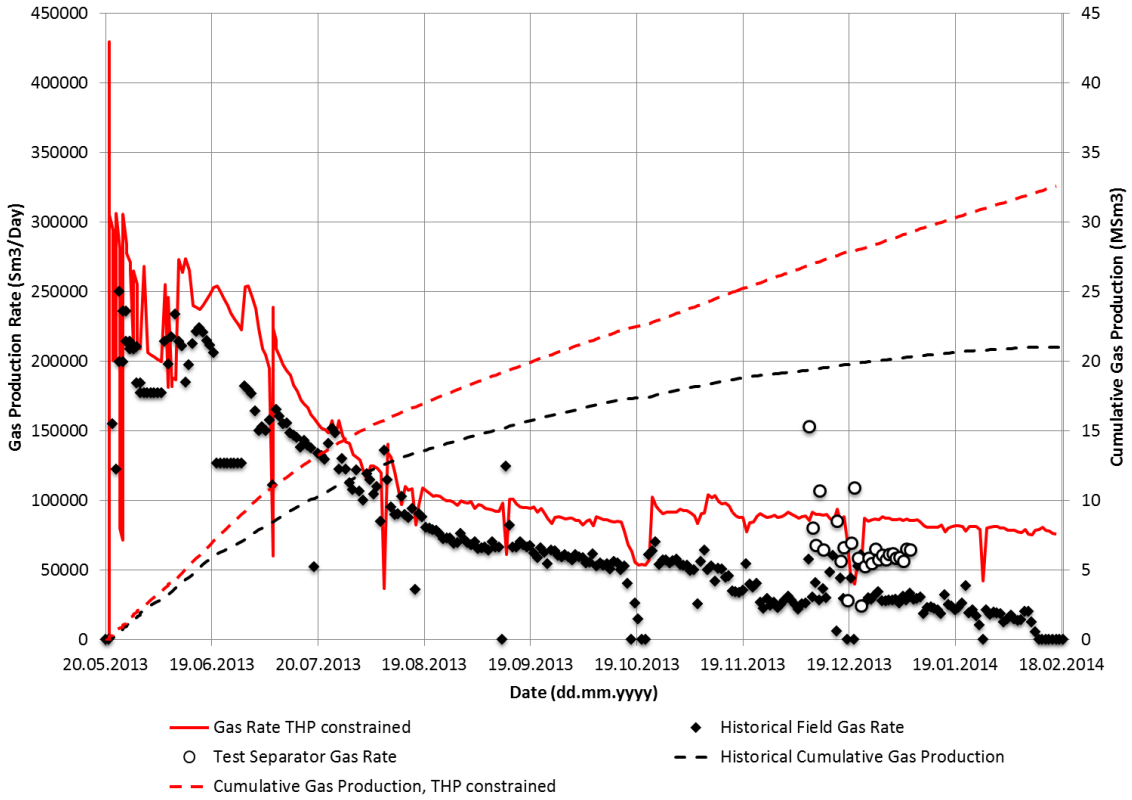

Figure F.1: Gas production in the history matched model when constrained from THP during simulation.

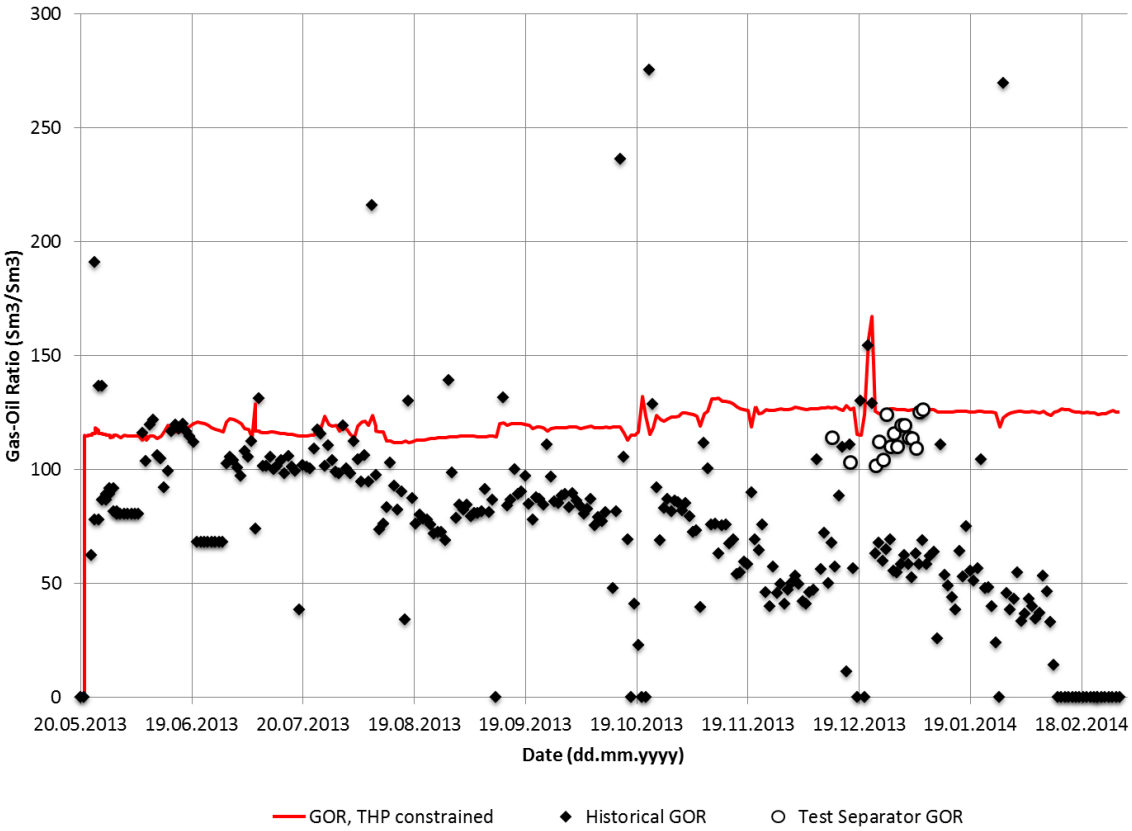

Figure F.2: GOR in the history matched model when constrained from THP during simulation.

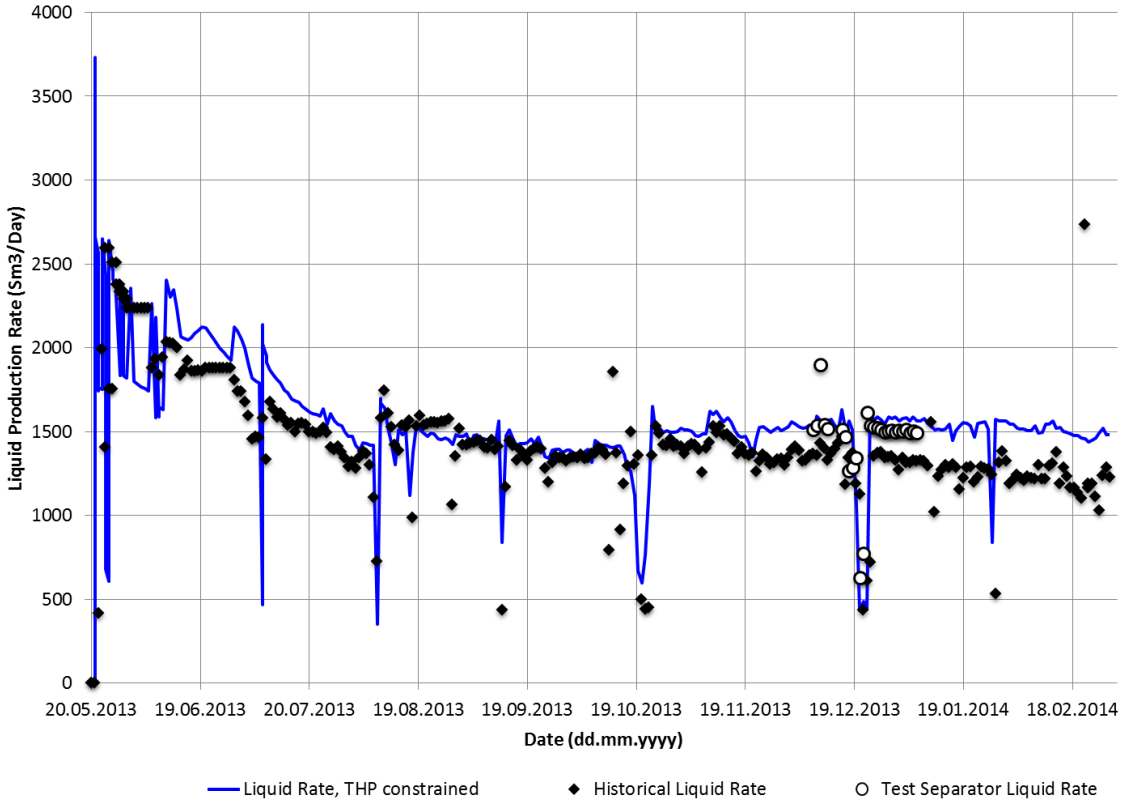

Figure F.3: Liquid production rate in the history matched model when constrained from THP during simulation.

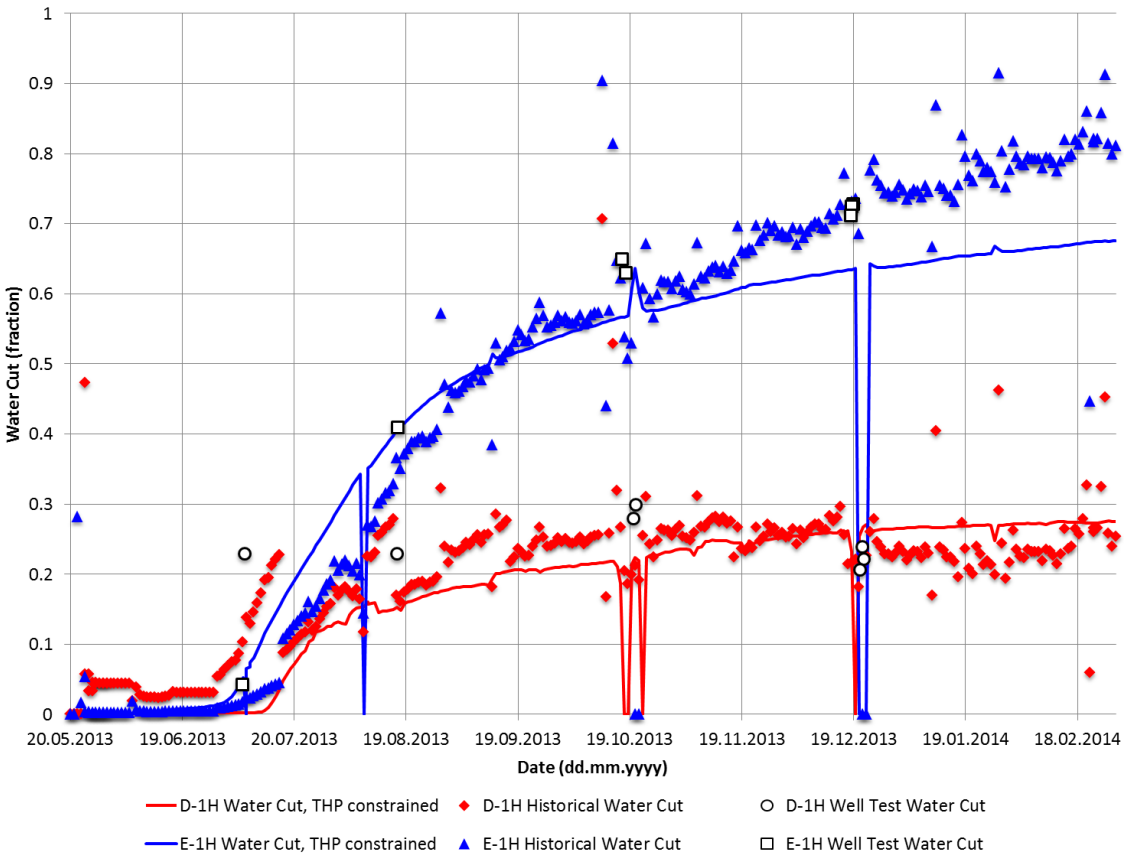

Figure F.4: Water cut in the history matched model when constrained from THP during simulation.

APPENDIX G

RESULTS FROM PRODUCTION FORECAST

This appendix presents additional results from the production forecast discussed in Chapter 9.2. The history matched model constrained from THP were used during prediction.

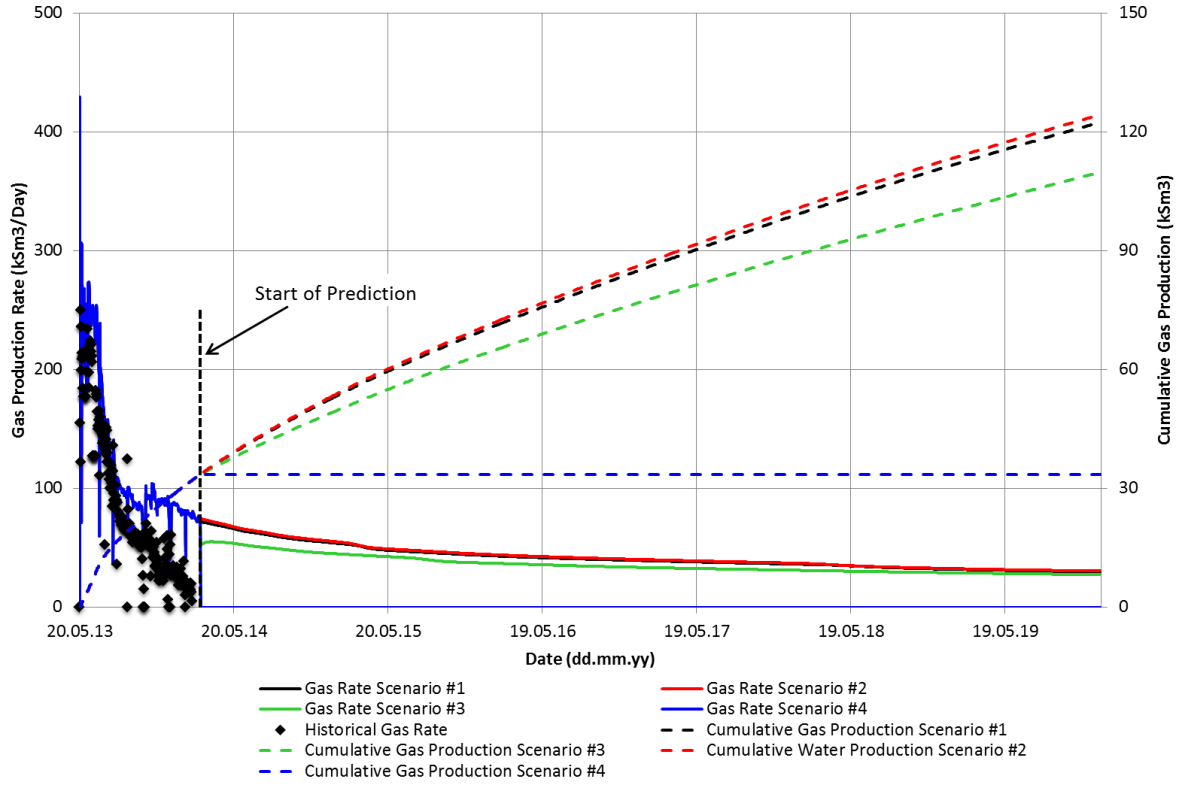

Figure G.1: Predicted gas production rate and cumulative gas production for the Jette field in the period 01.03.2014 to 01.01.2020.

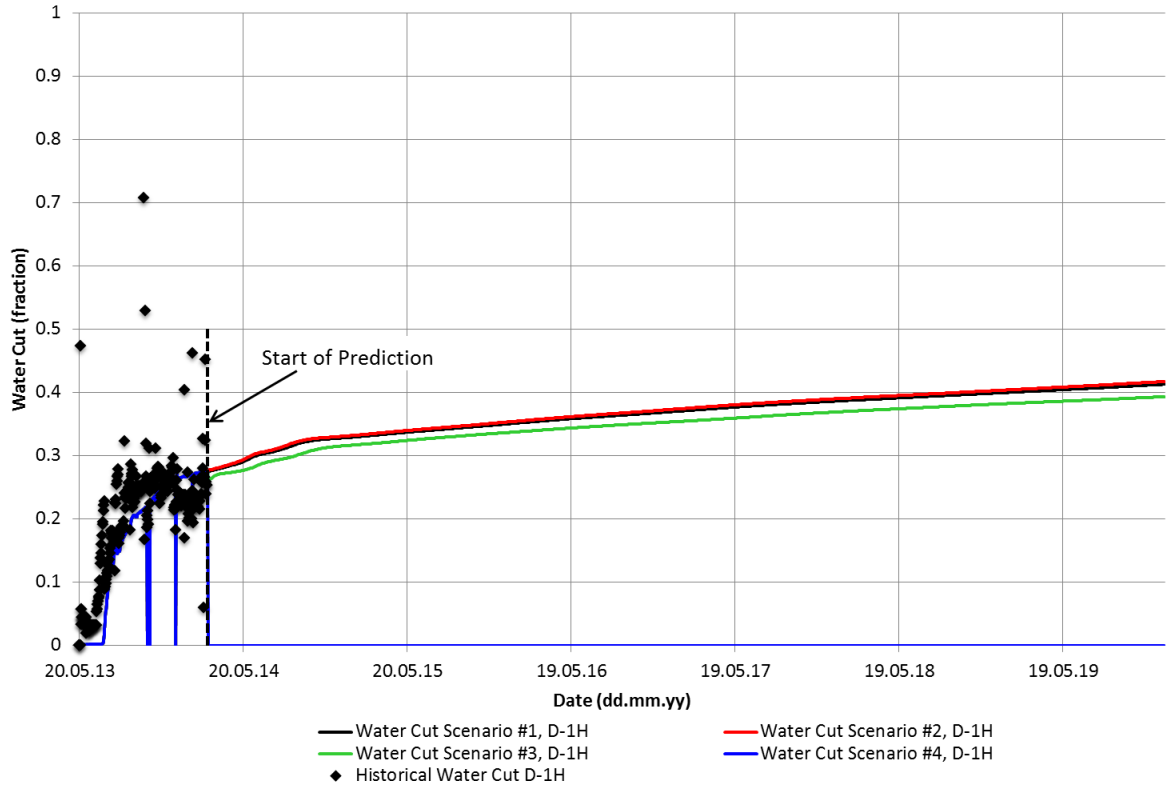

Figure G.2: Predicted water cut in well D-1H in the period 01.03.2014 to 01.01.2020.

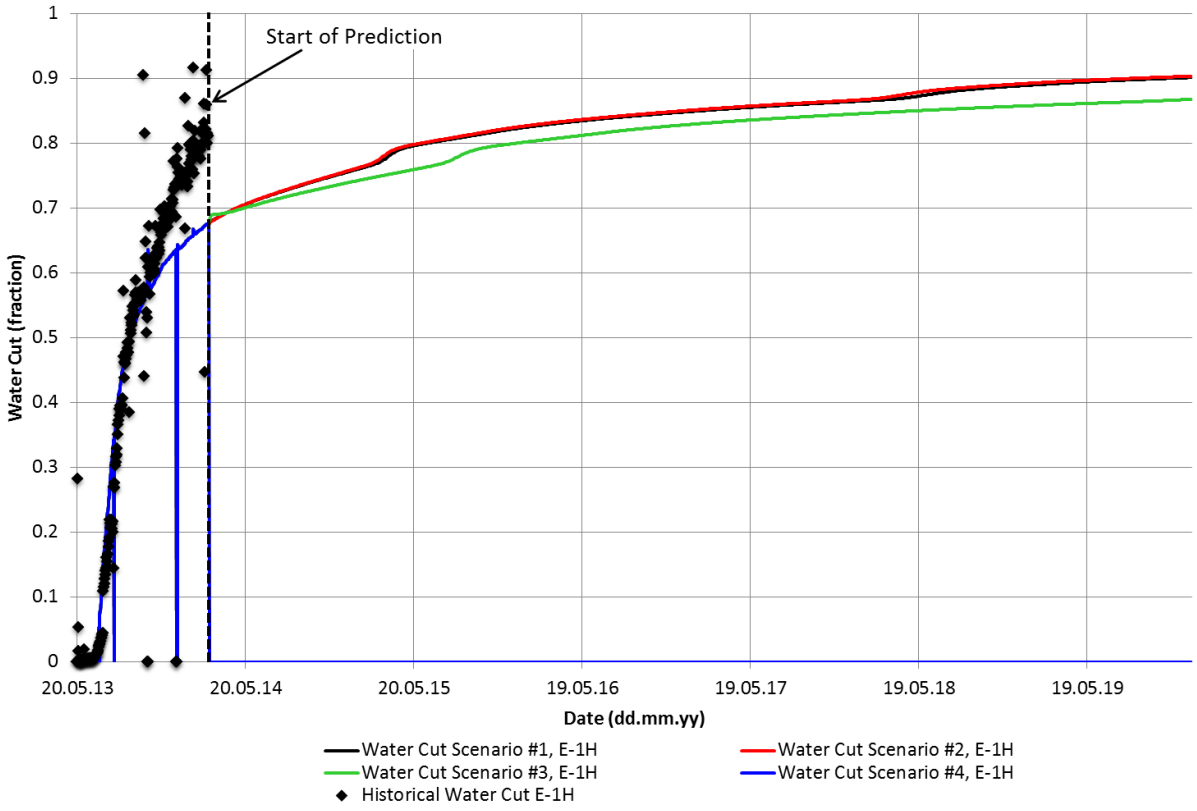

Figure G.3: Predicted water cut in well E-1H in the period 01.03.2014 to 01.01.2020.

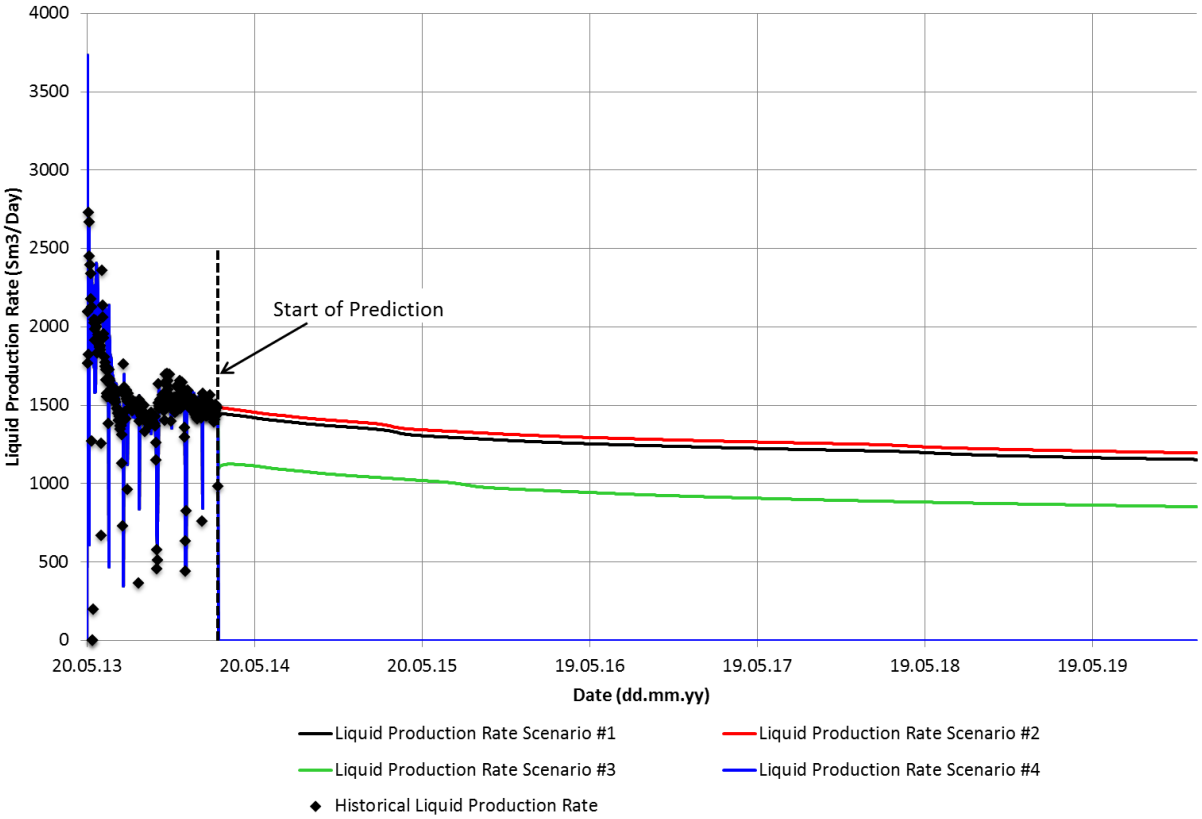

Figure G.4: Predicted liquid rate at the Jette field in the period 01.03.2014 to 01.01.2020.

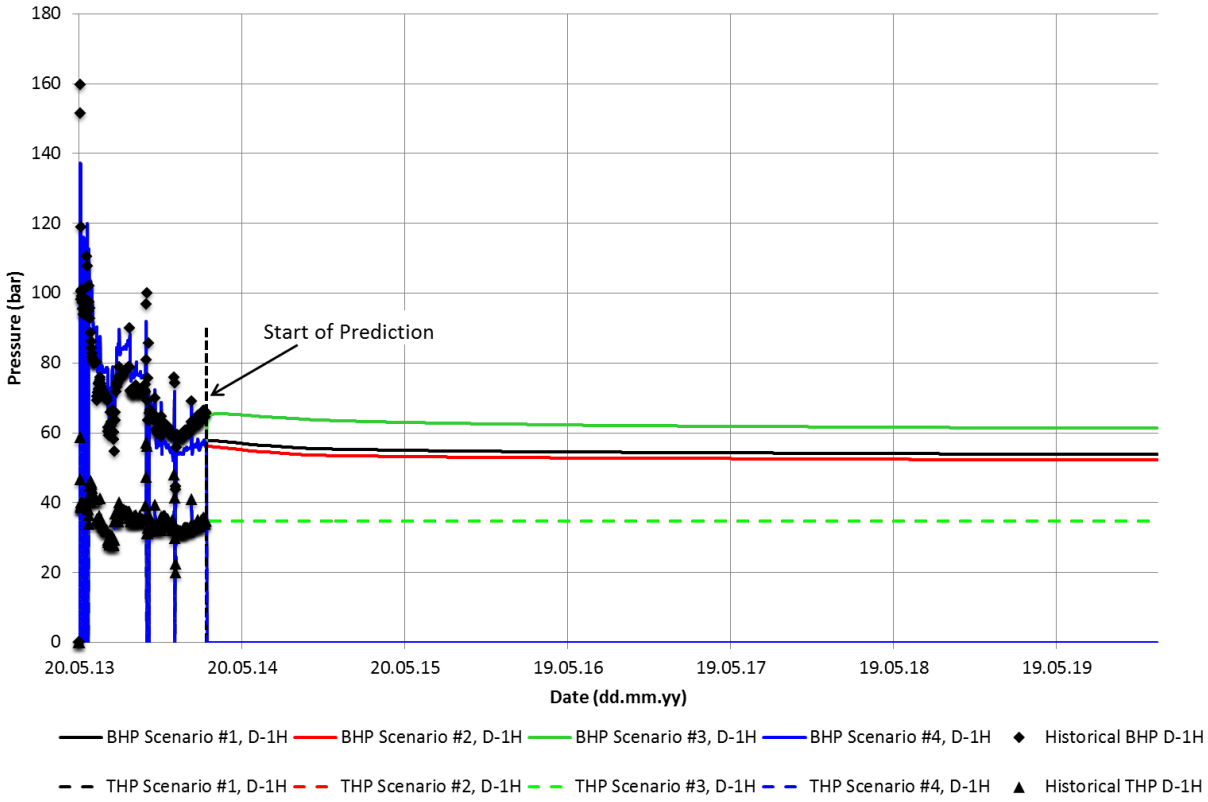

Figure G.5: Predicted BHP and THP in well D-1H in the period 01.03.2014 to 01.01.2020.

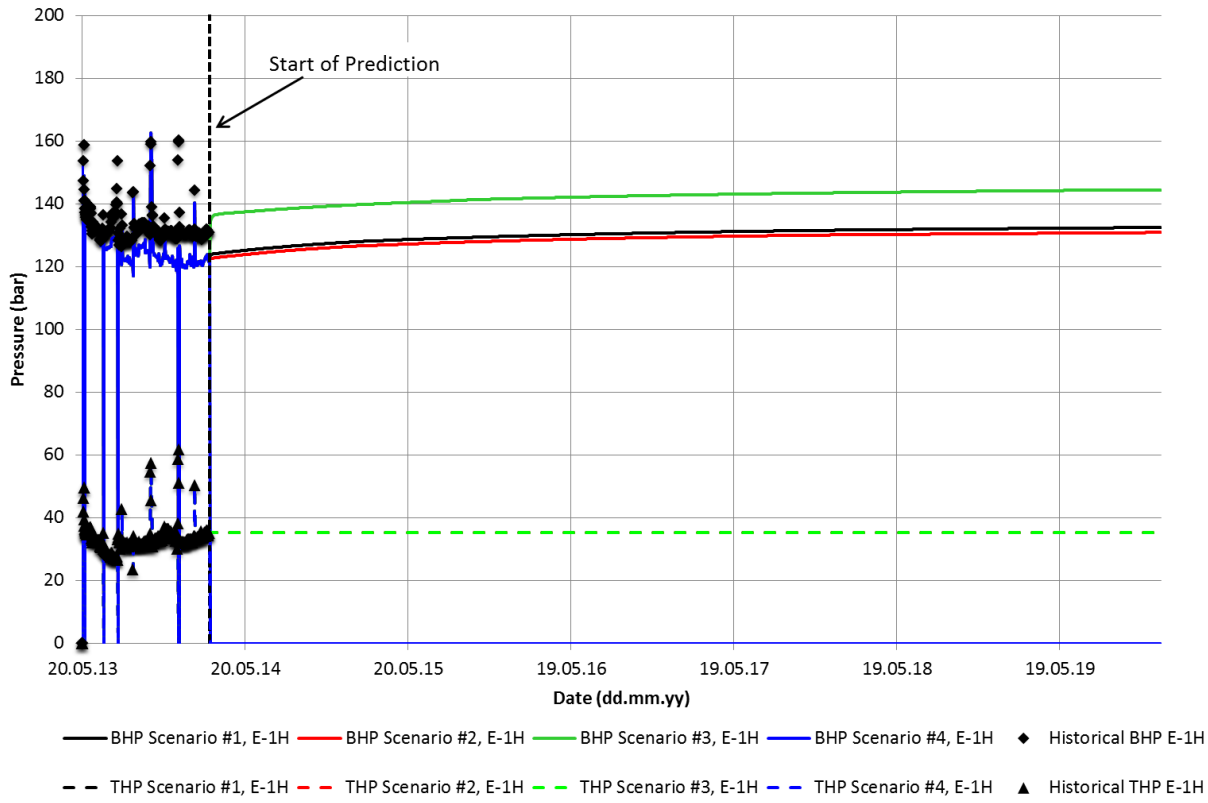

Figure G.6: Predicted BHP and THP in well E-1H in the period 01.03.2014 to 01.01.2020.